WITHIN-GENERATIONAL DISRUPTION OF THE STRESS RESPONSE BY FLUOXETINE AND OTHER ENVIRONMENTAL CONTAMINANTS IN ZEBRAFISH

AMIN NOZARI

Thesis submitted to the University of Ottawa
in partial Fulfillment of the requirements for the
Doctorate in Philosophy in Biology

Department of Biology
Faculty of Science
University of Ottawa

Acknowledgements

Now that I am coming to the end of this chapter of my life, I wish to express my utmost gratitude to people who stayed beside me throughout the ups and downs of this journey.

First and foremost, I would like to acknowledge my partner in life, my wife, Dr. Elham Karimi. Ellie, you have always been there for me and always put my needs first. During the first months of your arrival to Canada, you took charge to help our small family to go through financial struggles. At the times of my frustrations, you were always there and comforting me with your confidence. I wish I could repay you someday for all your kindness and generosity.

I wish to express my sincere gratitude to my mentor and my supervisor, Dr. Vance Trudeau. I joined his lab at the most challenging point in my life. I still can't believe how he saved me in less than a few hours from all the troubles and misery that I was in. You welcomed me to your lab and walked me through the steps like a real friend. I learned a lot from you. Not only how to be a scientist, but how to be a mentor in life. I am forever in your debt, and I wish our friendship lasts forever.

Also, I would like to thank my parents, Aliakbar and Parvin, my only sister, Rahil, and my brother-in-law, Omid, whom I have not seen in person for quite some time. The unconditional support and love that I received from these people is the only reason that I am who I am. I love you all and miss you so much. I wish to see you in a very near future.

Also, I would like to thank my dearest friend, Dr. Shahrokh Ghobadloo. Without your guidance, I would not be able to achieve what I did, Shahrokh. You have been, and still are, my most trusted consultant in both science and life. I am proud of being your friend.

To my PhD advisory committee, Dr. Jan Mennigen, Dr. Carol Yauk, and Dr. Kathleen Gilmour, I would like to express my sincere gratitude for all your supports, invaluable advice, and unconditional mentorship.

Also, I would like to express my gratitude to Remi Gagné, who without him the analysis of our massive data was not possible. Remi, you are a brilliant scientist and I enjoyed every bit of working with you.

To my great friends at TEAMENDO; Marylin, Chunyu, Katherine, Peng Di, Udeesha, Selena, and Izzy, it has been my privilege to work alongside you fine scientists. I enjoyed every bit of working with you guys. I want to thank Marilyn and Chun Yu, particularly, for their support even in the times that they were struggling with their own experiments. Also, I would like to particularly thank Selena, who helped me to develop the screening assay presented in this thesis. I wish all of you guys the bests in your future endeavours.

Last by not least, I wish to thank all members of my in-law family, Vadood and Mahnaz, my second parents who always cheered me up. My brothers-in-law, Vahid and Saeed, who supported me, way before I was a member of this family. Also, I want to thank Arezoo, my sister-in-law, who is gladly joining us in Canada soon alongside Vahid and my-nephew-in-law (not sure if such term is correct!), Pendar. Can't wait to have you with us guys.

I also would like to especially thank Dr. Markus Hecker and Dr. Marc Ekker for accepting to sit as my thesis defence committee. The time that you have allocated for this is greatly appreciated.

Abstract

Selective serotonin reuptake inhibitors (SSRIs), like fluoxetine, are widely used to treat depressive disorders during pregnancy. These antidepressants reach water reservoirs through sewage treatment facilities and expose the aquatic vertebrates, including fish. It has been shown that early-life exposure to fluoxetine could disrupt the normal function of the stress axis by decreasing the level of circulating glucocorticoids in humans, rodents, and teleosts. Our lab recently showed that early life exposure to fluoxetine resulted in transgenerational hyporcortisolism and altered exploratory behaviour in adult male zebrafish and their descendant male adults for at least three generations. In the current study, we used a stress-responsive transgenic zebrafish line (SR4G) that expresses green fluorescence protein (eGFP) under the control of six consecutive glucocorticoid response elements. The effects of developmental exposure to fluoxetine on the transcriptional profiles of genes in the larval head and male adult telencephalon and hypothalamus were analysed using high throughput RNA sequencing. We also assessed the potential of eGFP mRNA to evaluate blunted stress response as an alternative to cortisol immunoassay measurements. The effects of bisphenol A, vinclozolin and fluoxetine were ytested in the SR4G line. Developmental exposure to fluoxetine resulted in a life-long dysregulation of pathways involved in nervous system development, stress response, and lipid metabolism in both larvae and adult zebrafish. Numerous differentially expressed genes in zebrafish are orthologous to genes in *Homo sapiens* linked the development of the major depressive disorder and epigenetics regulation and include *bdnf*, *trkb*, *npas4, per1, per2, dnmt3a, adarb1, adaeb2, hdac4, hdac5, hdac8,* and *atf2*. It is suggested that the dysregulation of the primary transcription regulators of circadian rhythm (*clocka*) and *stress response (nr3c1), amongst others,* were the potential drivers of the observed life-long effects.

Furthermore, we report on a significant positive linear correlation between cortisol levels and eGFP mRNA levels in SR4G transgenic zebrafish larvae (R2> 0.9). Random forest and logistic regression models trained by eGFP mRNA levels both correctly predicted the blunted stress response. The negative predictive value (NPV) for both models was 100%. Models based on the mRNA levels of 11 genes associated with neurogenesis, stress response and depression resulted

in a similar 100% NPV. These findings provide evidence for a life-long effect of developmental exposure to fluoxetine. This study also provides a proof-of-concept for an *in vivo* biomonitoring assay to screen chemicals for their stress-disrupting potential.

Abbreviations

ACTH	Adrenocorticotropic hormon
ACVS	Animal care and veterinary services
adarb1	Adenosine Deaminase RNA Specific B1
adarb1b	Adenosine Deaminase RNA Specific b1-b
adarb2	Adenosine Deaminase RNA Specific B2
ANOVA	Analysis of variance
atf2	activating transcription factor 2
AVP	Arginine vasopressin
BDNF	Brain derived neurotrophic factor
BPA	bisphenol A
CaMKIIa	Ca2+/calmodulin-dependent protein kinase II
CLOCK	Clock circadian regulator
clocka	Clock circadian regulator a
CMLC	Cardiac myosin light chain-1
CORT	cortisol
CPM	count per million
CPT1C	Carnitine palmitoyltransferase 1C
CREB	cAMP response element-binding
crebzf	CREB/ATF bZIP transcription factor
CRH	Corticotropin releasing hormone
crhb	Corticotropin releasing hormone b
CRY1	Cryptochrome circadian regulator 1
CRY2	Cryptochrome circadian regulator 2
DAVID	Database for annotation, visualization and integrated discovery
DEG	Differentially expressed gene
DEX	Dexamethasone
DMSO	Dimethylsulfoxide
dnmt3a	DNA methyltransferase 3 alpha
dnmt3aa	DNA (cytosine-5-)-methyltransferase 3 alpha a
EDC	endocrine disruptive compound
eGFP	enhanced green fluorescence protein
egr2a	Early growth response 2a
egr4	Early growth response 4
elovl5	ELOVL fatty acid elongase 5
ERK	extracellular signal-regulated kinase
fabp2	Fatty acid binding protein 2
FC	fold change
FDR	false discovery rate
fkbp4	FK506 binding protein prolyl isomerase 4
fkbp5	FK506 binding protein prolyl isomerase 5
FLX	fluoxetine

fosab	V-fos FBJ murine osteosarcoma viral oncogene homolog Ab
fosl1a	FOS-like antigen 1a
GNRH	Gonadotropin releasing hormone
GO	gene ontology
GR	glucocorticoide receptor
GRE	Glucocorticoid Response elements
grm2a	Glutamate receptor, metabotropic 2a
grm3	Glutamate metabotropic receptor 3
hcn1	Hyperpolarization activated cyclic nucleotide gated potassium channel 1
hdac4	Histone deacetylase 4
hdac5	Histone deacetylase 5
hdac8	Histone deacetylase 8
HPA	hypothalamus-pituitary-adrenal
HPI	hypothalamus-pituitary-interreanl
htr1b	5-hydroxytryptamine receptor 1B
HTRs	serotonin receptors
HYP	hypothalamus
INR	interrenal
IPA	ingenuity pathway analysis
ITGB1	ntegrin subunit beta 1
JNK	c-Jun N-terminal kinase
klf11a	Kruppel-like factor 11a
klf15	Kruppel like factor 15
LINGO3	Leucine rich repeat and Ig domain containing 3
MAPK	mitogen-activated protein kinase
MAT1A	Methionine adenosyltransferase 1A
MBD-1	methyl-CpG binding domain-1
MDD	major depressive disorder
NCOA1	Nuclear receptor coactivator 1
NF-κB	Nuclear Factor kappa-light-chain-enhancer of activated B cells
npas4	Neuronal PAS domain protein 4
npas4a	Neuronal PAS domain protein 4 a
NPC1	NPC intracellular cholesterol transporter 1
nr1d1	Nuclear receptor subfamily 1 group D member 1
NR3C1	NUCLEAR RECEPTOR SUBFAMILY 3, GROUP C, MEMBER 1
nr3c2	Nuclear receptor subfamily 3 group C member 2
nr4a1	Nuclear receptor subfamily 4 group A member 1
Nrgn	Neurogranin
ntrk2a	Neurotrophic tyrosine kinase, receptor, type 2a
OECD	Organisation for Economic Co-operation and Development
OXTR	oxytocin receptor
pavalb6	Parvalbumin 6
PBDE	Polybrominated diphenyl ether
PBS	Phosphate-buffered saline

PC	pharmaceutical
PCA	Principal component analysis
pclob	Piccolo presynaptic cytomatrix protein b
per1	Period circadian regulator 1
per1a	Period circadian regulator 1 a
per1b	Period circadian regulator 1 b
per2	Period circadian regulator 2
PIT	pituitary
POU3F1	POU class 3 homeobox 1
PPARGC1A	PPARG coactivator 1 alpha
ptgdsb	Prostaglandin D2 synthase b, tandem duplicate 1
RIN	RNA integrity score
ROI	Region of interest
rorcb	RAR-related orphan receptor C b
SAPK	Mitogen-activated protein kinase 12
SCAP	Sterol regulatory element-binding transcription factor chaperone
sfpq	Splicing factor proline and glutamine rich
SIRT1	Sirtuin 1
SKA2	Spindle and kinetochore associated complex subunit 2
SR4G	stress responsive transgenic zebrafish line
SREBF1	Sterol regulatory element binding transcription factor 1
SREBF2	Sterol regulatory element binding transcription factor 2
srrt	Serrate, RNA effector molecule
SSRIs	Selective serotonin reuptake inhibitors
STAR	Spliced Transcripts Alignment to a Reference software
tefb	TEF transcription factor, PAR bZIP family member b
TEL	telencephalon
TMM	trimmed mean of M values
Trkb	Neurotrophin 3
tspo	Translocator protein
VIN	Vinclozolin
ZFET	Zebrafish Embryo Acute Toxicity Test

Contents

ACKNOWLEDGEMENTS ..... **II**

ABSTRACT ..... **IV**

ABBREVIATIONS ..... **VI**

LIST OF FIGURES ..... **XII**

LIST OF TABLES ..... **XIV**

LIST OF SUPPLEMENTARY FIGURES AND TABLES ..... **XV**

CHAPTER 1: GENERAL INTRODUCTION **1**

1.1. RATIONALE OF THE STUDY. 1
1.2. THE STRESS RESPONSE. 3
1.2.1. The physiology and endocrine pathways of the stress axis in mammals. *3*
1.2.2. The central nervous system response to stress. *4*
1.2.3. The mammalian models to study the stress axis. *5*
1.2.4. The teleost models to study the stress axis. *7*
1.2.5. The long-lasting adverse effects of early-life exposure to stress *8*
1.2.6. The long-lasting adverse effects of disruption of the stress response. *10*
1.3. DEPRESSION AND ANTI-DEPRESSANTS. 10
1.3.1. The different classes of anti-depressants. *11*
1.3.2. The selective-serotonin-reuptake inhibitors (SSRIs). *12*
1.3.3. The long-lasting adverse effects of early-life exposure to SSRIs. *12*
1.3.4. The SSRIs as emerging environmental contaminants. *14*
1.4. THE ZEBRAFISH MODEL. 17
1.4.1. The stress-inducible transgenic zebrafish (SR4G) line. *18*
1.5. THE HYPOTHESES AIMS, AND OBJECTIVES OF THE STUDY 19
1.6. THESIS OUTLINE 20

CHAPTER 2: APPLICATION OF SR4G TRANSGENIC ZEBRAFISH LINE IN THE STUDY OF THE STRESS RESPONSE. **22**

2.1. INTRODUCTION 22
2.2. MATERIALS AND METHODS 23
2.2.1. Animals and Husbandry *23*
2.2.3. Chemicals and exposure conditions *24*
2.2.4 Stress conditions and sample collection *24*
2.2.5. Whole-body cortisol measurement *25*
2.2.6. Total RNA extraction and quantitative PCR *25*
2.2.7. Whole-body fluorescence imaging *26*
2.2.7. Statistical analysis *27*
2.3. RESULTS 27
2.3.1. The highest level of cortisol was captured 30 minutes after the handling stress *27*
2.3.2. Whole-body eGFP mRNA levels reach the peak 60 minutes after handling stress. *30*
2.3.3. The fluorescence imaging revealed ubiquitous eGFP expression induced by exogenous and endogenous cortisol. *31*
2.4. DISCUSSION 38

2.5. STATEMENT OF CONTRIBUTION 39

CHAPTER 3: LIFE-LONG EFFECTS OF DEVELOPMENTAL EXPOSURE TO FLUOXETINE ON GLOBAL TRANSCRIPTION PROFILES IN THE BRAINS OF ZEBRAFISH 40

3.1. INTRODUCTION 40
3.2. MATERIALS AND METHODS 42
3.2.1. Animals and Husbandry 42
3.2.2. Study design 42
3.2.3. Chemical exposure 43
3.2.4. The net handling stress and sampling for RNA sequencing 44
3.2.5. Total RNA extraction and quality control 46
3.2.6. Next-generation high throughput RNA sequencing 46
3.2.7. Ingenuity pathway analysis and network prediction 48
3.2.8. The statistical analysis 49
3.3. RESULTS 49
3.3.1. Developmental exposure to fluoxetine altered gene transcription pattern of the central nervous system in both larva and adult zebrafish 49
3.3.2. Enrichment of pathways associated with neurotransmitter signalling and response to steroid hormones supports a life-long effect of developmental exposure to fluoxetine 55
3.3.3. The upstream transcriptional regulators associated with regulation of the stress response and circadian rhythm were affected life-longly upon developmental exposure to fluoxetine 67
3.3.4. Developmental exposure to fluoxetine dysregulated genes associated with lipid metabolism, nervous system development and behaviour 69
3.3.5. Several genes were dysregulated life-longly in both larvae and adult zebrafish upon developmental exposure to fluoxetine 71
3.3.6. Life-long effects of developmental exposure to fluoxetine on genes associated with depression, neuroplasticity and epigenetics 79
3.4. DISCUSSION 92
3.5. STATEMENT OF CONTRIBUTION 98

CHAPTER 4: APPLICATION OF SR4G TRANSGENIC ZEBRAFISH LINE AS A BIOMONITORING ASSAY TO DETECT ALTERED STRESS RESPONSE. 98

4.1. INTRODUCTION 98
4.2. MATERIALS AND METHODS 101
4.2.1. Animals and Husbandry 101
4.2.2. Study design 101
4.2.3. Chemicals and exposure concentrations 102
4.2.4. Stress conditions and sample collection 103
4.2.5. Total RNA extraction and quantitative PCR 103
4.2.6. Whole-body cortisol measurement 104
4.2.7. Whole-body fluorescence measurement 104
4.2.8. Statistical analysis 105
4.3. RESULTS 105
4.3.1. The whole-body cortisol response to handling stress is blunted following exposure to FLX, BPA, VIN, and DEX 105
4.3.2. The whole-body eGFP mRNA response to handling stress is blunted following exposure to FLX, BPA, VIN, and DEX 109
4.3.3. Whole-body eGFP mRNA are correlated to the whole-body cortisol levels in SR4G transgenic zebrafish larvae. 113

4.3.4. Whole-body eGFP mRNA levels are predictive of blunted stress response following exposure to stress disruptive chemicals in SR4G transgenic zebrafish larvae. 116
4.3.5. The global pattern of whole-body mRNA levels of 11 genes related to stress, depression, and neurogenesis was suggestive of blunted stress response following exposure to stress disruptive chemicals in SR4G transgenic zebrafish larvae....118
4.3.5. Whole-body mRNA levels of 11 genes related to stress, depression, and neurogenesis are predictive of altered stress response following chemical exposures in SR4G transgenic zebrafish larvae. 120
4.3.6. Whole-body fluorescence measurements are not sensitive enough to detect disruption of the stress response following chemical. exposure 139
4.4. DISCUSSION....142
4.5. Statement of contribution....146
CHAPTER 5: GENERAL DISCUSSION AND FUTURE DIRECTIONS 147
5.1. THESIS SUMMARY AND DISCUSSION....147
5.2. SIGNIFICANCE OF THESE FINDINGS....150
5.3. FUTURE PERSPECTIVES....151
SUPPLEMENTARY DATA 153
APPENDIX 1- THE STATISTICAL DETAILS FOR EGFP MRNA AND 11-TARGET GENES ALTERATION....193
REFERENCES.... 198

List of Figures

Figure 1.1. An illustration of the stress axis in zebrafish. 21
Figure 2.1. The handling stress protocol. 28
Figure 2.2. Whole-body cortisol measured before and after the handling stress. 29
Figure 2.3. The whole-body eGFP mRNA level measured before and after the handling stress. 30
Figure 2.4. The ubiquitous eGFP expression in 4dpf SR4G transgenic zebrafish line following exposure to exogenous cortisol. 33
Figure 2.5. The fluorescent intensity of four anatomical regions of the brain in 4dpf SR4G transgenic line 34
Figure 2.6. The time-lapse fluorescence imaging captures the ubiquitous eGFP expression in 4dpf SR4G transgenic zebrafish line following handling stress. 37
Figure 3.1. The net handling stressor for larvae and adult zebrafish. 45
Figure 3.2. Diagram depicting the comparison mode to determine the differentially expressed genes (DEGs) in both larvae and adults 48
Figure 3.3. The total numbers of differentially expressed genes (DEGs) in FLX exposed groups compared to respective controls in unstressed and stressed conditions. 52
Figure 3.4. Volcano plots of the mapped transcriptome in FLX exposed groups compared to the controls in unstressed and stressed conditions. 53
Figure 3.5. The effect of developmental fluoxetine exposure on transcriptome patterns in larvae and adult male zebrafish central nervous system in the unstressed and the stressed conditions. 54
Figure 3.7. Commonly dysregulated genes in larvae and adult zebrafish upon developmental exposure to fluoxetine in stressed and unstressed conditions 72
Figure 4.1 Whole-body cortisol levels in 7dpf transgenic zebrafish larvae exposed to different chemicals before and after handling stress. 107
Figure 4.2 Whole-body eGFP mRNA levels in 7dpf transgenic zebrafish larvae exposed to different chemicals before and after the handling stress 111
Figure 4.3. The correlation between whole-body cortisol and total eGFP mRNA levels in SR4G transgenic zebrafish larvae 114
Figure 4.5. The whole-body mRNA levels of the 11 genes in 7dpf SR4G transgenic zebrafish larvae in the control group 122
Figure 4.6. The whole-body mRNA levels of the 9 genes in FLX exposed 7dpf SR4G transgenic zebrafish larvae 124
Figure 4.7 The whole-body mRNA levels of bdnf and fosab in FLX-exposed 7dpf SR4G transgenic zebrafish larvae 126
Figure 4.8. The whole-body mRNA levels of the nine genes in BPA, VIN and DEX, exposed 7dpf SR4G transgenic zebrafish larvae 128
Figure 4.9. The whole-body mRNA levels of bdnf and fosab in BPA-, VIN- and DEX-exposed 7dpf SR4G transgenic zebrafish larvae 130
Figure 4.10. Comparing the whole-body mRNA levels of the 11 genes in FLX exposed 7dpf SR4G transgenic zebrafish larvae in the unstressed condition 132
Figure 4.11. Comparing the whole-body mRNA levels of the nine genes in BPA, VIN, and DEX exposed 7dpf SR4G transgenic zebrafish larvae in the unstressed condition 134

Figure 4.12. Comparing the whole-body mRNA levels of bdnf and fosab in BPA, VIN, and DEX exposed 7dpf SR4G transgenic zebrafish larvae in the unstressed condition 136
Figure 4.10. The whole-body fluorescence intensity in the crude homogenized extract of 7dpf transgenic zebrafish larvae exposed to different chemicals before and after handling stress..... 140

List of Tables

Table 3.1. Pathways affected life-longly by developmental exposure to fluoxetine in the unstressed condition 60
Table 3.2. Pathways affected life-longly by developmental exposure to fluoxetine in the stressed condition 65
Table 3.3. Pathways affected life-longly in adult zebrafish by developmental exposure to fluoxetine 66
Table 3.4. Upstream regulators affected life-longly by developmental exposure to fluoxetine in zebrafish 68
Table 3.5. Top 5 predicted networks affected by developmental exposure to fluoxetine 70
Table 3.6. Genes that were dysregulated life-longly upon developmental exposure to fluoxetine in the unstressed condition 73
Table 3.7. Genes that were dysregulated life-longly upon developmental exposure to fluoxetine in the stressed condition 75
Table 3.8. Life-long downregulation of genes associated with depressive disorders upon developmental exposure to fluoxetine 82
Table 3.9. Life-long upregulation of genes associated with depressive disorders upon developmental exposure to fluoxetine 83
Table 3.10. Life-long dysregulation of genes involved in neurogenesis and neural plasticity upon developmental exposure to fluoxetine 86
Table. 3.11. Life-long dysregulation of genes involved in epigenetics upon developmental exposure to fluoxetine 91
Table 4.1. Prediction of stress response based on the whole-body eGFP mRNA levels using regression random forest (RDF) and logistic regression (LOG) model trained by Ethanol (control) group 117
Table 4.2. The 11 genes implicated in stress response, neural plasticity, and development of depression 121
Table 4.3. Prediction of stress response based on the whole-body mRNA levels of the 11 genes using regression random forest (RDF) and logistic regression (LOG) model 138

List of Supplementary Figures and Tables

Supplementary Figure 1. The mass spectrometry analysis of the fluoxetine stock preparations. 153
Supplementary Figure 2. Principle component analysis of the differentially expressed genes obtained from each tissue sample in 24 samples 155
Supplementary Figure 3. Whole-body cortisol levels in 7dpf transgenic zebrafish larvae exposed to cortisol before and after handling stress. 156
Supplementary Figure 4. Whole-body eGFP mRNA levels in 7dpf transgenic zebrafish larvae exposed to cortisol before and after the handling stress 157
Supplementary Figure 5. The experimental design to study the life-long effects of developmental exposure to fluoxetine in zebrafish. 158
Supplementary Figure 6. The experimental design to study the life-long effects of developmental exposure to fluoxetine in zebrafish. 159
Supplementary Table 1. Pathways affected life-longly by developmental exposure to fluoxetine in the unstressed condition 161
Supplementary Table 2. Pathways affected life-longly by developmental exposure to fluoxetine in stressed condition 167
Supplementary Table 3. Life-long dysregulation of genes associated with depressive disorders upon developmental exposure to fluoxetine. 169
Supplementary Table 4. Gene list associate to neural plasticity, synaptogenesis, and neurogenesis in Homo sapiens 184
Supplementary Table 5. The primer list for qPCR experiments 187
Supplementary Table 6. Gene list associate to epigenetics in *Homo sapiens* 188

CHAPTER 1: General Introduction

The key components contributing to the rationale and design of this study are reviewed in the current chapter. Some topics briefly described here will be expanded further in the designated introduction to each chapter to reduced redundancy. This chapter emphasises our interest in fluoxetine (FLX) as an emerging stress-disrupting compound. The high level of prescription of FLX during pregnancy increases maternal exposure risks and increases the risks of aberrant environmental contamination. Fluoxetine, and its metabolite norfluoxetine, are excreted via urine and reaches waterbodies and found to bioconcentrate in the brains of fish. Chapter 2 is dedicated to establishing the animal model and the biological endpoints we used throughout the thesis in different experiments. Chapter 3 describes the study of the life-long effects of FLX on the global transcriptomic profile of brain regions in zebrafish. In Chapter 3, we discuss the impacts of life-long effects on health and the environment. Chapter 4 is dedicated to showcasing attempts to establish proof-of-concept of a biomonitoring assay to screen stress-disrupting compounds suggested as a tier-1 assay in environmental risk assessment studies.

1.1. Rationale of the study.

Our lab has been extensively studied FLX as an emerging environmental contaminant in aquatic ecosystems. Recently, Vera-Chang *et al.* (2018 and 2019) uncovered compelling evidence of transgenerational effects of the developmental exposure (0 to 6 days post-fertilization: dpf) to FLX, in both environmentally (0.54 µg/L; the amount reported downstream of the effluent of swage treatment facilities) and clinically (54 µg/L; the amount found in the embryonic cord blood sample of women consuming FLX during pregnancy) relevant doses [1-3]. This mode of exposure to FLX resulted in a decreased exploratory behaviour and hypocortisolism two and three generations withdrawn from FLX exposure in zebrafish, respectively [1-3]. This effect predominantly affected males in each generation. It was determined that the interrenal cells (a combination of steroidogenic cells in the head of the kidney of teleost that produce cortisol in response to stress) were one of the target tissues affected by FLX exposure [2]. The transcriptomic analysis of this tissue with the follow-up analysis showed significant enrichment of the pathways associated with glucocorticoid signalling and circadian rhythm signalling in the

FLX exposed lineage (F0 and F3) [2]. Furthermore, the functional analysis in the FLX-exposed lineage exhibited enriched networks associated with lipid metabolism, transport of molecules, protein synthesis, inflammatory responses, carbohydrate metabolism, cellular function, and cellular maintenance [2]. Overall, Vera-Chang *et al*. thus demonstrated transgenerational alterations of the cholesterol biosynthesis, cholesterol export, and steroidogenesis following developmental exposure to FLX in zebrafish [1-3].

In another related study, Martinez *et al.,* (2019), demonstrated a role for maternal transmission in intergenerational hypocortisolism following developmental exposure to FLX (0-6 dpf daily exposure to 54 µg/L FLX) in zebrafish [4]. Only offspring (12dpf old) from crossbreeding of developmentally exposed females and not exposed males showed decreased basal cortisol [4]. This observation was also time-dependent and only seen in offspring generated from sexually naïve five-month-old individuals, and not at their second breeding at 9 months [4]. Moreover, Martinez *et al.* (2019) showed that female zebrafish developmentally exposed to FLX deposited significantly less glucocorticoid receptor (gr) and *fkpb5* transcripts into their eggs based on the different age/breeding experience [4]. Furthermore, these eggs contained a significantly altered abundance of *dnmt3* paralogues and several micro-RNAs that target stress-related genes [4]. These observations suggested a possible role for epigenetic mechanisms in the inheritance of decreased basal cortisol in descendant offspring in zebrafish [4].

Following the study of transgenerational and intergenerational effects of FLX, I further examined the long-lasting effects of developmental exposure to FLX on the stress-induced transcriptomic profile of the central nervous system in adult male zebrafish. In the current study, the larval head and two brain regions (telencephalon and hypothalamus) in the developmentally-exposed adult male zebrafish were studied under unstressed and stressed conditions. Since it was crucial in my study design to discriminate between the unstressed and stressed states, I used a stress-responsive transgenic zebrafish line (SR4G). This transgenic zebrafish line expresses a short-lived variant of green fluorescent protein under the control of six different glucocorticoid response elements (GRE) [5]. The eGFP mRNA levels in the SR4G line was used as an internal control to confirm the stressed state in my study. Based on the experiments outlined in Chapter 1, I suggested measuring eGFP mRNA as an alternative route to assess the stress response.

Furthermore, given the potential of this transgenic line for the assessmemnt of emerging environmental contaminants, I developed a proof-of-concept study for an *in vivo* biomonitoring assay to screen stress-disruptive compounds.

1.2. The stress response.

Several neuroendocrine pathways participate in the reposne to a stressful event. Depending on the nature of the stimuls, different neural circuits are recruited, and the outcome is the perception of stress [6]. Two major types of stressors have been described in this regard; physical stressors, which are mostly perceived at the level of the brainstem and hypothalamic region [7] [6]; and psychological stressors which primarily engage the limbic circuits such as the pre-frontal cortex (PFC), amygdala, and hippocampus [8, 9]. The stressful stimuli simultaneously activate both the sympathetic adrenomedullary system (SAM) and Hypothalamic-Pituitary-Adrenal axis (HPA), in which the former evokes the short-lasting responses and the latter modulates the long-lasting responses [10, 11].

1.2.1. The physiology and endocrine pathways of the stress axis in mammals.

The hypothalamic paraventricular nucleus (PVN) is the main target for neural circuits relaying stress perception [6, 12]. In mammals, the parvocellular neurons of PVN receive direct innervations from multiple brainstem and forebrain regions, including the nucleus of the solitary tract (NTS), dorsomedial hypothalamus (DMH), locus coeruleus (LC), the rostral ventrolateral medulla (VLM), nucleus ambiguous (NA) [6] [13]. Moreover, PVN indirectly receives signals from PFC and hippocampus primarily via the bed nucleus of the stria terminalis (BST) and amygdala (the central nucleus of the amygdala, CeA; and the medial nucleus, MeA) [12] [14]. It should be mentioned here that not all neural connections with PVN are excitatory; several of these connections also relay inhibitory signals. For example, GABAergic neural connections between prelimbic area (PL) and BST in rodents trigger inhibition of PVN [15, 16].

Stimulation of the PVN activates the HPA axis. Three neuropeptides are synthesized and released from PVN, including oxytocin, vasopressin and corticotropin-releasing hormone (CRH) [17]. In mammals the CRH is delivered to the anterior pituitary via the hypophyseal portal system, where it targets the corticotrophs. Upon stimulation, corticotrophs in the pituitary synthesis and

secrete ACTH (adrenocorticotropin hormone) into the blood stream. The release of glucocorticoids (cortisol in human and corticosterone in rodents) from the adrenal cortex is the primary response to the increased ACTH levels in the systemic circulation.

Adrenocorticotropin hormone binds to its receptor, MC2R, in adrenal cells located at zona fasciculata in the adrenal cortex and results in activation of the steroidogenesis pathway. In the first step, cholesterol is transported to mitochondria's inner membrane by steroidogenic acute regulatory protein (StAR). Afterwards, through the action of the P450scc enzyme (CYP11A1 gene), cholesterol is converted to pregnenolone. This is the first rate-limiting step in the GCs synthesis. In humans, pregnenolone is converted to 17-a hydroxypregnenolone by the action of 17a-hydroxylase (P450C17, CYP17 gene). Three other enzymatic modification through 3B-hydroxysteroid dehydrogenase (3β-HSD, HSD3B1 gene), 21-hydroxylase (P450C21, CYP21 gene) and 11B-hydroxylase (P450C11, CYP11B1 gene) result in the production of cortisol. The synthesis of corticosterone in rodents is very similar, except that rodents do not have the CYP17 gene in their adrenal cortex. In rodents, pregnenolone directly goes through the three stages of enzymatic modification by 3β-HSD, P450C21, and P450C11 to produces corticosterone. The 11B-hydroxylase (P450C11, CYP11B1 gene) is the second rate-limiting enzyme in the biosynthesis of GCs and, like StAR, resides in mitochondria. The rest of the enzymes in the GCs biosynthesis are in the smooth endoplasmic reticulum [17].

Glucocorticoids are secreted in a fluctuating basal level throughout a day, which is both ultradian (multiple cycles with different peaks throughout the day) and circadian (the mean of peaks fluctuate based on the time of the day) [18]. The highest levels of basal GCs are observed before awakening in both diurnal and nocturnal animals. This is considered an adaptive response that prepares animals to cope with environmental stimuli (e.g. predation) during their active period [17].

1.2.2. The central nervous system response to stress.

Glucocorticoids control the activity of the HPA axis through short and long loop negative feedback affecting the anterior pituitary, PVN, and hippocampus [11, 14]). Aside from the negative feedback to control HPA axis activity, GCs in the brain modulate the transcription of

proteins involved in memory, cognitive, metabolic, and immune system processes, leading to altered physiology and behaviour. For example, ex vivo experiments have shown that GC stimulation of dorsal hippocampal CA1 pyramidal neurons results in altered electrical activity with L-type calcium currents were more prominent [19]. It has been shown that chronic corticosterone administration or daily physical restraint in rats results in reduced dendritic arborization and spine density in PFC, which manifests as memory deficit and impaired reversal learning [20]. Remodelling of the synapses connections in the amygdala has also been observed when exposed to high GC levels following both acute and chronic stress. The hippocampus is another region that is readily susceptible to GCs [21]. Hippocampus is one of the scant regions in the adult brain that maintains neural regeneration and plasticity levels, particularly in the dentate gyrus (DG) [21]. Adrenalectomised rats (surgical removal of adrenal glands to decrase endogenous GC production) exhibit extensive neural death in the DG (dentate gyrus)region of the hippocampus [22]. Supplementing water with low levels of corticosterone could reverse the rate of apoptosis in DG neurons. However, administration of dexamethasone, a very potent agonist of GR, accelerated neural death in DG in rats post adrenalectomy [22]. Similarly, high rates of apoptosis in the DG was observed in intact animals after chronic stress [23, 24].

Glucocorticoids may diffuse across the membranes of neurons or other cells in the brain [25]. However, GCs only exert effects in cells that express glucocorticoid receptors (GRs) and mineralocorticoid receptors (MRs) [25]. The MRs in neurons have 10-times more affinity to GCs compared to GRs. However, in contrast to GRs widely expressed throughout the brain, MRs have a stricter expression pattern and primarily found in the hippocampus, lateral septum, and CeA. There are also regions that GRs and MRs are co-expressed, such as PVN, NTS, LC, hippocampus, and amygdala [17]. Due to their high affinity for GCs, it is suggested that MRs regulate the physiological responses to basal endogenous GCs levels [26], and GRs are exerting responses to the higher levels of GCs, which are produced following a stressful event. Owing to this different affinity and regional expression of receptors, the response to GCs is both region dependant and dose dependant in the brain [18].

1.2.3. The mammalian models to study the stress axis.

Rodents have been the main mammalian models in the study of the stress response. The main paradigms are classified into two major stressors: physical and psychological [27]. Each paradigm aims to evoke a measurable biological endpoint such as behavioural, endocrine, metabolic, and neurochemical [27]. Physical stressors are mainly used to study short term aspects of the stress response. The first category in the physical stressor paradigm is deprivation (e.g., food deprivation, water deprivation, sleep deprivation, and mobility restriction). Mobility restriction, better known as restraint, is one of the most extensively studied stress paradigms and is considered a severe form of stress. Extreme environment exposure is another stress paradigm. A few examples are cold, heat, and danger (e.g., predator sound, sight, or olfactory cues). Pain (e.g., electric foot shock, tail pinch, or formalin injection) is another paradigm that can elicit severe stress in rodent models. However, due to concerns about animal welfare, it is less employed in recent years. Psychological stressors, although they could elicit acute effects like physical stressors, are mainly used to ascertain the long-lasting effects of stress. Some examples are social conflict (e.g., territory invasion, colony overcrowding, offspring protection) in population that have hierarchical relationships. Social deprivation (social isolation and maternal separation) is another commonly used paradigm, specifically of interest in the long-term generational study of stress impacts [27].

Modification of the stress response is another tool that has contributed to our understanding of physio-genomics of the stress axis. Adrenalectomy, or surgical removal of adrenal glands, was amongst the first attempts to physiologically modify stress response [25]. Brian injury-based models have extensively used to study the psychological aspect of the stress response [25]. More recently, pharmaceutical manipulation using agonists and antagonists of primary receptors in the stress axis, like GRs and MRs, has changed our understanding of the molecular pathways mediating a stress reponse. Natural agonists (cortisol and corticosterone for both GRs and MRs) and synthetic agonists such as dexamethasone (for GRs) have extensively studied. Development of specific antagonists that target GRs (RU486) or MRs (RU28318) revolutionized our understand of the extent of involvement of each receptor in aftermath of a stressful event in mammals [23-25].

Several genetically modified rodent lines have been created specifically for stress response studies. Due to the critical role of GRs in development, the double knockouts for NR3C1 (GR gene) snot survive [25]. However, a mouse line that expresses only one functional GR allele exists ($GR^{\pm}$) [28]. The $GR^{\pm}$ mice show a normal level of corticosterone; however, they have reduced GR expression in the hippocampus compared to the wildtypes. These $GR^{\pm}$ mice also have impaired HPA axis negative feedback and show significant impairment in coping with stress in helplessness challenges [28]. Tronche *et al*. (1999) developed a transgenic mouse that lack GR throughout the nervous system [29]. Their $Grl1^{LoxP}$ mice have significantly higher corticosterone levels in both basal conditions and 40 minutes after the restraint stressor compared to the wildtypes [29]. Moreover, the $Grl1^{LoxP}$ mice show anxiety-like behaviours and impaired cognition in forced swimming tests [29]. Another transgenic mouse line, FBGRKO, lack GR expression in the hippocampus, basolateral amygdala and most of the cortex when reaching 4-6 month of age [30]. The FBGRKO mice have higher corticosterone levels in different time points of circadian rhythm than the wildtypes [30]. This line provided extensive evidence for the negative feedback imposed on the HPA axis by the affected forebrain-specific regions. The $GR^{POMCCre}$ line lacks GR in POMC (precursor of corticotropin, melanotropin, endorphins, and many other neuroactive peptides) expressing cells in the pituitary [31]. The $GR^{POMCCre}$ interestingly show resilience when exposed to chronic social defeat stressor [32]. Also, there is a mouse strain, GRov, which demonstrates overexpression of GR in forebrain regions, including PFC, BTS, CeA, PVN and hippocampus [33]. Despite this overexpression of GR, GRov mice show regular HPA axis activity [33]. However, they show enhanced anxiety-like behaviour. Moreover, other transgenic lines have been created specifically to target MRs; like MRCaMKCre which lacks MR expression in forebrain [34], and MRov, which has a higher level of MR expression forebrain compared to the wildtypes [34].

1.2.4. The teleost models to study the stress axis.

Teleost fish share a similar physiological stress response with other vertebrates. Cortisol is the primary stress hormone in teleost [35]. There are some anatomical and genetic variations with regards to the stress axis. Teleost fish lack the adrenal glands typical of mammals, and instead, the steroidogenic interrenal cells are dispersed in the head of the kidney near the posterior cardinal veins [36]. The stress axis in fish is named the hypothalamo-pituitary-interrenal

()HPI) axis to emphasise this anatomical variation. The other main anatomical variation is that teleosts lacks the hypothalamic-hypophyseal portal system, and the anterior pituitary is directly innervated by axons and terminals originating from the pre-optic area that harbours the cell bodies of CRH-producing neurons [37]. The other main difference between HPI and HPA axis. function is the existence of duplicated genes in teleosts. Teleost fishes underwent a whole-genome duplication event about 320-350 million years ago and still harbour many duplicated genes [37]. In the HPI axis of teleost fish, several genes that express essential proteins are duplicated, including CRH, POMC (precursor of ACTH), GR, MR. Not all teleost fish retained the duplicated genes in the HPI axis [37]. For example, salmoniformes and cypriniformes retained two copies of the CRH gene; however, zebrafish and Acanthopterygii only harbour a single copy for CRH. Another example is tilapia (*O. mossambicus*) and sea bass (*Dicentrarchus labrax*), which only have one copy of the POMC gene while the rest of the teleost fish retained the two copies. Moreover, all teleosts except zebrafish have two copies of the GR gene [37]. Aside from these differences, the stress response is highly conserved amongst teleosts and mammals [36]. Many teleosts show the ultradian and circadian rhythm in circulatory cortisol levels as in mammals [36].

A similar classification of stress paradigms in mammalian models exists for fish. Examples of physical and environmental stressors include 1) fluctuation in the aquatic environment (e.g., temperature, oxygen, osmolarity, pH); 2) locomotory stressors (e.g., netting, chasing, artificial water turbulence), 3) deprivation of essentials (e.g., food, fresh water, normal light-dark cycle) [38, 39]. Psychological stressors in fish differ based on the species and social hierarchy; some examples are overcrowding, forced social dominance, and predation simulation [39, 40]. One of the main differences in some fish models compared to mammalian models is the lack of maternal care behaviour; therefore, the maternal separation paradigm used extensively in rodent studies is not applicable in the fish model [38]. However, this could be interpreted as advantageous for fish models such as the zebnrafish since the confounding factor of maternal behaviour is eliminated.

1.2.5. The long-lasting adverse effects of early-life exposure to stress

The transgenerational effects of a chemical compound or a social factor manifest adverse symptoms in the descendant generations that were not directly exposed to a specific substance or experience [41]. The life-long effects manifest adverse symptoms in individuals long after the withdrawal of compound exposure or the social factor [41]. Although stable chromosomal alterations have been associated with some transgenerational manifestations of adverse traits, recently, the sequence-independent phenomenon, the epigenetic alterations, has increasingly attracted the scientific community [42-48]. Epigenetics is the study of how the environment affects phenotype(s) of species. The prefix "*epi*" means "above" or "on top of" and implies to the inheritance of traits that may not be described solely based on the sequence of the genes [49]. There are different pathways associated with epigenetic alteration of genes, for which DNA methylation, histone modification, and micro-RNA dependent processes have been intensely studied [49]. Methylation of cytosine at carbon 5 of the pyrimidine ring through DNA methyltransferase enzymes is widely reported in genes with repressed expression [50]. There are two modes of epigenetic inheritance; the life-long inheritance is defined when the induced epigenetic marking only persists on somatic cells [51]. Intergenerational and transgenerational inheritance is defined when the induced epigenetic marking involves germ-line cells and could be passed down to the following generations [51].

One of the conditions that could result in both life-long and transgenerational inheritance of adverse effects is environmental stress [52]. Exposure to stressful conditions during early phases of development like parental stress and early-childhood stress is linked to the development of depression- or anxiety-like behaviours later in life and the descendant generations [53-58]. Early-life stress by maternal separation in rodent models showed broad changes in the histone modifications patterns and dysregulation of histone-modifying enzymes in the prefrontal cortex and DNA methylation changes in the hypothalamus [59-62]. It has been shown that environmental stress could induce epigenetic changes in many genes, including NR3C1, BDNF, FKBP5, SKA2, OXTR, LINGO3, POU3F1 and ITGB1 in rodent models [59, 63-68].

Most of our understanding of the impact of early-life exposure to stress originates from experimentally controlled animal studies. Although several studies conducted during pregnancy have shown an association between prenatal stress exposure and adverse outcome in children,

no casual relationship has been found due to inherent restriction to observational studies in human [69]. Furthermore, the measurable outcomes in human studies are restricted to behavioural, macroscopic neuroanatomy assessments (e.g. MRI), and genetic/epigenetic alterations in peripheral tissues [69].

1.2.6. The long-lasting adverse effects of disruption of the stress response.

The findings in our lab and others show that FLX at environmentally relevant doses disrupts the stress response. Other environmental contaminants reported having the potential to disrupt the stress response; these chemicals are grouped as endocrine-disrupting compounds (EDCs). The EDCs are chemicals that stimulate or inhibit hormone production by mimicking or blocking the effect of hormones (https://www.epa.gov/endocrine-disruption/what-endocrine-disruption). For instance, bisphenol A best known as a xeno-estrogen also competitively binds to the GRs in the HPA axis in rodents, an action that leads to neurobehavioral disorders like anxiety and depressive disorders. An *in silico* study showed BPA binds to the GR and could displace cortisol and dexamethasone and potentially elicit an agonistic biological function [70]. In rats, perinatal exposure to BPA (2 µg/kg/day was injected into the dam during gestation and lactation) resulted in a significant increase in corticosterone, ACTH, and GR mRNA in both unstressed and stressed conditions [71]. The molecular evidence of the effect of BPA on the HPA axis in humans during gestation has been recently published [72, 73]. Disruption of the HPA axis upon exposure to BPA has been extensively linked to anxiety-like behaviour and depressive disorders in rodent models**.** It should be emphasized that not all chemicals and pharmaceuticals (PCs) that reach the environment are considered EDCs.

1.3. Depression and anti-depressants.

Antidepressants are the second largest group of prescribed medications [74]. More than 264 million people worldwide are suffering from major depressive disorder (MDD) [75]. Depressive disorders have become one of the leading factors of disability in developed countries [76], and the risk of development of MDD peaks during pregnancy in women [77].

Several molecular pathways are hypothesized to be involved in the development of depression, including neurotransmitter (monoamines) depletion, disruption of neuroendocrine

systems such as stress (HPA) axis, increased inflammatory cytokines and decreased neurogenesis/neural plasticity [52, 78-82]. The monoaminergic theory is the dominant theory that explains the development of depressive disorder [81]. This theory states that the decreased amount of one or more of the monoamines (serotonin, dopamine, and norepinephrine) in the brain is the underlying cause for the development of depression [81]. All currently used antidepressants are designed based on this theory.

1.3.1. The different classes of anti-depressants.

The pharmacokinetic concept of all currently used antidepressants is to increase the concentration of one or more monoamines: serotonin, dopamine, and norepinephrine (nor-adrenaline) [52]. One way to classify antidepressants is by grouping them based on their primary function. For example, a few classes of antidepressants elicit their effects by inhibiting the reuptake transporters at the synaptic junctions. Examples of antidepressant classes in this major group are selective serotonin reuptake inhibitors (SSRIs; e.g. fluoxetine and sertraline), serotonin and norepinephrine reuptake inhibitors (SNRIs; venlafaxine and levomilnacipran), selective norepinephrine reuptake inhibitors (NRIs; Atomoxetine and Reboxetine), norepinephrine and dopamine reuptake inhibitors (NDRIs; Bupropion and Ritalin) and tricyclic antidepressants (TACs; e.g. amitriptyline and nortriptyline). The second major group of antidepressants is monoamine oxidase inhibitors (MAOIs), which inhibit one or both MAO-A and MAO-B isoenzymes. MAO-A inhibition prevents serotonin and norepinephrine breakdown, while dopamine is the substrate for both MAO-A and MAO-B. Selegiline, safinamide and rasagiline are examples of MAOIs antidepressants. The last major group is the atypical antidepressants which not fit the categories mentioned above, and each has a unique mechanism of action; for example, mirtazapine (an alpha$_2$-adrenoreceptor antagonist), agomelatine (a melatonin receptors agonist), Vortioxetine (an antagonist of serotonin reuptake transporter and a modulator of serotonin receptor).

The response to therapy is usually assessed four weeks after commencing the prescription of antidepressants [83]. Although there is no clear dose-related response for most antidepressants (except escitalopram, venlafaxine and TCAs), the usual strategy for unresponsive patients is to increase the doses gradually [84]. If the monotherapy strategy fails, switching to a

different class of antidepressant or multi-modal therapy would be the alternatives; however, the risk of adverse effects is much higher [83]. Combining mirtazapine with SSRIs or venlafaxine is recommended by the National Institute of Health and Care Excellence (NICE) [84].

The main side effects reported for antidepressants are related to serotonin's function, given its high distribution throughout the bodily systems. Increased risk of gastrointestinal bleeding, serotonin syndrome (diarrhoea, tremor, ataxia and seizure), and discontinuation syndrome are the main reported adverse effects [83]. Since no drug-seeking behaviour and craving symptoms are observed following the discontinuation, antidepressants are not considered addictive [83].

1.3.2. The selective-serotonin-reuptake inhibitors (SSRIs).

Selective serotonin reuptake inhibitors (SSRIs) target the serotonin transporter (SERT; SLC6A4) in the synaptic end of serotonergic neurons [85]. The inhibition of SERT results in elevation of serotonin (5-HT) concentration in synaptic junction, hypothesised to alleviate the depressive disorders' symptoms [86]. The SSRI group includes Prozac (fluoxetine), Zoloft (sertraline), Paxil (paroxetine), Celexa (citalopram), Lexapro (escitalopram) and Luvox (fluvoxamine). The SSRIs are the first line of medications in recently diagnosed patients and pregnant women due to their high tolerability and relative safety compared to the other antidepressants [87, 88]. However, given some reports on increased risk of pulmonary hypertension and heart defects, SSRIs are classified as group C when safety of prescription during pregnancy s considered [77]. Among SSRIs, fluoxetine (FLX) has the longest half-life and in human studies have shown the highest symptoms discontinuation rate [83].

1.3.3. The long-lasting adverse effects of early-life exposure to SSRIs.

Serotonin is synthesized from tryptophan by consecutive action of tryptophan hydroxylase 2 (TPH2) and L-amino acid decarboxylase (AADC). During the prenatal development period, serotonin, its receptors (5-HT receptors) and transporter (SERT) are highly expressed and involved in the modulation of neural development [89]. Evidence of transient expression of SERT in early brain development in different forebrain regions, including hippocampus, cortex, thalamus, and striatum, has been shown in rodents [90, 91]. This suggests a role for serotonin in

neurogenesis, neural differentiation, and synaptogenesis during early phases of development (embryonic days 10-17 in rodents) [92]. Tight regulation of serotonin levels in the pre-natal brain is crucial. It has been shown that the depletion of serotonin in developing brain via introducing insert mutation in Tph-2 gene, treatment with Tph-2 antagonist like p-chlorophenylalanine (PCPA), or treatment with 5,7-DHT, a neurotoxin with high affinity for serotonergic neurons, resulted in delayed neurogenesis, reduced forebrain growth, decreases hippocampal neurons, decreased cortical neurons, and dendritic maturation deficiencies in adult rodents [85]. Moreover, decreased cortical interneuron and pyramidal neuron migration have been shown in SERT deficient mutant mice with higher serotonin levels in their brains [93, 94]. Furthermore, elevated serotonin levels in mice with monoamine oxidase A (MAO-A) knock out have been linked to impaired cortical barrel formation, suppressing sensory perception in offspring [95]. Similar impaired cortical barrel formation has been observed following prenatal exposure to SSRIs [96, 97].

It has been shown that SSRIs pass the blood-placenta-barrier and potentially expose the developing fetus prenatally [98, 99]. It has also been demonstrated that placental transport of increased maternal serotonin levels could result in increased serotonin levels in the embryo, hence could disrupt serotonin-axonal growth in the forebrain of the fetus [100]. Several adverse effects have been reported following *in utero* exposure to SSRIs in humans, including disrupting normal social behaviour, altered neurodevelopment, irregular physiological hemostasis, and increased vulnerability to stressful situations. [101, 102]. Rodent studies have shown life-long effects of prenatal exposure to SSRIs, including anhedonia, troubled sleep, diminished sexual performance, and increased anxiety-like behaviours [85].

Neonatal abstinence syndrome (NAS) is the most commonly transient adverse effect reported in neonates with potential *in utero* exposure to SSRIs. The reported symptoms include one or a combination of the followings, which last for a few weeks after birth: vomiting, uncoordinated sucking, poor feeding, hyperhidrosis fever, tachypnea, restlessness, tremors, sleep irregularities, and hyper- or hypotonicity [103]. The long-lasting behavioural disorders are linked to post-natal NAS [104]. Blunted diurnal cortisol levels have been reported in three-month-

old infants who were prenatally exposed to SSRIs [105, 106]. Prenatally exposed infants showed blunted pain response at two months of age [107, 108].

Behavioural studies have shown *in utero* exposed children have lower social-emotional and adaptive behaviour test scores and increased internalizing behaviours like anxiety [85]. Population-based cohort studies have shown an increased risk of developing autism spectrum disorder (ASD) upon exposure to SSRIs during pregnancy, particularly in the first trimester [85]. There is a lack of evidence for long-lasting effects of prenatal exposure to SSRIs on adult individuals; however, several studies have recently shown the impacts of *in utero* exposure to SSRIs on adolescent-commenced depression [109].

1.3.4. The SSRIs as emerging environmental contaminants.

High levels of different SSRIs have been recorded in streams receiving wastewater effluent [110-113]. The concentrations of total SSRIs have been measured at approximately 3 µg/L downstream of wastewater effluents, which is above the threshold suggested by some regulatory organisations (e.g. EMEA) [114]. It is suggested that to the high level of prescription and inadequate removal during wastewater treatment results in such high amounts of SSRIs in aquatic environments [115]. The SSRIs are considered to be emerging environmental contaminants for aquatic environments [114]. The read-across hypothesis stipulates that the conservative nature of drug targets, which is exploited during drug development using animal models, could potentially result in a pharmacological effect in non-target organisms [116]. This has already been shown for SSRIs in fish. Fathead minnows (*Pimephales promelas*) exposed to 2.8, 9.4, and 28.1 µg/L of sertraline for 28 days showed plasma concentrations relevant to human therapeutic dose (305–1927 ng/ml), and this resulted in decreased anxiety evident by decreased shelter-seeking behaviour [117]. Similar anxiolytics effects observed when fathead minnows were exposed to 20, 38 and 72 µg/L of FLX for 28 days (equivalent to the human therapeutic dose of 91-302 ng/L) [118].

It is shown that the affinity of FLX and sertraline to SERT in zebrafish is lower than the human therapeutic dose for these medications. This further explains why low environmental SSRI concentrations are causing undesirable effects in fish [116]. Although several studies have

shown that the realistic environmental concentration of individual SSRIs might not reach the levels consistent with the read-across hypothesis; several fish pharmacokinetic factors should be considered; including the metabolism rate, the differences in cytochrome isoenzymes inventory in fish, the multimodal exposure to several SSRIs, and prolonged exposure time [116].

Except for serotonin receptor 5-HTR_{5B}, all other serotonin receptor subtypes are expressed in fish, with at least 11 being functionally annotated [116]. Fish SERT (*slc6a4*) shares an average of 68% sequence identity with human orthologue; however, the SSRIs binding site shows 93% sequence conservation between human and different fish species, including zebrafish, Japanese rice fish, Japanese puffer, mummichog, Australian ghost shark, and large yellow croaker [119]. Exposure to SSRIs affects several physiological responses in fish, including stress, reproduction, locomotion, and feeding behaviour, gastrointestinal, cardiovascular, and respiratory system have also been reported for fish exposed to SSRIs [116] This whole-body effect is partially stemmed from the involvement of serotonergic systems in different body systems. It is shown in adult zebrafish that SERT is highly expressed in the central nervous system, intestine, testis, liver, gill, and heart [120, 121].

Serotonin acts on the stress axis in both mammals and teleost fish. The mRNA for 5-HT_{1A} receptor is expressed in POA, pituitary, and interrenal cells of some fish [122]. It has been shown that elevated cortisol results in the downregulation of 5-HT_{1A} receptors in the Gulf toadfish brain [122]. Moreover, the injection of 8-OH-DPA, an agonist for 5-HT_{1A} receptor increased mRNA levels of CRH and significant elevation in ACTH and cortisol in the Gulf toadfish and rainbow trout *(Oncorhynchus mykiss)* [123]. In the context of social stressors, it has been shown that subordinate fish have a higher level of serotonergic neurons activity, measurable by an increase in 5-HIAA, the primary serotonin metabolite [116, 122]. These subordinate fish also have chronically high cortisol levels compared to the dominant dish in the same population.

Given the involvement of serotonergic systems in regulating the stress axis and the highly conserved stress and serotonin systems in teleost and mammals, SSRIs exposure could potentially alter stress responses in teleost [116]. Extensive evidence for such disruption has already been shown. Short-term exposure to FLX might not result in a significant alteration in the

stress response of different species of fish [124, 125]. However, with more prolonged exposure, between 7-21 days, pronounced effects of the HPI axis and stress-related behaviours have been reported. For example, Sebire *et al.,* (2015) showed that waterborne exposure to 32 µg/L of FLX for 21 days resulted in a significant increase in circulating cortisol in Chinook salmon, *Oncorhynchus tshawytscha* [126]. There is extensive evidence of altered anxiety-like behaviours in teleosts upon exposure to SSRIs [40, 127, 128]. Several behavioural endpoints are interpreted as anxiety-like behaviours in the teleost, including dark preference, reduced exploration, increased bottom-dwelling, increased shoal cohesion, increased erratic swimming, increased shelter seeking, and increased freezing [116]. Anxiety is a maladaptive response to chronic exposure to stress. Several serotonin receptors have been implicated in mediating the anxiety-like behaviour in fish, including 5-HT_{1A}, 5-HT_{1B}, 5-HT_{1D},5-HT_{2A}, 5-HT_{3},5-HT_{T5}, and 5-HT_{T6} receptors [129-132]. To date, a high level of inconsistency in the literature regarding the altered anxiety-like behaviour in fish. While there is evidence of anxiolytic effects of SSRIs (particularly FLX, citalopram, and sertraline), several studies show increased anxiety-like behaviours or even no response [116]. The differences in species, exposure dose, exposure time, and the behavioural endpoint (one or multiple) could partially explain the observed inconsistencies [133].

Besides stress, exposure to SSRIs has affected other physiological responses, for example, feeding and reproduction. It has been shown that exposure to FLX, citalopram, and sertraline decrease the feeding behaviour in different species of fish [121, 134, 135]. It is known that the activation of several serotonin receptors in the brain, including 5-HT_{1A}, 5-HT_{2C}, 5-HT_{1B}, 5-HT_{2B} receptors, results in suppressed appetite and feeding in goldfish, rainbow trout, and European sea bass [136-138]. The decrease in feeding upon exposure to SSRIs has been attributed to elevated serotonin's suppressive effect on appetite and decreased locomotion and food seeking observed in some fish species [116]. Serotonin is also involved in the regulation of the hypothalamic-pituitary-gonadal (HPG) axis in fish. The HPG axis regulates reproduction in vertebrates. Several receptors for serotonin have been found in the hypothalamus (5-HTR_{2C} and 5-HTR_{4}) and pituitary (5-HTR_{1} and 5-HTR_{2}, which their activation results in secretion of gonadotropin-releasing hormone (GnRH) and gonadotropins (follicle-stimulating hormone, FSH, and luteinizing hormone, LH) from the hypothalamus and pituitary; respectively [116].

The expression of serotonin receptors (5-HT_{1A} and 5-HT_{2A}) in gonads has been shown [139]. It is shown that chronic exposure to SSRIs decreased GnRH synthesis in the POA of zebrafish [140]. Decreased FSH expression in goldfish pituitary has been reported upon exposure to FLX [141, 142]. Decreased estradiol levels upon exposure to FLX is reported in both zebrafish and goldfish [141, 143].In male zebrafish, reduced synthesis of testosterone and milt production upon 14 days exposure to FLX (54 µg/L) was observed [121]. The alteration of the HPI axis upon exposure to SSRIs could impose adverse effects on the HPG axis and explain the observed reduced reproductive performance in exposed fish [144]. Several studies have shown that subordinate fish have a less active HPG axis supporting the role of anxiety and chronic elevation of stress in decreased reproductive performance [116].

1.4. The zebrafish model.

The zebrafish (*Danio rerio*) is a member of the cyprinid family (carps and minnows) of teleost fish. Zebrafish are increasingly being used in all aspects of life science research, particularly in developmental disease, behaviour, drug discovery, stress physiology and toxicology [145-148]. It is shown that more than 80% of human drug targets are conserved in zebrafish, making them a suitable model in pharmaceutical and environmental risk assessment studies [149]. Overall, the genetic diversity, large sample size, short generation time, transparent embryo, oviparous development, the documented stress response in larval and adults, and relatively low-cost maintenance compared to other mammalian models are some of the criteria that have made zebrafish an excellent model organism [148, 150-153].

Zebrafish have also been extensively used as a model organism to study stress response. The whole genome of zebrafish is sequenced, and more than 70% of genes have orthologues to *Homo sapiens* genes [154, 155]. A high percentage of conservation has been reported regarding the core genes involved in the stress response, like *crhb, pomc,* and *gr,* between zebrafish and other mammalians, including humans [148]. In general, zebrafish is the only teleost member with a singular gene system for the stress-axis, making the zebrafish HPI-axis relatively similar to the mammalian HPA axis [37]. Although zebrafish have two copies of the POMC gene, the cleavage site for ACTH at one copy is mutated and rendered non-functional [156]. Two splice variants have

been discovered for GR in zebrafish, GRα and GRβ [157]. It is shown that GRβ does not have transactivational properties [157]. Also, behavioural studies in zebrafish have demonstrated an extensive array of responses related to stress. For example, dominant/submissive behaviour, aggression, anxiety-like behaviour and coping strategy in stressful situations are well documented in zebrafish [152, 153]. The measurement of whole-body cortisol following exposure to different types of stressors alongside behaviour monitoring, during, and post-exposure has provided us with a better understanding of the stress axis in zebrafish [158]. Cumulatively, the unique molecular structure in zebrafish stress-axis compared to other teleost fish has made zebrafish an excellent model to study stress response, with results applicable to human health and development.

Zebrafish are increasingly used as a model organism in environmental risk assessment studies. According to the Organisation for Economic Co-operation and Development (OECD) guidelines, zebrafish may be used in the "Acute Fish Toxicity test" in risk assessment studies [159]. Given *ex vivo* development of zebrafish embryos, they could readily be used in high-throughput *in vitro* toxicity testing [150]. Moreover, rapid development to a multi-organism larva allows in vivo study of various compounds' toxicokinetics and toxicodynamics [150]. Since zebrafish share a high level of conservation regarding metabolic and genetic systems, they are considered to bridging *in vitro* and *in vivo* studies [160]. Zebrafish have been extensively used to study environmental contaminants like heavy metals, endocrine disruptors, and organic pollutants [161]. Besides the classic toxicity testing such as mortality and morphological abnormality assessments, several new approaches have been introduced in recent years using zebrafish, such as fluorescence and luciferase reporter transgenes that are responsive to certain compounds [162]. Zebrafish have also been used in ttoxicogenomic studies [163, 164]. Several of these applications will be reviewed further in the coming chapters.

1.4.1. The stress-inducible transgenic zebrafish (SR4G) line.

Recently, Krug *et al.,* (2014) has created a stress-responsive transgenic zebrafish line (SR4G) [5]. The SR4G transgenic line has been considered a model for studying neuropsychiatric diseases, including major depressive disorder, generalized anxiety disorder, and substance use

disorder [5, 165-167]. This line expresses an enhanced version of green fluorescent protein (eGFP) under control of the mouse cFos minimal promoter and six consecutive glucocorticoid response elements (GREs). The short 4 hours half-life of expressed eGFP allows one to capture stress response dynamics under different exposure modes [5]. The whole-body ubiquitous expression of eGFP provides high fluorescence intensity levels, which is detectable by standard laboratory imaging equipment [5].

1.5. The hypotheses aims, and objectives of the study

Three main null hypotheses were tested in this thesis:

- Developmental FLX exposure in zebrafish will not cause life-long changes pathways known to be involved in the development of depression, neurogenesis, and epigenetics in humans.
- Fluorescence and eGFP mRNA levels in the SR4G transgenic zebrafish line will not be predictive of stress-disrupting potential of environmental contaminants.
- The predictive models based on transcription of 11 genes associated with stress and neurogenesiss will not be predictive of stress-disrupting potential of environmental contaminants.

The current studies were designed to achieve three aims, 1) to determine the appropriate sampling time following a handling stressor routine to capture significant elevation of whole-body cortisol, whole-body eGFP mRNA, and whole-body eGFP fluorescence intensity, 2) to determine the life-long effects of developmental exposure to fluoxetine (FLX) on stress-induced transcriptomics of brain in zebrafish, and 3) to evaluate the potentials of SR4G transgenic line to track and/or predict altered stress response.

To achieve the first aim, transgenic SR4G zebrafish larvae were used, and serial sample collection was conducted at different time-points for the endpoints mentioned above. Several experiments using ELISA, qPCR, and fluorescence microscopy were conducted to measure the endpoints. To achieve the study's second aim, transcriptomic analysis of brain tissue in two stages of life (larvae and adult) was performed using high-throughput RNA sequencing. Moreover, to study the long-lasting effects of FLX on the stress response, associated treatment

and controls were generated in both larvae and adults. To achieve the third aim of the current study, SR4G larvae were exposed to different chemicals with known effect on stress disruption (BPA, VIN, FLX, DEX, and CORT) and different endpoints such as whole-body cortisol, whole-body eGFP mRNA, the whole-body fluorescence signal of a homogenized sample, and whole-body transcription profile of 11 target genes associated with stress and neurogenesis were studied. Several experiments using ELISA, qPCR, and fluorescence microscopy were conducted to measure the endpoints. Two predictive models using random forest regression and logistic regression were trained to evaluate each endpoint's predictive value in detecting blunted stress response in 7-dpf SR4G zebrafish larvae.

1.6. Thesis outline

The results of the experiments performed throughout this doctoral research are described in the following chapters:

Chapter 2: Application of SR4G transgenic zebrafish line in the study of the stress response.

Chapter 3: Life-long effects of developmental exposure to fluoxetine on global transcription profiles in the zebrafish brain.

Chapter 4: Application of SR4G transgenic zebrafish line as a biomonitoring assay to detect altered stress response.

The chapters are organized in a way to form the basis for future distinct publications. Given the closely related concepts, some level of redundancy in the introduction and methods was not avoidable. In sections 3.1 and 4.1, I present an introduction and overview of topics related to my thesis research.

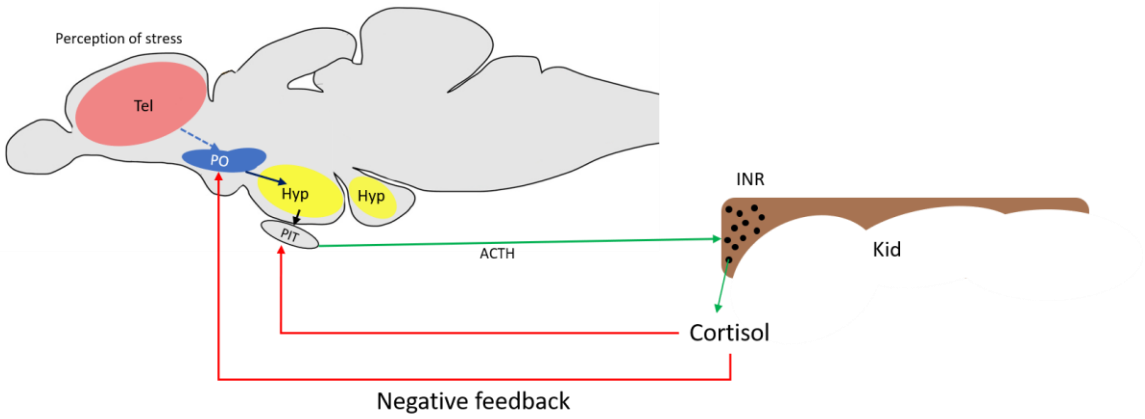

Figure 1.1. An illustration of the stress axis in zebrafish. The perception of a stressful condition (in the telencephalon, TEL) leads to the secretion of corticotropin-releasing hormone (CRH) from the preoptic area (PO) and hypothalamus (Hyp). The CRH, in turn, induces the synthesis and release of ACTH (adrenocorticotropic hormone) from the pituitary (PIT). Synthesis and release of cortisol from the interrenal cells (INR) in the head kidney (Kid) are the primary response to the increased ACTH levels in the systemic circulation. The negative feedback at the level of the PO and PIT are also illustrated. The solid line shows that the direct link has been discovered. The dashed line represents the suspected TEL-PO connection. For the control of CRH neurons, but this remains to be firmly established.

CHAPTER 2: Application of SR4G transgenic zebrafish line in the study of the stress response.

2.1. Introduction

In the 1960s, George Streisinger introduced *Danio rerio* as a vertebrate model to study genetics and development [168]. Since then, zebrafish has increasingly been used in all aspects of life science research, particularly in the fields of developmental diseases, behaviour, drug discovery, and toxicology [145-147]. The zebrafish genome is sequenced and shares more than 70% orthology to *Homo sapiens* genes, which shows this model's potentials in human health science as an alternative for mammalian models [154, 155]. The small size, high fecundity, short generation time, oviparity, transparent embryos and larvae, and relatively low-cost of maintenance compared to mammalian models have made zebrafish an amenable model for large scale studies [150, 151].

Moreover, based on the guidelines of the Organisation for Economic Co-operation and Development (OECD), several members of the teleost family, including zebrafish, fathead minnow, Japanese medaka, bluegill, and rainbow trout, are used in the "Acute Fish Toxicity test" as a part of "hazard and environmental risk assessment" [159]. Recently, a modified version of this test using zebrafish embryos (zebrafish embryo acute toxicity test, ZFET) has validated to be considered by regulatory bodies given its high predictive capacity [159, 162]. Zebrafish is considered a valuable animal model in toxicological assessments; particularly, for its potential to bridge *in vitro* and *in vivo* studies [146, 150, 160, 169]. Traditional assessment of morphological changes upon exposure to different arrays of potential toxicants is well documented for zebrafish embryos, and even automation protocols are described.

Recently, using a fluorescence signal of a transgene as a biomonitoring endpoint is introduced using zebrafish models. Several fluorescent transgenic zebrafish lines have already been created to detect environmental pollutants, including bisphenol A, xenoestrogens, pesticides, heavy metals, and aromatic hydrocarbons [151]. For example, two transgenic zebrafish lines, Tg(5xERE:GFP) and Tg(cyp19a1b:GFP) have been widely used to detect xenoestrogens in water samples [170, 171]. Recently, a stress-responsive transgenic zebrafish

line, SR4G, has been created that responds to both physical and chemical stressors by ubiquitous whole-body expression of a short-lived eGFP [5].

In the current study, we used the SR4G transgenic line to study the effects of developmental exposure to FLX in zebrafish larvae and adults' central nervous system. Due to the high variability of basal cortisol levels in zebrafish (both larvae and adults) [172], our study was imperative to elicit a consistent and reproducible stress response. This chapter studied several time points to determine the appropriate time to collect samples for cortisol and eGFP mRNA measurements. The goal was to capture the peak of elevation in the whole-body cortisol and the whole-body eGFP mRNA following handling stress. The appropriate time for eGFP mRNA was considered an arbitrary time that reflected the time needed to reach a significant alteration in the genes' transcription levels following handling stress. We also studied the fluorescence intensity in a time-lapse manner in SR4G transgenic larvae. The fluorescence measurement helped determine when the eGFP expression reaches its peak following handling stress. In this chapter of the study, we established the SR4G transgenic line in our laboratory setting and assessed its potential to track the HPI axis's activation in three levels: cortisol, eGFP mRNA, and eGFP protein.

2.2. Materials and Methods

2.2.1. Animals and Husbandry

The SR4G transgenic zebrafish line was kindly provided by Dr. Karl Clark (Mayo Clinic, Rochester, Minnesota, USA) and Dr. Xiao-Yan Wen (University of Toronto, Ontario, Canada). The one-day post-fertilization embryos were transferred from Toronto and placed in the quarantine room of the University of Ottawa's aquatic facility following the guidelines of the Animal Care and Veterinary Services (ACVS). The embryos were allowed to hatch and raised in the quarantine facility until they reached six months. These zebrafish were used to establish our founder generation. The post-fertilization embryos were raised in this facility equipped with controlled temperature (28 ^{o}C), 14 hours light and 10 hours dark daily and fed 2-3 times daily. The founder generation was raised to sexual maturity and used for breeding when it reached six months. The F_0 generation was bred from this founder line.

2.2.2. The design of the study and the statistical analysis

2.2.3. Chemicals and exposure conditions

All chemicals used in this study were purchased from commercial sources (Millipore-Sigma, Burlington, Massachusetts, USA). For the whole-body cortisol measurement and whole-body eGFP experiments, 7 days post-fertilization (7 dpf) larvae were used, which were not exposed to any exogenous compounds. For the fluorescence imaging experiments, two treatment groups were used. The 4 days post-fertilization (4dpf) larvae were exposed to cortisol (10 µM) for 4 hours (CORT-short) and 18 hours overnight (CORT-O/N), then imaged. The control fish were exposed to DMSO (0.02% final concentration). The unstressed groups and stress groups were randomly designated on the day of embryo collection and kept on separate shelves in the incubator (Percision^{TM} Plant growth incubator, Thermoscientific, USA) to minimize additional stressors. Unhatched or dead embryos/larvae were removed once daily. On the final sampling day, 24-26 larvae (unstressed or post handling stress) were humanely euthanized on ice-cold water and were pooled in a single 2 ml Eppendorf tube.

2.2.4 Stress conditions and sample collection

The unstressed groups were quickly netted and immediately euthanized in ice-cold water, and whole-body samples were collected for cortisol measurement, qPCR and fluorescence imaging. After removing the excess medium from each tube, samples were immediately placed on dry ice and later transferred to -80 ^{o}C freezer until further experiments. The stressed groups underwent a modified net-handling procedure previously described [173]. Briefly, the larvae from each group were exposed to air for 1 minute trapped in a mesh net, afterwards returned to the embryo medium for 3 minutes of rest, following by another 1-minute exposure to air (Fig 2.1). The time points for sample collections were determined based on several pilot studies conducted to capture each signal's peak.

The sample collection protocol was based on the different time-courses for each parameter assessed. Samples for whole-body cortisol contents were collected at 30 minutes and 60 minutes post handling stress (total of 6 replicates per sample). For RNA transcript measurements, samples were collected at 60 minutes and 90 minutes post handling stress (total of 9 replicates

per sample). For fluorescence imaging studies (eGFP protein) samples were collected at 30, 60, 90, 120, 180, 210- and 240-minutes post-handling stress.

2.2.5. Whole-body cortisol measurement

Whole-body cortisol was measured using a Cortisol ELISA kit (Cat# 500360 Cayman Chemicals, Michigan, USA) based on the manufacturer's recommendations. Cortisol was extracted from a pool of 24-26 larvae by ether lipid extraction protocol described previously [174]. Briefly, 200 µl of freshly prepared PBS was added to each sample and samples were sonicated (Qsonica- q700, CT, USA) at 20 kHz for two periods of 10 s while being incubated on ice. Afterwards, three times volumes of diethyl ether were added to each sample, vigorously mixed by vortex and centrifuged at 4000 rpm for 5 minutes at 4^{o}C, and supernatants were collected [174]. This procedure was repeated three times for each sample. The total collected supernatants were placed in an exhaust hood, and diethyl ether allowed to evaporate overnight. Following total evaporation, 50 µl of ELISA buffer was added to each sample and incubated at 4^{o}C for 24-30 hours with vortexing three times every 10-14 hours for full resuspension the lipid extracts. The resuspended samples were used for cortisol measurement. Samples with a high amount of cortisol which fell in the non-linear part of the standard curve, were diluted further with ELISA buffer and measured again. Based on the spiked samples with a known amount of cortisol (hydrocortisone), the extraction efficiency was > 85%. All experiments performed with six replicates.

2.2.6. Total RNA extraction and quantitative PCR

Total RNA extraction was carried out using the Qiagen Rneasy mini kit (Qiagen, Hilden, Germany) based on the manufacturer's recommendations. A fraction of total RNA extracts for each sample was converted to cDNA using Qiagen QuantiNova Reverse Transcription Kit (Qiagen, Hilden, Germany), based on the manufacturer's recommendations. The cDNA samples were kept in a -80 ^{o}C freezer until further experimentations. For qPCR experiments, the forward and reverse primer sequences for eGFP and *eef1a1l1* (*eukaryotic translation elongation factor 1 alpha 1, like 1*) were adopted from previously published data [5]. All oligonucleotides were synthesized by Integrated DNA Technologies (Coralville, Iowa, USA). The qPCR experiments were conducted

according to SYBR green chemistry using the SsoAdvanced universal SYBR Green supermix and Bio-rad CFX Thermal cycler (Bio-Rad, Hercules, California, USA) according to the manufacturer's recommendations, followed by melting curve analysis. Each qPCR experiments' efficiency was between 98-103%, with a slope between -3.58 to -3.10. Experiments were conducted using the same batch of materials in a single day. All experiments performed with N=6 replicates.

2.2.7. Whole-body fluorescence imaging

The 4dpf zebrafish larvae from the two treatment groups (CORT-short and CORT-O/N) and the two control groups (DMSO-short and DMSO-O/N) were anaesthetized using Tricaine mesylate as described in the ZFIN database (https://wiki.zfin.org/display/prot/TRICAINE) and fixed in a six-well plate containing low melting point agarose [175]. The heartbeat of the larvae was monitored throughout the experiment to assure stable anaesthesia. The light and fluorescence microscopy were performed using 485/20 filter for excitation and 530/25 filter for emission using Cytation 3 multi-well reader (Biotek, Winooski, Vermont, USA). This experiment was performed with N=6 replicates. The fluorescence intensity was measured on a single representative image of each treatment and control groups using ImageJ software (NIH; https://imagej.nih.gov/ij/) at four different anatomical regions. The areas of interest were encompassing the telencephalon, diencephalon, correct olfactory bulb, and left olfactory bulb. To measure similar regions, all images were scaled to a similar pixel ratio using the SCALE function of ImageJ version 1.8_172. Using an image acquired in the CORT-O/N group, the measuring areas were drawn on the highest intensity areas while avoiding skin pigmentations in the measuring area. In each anatomical section, ten similarly sized areas were drawn and measured. The mean of fluorescence intensity (mean grey value) and the standard deviation for each anatomical section, was calculated based on these measurements. The drawn areas were saved using the ROI (region of interest) function of ImageJ. The same ROI setting was used for all other images, and a similar calculation of fluorescence intensity (mean grey value) and the standard deviation was performed. The statistical analysis was performed as described below; briefly, one-way ANOVA was performed in each of the four anatomical sections in the related treatment and control groups and if significant, followed by a post hoc test for pairwise comparison.

For the time-lapse fluorescence study, a 4dpf SR4G larva was stressed via the handling stress routine described above. Afterwards, the larva was anaesthetized and fixed in a six-well plate containing low melting point agarose as described above. Serial fluorescence imaging of this larva's head area was performed (same settings as described above using the same equipment) starting at 30 minutes post handling stress and every 15 minutes afterwards until 240 minutes post handling stress time. The heartbeat of the larvae was monitored throughout the experiment to assure stable anaesthesia. This experiment was performed on six individual larvae (N=6). The fluorescence intensity measurement was performed using the similar ROI setting described above on the four anatomical positions described earlier (telencephalon, diencephalon, right olfactory bulb, and left olfactory bulb) at four different time points (60, 90, 120, and 180 minutes post handling stress) using a representative image. An unstressed larva was immediately anaesthetized and fixed on low melting point agarose as described. A similar image analysis process was performed on this unstressed larva designated as "0-minutes (unstressed)" condition in the time-lapse study. The statistical analysis was performed as described below; briefly, two-way ANOVA was performed in each of the four anatomical sections in the related time points (unstressed and the four post-stressed time points) and, if significant, followed by a post hoc test for pairwise comparison.

2.2.7. Statistical analysis

All statistical analysis was performed by XLSTAT (Addinsoft Inc, N.Y. USA). The Shapiro-Wilk or Jarque-Bera tests of normality were performed on each data set to determine each data set's normal distribution. Also, the homogeneity of variances was assessed in these samples using Levene's test, and if homogenous, parametric tests were employed. Given each experiment's design, one-way ANOVA or two-way ANOVA was performed between each treatment group and the associated control. All tests were performed with six replicates to determine the significance level, followed by Tukey's post-hoc test for pairwise comparison. The level of significance was selected as $p \leq 0.05$.

2.3. Results

2.3.1. The highest level of cortisol was captured 30 minutes after the handling stress

Figure 2.2 shows the cortisol levels at different time points before and following the handling stress. The one-way ANOVA indicated that time after the handling stress had a significant effect on the cortisol levels ($p<0.05$). The mean cortisol levels increased 2.2-fold at 30-minutes ($p<0.05$) compared to the unstressed state and returned to pre-stress (unstressed) levels by 90 minutes. Our findings indicate that collecting samples at 30 minutes following the final handling stress was the appropriate time to capture elevation of endogenous cortisol ($p<0.05$).

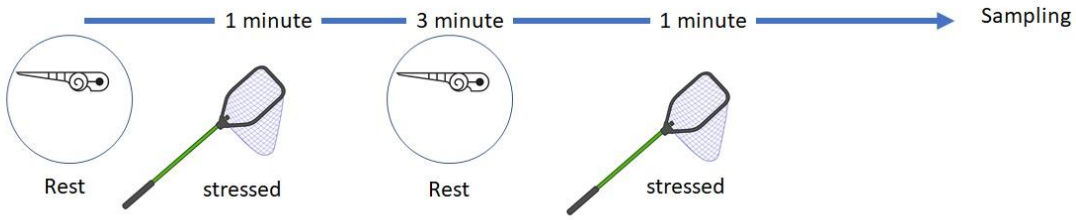

Figure 2.1. The handling stress protocol. The top portion of the design shows the handling stress routine for 7dpf larvae consisting of two 1-minute net stressing and room air exposure separated by 3-minutes resting for free-roaming in the water tank; following by sample collection 1 hour after the last stressed episode. The bottom part of the design shows the handling stress routine for adult zebrafish consisting of two 3-minute net stressing and room air exposure separated by 3-minutes resting for free-roaming in the water tank; following by sample collection 1 hour after the last stressed episode.

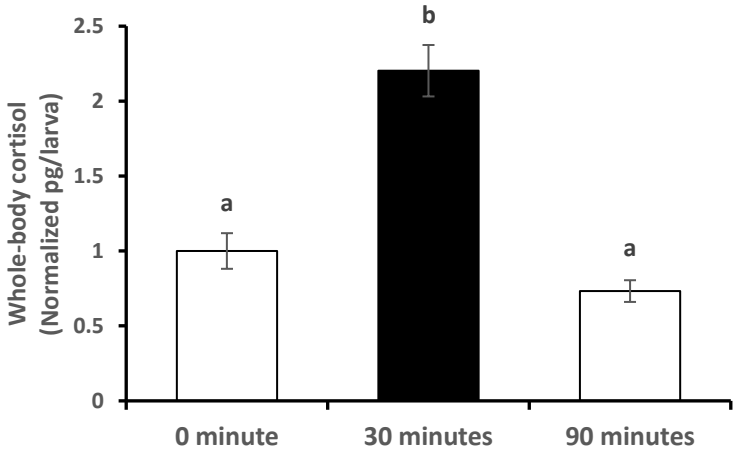

Figure 2.2. Whole-body cortisol measured before and after the handling stress. The levels of whole-body cortisol are shown in 7dpf SR4G transgenic larvae at different time points. The 0 minute is equivalent to the unstressed state. The 30 minutes and 90 minutes is the time-lapsed following the last stage of handling stress. Each sample contained 24-26 7dpf SR4G transgenic zebrafish larvae. Means (± SEM) with different letters (a, b) are significantly different; $p < 0.01$, N=6.

2.3.2. Whole-body eGFP mRNA levels reach the peak 60 minutes after handling stress.

Our findings indicated that the time after the handling stress had a significant effect on the eGFP mRNA levels ($p<0.05$) (Figure 2.3). The mean of eGFP mRNA levels increased 2.25-fold at 60-minutest ($p<0.05$) compared to the unstressed state and returned to pre-stress (unstressed) levels by 180 minutes. Our findings indicated that collecting samples at 60 minutes following the final handling stress was the appropriate time of collection ($p<0.05$).

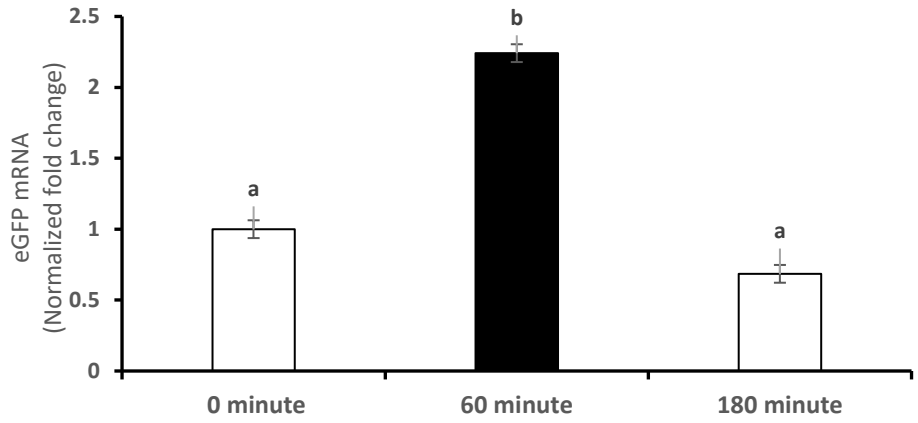

Figure 2.3. The whole-body eGFP mRNA level measured before and after the handling stress. The levels of whole-body eGFP mRNA are shown for 7dpf SR4G transgenic larvae at different time points. The 0 minute is equivalent to the unstressed state. The 60 minutes and 180 minutes is time-lapsed following the last stage of handling stress. Each sample contained a pool of 23-27 7dpf SR4G transgenic zebrafish larvae. Means (± SEM) with different letters (a, b) are significantly different; $p<0.01$, N=9.

2.3.3. The fluorescence imaging revealed ubiquitous eGFP expression induced by exogenous and endogenous cortisol.

The two-way ANOVA performed showed that the treatment (DMSO vs cortisol; $p<0.01$), the length of exposure (4 hours vs 18 hours overnight; $p<0.01$) and their interaction (treatment vs length of exposure; $p<0.01$) had significant effects on the fluorescence intensity of the four anatomical regions studied (Figure 2.5). The measured fluorescence intensity showed that cortisol exposure for 4 hours increased fluorescence intensity in all four anatomical regions compared to the control: left olfactory bulb [9-fold, $p<0.01$], right olfactory bulb [9.6-fold, $p<0.01$], diencephalon [51-fold, $p<0.01$] and telencephalon [52-fold, $p<0.01$]. Moreover, the measured fluorescence intensity showed that cortisol exposure for 18 hours overnight increased fluorescence intensity in all four anatomical regions to significantly higher levels compared to the control: left olfactory bulb [27.6-fold, $p<0.01$], right olfactory bulb [27.6-fold, $p<0.01$], diencephalon [77-fold, $p<0.01$] and telencephalon [91-fold, $p<0.01$]. There was no difference between control groups concerning the length of exposure in three anatomical positions; left olfactory bulb, right olfactory bulb; and telencephalon [DMSO-short vs DMSO-O/N; $p>0.05$]. There was a significant difference between control groups regarding the length of exposure in the diencephalon with fluorescence intensity following overnight exposure to DMSO was 1.6-fold less compared to the fluorescence intensity following short 4 hours exposure to DMSO [DMSO-short vs DMSO-O/N; $p<0.05$]. Our findings showed that global eGFP expression following exposure to exogenous cortisol increased in the four anatomical regions assessed ($p<0.01$), and the more prolonged exposure resulted in higher fluorescence signal related to eGFP expression in the four anatomical regions assessed ($p<0.01$).

The one-way ANOVA performed showed sampling at different time points after the handling stress had a significant effect on the fluorescence intensity in four different anatomical regions in the SR4G larva head ($p<0.01$) (Figure 2.6). The mean of fluorescence intensity was consistently elevated at 120 minutes post-handling stress across all four anatomical regions compared to the control (unstressed state): left olfactory bulb [5-fold, $p<0.01$], right olfactory bulb [6-fold, $p<0.01$], diencephalon [5-fold, $p<0.01$] and telencephalon [6-fold, $p<0.01$]. Our findings showed that sampling at 120 minutes following the last stage of the handling stress

captured the highest fluorescence intensity associated with the eGFP expression in the four anatomical regions in the SR4G larvae head.

These experiments show that eGFP expression responds promptly to both endogenous and exogenous glucocorticoids, and the response to both stressors are comparable. Also, it was determined that the peak of the eGFP fluorescence signal was reached after 120 minutes following the handling stress ($p<0.01$) regardless of the anatomical region selected (Fig 2.6).

A) B)

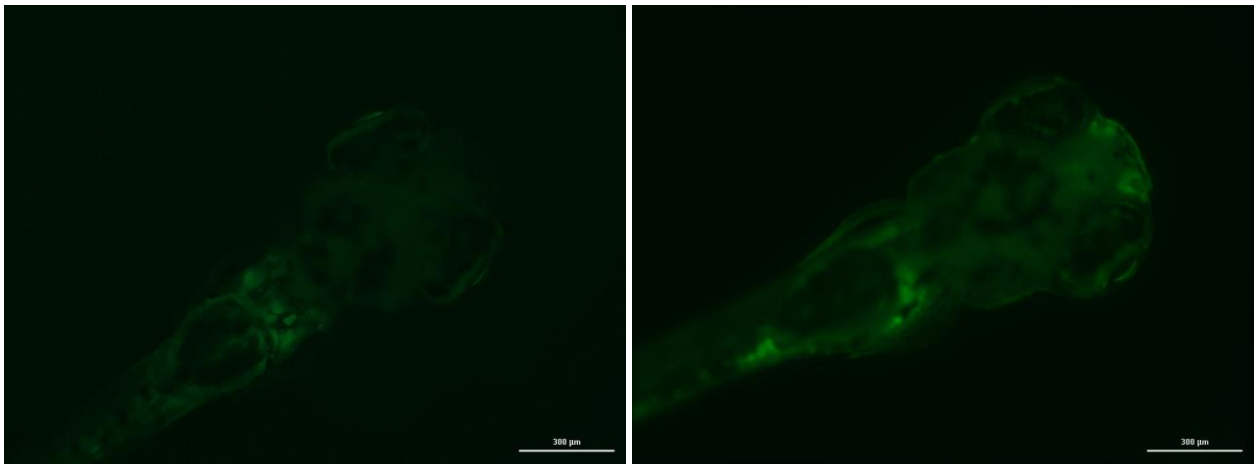

C) D)

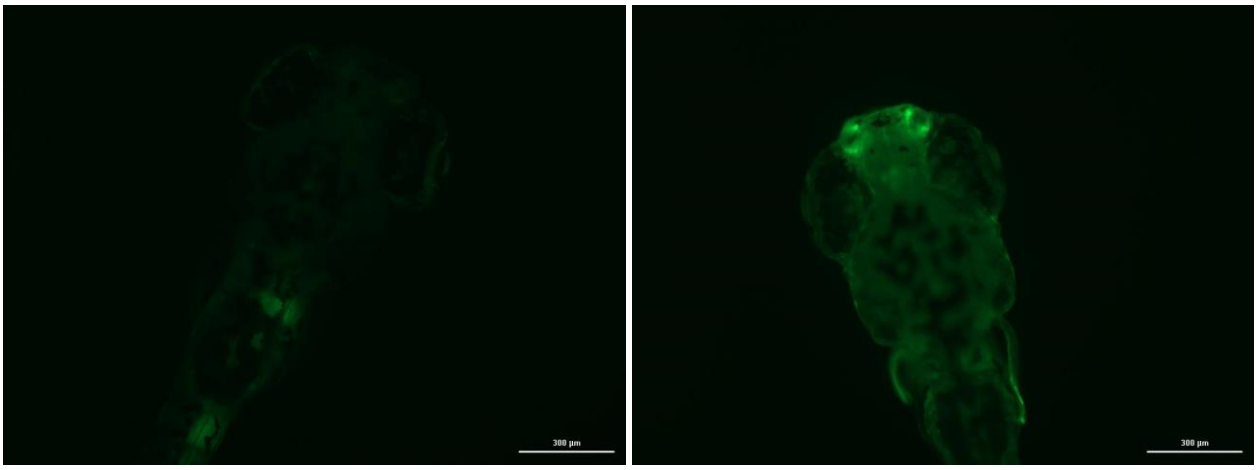

Figure 2.4. The ubiquitous eGFP expression in 4dpf SR4G transgenic zebrafish line following exposure to exogenous cortisol. A: DMSO-short: 4 hours exposure to 0.02% DMSO; **B**: CORT-short: 4 hours exposure to 10 µM exogenous cortisol (hydrocortisone); **C**: DMSO-O/N: 18 hours exposure to 0.02% DMSO; **D**:CORT-O/N: 18 hours exposure to 10µM exogenous cortisol. The scale bar is 300 µm. All images acquired using the same parameters.

A)

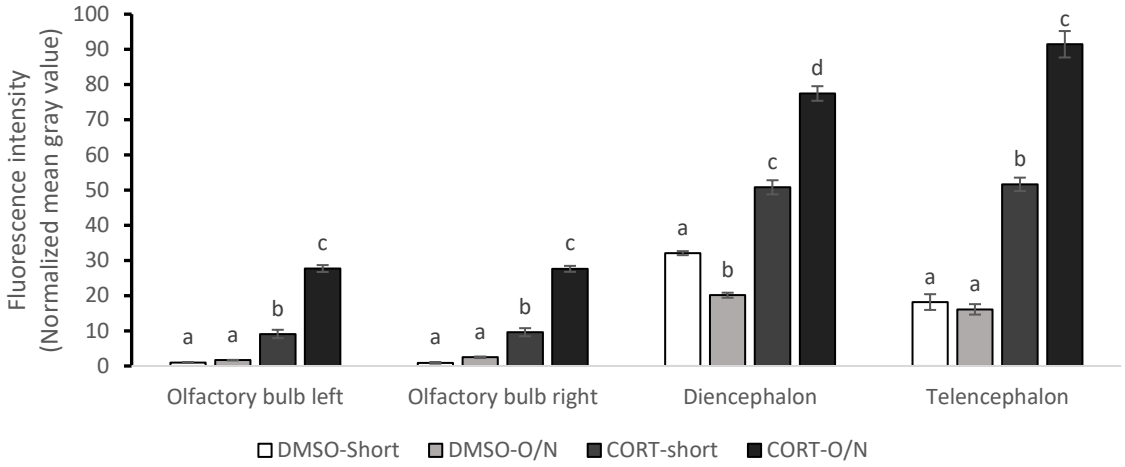

B)

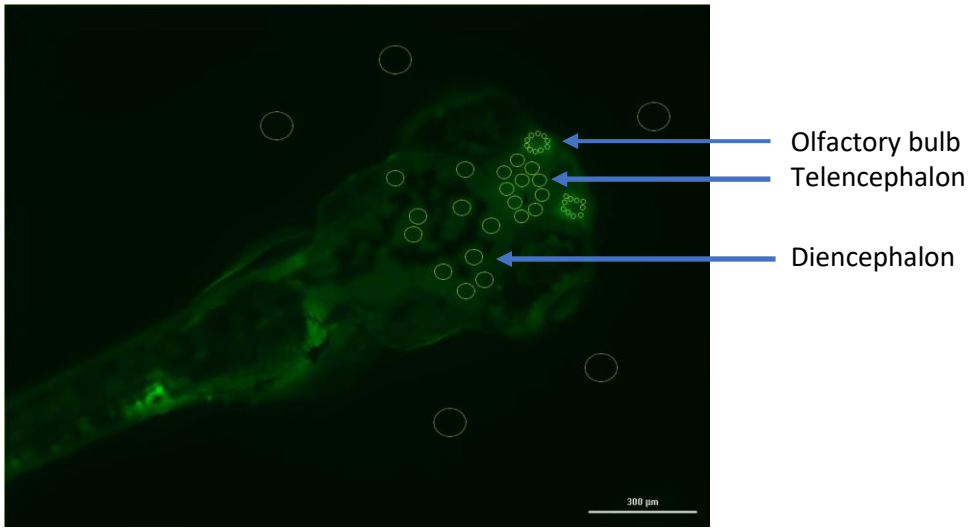

Figure 2.5. The fluorescent intensity of four anatomical regions of the brain in 4dpf SR4G transgenic line. Panel **A** shows the quantified fluorescence intensity (mean grey value) after exposure to DMSO control or cortisol compounds in four different anatomical positions; diencephalon, telencephalon, left olfactory bulb and right olfactory bulb of the brain in 4dpf SR4G larvae. Panel **B** shows the sampling method. The mean grey value of ten equally sized areas was measured to acquire the overall mean grey value of each of the four anatomical positions. The measured intensity was subtracted from the background intensity (large circles out around the larvae). DMSO-short: 4 hours exposure to 0.02% DMSO; CORT-short: 4 hours exposure to 10 µM exogenous cortisol (hydrocortisone); DMSO-O/N: 18 hours exposure to 0.02% DMSO; CORT-O/N: 18 hours exposure to 10 µM exogenous cortisol (hydrocortisone).

Means (± SEM) with different letters (a, b, c, d) are significantly different; $p<0.01$; $N=10$ area in each anatomical region in a representative image.

A)

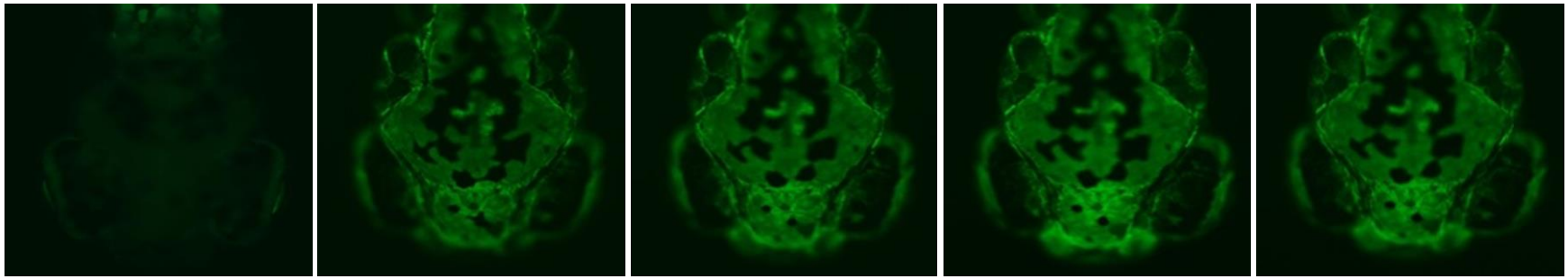

Unstressed (0 minute) **60 minutes** **90 minutes** **120 minutes** **180 minutes**

B)

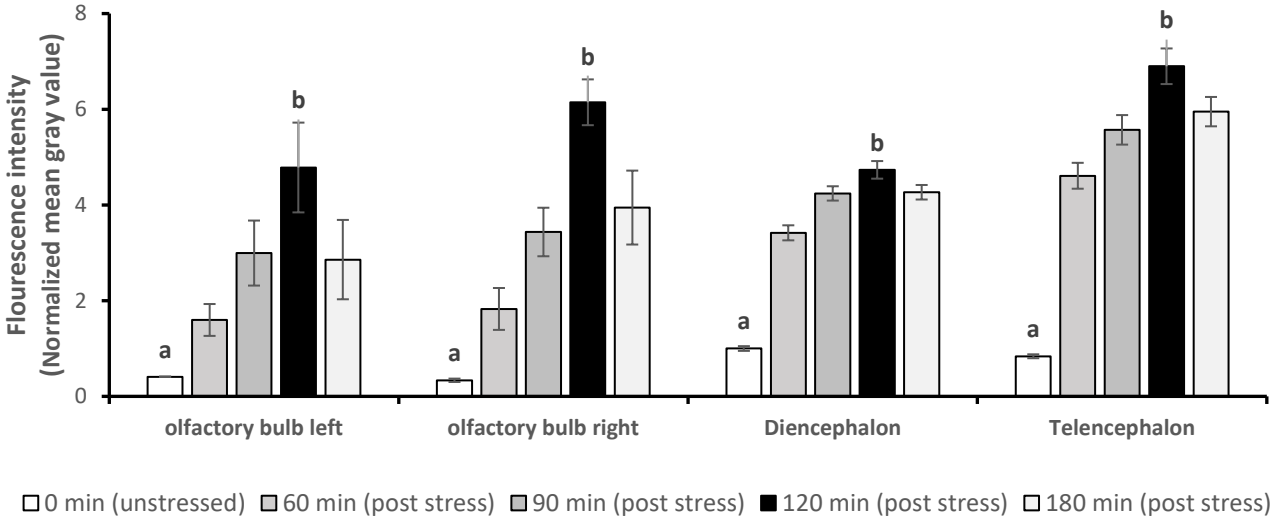

Figure 2.6. The time-lapse fluorescence imaging captures the ubiquitous eGFP expression in 4dpf SR4G transgenic zebrafish line following handling stress. Panel A shows the direct fluorescent imaging of 4dpf SR4G transgenic larva head at four different time-points after the handling stress. Panel B shows the quantified fluorescence intensity (mean grey value) after the handling stress in four different anatomical positions; diencephalon, telencephalon, left olfactory bulb and right olfactory bulb, in 4dpf SR4G transgenic larva head at four different time-points. Means (± SEM) marked with different letters (a,b) are significantly different within each anatomical position; $p<0.01$; N=10.

2.4. Discussion

We showed that using the SR4G transgenic zebrafish line, one could determine the activation of the HPI axis following a physical stressor in zebrafish larvae in three different levels: whole-body, cortisol, whole-body eGFP mRNA, and fluorescence imaging of the larvae head. We determined that samples should be collected at 30 minutes and 60 minutes after the handling stress to capture the significant elevation in the whole-body cortisol and the whole-body eGFP mRNA levels, respectively. Our findings were consistent with other studies in the SR4G transgenic line [5, 165]. The measurement of a fluorescence signal in different anatomical regions of the brain could significantly capture the activated stress response. Based on the time-lapse study performed, it was determined that the eGFP fluorescence signal reached its peak 120 minutes after handling stress in different anatomical regions of the larval brain. Some part of the brain (for example, the diencephalon) might express the fluorescence signal faster than other regions following the handling stress. However, this concept needs further evaluation and was not pursued in the current study.

The fluorescence imaging on the 4dpf larvae showed a similar increase in fluorescence intensity upon exposure to chemical (exogenous glucocorticoid) and physical (netting) stressors. It has been already shown that the stress axis is functional and responsive to exogenous stimuli in zebrafish larvae as early as 4dpf [37, 173, 176]. To avoid potential blockage of the fluorescence signal, 4dpf larvae were used due to less pigmental development compared to 7 dpf larvae. However, measurements at this age might not be optimum under all laboratory settings, mainly since there is still debate on the timing of the HPI axis's full functionality at this age in zebrafish [148, 177, 178]. A more sophisticated imaging tool or technique might alleviate this problem, for example, confocal microscopy study of histopathology sections. The other approach to enhancing fluorescence imaging could be developing stress-inducible transgene models based on existent transparent mutants like *casper* [179] or *crystal* [180]. These mutants lack melanophores and iridophores.

Zebrafish have been successfully used for biomonitoring of environmental pollutants, including bisphenol A, xenoestrogens, pesticides, heavy metals, and aromatic hydrocarbons [151]. For example, induction of transcription of metalloproteins in zebrafish has been observed

upon exposure to Hg^{2+}, Cu^{2+}, Zn^{2+}, and Cd^{2+} [181]. Moreover, zebrafish have been used to detect EDCs in aquatic environments, like PBDEs (Polybrominated diphenyl ethers) which upon exposure resulted in altered swimming behaviour [182]. Many EDCs are shown to affect the stress-axis in zebrafish and other teleost models [183]. For example, exposure to environmentally relevant doses of PBDEs resulted in upregulation of *crhb* (corticotropin-releasing hormone) and *tshba* (thyroid-stimulating hormone) genes in zebrafish larvae [184]. Measuring eGFP mRNA and eGFP fluorescence signal in SR4G transgenic larvae could potentially monitor the dynamic alterations in the stress axis. These values could be considered as new endpoints to monitor stress response compared to the classic measurement glucocorticoids.

In the next chapter of the study, we introduced using eGFP mRNA in the SR4G transgenic line as a mean to track stressed individuals in our study of long-lasting effects of developmental exposure to FLX. The proper sampling time is crucial in the study of the dynamic process like stress response. There is a delay between increased cortisol levels and transcription of responsive genes (eGFP mRNA) and the translation of endpoint proteins (eGFP protein). Missing the proper sampling time could have dire consequences on the measured signals, particularly in transcriptomic studies [185, 186]. Using eGFP mRNA or eGFP fluorescence as the internal controls for response to a stressor shows the potentials of the SR4G transgenic line and other similarly designed models in the study of dynamic physiological processes stress or other endocrine pathways. In Chapter 4 of this thesis, we elaborate more on such potentials.

2.5. Statement of contribution

Amin Nozari designed the study and methodology, conducted the experiments and analyses and prepared the manuscript. Dr. Vance Trudeau helped with the design of the study and manuscript editing.

CHAPTER 3: Life-long effects of developmental exposure to fluoxetine on global transcription profiles in the brains of zebrafish

3.1. Introduction

Selective serotonin reuptake inhibitors (SSRIs) are classified as class C pharmaceuticals that indicate they might have adverse effects on the developing fetus; however, SSRIs have been widely used to treat depression and mood disorders in pregnancy and early post parturition [187, 188]. It is shown that SSRIs could cross the placental barrier during pregnancy [98, 99]. In early development, serotonin has heavily involved in the development of neural circuits, particularly in cell division, cell differentiation, cell migration, myelination, and synaptogenesis [189-193]. Therefore, dysregulation of serotonin production in the developing brain by SSRIs could have potential long-lasting effects on the fetal brain's neuronal networks [85].

Human and rodents' studies show that developmental exposure to SSRIs could adversely affect social behaviour, neurodevelopment, vulnerability to stressful situations, and physiological hemostasis [194-201]. Recently, teleost has been used as a new model to study SSRIs' developmental effects [147, 202]. The serotonergic pathways are highly conserved between teleost and other mammals, with 93% of the amino-acid sequence in SSRIs binding site in serotonin reuptake transporter (*sert*, *slc6a4a*) is conserved between human and different fish species [116, 119]. SSRIs' anxiolytic effects have been reported in fathead minnows (*Pimephales promelas*) upon exposure to sertraline and FLX following 28 days exposure in different concentrations [117, 118]. Several serotonin receptors have been implicated in mediating the anxiety-like behaviour in fish, including 5-HT_{1A}, 5-HT_{1B}, 5-HT_{1D},5-HT_{2A}, 5-HT_{3},5-HT_{T5}, and 5-HT_{T6} receptors [129-132]. Moreover, using teleost models has helped to discern the environmental impacts of SSRIs which reach aquatic systems through sewage treatment facilities [150]. Using teleost models in environmental studies has further discussed in the next chapter of the current thesis.

It has been suggested that the altered regulation of the stress-axis mediates the long-lasting effects of SSRIs on behaviour in humans and rodents. For example, it is shown that FLX could disrupt the stress-axis's normal function by decreasing the circulation of glucocorticoids

and the downregulation of GR in the nervous system in humans and rodents [203-207]. The downregulation of GR has been linked to depressive-like behaviours in rodents [208]. It is shown that impaired GR function in the central nervous system could result in hyperactivity of the HPA axis, resulting in behavioural abnormalities observed in depression [18]. Also, rodents' studies have shown that stress contributes to serotonergic pathways' dysregulation [18]. A subpopulation of serotonergic neurons in raphe nuclei responds to an elevation of corticotropin-releasing hormone (CRH) and anxiety-like behaviour in rats [209]. The close interaction between the serotonergic system and the stress-axis has also been shown in teleost. For example, high levels of the 5-HT_{1A} receptor have been detected in POA, pituitary and interrenal cells of Gulf toadfish (*Opsanus beta*) [122]. Activation of the 5-HT_{1A} receptor has increased *crh* transcription and elevation of whole-body cortisol in Gulf toadfish and rainbow trout (Oncorhynchus mykiss) [123]. Moreover, it is shown that subordinate fish have higher cortisol levels and serotonergic neural activity than dominant fish [116, 122, 210]. The subordinate fish are shown to have an elevated transcription of 5-HT_{1A} and 5-HT_{2A} receptors in their telencephalon and increased levels of 5-HIAA (the primary metabolite of serotonin, an indicator of serotonergic neural activity) in their POA [210].

Recent studies in our lab by Vera Chang *et al.* (2018, 2019) showed that developmental exposure to FLX resulted in hyporcortisolism in the descendant male adults for at least three generations [1, 2, 199]. Such decreases in whole-body cortisol levels coincided with a decrease in exploratory behaviour in the novel tank test, an anxiety-like behaviour in zebrafish [1, 2, 199]. Also, based on the transcriptomic study on interrenal cells, Vera Chang *et al.,* (2018, 2019) showed significant dysregulation of glucocorticoid signalling and circadian rhythm signalling pathways in the FLX exposed lineage (F0 and F3) compared to unexposed controls zebrafish [1, 2, 199]. In the current study, using a transgenic zebrafish line, we studied the long-lasting effects of developmental exposure to FLX on genes involved in stress and neurogenesis in larvae and adult telencephalon and hypothalamus. Moreover, using orthologue pathways analysis, we evaluated the effect of such exposure on genes involved in the development of depression in human.

Furthermore, in this study, we used the SR4G transgenic line, which expresses an enhanced green fluorescent protein (eGFP) when exposed to physical stress [5]. We aimed to use the transgene transcript (GFP mRNA) as an internal control to confirm the stress response activation in our transcriptomic analysis. The experiments performed in the previous chapter (Chapter 2) have provided us with appropriate sampling time to capture the significant activation of stress response in the SR4G zebrafish line. Since it has been suggested that the effect of FLX is sex-dependent in zebrafish and more prominent in male individuals [211], only male adults were studied in the current study. The current chapter's findings have provided extensive evidence for the life-long effects of developmental exposure to FLX on neural development, stress response, and cholesterol metabolism in adult male zebrafish. Furthermore, our orthologue pathway analysis showed the benefits of using the zebrafish model to study neuropsychiatric disorders in humans.

3.2. Materials and Methods

3.2.1. Animals and Husbandry

The SR4G transgenic zebrafish line was kindly provided by Dr. Karl Clark (Mayo Clinic, Minnesota, USA) and Dr. Xiao-Yan Wen (University of Toronto, Ontario, Canada) [5]. The one-day post-fertilization embryos were transferred to Ottawa and placed in the quarantine room of the University of Ottawa's aquatic facility per regulations of Animal Care and Veterinary Services (ACVS). The embryos allowed to hatch and were raised in the quarantine facility until they reached six months of age. These zebrafish were used to establish our founder generation. The F_0 generation was bred from this founder line.

3.2.2. Study design

To study the life-long effect of developmental exposure to FLX on the central nervous system, the larvae head and brain’s tissues (telencephalon and hypothalamus) of male adult zebrafish were studies. Two independent variables were studied, stress condition and FLX exposure (Supplementary Figure 5). A total of 12 treatment and control groups were studied. For the larval study, all experiments were conducted with six replicates (experimental units) which consisted of 22-28 larvae head (sampling unit) that were raised in separate containers to avoid

pseudo-replication (Supplementary Figure 5). For adults' study, similarly, all experiments were conducted with six replicates (experimental units) prepared by pooling of 5 tissue samples (sampling unit; either telencephalon or hypothalamus) harvested from adult male zebrafish. The same adult was used to harvest the telencephalon and hypothalamus so that the pooled samples were from the same five adult zebrafish for telencephalon and hypothalamus in each replicate. The five individuals pooling together were raised in separate containers from other groups of 5 to avoid pseudo-replication (Supplementary Figure 5). The details about FLX exposure and stress routine is provided in the following sections.

3.2.3. Chemical exposure

The stock of 1 mg/ml of fluoxetine (Millipore-Sigma, Burlington, MA, USA) was prepared in 99% ethanol as the vehicle. To confirm that the storage in -80 ^{o}C does not affect the concentration of FLX, in freshly prepared working dilution from stock solution, the concentration working solution (54 µg/L) was assessd by liquid chromatography-Mass spectropmetry (LC/MS) (LC: Agilent 1100 capillary HPLC, Agilent, Santa Clara, CA, US; MS: Thermo LTQ Linear Ion Trap mass spectrometer, Thermo scientific, CA, US) . The procedure was performed in collaboration with PhD student C. Lu in our laboratory (Supplementary Figure 1). Embryos from 0 days post fertilization (0 dpf) were exposed to freshly prepared 54 µg/L fluoxetine daily until they reached 6 dpf. The control groups were exposed to the vehicle only (final concentration of 0.005% ethanol) from 0-6 dpf. The total volume of the rearing tanks was adjusted to approximately 1ml per larva. The treatment and control larvae were further divided into unstressed and stressed groups and were housed in separate shelves in the incubator (Percision^{TM} plant growth chamber, 504L; Thermoscientific, USA) to avoid unwanted stressors. The unhatched or dead embryos/larvae were collected once daily. Several larvae with fluoxetine-exposure background and control-exposure background were raised until they reached six months with no further exposure to FLX or any other chemicals. At six months, the male and female adult zebrafish were segregated, and the experiments performed on male adult zebrafish. The treatment-lineage and control-lineage were further divided into unstressed and stressed groups and were housed in separate shelves in the incubator to avoid unwanted stress.

3.2.4. The net handling stress and sampling for RNA sequencing

For both treated larvae and adults and their corresponding control, the unstressed groups were not exposed to any handling or mechanical stress and sacrificed immediately using ice-cold water on the day of an experiment. The stressed groups were exposed to a modified handling net stress described previously [2]. Briefly, the larvae from each group were exposed to air for 1 minute trapped in a mesh net, afterwards returned to the embryo medium for 3 minutes for rest, followed by another 1-minute exposure to air trapped in a mesh net (Figure 3.1). The sample collection was carried out 60 minutes after the last net stress based on the findings reported in Chapter 2. The adults from each group were exposed to air for 3 minutes trapped in a mesh net, afterwards returned to the water for 3 minutes for rest, followed by another 3-minute exposure to air trapped in a mesh net. The sample collection was carried out 60 minutes after the last net stress based on the findings reported in Chapter 2. For 7 dpf larvae, a pooled sample of the body's cranial part (head) was acquired by removing the trunk and tail sections. This was done to reduce the number of abundant muscular and gastrointestinal-related genes in our data set. Each larval sample was a pool of 22-28 heads. The tissue samples were immediately frozen on dry ice and stored at -80 ^{o}C until further assessments. After careful dissection of the skull, the telencephalon and the hypothalamus were separately dissected and immediately placed on dry ice for adults. The designated brain parts from 5 adult fish were pooled and placed in -80^{o}C until further experimentations. All pooled tissue samples were prepared in 6 replicates across all treatment (FLX-L: fluoxetine exposed larvae; FLX-Tel: adult telencephalon from descendants of FLX-L; FLX-Hyp: adult hypothalamus from descendants of FLX-L; cL: control larvae, cTel: control adult telencephalon; cHyp: control adult hypothalamus)(Supplementary Figure 5).

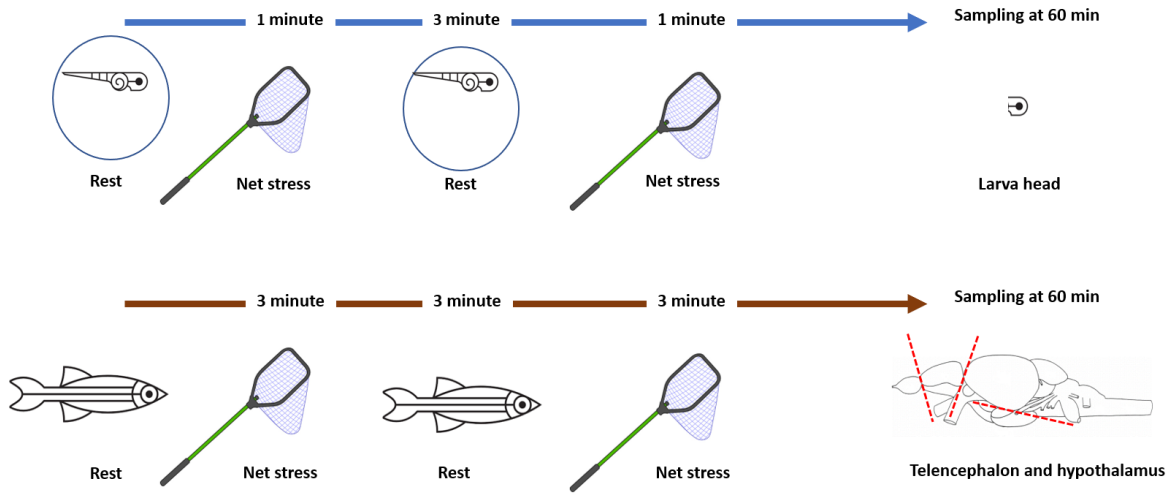

Figure 3.1. The net handling stressor for larvae and adult zebrafish. The top panel depicted the handling stress for 7 dpf larvae and consisted of two 1-minute net stress and room air exposure separated by a 3-minutes resting and free-swimming episode. Larvae were sacrificed 60 minutes after the last net stress, and larval heads were collected and 22-28 pooled in a single 2 ml sample tube. The bottom panel depicted the handling stress protocol for adult zebrafish and consisted of two 3-minute net stressing and room air exposure separated by a 3-minutes resting and free-swimming. Adult zebrafish were sacrificed 60 minutes after the last net stress, and telencephalon and hypothalamus tissue were collected. The red dashed line depicts the incision sites on the brain anatomy to acquire telencephalon and hypothalamus samples. The telencephalon and hypothalamus from five adult fish were pooled in a single 2 ml sample tube. All experiments were performed with six experimental replicates (N=6).

3.2.5. Total RNA extraction and quality control

Total RNA extraction from all samples was carried out by using Qiagen Rneasy mini kit, (Qiagen, Hilden, Germany) based on the manufacturer recommendations. The quality of the total extracted RNA was assessed using Agilent 4150 TapeStation system (Agilent, Santa Clara, CA, USA). The RNA integrity number (RIN) was acquired for all samples, and only those with RIN >8.5 were of sufficiently high quality and used for RNA sequencing [212].

3.2.6. Next-generation high throughput RNA sequencing

Next-generation high-throughput RNA sequencing was carried out using Illumina technology (Illumina, San Diego, CA, USA) in the laboratory of Dr. C. Yauk (Health Canada, Ottawa, ON, Canada). A total of 72 samples were sequenced, considering three tissues (L, Tel, and Hyp), two independent factors (stressed vs unstressed) and (FLX treatment vs vehicle control), and six experimental replicates for each studies conditions (Supplementary Figure 5). Standard single-read mRNA libraries were built using the TruSeq Stranded mRNA Library Prep kit (Cat. # 20020595, Illumina) with initial 150 ng of total RNA extracts. The Poly-A enrichment technique was used to purify mRNA. Afterwards, all mRNAs were fragmented, converted to cDNA using random hexamers, and indexed using TruSeq RNA CD Idx (Cat. # 20019792, Illumina) for downstream multiplex analysis. The prepared libraries were assessed for the final size using Agilent 4150 TapeStation system (Agilent, Santa Clara, CA, USA). The approximate band size was 260 bp for each prepared library. The samples were randomly assigned to two 36 samples groups. The indexed libraries were normalized to 10nM and pooled in equal volumes. Afterwards, clustered were generated using NSQ 500/550 Hi Output KT v2.5 (Cat. # 20024906, Illumina) with 75 cycle cartridges. Each pooled library was run on two separate Flow cells as technical replicates. An average of 18 million reads per sample was obtained.

For quality assessment, raw counts were transformed to logarithmic pseudo counts, and Boxplot and PCA (principal component analysis) functions were used to visualize between sample distribution of pseudo counts. Parallel boxplots and median marker between samples interpreted as the similar distribution of pseudo counts between samples. Approximate clustering of samples in PCA allowed ruling out the existence of outlier samples (Supplementary Figure 2). The raw

reads were assessed for Median Phred Quality Score (median score 36), GC Content (mean 35%), Missing Nucleotide Rate (median 2E-05), and Nucleotide Rate by Cycle. Reads were trimmed to remove prefixes and suffixes with cutAdapt. The reads were aligned to the zebrafish reference genome (GRCz11; GCA_000002035.4)) using STAR and gene counting performed by HT-Seq count.

An average of 18 million reads was mapped across different samples (range considering all samples: 12-24 million reads). The Gene−Body Coverage was assessed, showing mean ranges between 55% to 60% coverage across different samples for both Low Expressed Genes category and Upper Middle Quartile Genes category. Read mapping analysis showed that 70%-90% of reads across different samples were mapped to unique genes, with 20%-30% of reads mapped to Unique Gene UTRs. Following these quality control tests, the reads were filtered based on genes count per million (CPM), keeping genes that had ≥1 CPM at least in one sample. Library sizes were normalized using the Trimmed Mean of M-values (TMM) to eliminate the difference in sequencing depth between samples. The TMM is a global normalization method that assumes most of the genes are not differentially expressed, and the differences observed between samples are strongly dependant on a few highly transcribed genes. The normalized CPM for each gene was fitted to the negative binomial model and dispersion estimates were calculated using the DESeq2 package [213]. Given our study design had 2 independent variables, FLX exposure and stress status, the nbinomWaldTest function was used for comparing stressed and unstressed groups considering the FLX exposure (using the following code: DESeqDataSetFromMatrix(countData = dataCountTable, colData = dataDesign, design = ~ treatment*condition) (Figure 3.2). This function also reported an adjusted p-value (padj) based on the Benjamini-Hochberg procedure, which controls the false discovery rate (FDR). Statistical significance was evaluated using the criteria of adjusted p value ≤ 0.05. The threshold was selected as 1.2 (FC≥1.2) for fold-change analysis, already reported as the optimal FC for nervous system transcriptomic analysis [214]. The RNA sequencing was conducted in Dr. C. Yauk's laboratory with the assistance of Mr. R. Gagné at Health Canada (Ottawa).

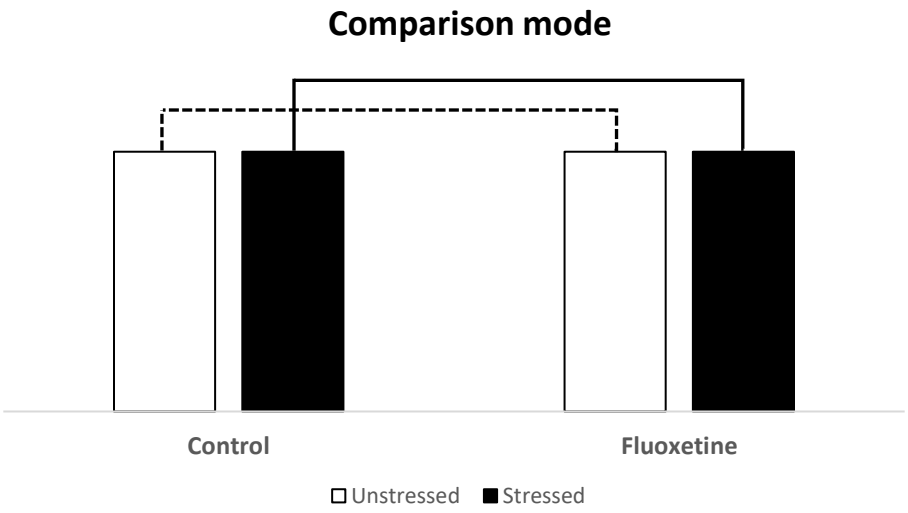

Figure 3.2. Diagram depicting the comparison mode to determine the differentially expressed genes (DEGs) in both larvae and adults. The black bar represents the stressed groups, and the white bars represent the unstressed groups. The solid and dashed lines connect the groups that were compared to each other.

3.2.7. Ingenuity pathway analysis and network prediction

The lists of differentially expressed genes were analysed further using Qiagen Ingenuity Pathway Analysis (Qiagen, Hilden, Germany) to retrieve clusters of affected canonical pathways. Since IPA does not have zebrafish genome annotation currently, the gene Ensembl IDs were converted to human orthologs using ID converter on DAVID (The Database for Annotation, Visualization and Integrated Discovery; https://david.ncifcrf.gov/tools.jsp). The duplicated paralogue genes in the zebrafish genome were assigned similar *Homo sapiens* orthologue Ensemble ID. All annotations reported here for pathways, networks, transcription regulators, and individual genes are according to *Homo sapiens* orthologue annotations. When applicable zebrafish specific gene annotations are shown throughout this thesis.

A total of 27,162 (85%) gene IDs were successfully mapped by IPA. To avoid losing sensitive information, no attempt to delete or adjust duplicated probes was made; therefore, IPA's function to assign a Z-score for activation or inhibition of any canonical pathway was not used. All analysis reported here is solely based on gene enrichment in canonical pathways.

Furthermore, IPA's network prediction tool was used to cluster affected genes in functional molecular networks. This functionality was also used to determine potential upstream transcription regulators driving the observed alterations in the DEGs.

3.2.8. The statistical analysis

The study designed to create a list of differentially expressed genes in two different conditions (stressed vs unstressed) while considering the developmental exposure to FLX (FLX-treated vs control). The experimental units contained six biological replicates (experimental units, N=6) of pooled samples of larvae heads (sampling units: 22-28 individual), adult telencephalon (sampling units: 5 individuals), and adult hypothalamus (sampling units: 5 individuals) (Supplementary Figure 5). The telencephalon and hypothalamus tissues were harvested from the same individual fish to create a pooled designated sample. The multiplex design was used for the high-throughput sequencing by sample-specific barcoding immediately after fragmentation during library preparation. Two technical replicates were used for flow cell loading to balance batch and lane effect. The internal statistical analysis in the DESeq2 package was used to determine DEGs, which is based on the Wald test considering the negative binomial model and using Benjamini-Hochberg correction for FDR. The genes with FC≥1.2 and $p\ adj \leq 0.05$ considered significantly expressed.

3.3. Results

3.3.1. Developmental exposure to fluoxetine altered gene transcription pattern of the central nervous system in both larva and adult zebrafish

Our transcriptomic analysis showed that a total of 4456, 3172, and 5778 genes were significantly affected by developmental exposure to FLX in larvae (L), adult telencephalon (Tel), and adult hypothalamus (Hyp); respectively, regardless of stress condition. The total number of up-and down-regulated genes following developmental exposure to FLX in unstressed condition was 941, 1927, and 5055 for L, Tel, and Hyp, respectively (Figure 3.3). In the unstressed state, 68% of DEGs were downregulated, and 32% were upregulated in the fluoxetine exposed larvae (unstr-FLX-L). Interestingly, this ratio was reversed in the same unstressed condition in Hyp (unstr-FLX-Hyp), with 63% and 37% of genes upregulated and downregulated, respectively. For

the adults' telencephalon in the unstressed condition (unstr-FLX-Tel), 57% and 43% of genes were upregulated and downregulated, respectively. The total number of up-and down-regulated genes following developmental exposure to FLX in the stressed condition was 3515, 1245, and 723 for L, Tel, and Hyp, respectively (Figure 3.3). In the stressed state, the ratio of up-and down-regulated genes was similar across all samples. The stressed larvae group (str-FLX-L) developmental exposure to FLX resulted in downregulation of 60% of the affected genes; the remaining 40% were upregulated. In the hypothalamus of stressed adult zebrafish (str-FLX-Hyp), 44% and 56% of genes were upregulated and downregulated, respectively, following developmental exposure to FLX. Moreover, 43% and 57% of genes were upregulated and downregulated in the str-FLX-Tel group, respectively (Figure 3.3). The relation of significantly affected DEGs to the complete transcript mapped across all tissue samples in the two unstressed and stressed conditions is shown (Figure 3.4). The genes with high fold change and the most significance are marked for each group (Figure 3.4).

The hierarchical clustering of DEGs revealed the effect of treatment (FLX vs control) and stress status (unstressed vs stressed)(Figure 3.3). For larvae and adult hypothalamus, treatment (FLX vs control) was the main clustering factor; and for telencephalon, the stress status (unstressed vs stress) divided the main clusters (Figure 3.3). The replicates of stressed and unstressed groups were clustered together in FLX exposed groups across all tissue samples (L, Tel, Hyp). Although the replicates of control larvae (not exposed to FLX) were clustered together in a stressed condition, there was a division in the unstressed condition. For TEL and HYP, a similar division in clustering of stressed and unstressed replicates was observed only for control (not exposed to FLX) groups. The principal component (PCA) analysis also showed similar results (Supplementary Figure 2). Levels of eGFP mRNA followed the stress pattern, with a higher count per million reads (CPM) for eGFP transcripts in stressed subgroups. However, the distinction between stressed and unstressed groups using the eGFP transcription was less robust in Hyp compared to L and Tel.

Overall, our findings show that developmental exposure to FLX alters the central nervous system's transcription profile in the affected larvae in the unstressed and stressed condition. This effect of FLX lasts to adulthood and is evident in the altered transcriptomic profiles of

telencephalon and hypothalamus in both stressed and unstressed conditions. Our findings support a possible life-long effect of developmental exposure to FLX. Moreover, our findings showed the potentials of tracing eGFP transcript in RNAseq samples as an alternative route to confirm stress induction in subject individuals.

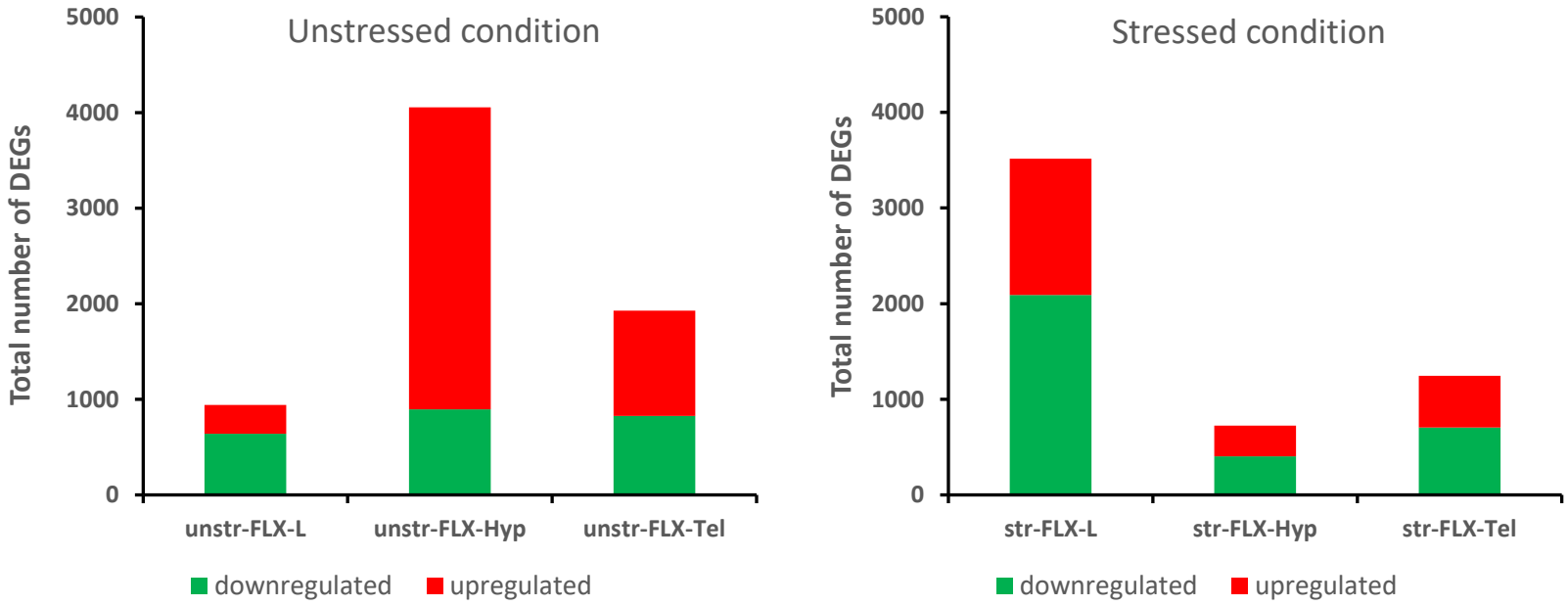

Figure 3.3. The total numbers of differentially expressed genes (DEGs) in FLX exposed groups compared to respective controls in unstressed and stressed conditions. The total numbers of DEGs are shown in a stacked format with downregulated and upregulated genes are colour-coded in green and red, respectively.

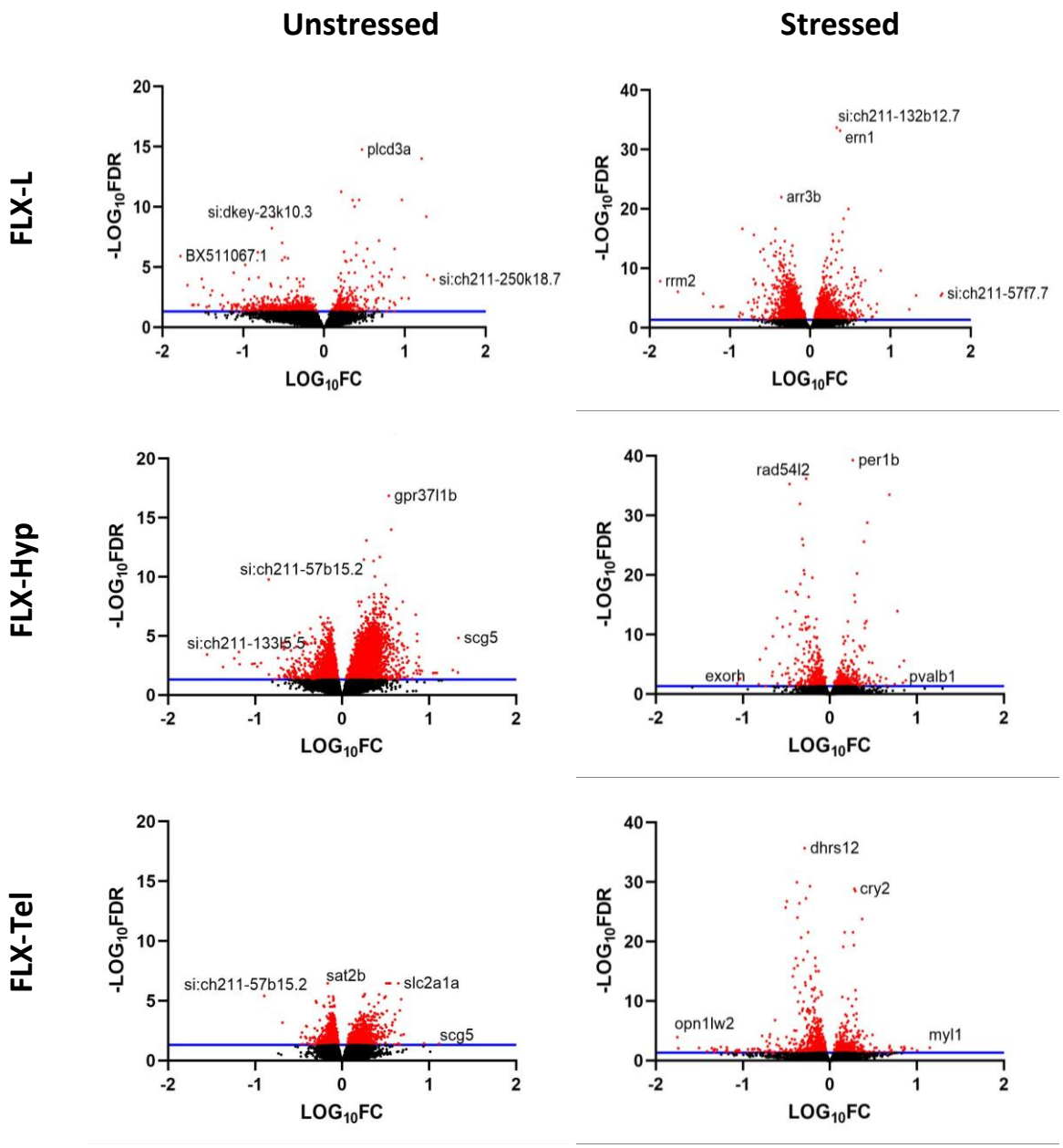

Figure 3.4. Volcano plots of the mapped transcriptome in FLX exposed groups compared to the controls in unstressed and stressed conditions. The volcano plots in the three studied tissues (L, Hyp, and Tel) in the unstressed and stressed conditions are shown. The x-axis shows the fold change (FC) on a logarithmic scale. Only genes with FC> 1.2 are depicted here. The y-axis shows the level of significance on a negative logarithmic scale. The scales of the y-axis are different for unstressed and stressed conditions to illustrate the data points clearly. The blue line shows the FDR ≤ 0.05 (equal to 1.3 on a negative logarithmic scale). The genes with significant FC are demonstrated as red dots above the blue threshold line. The genes with the most significant fold change and the highest significance are marked in each graph.

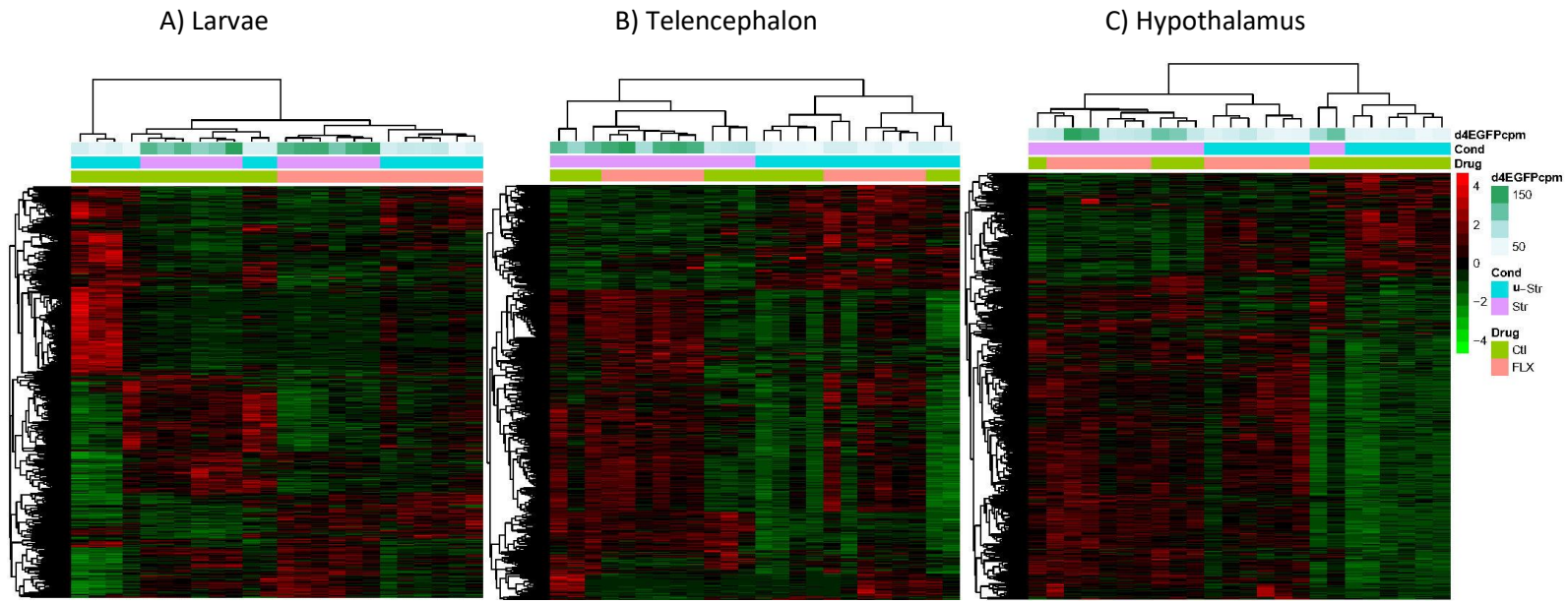

Figure 3.5. The effect of developmental fluoxetine exposure on transcriptome patterns in larvae and adult male zebrafish central nervous system in the unstressed and the stressed conditions. Each heatmap shows the gene clustering across all 24 samples (stressed, unstressed, FLX exposed and control ethanol exposed) in a single tissue (Larvae, hypothalamus, and telencephalon) and their relation to FLX and stress treatment. Panel (A) depicts the data set for FLX exposed larvae compared to the control larvae. Panel (B) depicts the data set for telencephalon from adults exposed to FLX in the early life developmental stage compared to control adults exposed to vehicle compound (ethanol) in the early life developmental stage. Panel (C) depicts the data set for the hypothalamus from adults exposed to FLX in the early life developmental stage compared to control adults exposed to vehicle compound (ethanol) in the early life developmental stage. The Y-axis consists of all genes with significant fold change (FDR ≤0.05 and FC≥ 1.2) in the treatment groups relative to the control groups. Red: up-regulation, green: down-regulation. The count per million (CPM) of the reads associated with the green fluorescent protein (d4eGFP) transgene in the SR4G zebrafish line is shown. The different shades of green show different CPM. Blue: unstressed condition, lavender: stressed condition, light green: control (ethanol), pink: Fluoxetine.

3.3.2. Enrichment of pathways associated with neurotransmitter signalling and response to steroid hormones supports a life-long effect of developmental exposure to fluoxetine

Enrichment clustering analysis was performed to assess the common pathways affected by developmental exposure to FLX in zebrafish larvae and adults in stressed or unstressed conditions. The DEGs list was evaluated using the Qiagen Ingenuity Pathway Analysis (Qiagen, Hilden, Germany) to retrieve clusters of affected canonical pathways across all six groups. The canonical pathways were ranked based on their p-value ($p \leq 0.05$). The top 10 pathways for each of the six main groups are shown for unstressed (Figure 3.6) and stressed (Figure 3.7) conditions, separately. Our findings showed that the canonical pathways were more significantly affected in unstressed conditions in both FLX-exposed larvae and FLX-exposed adults than the stressed condition in the same age group.

Cholesterol biosynthesis was significantly affected in the FLX-exposed larvae in the unstressed condition (unstr-FLX-L), evident with 8 of 10 significantly affected pathways were associated with cholesterol metabolism. In the unstressed telencephalon and hypothalamus (unstr-FLX-Tel and unstr-FLX-Hyp), several pathways associated with neural cell-signalling, neurotransmitter signalling, and regulation of synaptic junctions were affected. Our findings showed that a few pathways were affected in both larvae and adults in unstressed condition; including Paxillin Signaling ($p= 4^{E-06,}$ $p= 9^{E-04}$, $p=4^{E-06}$, for unstr-FLX-L, unstr-FLX-Hyp, and unstr-FLX-Tel; respectively); Clathrin-mediated Endocytosis Signaling (p= 0.009, p= 0.008, p=0.02, for unstr-FLX-L, unstr-FLX-Hyp, and unstr-FLX-Tel; respectively); ILK (integrin-linked kinase) Signaling (p= 0.001, p= 0.001, p=0.001, for unstr-FLX-L, unstr-FLX-Hyp, and unstr-FLX-Tel; respectively); and Agrin Interactions at Neuromuscular Junction (p= 0.012, p= 0.019, $p=3^{E-04}$, for unstr-FLX-L, unstr-FLX-Hyp, and unstr-FLX-Tel; respectively) (Table 3.1). Our findings revealed that 11 canonical pathways were affected by developmental exposure to fluoxetine in larval heads and adult hypothalamus in the unstressed condition (Table 3.1). Among these, Glucocorticoid Receptor Signaling (unstr-FLX-L, p=0.004 ;unstr-FLX-Hyp, p=0.028); Aldosterone Signaling in Epithelial Cells (unstr-FLX-L , p=0.011 ;unstr-FLX-Hyp, p=0.01); and SAPK/JNK Signaling (unstr-FLX-L , $p=5^{E-05}$;unstr-FLX-Hyp, p=0.04). Our findings showed that several pathways were affected only in adulthood by developmental exposure to FLX in the unstressed condition, evident in the

hypothalamus and telencephalon (Table 3.1). Among these, CREB Signaling in Neurons (unstr-FLX-Hyp, p=0.04; unstr-FLX-Tel, $p=1^{E-09}$), GnRH Signaling (unstr-FLX-Hyp, p=0.01; unstr-FLX-Tel, $p=1^{E-09}$), Synaptogenesis Signaling Pathway (unstr-FLX-Hyp, $p=5^{E-04}$; unstr-FLX-Tel, $p=4^{E-08}$), NF-κB Signaling (unstr-FLX-Hyp, p=0.02; unstr-FLX-Tel, p=0.01), Axonal Guidance Signaling (unstr-FLX-Hyp, $p=3^{E-04}$; unstr-FLX-Tel, $p=9^{E-06}$), and ERK/MAPK Signaling (unstr-FLX-Hyp, p=0.03; unstr-FLX-Tel, p=0.0001) (Table 3.1 and Supplementary Table 1).

The DNA base pair metabolism (4 out of 10 pathways) and neurotransmitter signalling (3 out of 10 pathways) were most significantly affected by developmental exposure to FLX in stressed larvae (Figure 3.7). In the stressed telencephalon and hypothalamus (str-FLX-Tel and str-FLX-Hyp), pathways associated with neural cell-signalling, circadian rhythm, and energy metabolism were affected (Figure 3.7). Our findings showed that the Androgen Signaling pathway was affected in both larvae and adults in the stressed condition (str-FLX-L, p=0.026; str-FLX-Hyp, p=0.04) (Table 3.2). Our finding showed the life-long effect of developmental exposure to FLX in the stressed condition, mainly manifested in the adult telencephalon and hypothalamus (Table 3.2). Amongst the pathways that affected in both tissues were Circadian Rhythm Signaling (str-FLX-Hyp, $p=2^{E-05}$; str-FLX-Tel, p=0.003), Sirtuin Signaling Pathway (str-FLX-Hyp, p=0.001; str-FLX-Tel, p=0.005), Oxidative Phosphorylation (str-FLX-Hyp, p=0.04; str-FLX-Tel, p=0.02), and Aldosterone Signaling (str-FLX-Hyp, p=0.03 str-FLX-Tel, $p=3.8^{E-07}$) (Table 3.2). Our findings also show that several other pathways were affected by developmental exposure to FLX only in one of the target tissues (larvae, hypothalamus, and telencephalon) in stressed condition (Supplementary Table 2).

Table 3.3. shows the hypothalamus and telencephalon pathways, which were affected by developmental exposure to FLX in both stressed and unstressed conditions. Our findings showed that more pathways were affected in the hypothalamus compared to the telencephalon. The Oxidative Phosphorylation pathway was affected in both the hypothalamus and the telencephalon of male adult zebrafish in both stressed and unstressed conditions (unstr-FLX-Hyp, p=0.0001; unstr-FLX-Tel, p=0.03; str-FLX-Hyp, p=0.04; str-FLX-Tel, p=0.02). Several pathways were affected life-longly in hypothalamus including Glucocorticoid Receptor Signaling (unstr-FLX-Hyp, p=1.8E0-8; str-FLX-Hyp, p=0.03), GnRH Signaling (conditions (unstr-FLX-Hyp, p=0.004; str-

FLX-Hyp, p=0.03), Aldosterone Signaling (unstr-FLX-Hyp, p=0.01; str-FLX-Hyp, p=0.03), Circadian Rhythm Signaling (unstr-FLX-Hyp, $p=3.8^{E-08}$; str-FLX-Hyp, $p=2.1^{E0-5}$), Androgen Signaling (unstr-FLX-Hyp, p=0.0005; str-FLX-Hyp, p=0.04), Prolactin Signaling (unstr-FLX-Hyp, p=0.005; str-FLX-Hyp, p=0.04), and Relaxin Signaling (unstr-FLX-Hyp, $p=3.4^{E-05}$; str-FLX-Hyp, p=0.02).

Overall, our findings showed that developmental exposure to FLX results in life-long alteration of several pathways in the adult nervous system. Our findings showed that more pathways were affected in the hypothalamus than the telencephalon in both unstressed and stressed conditions. Our data showed a life-long alteration of several pathways involved in neuroendocrine signalling, cholesterol metabolism, and synaptogenesis signalling.

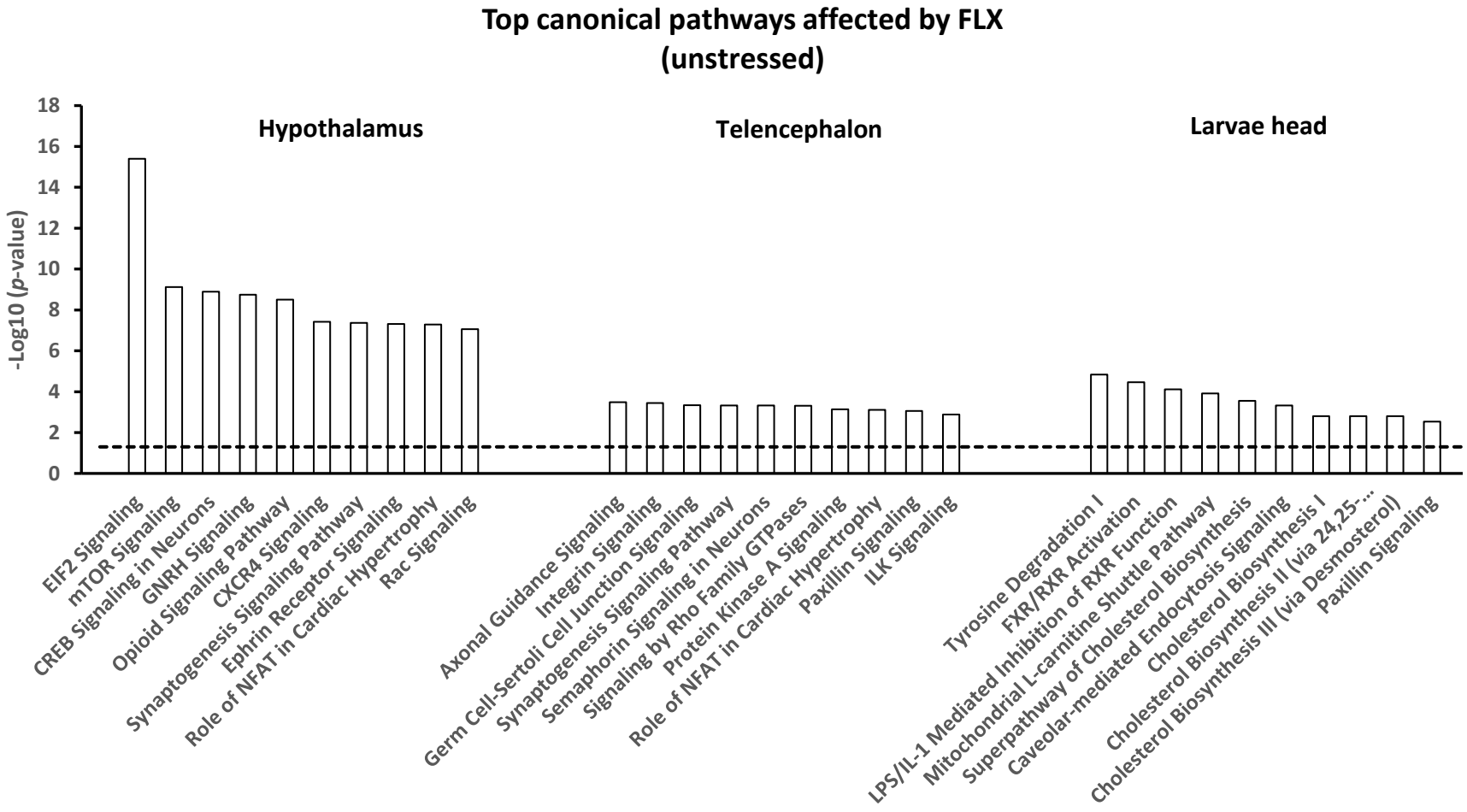

Figure 3.6. Top ten affected canonical pathways by early-life exposure to fluoxetine in the unstressed condition. Pathways with the highest level of significance shown in each target tissue in both larvae and adult groups in the unstressed condition. The y-axis presents the p-value

associated with each pathway in a negative logarithmic scale (-log p-value). The horizontal dash line marks the negative logarithmic value related to the significance level ($p \leq 0.05$; $-\log10(p) = 1.3$). Each bar is presenting a canonical pathway identified from the gene cluster enrichment function of IPA. The analysis was performed after converting the gene Ensembl ID of zebrafish (*Danio rerio*) to human (*Homo sapiens*) orthologues. Only genes with significant fold change (FC>1.2; FDR≤0.05) were used for pathway enrichment analysis. FLX: fluoxetine.

Table 3.1. Pathways affected life-longly by developmental exposure to fluoxetine in the unstressed condition.

Canonical pathway	unstressed		
	L	H	T
Agrin Interactions at Neuromuscular Junction			
Clathrin-mediated Endocytosis Signaling			
ILK Signaling			
Paxillin Signaling			
Glucocorticoid Receptor Signaling			
Aldosterone Signaling in Epithelial Cells			
April Mediated Signaling			
B Cell Activating Factor Signaling			
IL-17A Signaling in Airway Cells			
Myc Mediated Apoptosis Signaling			
Sertoli Cell-Sertoli Cell Junction Signaling			
NRF2-mediated Oxidative Stress Response			
HIF1α Signaling			
IL-22 Signaling			
SAPK/JNK Signaling			

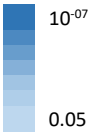

Different shades of blue represent the negative logarithmic scale of the associated p-value (-logp value); the dense colours present lower p values, and lighter colours present a higher p-value. Only significant data ($p \leq 0.05$) are shown in the blue gradient. Gray represents statistically non-significant data ($p > 0.05$). L: larval heads (unstr-FLX-L); H: the hypothalamus (unstr-FLX-Hyp); T: telencephalon (unstr-FLX-Tel).

Table 3.1. Pathways affected life-longly by developmental exposure to fluoxetine in the unstressed condition (cont…).

Canonical pathway	unstressed		
	L	H	T
14-3-3-mediated Signaling			
AMPK Signaling			
Apelin Endothelial Signaling Pathway			
Apelin Pancreas Signaling Pathway			
Axonal Guidance Signaling			
Calcium Signaling			
Cardiac Hypertrophy Signaling			
Cardiac Hypertrophy Signaling (Enhanced)			
Cdc42 Signaling			
Cholecystokinin/Gastrin-mediated Signaling			
CREB Signaling in Neurons			
CXCR4 Signaling			
Dopamine-DARPP32 Feedback in cAMP Signaling			
Epithelial Adherens Junction Signaling			
ERK/MAPK Signaling			
Germ Cell-Sertoli Cell Junction Signaling			
Glioblastoma Multiforme Signaling			
Glioma Invasiveness Signaling			
GNRH Signaling			
Gαq Signaling			
Hypoxia Signaling in the Cardiovascular System			
IGF-1 Signaling			
IL-15 Production			
IL-8 Signaling			
Integrin Signaling			
Leukocyte Extravasation Signaling			
Macropinocytosis Signaling			
Mitochondrial Dysfunction			
mTOR Signaling			
Neuropathic Pain Signaling In Dorsal Horn Neurons			
NF-κB Signaling			

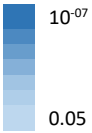

Table 3.1. Pathways affected life-longly by developmental exposure to fluoxetine in unstressed condition (cont…).

Canonical pathway	unstressed		
	L	H	T
Oxidative Phosphorylation			
p70S6K Signaling			
PAK Signaling			
Phospholipase C Signaling			
Protein Kinase A Signaling			
PTEN Signaling			
Rac Signaling			
Regulation of Actin-based Motility by Rho			
Remodeling of Epithelial Adherens Junctions			
Role of NFAT in Cardiac Hypertrophy			
Semaphorin Signaling in Neurons			
Signaling by Rho Family GTPases			
Sperm Motility			
STAT3 Pathway			
Synaptogenesis Signaling Pathway			
Virus Entry via Endocytic Pathways			

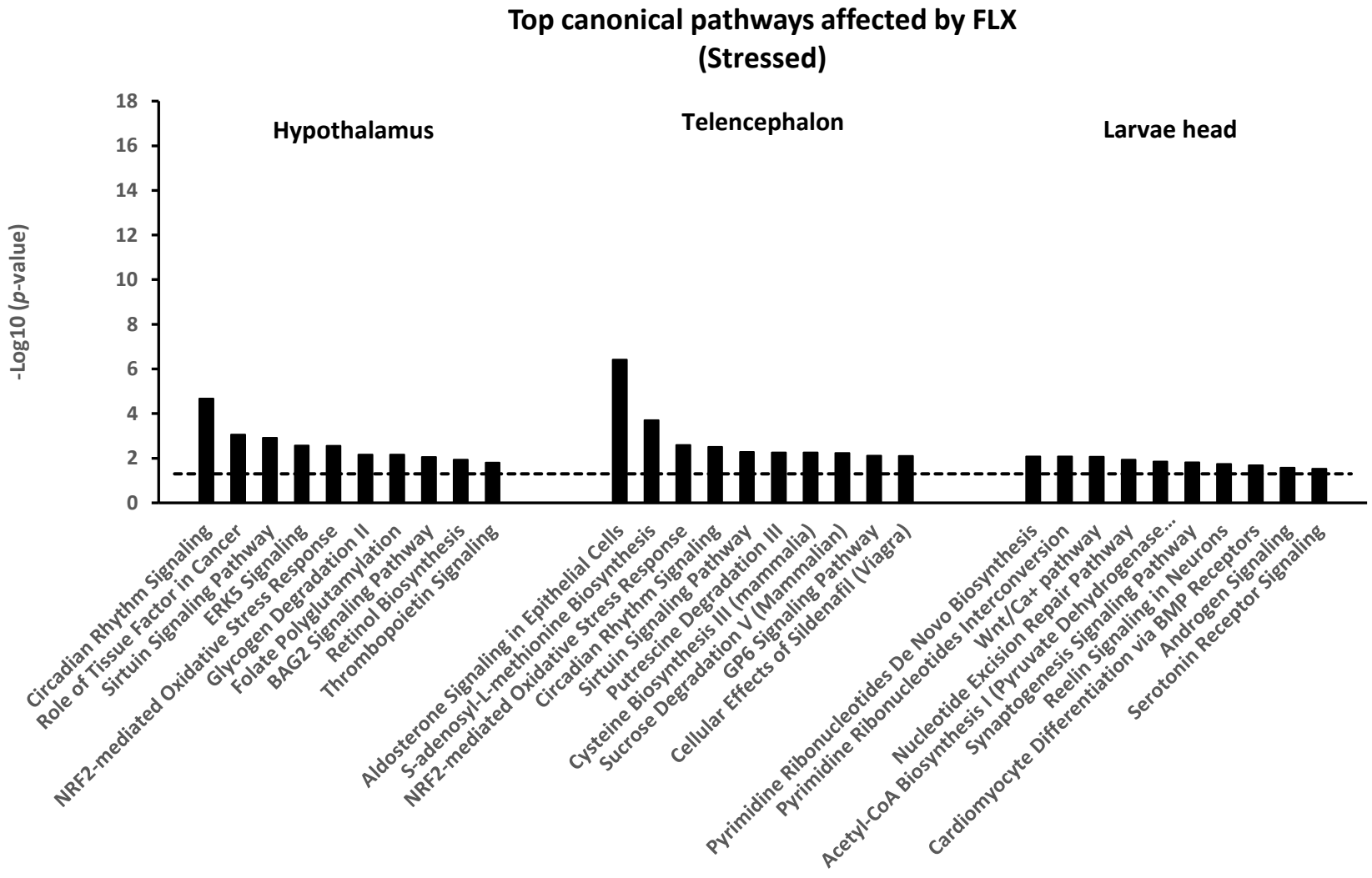

Figure 3.7. Top ten affected canonical pathways by early-life exposure to fluoxetine in the stressed condition. Pathways with the highest level of significance shown in each target tissue in both larvae and adult groups in the stressed condition. The y-axis presents the p-value associated

with each pathway in a negative logarithmic scale (-log p-value). The horizontal dash line marks the negative logarithmic value related to the significance level (p ≤0.05; -log10(*p*)= 1.3). Each bar is presenting a canonical pathway resulted from the gene cluster enrichment function of IPA. The analysis was done after converting the gene Ensembl ID of zebrafish (Danio rerio) to human (Homo sapiens) orthologues. Only genes with significant fold change (FC>1.2; FDR≤0.05) were used for pathway enrichment analysis. FLX: fluoxetine.

Table 3.2. Pathways affected life-longly by developmental exposure to fluoxetine in the stressed condition.

Canonical pathways	stressed		
	L	H	T
Androgen Signaling			
Aldosterone Signaling in Epithelial Cells			
BAG2 Signaling Pathway			
Circadian Rhythm Signaling			
NRF2-mediated Oxidative Stress Response			
Oxidative Phosphorylation			
Sirtuin Signaling Pathway			
TCA Cycle II (Eukaryotic)			
Unfolded protein response			

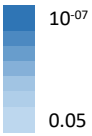

Different shades of blue represent the negative logarithmic scale of associated p-value (-logp value); the dense colours present lower p values and, lighter colours present a higher p-value. Only significant data ($p \leq 0.05$) are shown in the blue gradient. Gray represents statistically non-significant data ($p > 0.05$). L: larval heads (str-FLX-L); H: hypothalamus (str-FLX-Hyp); T: telencephalon (str-FLX-Tel).

Table 3.3. Pathways affected life-longly in adult zebrafish by developmental exposure to fluoxetine

Canonical pathways	unstressed		stressed	
	H	T	H	T
Oxidative Phosphorylation				
Cholecystokinin/Gastrin-mediated Signaling				
CXCR4 Signaling				
GNRH Signaling				
Aldosterone Signaling in Epithelial Cells				
Circadian Rhythm Signaling				
NRF2-mediated Oxidative Stress Response				
Androgen Signaling				
BAG2 Signaling Pathway				
Cancer Drug Resistance By Drug Efflux				
Chemokine Signaling				
D-myo-inositol (1,4,5,6)-Tetrakisphosphate Biosynthesis				
D-myo-inositol (3,4,5,6)-tetrakisphosphate Biosynthesis				
Endothelin-1 Signaling				
Ephrin B Signaling				
Ephrin Receptor Signaling				
ERK5 Signaling				
Glucocorticoid Receptor Signaling				
HER-2 Signaling in Breast Cancer				
JAK/Stat Signaling				
Prolactin Signaling				
RAR Activation				
Relaxin Signaling				
Thrombopoietin Signaling				
UVA-Induced MAPK Signaling				
VEGF Family Ligand-Receptor Interactions				
Role of Tissue Factor in Cancer				
Sirtuin Signaling Pathway				
TCA Cycle II (Eukaryotic)				
Unfolded protein response				

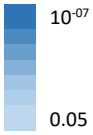

3.3.3. The upstream transcriptional regulators associated with regulation of the stress response and circadian rhythm were affected life-longly upon developmental exposure to fluoxetine

An upstream regulator analysis was conducted in IPA to identify the potential key transcriptional regulators that drive the gene dysregulation observed. Table 3.4 shows the affected transcriptional regulators in larvae and adults in both the stressed and unstressed condition. Our findings showed that a higher number of transcriptional regulators were affected by FLX in zebrafish larvae in unstressed condition (Table 3.4). Our findings showed that CLOCK, a key transcription factor in regulating circadian rhythm, was affected in both larvae and adults and was more affected in stressed condition (unstr-FLX-L, p=0.02; str-FLX-L, p=0.04; str-FLX-Hyp, $p=5^{E-06}$; str-FLX-Tel, $p=9^{E-06}$). Such significant effects were not observed on the hypothalamus and the telencephalon in the unstressed condition (unstr-FLX-Hyp, p>0.05; unstr-FLX-Tel, p>0.05). Our findings indicate that other transcriptions regulators were affected life-longly in the adult hypothalamus and telencephalon. For example in stressed condition NR3C1 (str-FLX-L, p=0.03; str-FLX-Tel, p=0.02), MAT1A (str-FLX-L, p=0.002; str-FLX-Tel, p=0.02), NPC1 (str-FLX-Hyp, p=0.02 ; str-FLX-Tel, p=0.04), SIRT1 (str-FLX-Hyp, p=0.02 ; str-FLX-Tel, p=0.02), and NCOA1 (str-FLX-Hyp, $p=6^{E-04}$; str-FLX-Tel, p=0.0001). Moreover, in the unstressed condition we observed several transcriptions regulators were affected life-longly in adult hypothalamus and telencephalon; for example, CPT1C (unstr-FLX-Hyp, p=0.03; unstr-FLX-Tel, p=0.002), SREBF1 (unstr-FLX-L, p=0.02; unstr-FLX-Tel, $p=8^{E-04}$), , and SREBF2 (unstr-FLX-L, p=0.001; unstr-FLX-Tel, $p=2^{E-04}$), SCAP (unstr-FLX-L, p=0.01; unstr-FLX-Tel, p=0.002), and PPARGC1A (unstr-FLX-L, p=0.009; unstr-FLX-Tel, p=0.004) (Table3.4).

Overall, our findings showed that several upstream transcription factors involved in regulating circadian rhythm, stress response, cholesterol metabolism, and histone modification were affected life-longly by developmental exposure to fluoxetine in zebrafish.

Table 3.4. Upstream regulators affected life-longly by developmental exposure to fluoxetine in zebrafish

Upstream regulator	Gene ontology: Biological process	Unstressed			Stressed		
		L	H	T	L	H	T
CLOCK	circadian regulation of gene expression						
NPC1	cholesterol metabolic process						
SIRT1	circadian regulation of gene expression, histone H3 deacetylation						
NFE2L2	protein catabolic process						
RICTOR	TOR signaling						
CPT1C	fatty acid beta-oxidation						
CCL4	immune response						
PPARD	cholesterol metabolic process						
DERL1	positive regulation of protein binding						
NR0B2	cholesterol metabolic process						
PML	circadian regulation of gene expression						
GCK	cellular glucose homeostasis						
PPARGC1A	circadian regulation of gene expression						
SCAP	cholesterol metabolic process						
SREBF1	cholesterol metabolic process						
SREBF2	cholesterol metabolic process						
ABCA1	cholesterol metabolic process						
SIRT3	histone H3 deacetylation						
NCOA1	histone H4 acetylation						
STAT3	negative regulation of neuron death						
NR3C1	stress response						
MAT1A	methylation						

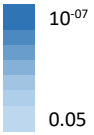

Different shades of blue represent the negative logarithmic scale of associated p-value (-logp value); the dense colours present lower p values and, lighter colours present a higher p-value. Only significant data ($p \leq 0.05$) are shown in the blue gradient. Gray represents statistically non-significant data ($p > 0.05$). L: larval heads, H: hypothalamus T: telencephalon. Gene ontology is associated with *Homo sapiens* orthologs.

3.3.4. Developmental exposure to fluoxetine dysregulated genes associated with lipid metabolism, nervous system development and behaviour

The top 5 networks in each tissue sample and their IPA functional category are shown (Table 3.5). The scoring is based on the number of genes involved and the internal scoring algorithm of IPA. Our findings suggest that several predicted networks were affected life-longly upon developmental exposure to FLX; for example, “lipid metabolism” and “molecular transport” were affected in larvae and adult in both stressed and unstressed condition. Moreover, networks involved in “nervous system development” and “endocrine system development” were affected by the adult hypothalamus and telencephalon.

Overall, our findings support a life-long effect of developmental exposure to FLX on networks involved in lipid metabolism, molecular transport, and nervous system development in male zebrafish that lasts to adulthood.

Table 3.5. Top 5 predicted networks affected by developmental exposure to fluoxetine.

Group	Score	# Genes	Functional clustering
Larvae heads (unstressed)	43	35	Lipid Metabolism, Molecular Transport
	14	19	Hepatic System Disease, Liver Steatosis
	13	18	Lipid Metabolism, Molecular Transport
	11	17	Lipid Metabolism, Molecular Transport
	10	16	Lipid Metabolism, Molecular Transport
Hypothalamus (unstressed)	24	35	Drug Metabolism, Small Molecule Biochemistry
	24	35	Lipid Metabolism, Molecular Transport
	24	35	Endocrine System Development and Function
	24	35	Hepatic System Disease, Liver Steatosis
	11	26	Cancer, Gene Expression, Organismal Injury and Abnormalities
Telencephalon (unstressed)	34	35	Lipid Metabolism, Small Molecule Biochemistry
	34	35	Cellular Development, Cellular Growth and Proliferation
	13	16	Cell Morphology, Cellular Function and Maintenance
	11	16	Cell-To-Cell Signaling and Interaction, Cellular Function and Maintenance
	10	19	Cellular Compromise, Organismal Injury and Abnormalities
Larvae heads (stressed)	29	35	Lipid Metabolism, Molecular Transport
	29	35	Lipid Metabolism, Small Molecule Biochemistry
	12	16	Developmental Disorder, Hereditary Disorder, Metabolic Disease
	9	21	Lipid Metabolism, Molecular Transport
	9	17	Behavior, Nervous System Development and Function
Hypothalamus (stressed)	12	16	Lipid Metabolism, Molecular Transport
	12	16	Lipid Metabolism, Molecular Transport
	12	16	Lipid Metabolism, Molecular Transport
	12	16	Behavior, Nervous System Development and Function
	9	14	Lipid Metabolism, Molecular Transport
Telencephalon (stressed)	11	16	Lipid Metabolism, Behavior, Nervous System Development and Function
	11	17	Lipid Metabolism, Small Molecule Biochemistry
	11	17	Lipid Metabolism, Molecular Transport
	11	17	Cellular Development, Tissue Development
	11	17	Metabolic Disease, Organismal Injury and Abnormalities

3.3.5. Several genes were dysregulated life-longly in both larvae and adult zebrafish upon developmental exposure to fluoxetine

Many genes were dysregulated in both larvae and adults. We report that 46 and 117 genes were dysregulated (up or down-regulated) upon developmental exposure to FLX in all tissue samples (L, Hyp, Tel) in the unstressed and stressed conditions, respectively (Figure 3.7). The associated functional clustering of these genes based on Gene Ontology annotations of *Homo sapiens* orthologues are shown in Table 3.5 and Table 3.6 for the unstressed and stress conditions, respectively. Downregulation was the main feature in the unstressed larvae (unstr-FLX-L, 38 out of 46 genes), and upregulation was the main feature in the unstressed adults (unstr-FLX-Hyp, 34 out of 46; unstr-FLX-Tel, 34 out of 46). Upregulation was the main feature in the stressed larvae (str-FLX-L, 95 out of 117 genes), and downregulation was the main feature in the stressed adults (str-FLX-Hyp, 91 out of 117; str-FLX-Tel, 91out of 117). Interestingly, for most of the genes in the unstressed and stressed responses, the direction of the gene expression change in larvae was opposite to that in adults; 93% of genes and 82% of genes for unstressed and stressed conditions, respectively.

Our analysis indicated life-long alterations in several genes with suggested involvement in neurodevelopment, synaptogenesis, neural cell migration, circadian rhythm, behaviour response, lipid metabolism, steroid hormone metabolism, histone modification, and chromatin remodelling were affected in both the unstressed and stressed conditions.

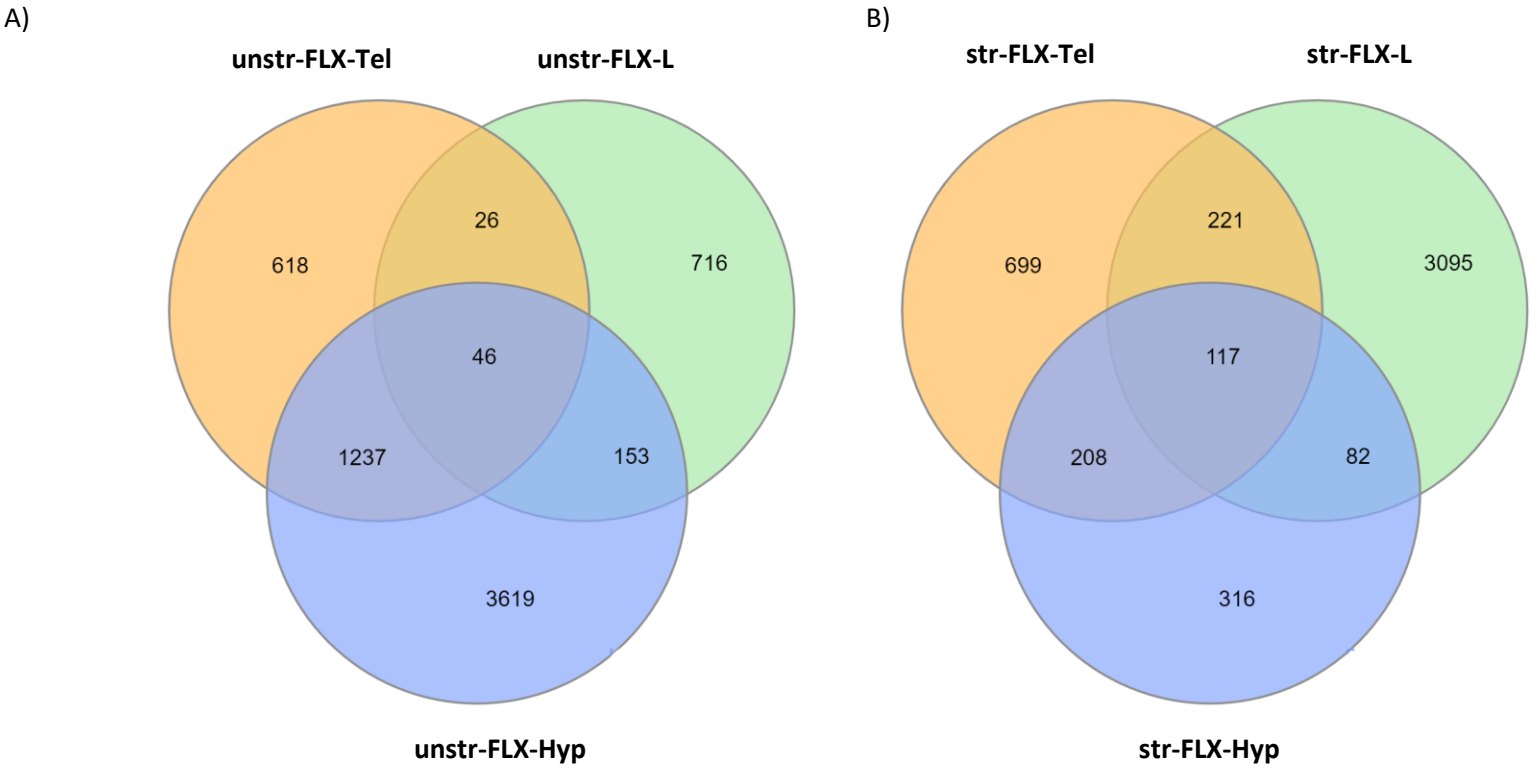

Figure 3.7. Commonly dysregulated genes in larvae and adult zebrafish upon developmental exposure to fluoxetine in stressed and unstressed conditions. A) Venn diagram illustrating the common differentially expressed genes between larval heads and adult telencephalon and hypothalamus in the unstressed condition. B) Venn diagram illustrating the common differentially expressed genes between larval heads and adult telencephalon and hypothalamus in the stressed condition. All significantly dysregulated genes (up or downregulated) were compared (FC≥1.2; p≤0.05). unstr: unstressed condition, str: stressed condition, FLX: fluoxetine, L: larvae, Hyp: hypothalamus, Tel: telencephalon.

Table 3.6. Genes that were dysregulated life-longly upon developmental exposure to fluoxetine in the unstressed condition

Gene symbol		Unstressed			Gene ontology: Biological process
Homo sapiens	***Danio rerio***	**L**	**T**	**H**	
ALCAM	alcama				neuron migration, axonogenesis, neuropeptide hormone activity, circadian rhythm regulation
CCK	cckb				
ITGB1	itgb1b				
CTNNA1	ctnna1				
ABHD17A	abhd17aa				
RAB5A	rab5ab				
PASD1	npas2				
GDPD1	gdpd1				lipid and cholesterol metabolic process
HIGD1B	higd1a				
MLC1	mlc1				
PKD1L3	pkd1a				
ITGAV	itgav				
PARP10	si:ch1073-296d18.1				regulation of chromatin assembly, cell division, and transcription
DYNC1I2	dync1i2b				
SPECC1L	zbtb37				
PURB	purbb				
LARP4	larp4aa				
ZBTB37	specc1lb				
PIGP	pigp				biosynthesis process
ALDH1L2	aldh1l2				

Table 3.6. Genes that were dysregulated life-longly upon developmental exposure to fluoxetine in the unstressed condition (cont…)

Gene symbol is shown for *Danio rerio* (zebrafish) and its associated *Homo sapiens* (human) orthologue. Gene ontology clustering is associated with

Gene symbol		Unstressed			Gene ontology: Biological process
Homo sapiens	***Danio rerio***	**L**	**T**	**H**	
SLC9A3R1	slc9a3r1b				negative regulation of intercellular signaling
RASL11B	rasl11b				
RILPL2	rilpl2				cell morphogenesis
NOXO1	noxo1a				
FAM118B	fam118b				
MFSD14B	mfsd14bb				transmembrane transport
C2orf83	slc19a2				
SLC7A13	si:ch73-352p4.8				
C20orf173	st3gal8				protein binding[+]
CRELD2	creld2				
PTRHD1	ptrhd1				
SLC9A3R1	slc9a3r1b				negative regulation of intercellular signaling
RASL11B	rasl11b				

Homo sapiens orthologs. Red: upregulation, Green: downregulation. L: larvae, T: telencephalon, H: hypothalamus. ([+]) shows GO molecular function instead of GO: Biological process due to no annotation.

Table 3.7. Genes that were dysregulated life-longly upon developmental exposure to fluoxetine in the stressed condition.

Gene symbol		Stressed			Gene ontology: Biological process
Homo sapiens	***Danio rerio***	**L**	**T**	**H**	
ARNTL2	arntl2				regulation of circadian rhythm
ARNTL	arntl1a				
PASD1	npas2				
BHLHE41	bhlhe41				
CIART	ciarta				
SFPQ	sfpq				
IGSF9B	igsf9bb				nervous system, hippocampus, cerebral cortex, and pituitary gland development, response to steroid hormones
NME1	nme2b.2				
MYLIP	mylipb				
DIXDC1	dixdc1b				
KDM1A	kdm1a				
IFRD1	ifrd1				
FAM107B	fam107b				
HSPD1	hspd1				
SRRT	srrt				
BATF2	fosaa				transcription factor activity, sequence-specific DNA binding, negative regulation of transcription
BHLHE41	bhlhe41				
HSF2	hsf2				
ZHX3	si:ch211-232b12.5				
ERCC6	ercc6				

Table 3.7. Genes that were dysregulated life-longly upon developmental exposure to fluoxetine in the stressed condition (Cont…)

Gene symbol		Stressed			Gene ontology: Biological process
Homo sapiens	**Danio rerio**	**L**	**T**	**H**	
HSD11B2	hsd11b2				glucocorticoid biosynthetic process, response to glucocorticoid
ABCA7	abca7				regulation of lipid and cholesterol synthesis, regulation of mitochondrial transport, translation, and respiratory chain
TSPO2	tspo				
PTGES2	ptgesl				
LCN12	ptgdsb.1				
NDUFAF4	ndufaf4				
CHCHD4	chchd4a				
MRPL57	mrpl57				
SURF1	surf1				
TIMM50	timm50				
TOMM40	tomm40				
TRIT1	trit1				
UQCC1	uqcc1				
SLC7A13	si:ch73-352p4.8				regulation of transmembrane transport
SMU1	smu1b				
SLC22A8	slc22a6l				
KCNJ5	kcnj5				
OSGIN2	osgin2				
CARF	carf				calcium channel regulator activity
ATP2A3	atp2a3				
CRISP1	glipr1b				

Table 3.7. Genes that were dysregulated life-longly upon developmental exposure to fluoxetine in the stressed condition (Cont…)

Gene symbol		Stressed			Gene ontology: Biological process
Homo sapiens	***Danio rerio***	**L**	**T**	**H**	
AAMP	aamp				cell differentiation, organs development, vasculogenesis
AIMP1	aimp1b				
F10	f10				
OSR1	osr1				
PAQR7	paqr7b				
HCCS	hccsa.1				
TIPARP	tiparp				
P3H3	p3h3				regulation of mitosis, cell cycle arrest
ERF	erfl3				
PPP1R1C	ppp1r1c				
TBRG4	tbrg4				
CDV3	cdv3				
CAB39	cab39				
FMNL2	fmnl2a				
UBXN6	ubxn6				
C9orf72	zgc:100846				
NEIL1	neil1				regulation of DNA damage checkpoint
WDR76	wdr76				
RAD54L2	rad54l2				
TUT7	tut7				
ECSIT	ecsit				innate immune response
SDHAF4	sdhaf4				

Table 3.7. Genes that were dysregulated life-longly upon developmental exposure to fluoxetine in the stressed condition (Cont…)

Gene symbol		Stressed			Gene ontology: Biological process
Homo sapiens	***Danio rerio***	**L**	**T**	**H**	
GRN	grnb				protein binding and protein folding
SERPINB8	serpinb14				
FAM43B	fam43b				
HSPE1	hspe1				
DNAJC4	dnajc4				
LONRF1	lonrf1l				
RPIA	rpia				ATP biosynthesis process
MT-ATP6	mt-atp6				
GYG1	gyg1b				
RABEP2	rabep2				signal transduction
GUCY1A2	GUCY1A2*				
CBR3	zgc:110339				oxidation-reduction process
SELENOW	selenow1				
TPMT	tpmt.1				methylation
EPHX1	ephx1				xenobiotic metabolic process

Gene symbol is shown for *Danio rerio* (zebrafish) and its associated *Homo sapiens* (human) orthologue. Gene ontology clustering is associated with *Homo sapiens* orthologs. Red: upregulation, Green: downregulation. L: larvae, T: telencephalon, H: hypothalamus. Asterisk (*) represent predicted orthologue.

3.3.6. Life-long effects of developmental exposure to fluoxetine on genes associated with depression, neuroplasticity and epigenetics

A list of 512 genes which are reportedly associated with the major depressive disorder was extracted from the DisGeNET database [215]. Our transcriptome analysis shows that more than 80% of the orthologues of these genes were affected by developmental exposure to FLX at least in one of the studied tissue samples (Supplementary Table 3). Our findings showed that the main dysregulation was in adults hypothalamus in the unstressed condition with 271 depression-associated genes significantly affected. Among these, 73% of genes upregulated and 26% downregulated upon developmental exposure to FLX (Supplementary Table 3).Several genes in the list were downregulated in adult brain following developmental exposure to FLX; for example, in unstressed condition *nrgn* (unstr-FLX-Hyp: FC= -1.4 , p=0.04 ; unstr-FLX-Tel: FC= -1.3 , p=0.008), *fabp2* (unstr-FLX-Hyp: FC=-1.6 , p=0.02 ; unstr-FLX-Tel: FC=-2 , p=0.04), *klf11a* (unstr-FLX-Hyp: FC=-1.4 , p=0.007 ; unstr-FLX-Tel: FC= -1.45 , p= 0.005), and *pvalb6* (unstr-FLX-Hyp: FC=-1.2 , p=0.01 ; unstr-FLX-Tel: FC= -1.6 , p= 0.03) (Table 3.7). Similar life-long downregulation was also observed in the stressed adult zebrafish; for example, *abcc1* (str-FLX-Hyp: FC= -1.7, p= 1.5^{E0-8}; str-FLX-Tel: FC= -1.5 , p= 1.4^{E0-12}), *fkbp4* (str-FLX-Hyp: FC= -1.4, p=1.2^{E0-7} ; str-FLX-Tel: FC=-1.3 , p=9^{E-016}), *pclob* (str-FLX-Hyp: FC= -1.4, p= 0.04; str-FLX-Tel: FC=-1.2 , p= 0.02), *srrt* (str-FLX-Hyp: FC= -1.4, p= 0.00002 ; str-FLX-Tel: FC= -1.3 , p= 0.002), and *tspo* (str-FLX-Hyp: FC= -2, p= 7^{E0-7} ; str-FLX-Tel: FC=-1.7, p= 2^{E0-9}).

We also found that several genes associated with development of depressive disorders were upregulated in adult brain following developmental exposure to FLX; for example, *elovl5* (unstr-FLX-Hyp: FC= 1.7, p=0.001 ; unstr-FLX-Tel: FC= 1.9, p= 0.04; str-FLX-Hyp: FC=1.9, p= 9^{E0-6}; str-FLX-Tel: FC=1.9 , p=0.008) , *tefb* (unstr-FLX-Hyp: FC=2 , p= 4^{E0-6}; unstr-FLX-Tel: FC= 1.5, p= 0.002; str-FLX-Hyp: FC= 1.6, p= 0.002; str-FLX-Tel: FC= 1.8, p= 7^{E0-10}) and *klf15* (unstr-FLX-Hyp: FC= 2.5, p= 2^{E0-7}; unstr-FLX-Tel: FC= 1.7, p= 0.002; str-FLX-Hyp: FC= 1.6, p= 0.006; str-FLX-Tel: FC= 1.4, p=0.03)*;* were upregulated in both adult telencephalon and hypothalamus in both unstressed and stressed conditions (Table 3.8). Our findings also reveal that several members of the genes associated with development of depressive disorders were upregulated in adult brain following developmental exposure to FLX only in the unstressed condition; for example: *nr3c2* (unstr-FLX-

Hyp: FC= 3.12, p= 2^{E0-5}; unstr-FLX-Tel: FC= 1.6, p= 0.01), *clocka* (unstr-FLX-Hyp: FC= 2, p= 2^{E0-6}; unstr-FLX-Tel: FC= 1.4, p= 0.03), *grm3* (unstr-FLX-Hyp: FC= 2.3, p= 5^{E0-6}; unstr-FLX-Tel: FC= 1.8, p= 0.02), and *ntrk2a* (unstr-FLX-Hyp: FC= 1.7, p= 3^{E0-12}; unstr-FLX-Tel: FC= 1.4, p= 0.006) (Table 3.8). Additionally, genes associated with development of depressive disorders were upregulated in adult brain following developmental exposure to FLX only in stressed condition; for example: *grm2a* (str-FLX-Hyp: FC=1.2, p= 0.01; str-FLX-Tel: FC= 2, p= 1.2^{E0-7}), *per1b* (str-FLX-Hyp: FC= 1.8, p= 5^{E0-4}; str-FLX-Tel: FC= 1.7, p= 2^{E0-8}) and *per1a* (str-FLX-Hyp: FC= 3, p= 5^{E0-6}; str-FLX-Tel: FC= 2.6, p= 2^{E0-7}) (Table 3.8).

A list of genes annotated for neural plasticity, synaptogenesis, and neurogenesis was extracted from the Gene Ontology database using *Homo sapiens* GO biological process annotations (Supplementary Table 4). Table 3.9 shows the significantly dysregulated genes upon developmental exposure to FLX in larvae and adult zebrafish in a both unstressed and stressed condition. The hypothalamus and telencephalon in the unstressed condition were affected more by developmental exposure to FLX than other groups. From the common 19 genes affected by developmental exposure to FLX in adult brain tissues, 14 genes were upregulated, and 4 genes downregulated.

Moreover, a list of genes involved in epigenetics was extracted from the Gene Ontology data base using *Homo sapiens* GO: biological process annotations (Supplementary Table 6). Table 3.10 shows the significantly dysregulated genes upon developmental exposure to FLX in larvae and adult zebrafish in both unstressed and stressed condition. Our findings showed that upregulation of these genes in unstressed condition the hypothalamus and telencephalon of adult zebrafish was the main effect. For example, *hdac4* (unstr-FLX-Hyp: FC=2.2, p= 2.2^{E0-5}; unstr-FLX-Tel: FC= 1.5, p= 0.005) *hdac5* (unstr-FLX-Hyp: FC=2, p= 1.4^{E0-6}; unstr-FLX-Tel: FC= 1.4, p= 0.02), *adarb1b* (unstr-FLX-Hyp: FC=2.6, p= 0.0002; unstr-FLX-Tel: FC= 1.6, p= 0.4), *adarb2* (unstr-FLX-Hyp: FC=2.6, p= 0.0001; unstr-FLX-Tel: FC= 1.8, p= 0.04), *dnmt3aa* (unstr-FLX-Hyp: FC= 2, p= 5^{E0-5}; unstr-FLX-Tel: FC= 1.7, p= 0.004), and *hcn1*(unstr-FLX-Hyp: FC= 2.7, p= 1.2^{E0-5}; unstr-FLX-Tel: FC= 1.6, p= 0.03) were upregulated upon developmental exposure to FLX.

Overall, our findings showed that a high number of genes associated with the development of depressive disorders, neural plasticity and epigenetics were life-longly dysregulated by

developmental exposure to FLX. We also report that developmental exposure to FLX affected gene expression in the adult brain, particularly in the unstressed condition.

Table 3.8. Life-long downregulation of genes associated with depressive disorders upon developmental exposure to fluoxetine

Gene symbol		Unstressed			Stressed			Gene ontology: Biological process
Homo sapiens	***Danio rerio***	**L**	**H**	**T**	**L**	**H**	**T**	
CITED1	cited1							brain development
CITED2	cited2							brain development
FABP2	fabp2							triglyceride catabolic process
GSK3B	gsk3b							circadian rhythm
KLF11	klf11a							negative regulation of transcription
LDHA	ldha							positive regulation of apoptotic process
OLIG1	olig1							neuron fate commitment, regulation of transcription
PTPRR	ptprr							negative regulation of ERK1 and ERK2 cascade
PVALB	pvalb6							regulation of cytosolic calcium ion concentration
SIGMAR1	sigmar1							nervous system development, lipid transport
VEGFA	vegfab							angiogenesis, organogenesis
NRGN	nrgna							nervous system development, telencephalon development
ABCC1	abcc1							transport across blood-brain barrier
FKBP4	fkbp4							regulation of neuron development, steroid hormone receptor assembly
HSP90AA1	hsp90aa1.2							central nervous system neuron axonogenesis
LRP8	lrp8							cellular response to cholesterol
NDUFV1	ndufv1							mitochondrial respiratory chain complex I assembly
PCLO	pclob							pre-synapse to nucleus signaling pathway
SOD2	sod2							neuron development
SRRT	srrt							gene silencing by RNA
TEF	tefa							regulation of transcription
TOMM40	tomm40							transmembrane transport
TSPO2	tspo							intracellular cholesterol transport

Gene symbol is shown for *Danio rerio* (zebrafish) and its associated *Homo sapiens* (human) orthologue. Gene ontology clustering is associated with *Homo sapiens* orthologs. Red: upregulation, green: downregulation, Grey: statistically non-significant fold change. L: larval heads, T: telencephalon, H: hypothalamus

Table 3.9. Life-long upregulation of genes associated with depressive disorders upon developmental exposure to fluoxetine

Gene symbol		Unstressed			Stressed			Gene ontology: Biological process
Homo sapiens	***Danio rerio***	**L**	**H**	**T**	**L**	**H**	**T**	
BCL2L1	bcl2l1							neuron apoptotic process
CFP	si:ch73-237c6.1							immune response
CHRFAM7A	chrna7							cellular calcium ion homeostasis
GRM2	grm2a							regulation of synaptic transmission
PER1	per1b							regulation of circadian rhythm
PER1	per1a							regulation of circadian rhythm
TEF	tefb							positive regulation of transcription from RNA polymerase II promoter
ELOVL5	elovl5							sphingolipid biosynthetic process
KLF15	klf15							positive regulation of transcription from RNA polymerase II promoter
NR3C2	nr3c2							steroid hormone mediated signaling pathway
ADARB1	adarb1b							RNA processing, negative regulation of cell migration
ADARB2	adarb2							RNA processing
ARRB1	arrb1							regulation of ERK1 and ERK2 cascade
CDK5R1	cdk5r1a							brain development
CHRM2	chrm2a							nervous system development
CLOCK	clocka							regulation of circadian rhythm
CREM	crema							regulation of circadian rhythm
DRD1	drd1b							behavioral fear response, synaptic transmission
GABBR1	gabbr1a							gamma-aminobutyric acid signaling pathway
GRM3	grm3							regulation of synaptic transmission
HLF	hlfb							multicellular organism development
KLHL5	klhl5							protein ubiquitination

Gene symbol is shown for *Danio rerio* (zebrafish) and its associated *Homo sapiens* (human) orthologue. Gene ontology clustering is associated with *Homo sapiens* orthologs. Red: upregulation, Green: downregulation, Grey: non-significant fold change. L: larvae, T: telencephalon, H: hypothalamus.

Table 3.9. Life-long upregulation of genes associated with depressive disorders upon developmental exposure to fluoxetine (cont…)

Gene symbol		Unstressed			Stressed			Gene ontology: Biological process
Homo sapiens	***Danio rerio***	**L**	**H**	**T**	**L**	**H**	**T**	
MAGI2	magi2b							positive regulation of neuron projection development
MAPK10	mapk10							regulation of circadian rhythm
NCAM1	ncam1a							regulation of synaptic plasticity
NCAN	CU861477.1							central nervous system development
NOTCH1	notch1b							axonogenesis
PEA15	pea15							DNA damage checkpoint
PHF21B	PHF21B							regulation of transcription
SLC2A1	slc2a1a							glucose transmembrane transport
SLC2A1	slc2a1b							glucose transmembrane transport
TBC1D9	tbc1d9							intracellular protein transport
TBC1D9B	tbc1d9							intracellular protein transport
THSD7A	thsd7ab							cell differentiation, angiogenesis
TNFAIP3	tnfaip3							immune response
TPPP	TPPP							microtubule bundle formation
VDR	vdrb							cellular calcium ion homeostasis
ZNF804A	znf804a							regulation of neuron projection development
AVPI1	si:ch211-197k17.3							activation of MAPK activity, cell cycle
CC2D1A	FO704915.1							positive regulation of I-kappaB kinase/NF-kappaB signaling
CIT	citb							nervous system development
CIT	cita							nervous system development
FGFR2	fgfr2							positive regulation of cell proliferation
GRIK3	GRIK3*							glutamate receptor signaling pathway

Table 3.9. Life-long upregulation of genes associated with depressive disorders upon developmental exposure to fluoxetine (cont…)

Gene symbol		Unstressed			Stressed			Gene ontology: Biological process
Homo sapiens	***Danio rerio***	**L**	**H**	**T**	**L**	**H**	**T**	
HDAC5	hdac5							chromatin silencing
KDR	kdr							positive regulation of cell proliferation
KLF12	klf12b							positive regulation of transcription from RNA polymerase II promoter
KLHL25	enc2							regulation of translational initiation
LRFN5	lrfn5a							chemical synaptic transmission, axonogenesis
NTRK2	ntrk2a							positive regulation of neuron projection development
QKI	qkib							positive regulation of gene expression, myelination
RAPGEF5	rapgef5a							nervous system development
SLC2A12	slc2a12							glucose transmembrane transport
SLC6A13	SLC6A13*							neurotransmitter transport
SOX9	sox9a							positive regulation of cell proliferation
TNFRSF4	tnfrsfa							immune response
SLC1A3	slc1a3b							neurotransmitter transport

Table 3.10. Life-long dysregulation of genes involved in neurogenesis and neural plasticity upon developmental exposure to fluoxetine.

Gene symbol		Unstressed			Stressed			Gene ontology: Biological process
Homo sapiens	***Danio rerio***	**L**	**T**	**H**	**L**	**T**	**H**	
BAIAP2	baiap2a							regulation of synaptic plasticity
BAIAP2	baiap2b							
CALB1	calb1							
CDK5	cdk5							
NPAS4	npas4a							
NPAS4	NPAS4B							
P2RX3	p2rx3b							
RAPGEF2	rapgef2							
SYT7	syt7a							regulation of short-term neuronal synaptic plasticity
RAB3A	rab3ab							
SHISA8	SHISA8							
SHISA7	shisa7a							
SHISA8	shisa8b							
SHISA8	shisa9b							
SHISA6	shisa6							
SHISA8	shisa9a							
UNC13A	unc13a							
UNC13B	UNC13B							

Gene symbol is shown for *Danio rerio* (zebrafish) and its associated *Homo sapiens* (human) orthologue. Gene ontology clustering is associated with *Homo sapiens* orthologs. Red: upregulation, Green: downregulation, Grey: non-significant fold change. L: larvae, T: telencephalon, H: hypothalamus.

Table 3.10. Life-long dysregulation of genes involved in neurogenesis and neural plasticity upon developmental exposure to fluoxetine (cont…)

Gene symbol		Unstressed			Stressed			Gene ontology: Biological process
Homo sapiens	*Danio rerio*	L	T	H	L	T	H	
KCNB1	kcnb1							positive regulation of long-term synaptic depression
ADORA1	adora1b							nervous system development
APP	appb							
BDNF	bdnf							
SLC4A10	slc4a10b							
CRH	crhb							long-term synaptic potentiation
DRD1	drd1b							
MAPK1	mapk1							
NLGN1	nlgn1							
NPTN	nptna							
NTRK2	ntrk2a							
NTRK2	ntrk2b							
PRKCZ	prkcz							
PTK2B	ptk2ba							
SHANK3	shank3a							
SLC24A2	SLC24A2							
SLC8A2	slc8a2b							
SLC8A3	slc8a3							
SNAP25	snap25a							
SNAP25	snap25b							
SNAP47	snap47							
GRIA1	gria1b							long term synaptic depression
PICK1	pick1							
STXBP1	stxbp1a							

Table 3.10. Life-long dysregulation of genes involved in neurogenesis and neural plasticity upon developmental exposure to fluoxetine (cont…)

Gene symbol		Unstressed			Stressed			Gene ontology: Biological process
Homo sapiens	***Danio rerio***	**L**	**T**	**H**	**L**	**T**	**H**	
CAMK2B	camk2b2							regulation of long-term neuronal synaptic plasticity
DLG4	dlg4a							
GRIK2	GRIK2							
GRM5	grm5b							
HRAS	hrasa							
KCNJ10	kcnj10a							
KCNJ10	KCNJ10							
KRAS	kras							
NF1	nf1b							
RAB11A	rab11a							
RAB8A	rab8a							
SYNGAP1	syngap1a							
SYNGAP1	syngap1b							
SYNGR1	syngr1a							
SYP	sypb							
DGKI	DGKI							regulation of long-term synaptic depression
CDC42	cdc42							regulation of filopodium assembly
PPP1R9A	ppp1r9a							
RAB5A	rab5ab							

Table 3.10. Life-long dysregulation of genes involved in neurogenesis and neural plasticity upon developmental exposure to fluoxetine (cont…)

Gene symbol		Unstressed			Stressed			Gene ontology: Biological process
Homo sapiens	*Danio rerio*	L	T	H	L	T	H	
APOE	apoeb							regulation of neuronal synaptic plasticity
APOE	apoea							
CAMK2A	camk2a							
CNTN2	robo4							
DBN1	dbn1							
EGR2	egr2b							
NSMF	nsmfa							
RASGRF1	RASGRF1							
CRTC1	crtc1a							positive regulation of long-term synaptic potentiation
CRTC1	crtc1b							
NRGN	nrgna							
STAU1	stau1							
EPHB2	ephb2a							positive regulation of long-term neuronal synaptic plasticity
KIT	kitb							
NEURL1	neurl1aa							

Table 3.10. Life-long dysregulation of genes involved in neurogenesis and neural plasticity upon developmental exposure to fluoxetine (cont…)

Gene symbol		Unstressed			Stressed			Gene ontology: Biological process
Homo sapiens	Danio rerio	L	T	H	L	T	H	
ADCY8	adcy8							learning
JPH3	jph3							
ABL1	abl1							associative learning
RIN1	rabgef1l							
RIN1	rin1a							
SYNPO	LO018188.1							regulation of stress fiber assembly
EPHA4	epha4l							regulation of axonogenesis
MAPT	maptb							neuron migration, axon extension
MAPT	mapta							

Table. 3.11. Life-long dysregulation of genes involved in epigenetics upon developmental exposure to fluoxetine.

Gene symbol		Unstressed			Stressed			Gene ontology: Biological process
Homo sapiens	**Danio rerio**	**L**	**T**	**H**	**L**	**T**	**H**	
ACTR2	actr2b							Arp2/3 complex-mediated actin nucleation
ACTR3B	actr3b							
HDAC4	hdac4							chromatin remodeling
HDAC5	hdac5							
KAT2A	kat2a							
KAT2B	kat2b							
ACTR1A	actr1							G2/M transition of mitotic cell cycle
ADARB1	adarb1b							mRNA processing
ADARB2	adarb2							
ATF2	atf2							negative regulation of transcription from RNA polymerase II promoter
DNMT3A	dnmt3aa							
FOSB	fosb							
HDAC8	hdac8							
MECP2	mecp2							
FP565260.4	dnmt3bb.3							novel protein
HCN1	hcn1							regulation of postsynaptic membrane potential

Gene symbol is shown for *Danio rerio* (zebrafish) and its associated *Homo sapiens* (human) orthologue. Gene ontology clustering is associated with *Homo sapiens* orthologs. Red: upregulation, Green: downregulation, Grey: non-significant fold change. L: larvae heads, T: telencephalon, H: hypothalamus.

3.4. Discussion

Our findings provide extensive evidence for life-long dysregulation of genes upon developmental six-days exposure to FLX. Numerous genes were affected in both larvae and adult zebrafish, with many involved in neural development, cell signalling, and lipid metabolism. We report that 1927 and 1245 genes were significantly affected in the unstressed and stressed adult telencephalon, respectively, following developmental exposure to FLX. Such life-long effects were also observed in the hypothalamus, with 5055 and 723 genes being significantly dysregulated in unstressed and stressed adult zebrafish, respectively. There are many studies in teleosts on the potential adverse effects of FLX; however, to our knowledge, only a few studies investigated the transcriptomic effects of this psychoactive compound [216-218]. For example, Wong *et al*., (2013) showed that two weeks of exposure to FLX (100 µg/L) resulted in the dysregulation of 411 genes in the whole brain of adult male zebrafish [218]. The GO term analysis performed showed enrichment of pathways associated with lipid metabolism and small molecule biosynthesis [218]. Wu *et al.,* (2017) determined that five days embryonic-exposure to FLX (10 µg/L) affected the expression of 32 genes in 124 hpf larvae; amongst them, *egr4, ptgdsb, per1, per2, sfpq, crebzf,* and *nr1d1* which are involved in circadian rhythm regulation [216]. In another study using the Affymetrix GeneChip Zebrafish Array, Park *et al.,* (2012) showed that 96h exposure to FLX in two different concentrations, 25 µg/L and 250 µg/L, resulted in significant dysregulation of 288 and 131 genes in 3 dpf zebrafish whole larvae, respectively [217]. In their study, amongst the shared 81 genes affected by both concentrations of FLX, the gene ontology (GO) terms associated with Physiological Process, Cellular Process, and Metabolism were enriched [217]. Moreover, in a recently published study, Huang *et al.*, (2020) showed dysregulation of 1518 and 170 genes in the individual larval brain upon developmental 6 days exposure to paroxetine (100µg/L) and FLX (100µg/L); respectively. The functional clustering analysis showed enrichment of GO terms associated with mitochondrial and neuronal structures, mitochondrial respiration, and neurodevelopmental processes [219].

In this study, we used Qiagen IPA software for pathway analysis, and since IPA was not cover zebrafish annotation at the time of writing this manuscript, we had to convert the list of DEGs to their *Homo sapiens* orthologues. Given the high level of genome conservation between

humans and zebrafish, we believe the inferred pathway dysregulations are valid, particularly when our data is compared to human and other mammalian models. In the current study, we report that more pathways were affected in the hypothalamus than the telencephalon in both unstressed and stressed conditions in adult zebrafish, which were developmentally exposed to FLX. Our data showed the life-long alteration of several orthologue pathways involved in neuroendocrine signalling, cholesterol metabolism, and synaptogenesis. Moreover, the network prediction study performed supported similar findings with networks involved in lipid metabolism, molecular transport, and nervous system development were enriched and presented in both larvae and as adults, also suggestive of life-long effects.

The upstream regulator analysis performed showed potential dysregulation of transcription factors involved in circadian rhythm, stress response, cholesterol metabolism, and histone modifications that may drive observed life-long effects. For example, the transcriptomic pattern analysis showed a dysregulation signalling pathway associated with *clocka* (orthologue to CLOCK in *Homo sapiens*). This dysregulation was observed in unstressed larvae, stressed larvae, and stressed adults upon developmental exposure to FLX. Circadian locomotor output cycles kaput protein (CLOCK) plays a central role in regulating circadian rhythms in all vertebrates [220]. This gene is related to Period (PER1, PER2, PER3) and Cryptochrome (CRY1 and CRY2) genes [220]. Several mental and metabolic disorders in human are associated with dysregulation of CLOCK and its related genes, including major depressive disorder, bipolar disorder, schizophrenia, diabetes mellitus and obesity [221]. Disruption of CLOCK related genes have already been reported in both rodent and teleost models. For example, Kiryanova *et al.,* (2016) showed that developmental exposure to FLX in mice (administering 25 mg/kg/day FLX to the drinking water of the pregnant dam) could disrupt the normal circadian rhythm in the adolescent two months old male offspring [222]. This was evident by a significantly higher number of days needed for the affected individuals to adapt to a new day-light cycle [222]. Moreover, it is known in zebrafish that FLX exposure decreases the amount of melatonin production, potentially leading to altered circadian rhythm [114]. For example, Wu *et al.,* (2017) have shown several genes associated with circadian rhythm regulations, including *nr1d1* and *per2*, were affected upon exposure to FLX (10 µg/L), amitriptyline (0.1 µg/L), and mianserin (10 µg/L) [216].

The transcriptomic patterns also showed a life-long dysregulation in signalling pathways associated with *nr3c1* (orthologue to NR3C1 in *Homo sapiens*), the glucocorticoid receptor (GR). This dysregulation was observed in both larvae and adult hypothalamus in stressed condition upon developmental exposure to FLX. Impairment of stress axis upon exposure to FLX is also reported in both rodents and teleost models. It is shown that perinatal exposure to SSRIs resulted in decreased circulatory cortisol in human infants and rodents [197, 223-225]. For example, *Pawloski et al.*, (2018) also showed 28-days maternal prenatal exposure to FLX in rats resulted in blunted corticosterone levels and reduced GR expression in the hippocampal region more prominent in adolescent male offspring [226]. Such decreased levels of cortisol also reported in zebrafish. For example, Giacomini *et al.,* (2016) reported that adult male zebrafish exposed to FLX (50µg/L) for 15 days showed reduced cortisol levels and a blunted stress response upon exposure to the novel tank test [127]. Abreu *et al*., (2017) also reported a blunted cortisol levels in six-month-old adult zebrafish exposed to FLX (50µg/L) following both physical (chasing) and chemical (osmotic shock) stress [211]. A similar blunted cortisol level was reported upon 15 minutes of exposure to a lower concentration of FLX (1µg/L) before the osmotic stressor in adult zebrafish [227]. Recently in our lab, Vera-Chang *et al.*, (2018, 2019) reported that developmental six-days exposure to FLX (54µg/L) could result in a blunted stress response in the descendant adults and descendant generations; at least for three generations in male zebrafish [2]. We found that the developmental exposure to FLX affected many endocrine pathways in the adult hypothalamus. Among these pathways associated with GNRH signaling, glucocorticoid receptor signaling, aldosterone receptor signaling, androgen signaling, relaxin signaling, and prolactin signaling in both stressed and unstressed conditions. It should be noted that zebrafish and other teleost do not have aldosterone and it is cortisol that binds to *nr3c2* (mineralocorticoid receptor, *mr*) to control electrolyte balance [228]. The aldosterone receptor signaling canonical pathway that is shown affected in our data set is likely due to using *Homo sapiens* orthologues for our IPA analysis. It is also well-documented that MR in the brain has 10 times more affinity for GCs in mammalians and is believed to be the main responder to basal cortisol [25, 228]. The clustering of genes associated with *mr*, in our transcriptomic analysis of the brain, could be another explanation of the observed feature regarding the aldosterone receptor signalling pathway.

The genes whose *Homo sapiens* orthologues are associated with the development of major depressive disorder were affected by developmental exposure to FLX in our study. To date, 512 genes have been clinically associated with the development of the major depressive disorder and similar mental ailments [215]. Our findings showed that the orthologues of many of these genes were upregulated in the adult telencephalon and hypothalamus, particularly in the unstressed conditions in the zebrafish model. Based on a separate GO-term clustering analysis performed using DAVID, many of these genes were implicated in nervous system development, regulation of synaptic transmission, circadian rhythm, cholesterol metabolism, and steroid hormone signalling.

A life-long dysregulation of several genes observed which their *Homo sapiens* orthologues are implicated in neurogenesis and synaptogenesis. It is known that the neurogenesis in adult zebrafish telencephalon shares high levels of cellular and molecular similarities with mouse telencephalon [229, 230]. The radial glial cells in zebrafish brains are considered homologous to the rodents' neural stem cells [230]. For example, we observed life-long dysregulation of *bdnf*, *trkb* (bdnf receptor), and *npas4* (a *bdnf* transcriptional regulator) in FLX-exposed larvae and their descendant adults. These genes' regulation is essential for neurogenesis in adult zebrafish and is affected by stress and SSRI exposure [229-231]. For example, it is shown that chronic stress (daily crowding, chasing, and irregular 15 minutes of light exposure) could upregulate bdnf in zebrafish brain [231].

Theodoridi *et al.,* (2017) have shown FLX exposure has anti-aggression properties in dominant zebrafish which is likely mediated by upregulation of BDNF in the adult brain [232]. Several studies in humans and mammalian models suggested a correlation between the development of depression and a decreased level of neurogenesis [75, 82, 233]. The inhibition of neurogenesis by neurotoxins, chronic corticosteroid treatment, or irradiation could result in depression and anxiety-like behaviours in mice and hinders the positive effect of FLX treatment [234-236]. Other studies suggested that the response to SSRIs therapy is related to changes in neurogenesis as well [76]. For example, the promotion of neurogenesis by inactivation of the pro-apoptotic gene, Bax, could alleviate the depression-related behaviours in chronically stressed mice [237]. The BDNF and TrKB-mediated neurogenesis and synaptogenesis are suggested as

therapeutic means for FLX in humans [60]. Also, it is shown that NPAS4 is significantly downregulated in the hippocampus and prefrontal cortex of SERT-/- rats; a mammalian model for mood disorders [238]. Also, in rats, early life exposure to SSRIs reduced social behaviours and social preference later in life during the juvenile period and adulthood in both sexes [239, 240]. This could be explained by the time needed for neural reprogramming and hippocampus reinstitution of plasticity as the mean therapeutic effects of SSRIs [75].

It is known that SSRIs may reinstate the plasticity of the nervous system by enhancing neurogenesis and synaptogenesis through the adjustment of epigenetics markings of genes [52, 76, 101, 241]. Our study showed evidence of life-long effects of developmental exposure to FLX by tracing the expression pattern of genes associated with epigenetic machinery. Several genes, including *dnmt3a, adarb1, adarb2, hdac4, hdac5, hdac8,* and *atf2* were significantly affected by FLX exposure in our study. Interestingly, the upregulation of these genes in the adult neural circuits was the main trait. Similar findings are reported in zebrafish upon exposure to SSRIs. Alteration of epigenetic-related mechanisms has already been reported in zebrafish upon exposure to FLX. For example, Martinez *et al.,* (2019) have shown a similar developmental exposure to FLX, resulted in decreased *dnmt3a* transcript deposit in the eggs collected from 5 months old female zebrafish [4]. Moreover, they reported an increased amount of several microRNAs, which could target stress-related transcripts in the eggs from the same female zebrafish [4]. Although the exact mechanism was not studied, the recent study in our lab, reporting a transgenerational hypocortisolism in zebrafish for at least three generations upon developmental exposure to FLX, supports the possible involvement of epigenetic mechanisms [1, 2].

Epigenetic mechanisms in the development of clinical depression in humans have been extensively investigated [75, 78, 81, 242-244]. An increasing body of evidence attributes the beneficiary response to antidepressant therapies to epigenetics [245, 246]. For example, Vatencourt *et al.,* (2011) showed that FLX therapy transiently increased *Bdnf* expression in adult rats' visual cortex [247]. This was accompanied by increased H3K9 acetylation of the *Bdnf* promoter, a chromatin remodelling associated with the epigenetic marking of DNA [247]. Moreover, Wang *et al.,* (2011) showed that FLX treatment after traumatic brain injury could

increase the rate of neurogenesis. This increase in neurogenesis coincided with an increase in H3K9 acetylation and MBD-1 (methyl-CpG-binding protein 1) immunoreactive cells in the hippocampal region treated mice [248]. In yet another study, Robinson *et al.* reported that FLX reduced the acetylation of histone three(H3) at the promoter region of CaMKIIa in mice model for anxiety-like behaviour [249]. This resulted in a downregulation in CaMKIIa, which improved the mood and behaviour of mice [249]. Zaidan *et al.* (2018) demonstrated that pre-gestational FLX treatment of the dam enhances ADAR enzymes' expression, a family of RNA editing enzymes associated with epigenetic marking, in the offspring amygdala in rats [250]. This change was associated with the reversal of the effects of pre-reproductive stress of dam on adult offspring's social behaviour [250].

The technical considerations in our study's design have improved the impact of our results. Based on our knowledge, this is the first time that the life-long effects of developmental exposure to FLX on brain transcriptome are studied in both stressed and unstressed conditions in zebrafish. Moreover, by using eGFP mRNA as an alternative route to measure stress response, we could track the stress axis's activation in our animal models. Based on our knowledge, this is the first time that such an approach is used in the transcriptomic analysis of stress response in zebrafish. By focusing our transcriptomic analysis on brain tissues, we could decrease the background noise compared to previous whole-body transcriptomic studies, which dramatically affected the number of our DEGs.

By studying the telencephalon and hypothalamus separately, we were able to increase our data set's resolution by reducing the effect of whole brain heterogenicity, which is reported to affect transcriptomic data [251]. Although we used the recommended FC≥ 1.2 for analysis of brain transcriptomic data [214], our findings showed that using higher thresholds, for example, FC≥1.5 or even FC≥2, likely provide a similar finding. A repeated data analysis using these strict thresholds should be performed in future.

In conclusion, we provided extensive evidence of life-long dysregulation of numerous genes upon developmental exposure to FLX in the adult zebrafish brain. We also showed many similar findings to mammalian models, which further supports the benefits of using zebrafish in neuropsychological studies of anti-depressants' effects. Using orthologue conversion, we showed

life-long disruption of several pathways associated with neuroendocrine signalling, stress response and circadian rhythm upon developmental exposure to FLX, all of which are implicated in the development of depressive disorders in humans. Also, the observed life-long alterations of epigenetic modifying enzymes and genes involved in the neurogenesis could explain the dysregulation observed in these major hypothalamic pathways. Overall, our study provided more insight into the potential pathways responsible for the long-lasting effects of FLX using a zebrafish model andshowed the benefits of using a stress-inducible transgenic line to track stress response in transcriptomic analysis.

3.5. Statement of contribution

Amin Nozari, designed the study and methodology, conducted most of the experiments and analyses and prepared the manuscript. Rémi Gagné (Environment Health Centre of Health Canada) performed the RNA Sequencing and all associated analysis. Dr. Carole Yauk (Environment Health Centre of Health Canada) assisted with the RNA Sequencing experimental design. Dr. Vance Trudeau helped with the design of the study and manuscript editing.

CHAPTER 4: Application of SR4G transgenic zebrafish line as a biomonitoring assay to detect altered stress response.

4.1. Introduction

According to the Environmental Risk Assessment Guidelines of the European Medicines Agency (EMEA), the study of potential risks of pharmaceuticals consists of two phases [119]; in phase I, the environmental concentration of the pharmaceutical is predicted (PEC), and the risk of bioaccumulation of the pharmaceutical in the aquatic food chain is assessed. If the PEC was less than 0.01 µg/L, and no bioaccumulation concern was apparent, the environmental risk is considered unlikely. When one or both clauses were false, phase II is conducted by environmental fate and effect analysis. In this phase, all data from the toxicity tests (ecological effects), the exposure information, and assumptions are combined to characterize exposure and risk. The compound's behaviour in the environment is predicted using computational modelling, and risk management advice is generated. Potential endocrine disrupting compounds (EDCs) enter phase II of the risk assessment directly regardless of their PEC according to EMEA guidelines[119].

The eggs and embryos of aquatic vertebrates such as fish and frogs are directly exposed to environmental contaminants and are vulnerable to the potential adverse effects because of their external fertilization and development [146]. Many environmental hazards originate from municipal and industrial waste management facilities [252, 253]. Among the most studied environmental contaminants, EDCs, pharmaceuticals (PCs), and agricultural pesticides have shown to affect many aspects of embryonic development in aquatic vertebrates [162]. Moreover, EDCs with their potential to interfere with hormonal systems are of potenital risk for a developing embryo [254-256]. These endocrine disruption properties affect the survivability and normal development of an exposed embryo, but an increasing body of evidence supports the long-lasting effects of such an exposure to adulthood and even to the descendant generations [254, 256-258]. For example, reduced fertility, altered sexual behaviour, altered locomotion, and reduced stress and anxiety-like responses have been reported in adult teleost exposed to EDCs during early life stages [199, 259].

According to guidelines from the Organization for Economic Co-operation and Development (OECD), several members of the teleost family, including zebrafish (*Danio rerio*), fathead minnow (*Pimephales promelas*), Japanese medaka (*Oryzias latipes*), bluegill (*Lepomis macrochirus*), and rainbow trout (*Oncorhynchus mykiss*) have been used in the Acute Fish Toxicity test as a part of “hazard and environmental risk assessment” studies [159]. Recently,

a modified version of this, the zebrafish embryo acute toxicity test (ZFET) has been validated by regulatory bodies for environmental exposure risk assessment, given its high predictive capacity [159, 162]. Zebrafish larvae are considered a valuable animal model in toxicological assessments, particularly for their potential to bridge *in vitro* and *in vivo* studies [146, 150, 160, 169]. Zebrafish embryos rapidly develop from a single-cell stage to fully functional multi-organs larvae in 4 to 5 days; therefore, an excellent model to study developmental toxicology [260]. Their external development makes the experimental manipulations more feasible compared to mammalian models [260]. High fecundity provides an adequate sample size for high-throughput studies, which is less convenient with many other *in vivo* animal models [260]. The traditional assessment of morphological changes upon exposure to different arrays of potential toxicants is well-documented for zebrafish embryos, and automation protocols have already been described [261]. Gene expression analysis, behavioural monitoring, and fluorescence imaging of inducible transgenes have been recently described as potential endpoints for biomonitoring approaches using zebrafish [150]. Overall, the small size, easy dosing, moderate skin transparency, and rapid development further contribute to the choice of zebrafish embryos and larvae for high-throughput screening for potential toxicants [150, 160, 161, 163, 202, 262].

In the current study, we propose using a stress-inducible eGFP (at mRNA and protein levels) in the transgenic zebrafish SR4G line to detect normal and blunted stress responses [5]. Several environmental contaminants have been shown to affect the stress-axis in zebrafish larvae. For example, exposure to PBDEs (the main compound in flame retardants) resulted in *crhb* and *tshba* upregulation in zebrafish larvae [184]. In another example, exposure to low doses of BPA (0.0068 µM), a widely used plasticizer, has altered neurogenesis in the hypothalamus of developing zebrafish larvae [263]. There is extensive evidence regarding the effects of SSRIs on stress response in fish. Recent studies from our lab, including the previous chapter (Chapter 3), have shown blunted stress response in zebrafish larvae upon developmental exposure to FLX [1, 2, 4, 199]. In Chapter 2 of this thesis, using the SR4G transgenic line, we showed that the whole-body ubiquitous expression of eGFP, following exposure to stress, provides high fluorescence intensity levels in zebrafish larvae which is detectable by standard laboratory imaging equipment. Also, we provided some evidence of a close correlation between cortisol and eGFP mRNA in this line.

Furthermore, in Chapter 3, we showed the potential of using eGFP transcript as an internal control to track stress response in both larvae and adult zebrafish. Here we tested the hypothesis of using the whole-body eGFP mRNA and the whole-body eGFP fluorescence in the SR4G transgenic line as alternative to cortisol measurements to assess stress disruption.

As a proof-of-concept, the whole-body levels of cortisol, eGFP mRNA, eGFP fluorescence and mRNA levels of 11 target genes were studied upon exposure to BPA, FLX, and vinclozolin (VIN) [52, 183, 219, 258, 264-266]. Cortisol (CORT) and dexamethasone (DEX) were used as positive and negative controls, respectively. The 11 target genes with known involvement in stress response and neurogenesis in *Homo sapiens* and rodent models were selected. Our findings suggested that two predictive models trained on whole-body eGFP mRNA and 11 target genes could predict stress disruption in transgenic zebrafish larvae. Our findings support the use of stress-inducible transgenic zebrafish for medium- to high-throughput screening as a tier-1 test in risk assessment studies.

4.2. Materials and methods

4.2.1. Animals and Husbandry

The SR4G transgenic zebrafish line was kindly provided by Dr. Karl Clark (Mayo Clinic, Minnesota, USA) and Dr. Xiao-Yan Wen (University of Toronto, Ontario, Canada). The one-day post-fertilization embryos were transferred to Ottawa and placed in the quarantine room of the University of Ottawa's aquatic facility per regulations of Animal Care and Veterinary Services (ACVS). The embryos allowed to hatch and were raised in the quarantine facility until they reached six months of age. These zebrafish were used to establish our founder generation. The F_0 generation was bred from this founder line.

4.2.2. Study design

All experiments were conducted with six experimental replicates containing 22-28 individual zebrafish larvae (sampling unit; 7 dpf) raised in a separate container from other experimental replicates to avoid pseudo-replication (Supplementary Figure 6). The following endpoints were studied: whole-body cortisol, whole-body eGFP mRNA levels, whole-body mRNA

levels of 11 target genes, and whole-body fluorescence in a homogenized sample. The details regarding the chemical exposure, stress routine and time points for collecting samples are described in the following sections. For statistical analysis, ANOVA test (one or two way) was used according to the study type.

4.2.3. Chemicals and exposure concentrations

All candidate chemicals studied in this study were purchased from commercial sources (Millipore-Sigma, Burlington, Massachusetts, USA). The exposure doses were determined based on several pilot studies using the published LC10 and/or therapeutic doses of the specific compounds. The final exposure concentration for BPA and VIN were at environmentally relevant concentrations based on the previously published literature [167, 267-272]. The DEX concentration was 100 times less than the approved dose for children (paediatric) conditions (https://www.drugs.com/dosage/dexamethasone.html). The FLX concentration was based on the clinically relevant dose used in the previous study in our lab [2], which was within the lower range found in the cord blood of pregnant women receiving FLX [273-275]. The SR4G transgenic zebrafish embryos allowed to reach six days post-fertilization with daily fresh embryo medium change. On the evening of the 6^{th} day, embryos were treated with either of the following compounds and the assigned concentrations for a total of 18 hours of exposure: bisphenol A (BPA, 5 µM, 1mg/L), vinclozolin (VIN, 17 µM, 4mg/L), dexamethasone (DEX, 0.2 nM, 0.07 µg/L), cortisol (CORT, 10 mM, 3.6g/L) and fluoxetine (FLX-O/N, 54 µg/L, 0.17 µM). The selected ocncentrations were selected based on 100 times dilutions below LC10 for BPA and VIN. The control groups only received the final concentration of 0.001% of DMSO as the vehicle for BPA, VIN and DEX, and the final concentration of 0.005% of ethanol as the vehicle for the FLX group. Another FLX-exposed group (FLX-6D) was generated by exposing 0-day post fertilization (dpf) embryos to 54 µg/L of fluoxetine for six days (6 dpf) with daily change of embryo medium and with freshly prepared FLX from the stock solution. The associated control group (Ethanol-6D) only received the vehicle with the same daily embryo medium changes. The exposed treatment and control groups were further divided into four subgroups, unstressed (0 minutes), stressed for cortisol study (30 minutes post handling stress), stressed for mRNA study (60 minutes post handling stress) and stressed for fluorescent study (120 minutes post handling stress). Each

group's tank was prepared on the day of embryo collection and kept on separate shelves in the incubator to avoid unwanted stress in the unstressed groups. The unhatched or dead embryos/larvae were collected once daily.

4.2.4. Stress conditions and sample collection

Following the 18hr overnight exposure, the unstressed groups were immediately euthanized in cold water; and samples were collected for cortisol measurement, qPCR, and fluorescence measurements. After removing the excess medium from each tube, samples were immediately placed on dry ice and later transferred to -80 ^{o}C freezer until further experiments. The stressed groups were submitted to the handling procedure described and validated in chapter 2. Briefly, the larvae from each group were exposed to air for 1 minute trapped in a mesh net, afterwards returned to the embryo medium for 3 minutes of rest, following by another 1-minute exposure to air trapped in a mesh net. The sample collection was carried out based on the measuring criteria; for cortisol measurement samples were collected 30 minutes post handling stress, for RNA transcript measurement samples were collected 60 minutes (1 hr) post handling stress, and for fluorescence measurement samples were collected 120 minutes (2 hr) post handling stress. The time points for sample collections were determined based on findings reported in Chapter 2.

4.2.5. Total RNA extraction and quantitative PCR

Total RNA extraction was carried out using the same protocol and commercial kit described in Chapter 3. After total RNA extraction, the samples were kept in -80 ^{o}C freezer until further experimentations. A fraction of total RNA extracts for each sample was converted to cDNA using Qiagen QuantiNova Reverse Transcription Kit (Qiagen, Hilden, Germany), based on the manufacturer recommendations. The cDNA samples were kept in -80 ^{o}C freezer until further experimentations.

For qPCR experiments, eleven genes related to stress response and neurogenesis (based on mammalian studies) were studied; including *crhb, bdnf, egr2a, fkbp5, fosab, fosl1a, htr1b, npas4a, nr4a1, per2*, and *rorcb.* The forward and reverse primers for the 11 selected genes were designed using “Primer Blast” function of NCBI’s BLAST project. The sequence of each of the

primers is shown in the supplementary data (Supplementary Table 5). The forward and reverse primers sequence for eGFP and *eef1a1l1* were adopted from the previously published data [5]. All oligonucleotides were synthesized by Integrated DNA Technologies (Coralville, Iowa, USA). The qPCR experiments were conducted according to SYBR green chemistry principle using the SsoAdvanced universal SYBR Green supermix and Bio-rad CFX Thermal cycle (Bio-rad, Hercules, California, USA) according to the manufacturer's recommendations. As it was determined in the previous experiments described in chapter 2, the collection times to cover the peak changes in eGFP expression were 0 minutes (before handling stress) and 60 minutes after the final round of handling stress for unstressed and stressed conditions, respectively.

4.2.6. Whole-body cortisol measurement

Whole-body cortisol was measured using the Cayman Cortisol ELISA kit (Cayman chemicals, USA) based on the manufacturer's recommendations. Cortisol was extracted from a pool of 22-28 larvae by an ether lipid extraction protocol described elsewhere [174]. Briefly, about 200 µl of freshly prepared PBS was added to each sample and samples were sonicated using a commercial sonicator(Qsonica- q700, CT, USA) at Hz for two 10 s periods while incubating on ice. Afterwards, ether was added at three times the initial volume (600 µl), samples were centrifuged on 4^{o}C at 4000 rpm for 5 minutes, and supernatants were collected. This procedure was repeated three times for each sample. The total collected supernatants were placed under the chemical hood for ether to get evaporated overnight. Following total evaporation, 50 µl of ELISA buffer was added to each sample and incubated on 4^{o}C for 24-30 hours with occasional vortex for the lipid extracts' full resuspension. The resuspended samples were used for ELISA cortisol measurement. Samples with a high amount of cortisol fell in the standard curve's none-linear part were diluted and measured again. Based on the spiked samples with known amounts of cortisol, the extraction efficiency was >85%.

4.2.7. Whole-body fluorescence measurement

Freshly prepared PBS (200 µl) containing a protease inhibitor cocktail mix was added to all larval samples before sonication (1:1000 dilution of #P8340-5ML, Millipore-Sigma, Burlington, Massachusetts, USA). Samples were sonicated at 20 kHz for two periods of 10 s while incubated

on ice (Qsonica- q700, CT, USA). The samples were centrifuged afterwards at 10000 rpm on a refrigerated centrifuge at 4^{o}C for 4 minutes. Fifty microliters of the supernatant were transferred into a well of a 96-well flat-bottom plate, and fluorescence signal of eGFP was measured using 485/20 filter for excitation and 530/25 filter for emission using Cytation 3 multi-well reader (# BTCYT3V, Biotek, Winooski, Vermont, USA).

4.2.8. Statistical analysis

All statistical analysis was performed by XLSTAT (Addinsoft Inc, N.Y. USA). The Shapiro-Wilk or Jarque-Bera tests of normality were performed on each data set to determine each data set's normal distribution. The homogeneity of variances was assessed using Levene's test, and if homogenous, parametric tests were employed. Given each experiment's design, one-way ANOVA or two-way ANOVA was performed between each treatment group and the associated control. All tests were performed with six experimental replicates to determine the significance level, followed by Tukey's post-hoc test for pairwise comparison. The level of significance was selected as $p \leq 0.05$.

The Pearson test was performed to assess the linear correlation between cortisol levels and eGFP mRNA levels. The statistical modelling to predict a blunted stress response was performed by Binomial Logistic Regression (LOG) and regression Random Forest (RDF). The R^2 and Out-Of-Bag (OOB) ratio was used to assess each model's fitness to the original data set and the predicted data set for LOG and RDF, respectively.

4.3. Results

4.3.1. The whole-body cortisol response to handling stress is blunted following exposure to FLX, BPA, VIN, and DEX

Our findings showed that the mean of whole-body cortisol levels 30 minutes after the handling stress increased by 4.4-fold in the Ethanol-6D (control) group compared to the unstressed condition ($p \leq 0.05$). Such increase was not observed upon developmental exposure to FLX (FLX-6D) in a stressed condition, and the whole-body cortisol levels were significantly decreased compared to the control group ($p \leq 0.01$; Figure 4.1). Moreover, the two-way ANOVA

study performed did not show any significant alteration in stress response upon overnight exposure to FLX (FLX-O/N) in the 7-dpf zebrafish larvae ($p>0.05$; Figure 4.1)

Our findings showed that the mean of whole-body cortisol levels 30 minutes after the handling stress increased by 3-fold in the DMSO group compared to the unstressed condition ($p\leq0.01$). This increase was not observed in all other treatment groups (0.7-fold in BPA, $p>0.05$; 0.8-fold in VIN, $p>0.05$; 0.4-fold in DEX, $p>0.05$). There was no significant difference between stressed and unstressed state within each treatment groups (BPA, VIN and DEX; $p>0.05$), and both values (stressed and unstressed) were similar to the whole-body cortisol levels in the unstressed state in control (DMSO) (Figure 4.1). Our findings show that overnight exposure to BPA, VIN, and DEX blunted the elevation of whole-body cortisol response to handling stress.

In our study, the cortisol (CORT) group exposed to 10 µM of cortisol overnight was used as the positive control and had a distinct pattern compared to the other groups (Supplementary Figure 4). The larvae in the pre-handling stress group (equivalent to the unstressed compared to the other treatment groups studies) showed a higher elevation of whole-body cortisol (9.2fold ($p\leq0.05$). Our findings showed that the mean of whole-body cortisol after overnight exposure to cortisol was elevated at 0- min sampling time point (9.2-fold, $p\leq0.05$) and 30 minutes after the handling stress when the source of exogenous cortisol was removed decreased by 3-fold ($p\leq0.05$; Supplementary Figure 4).

Overall, our whole-body cortisol measurements showed that BPA, VIN, and FLX in the concentrations and exposure times used in this study could blunt the stress response in the transgenic SR4G zebrafish larvae ($p\leq0.05$). A similar finding was observed for the DEX group used as our positive control group for disrupted stressed responses.

A)

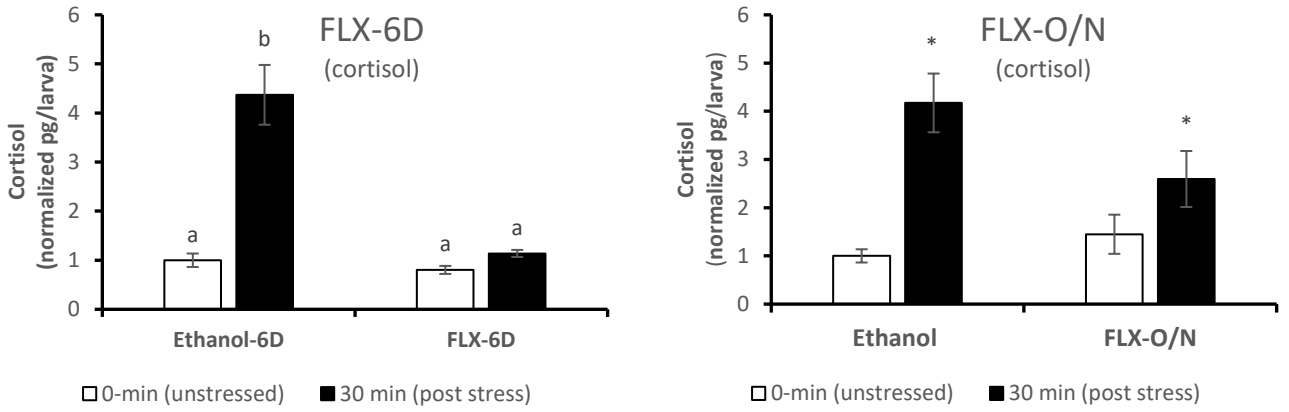

B)

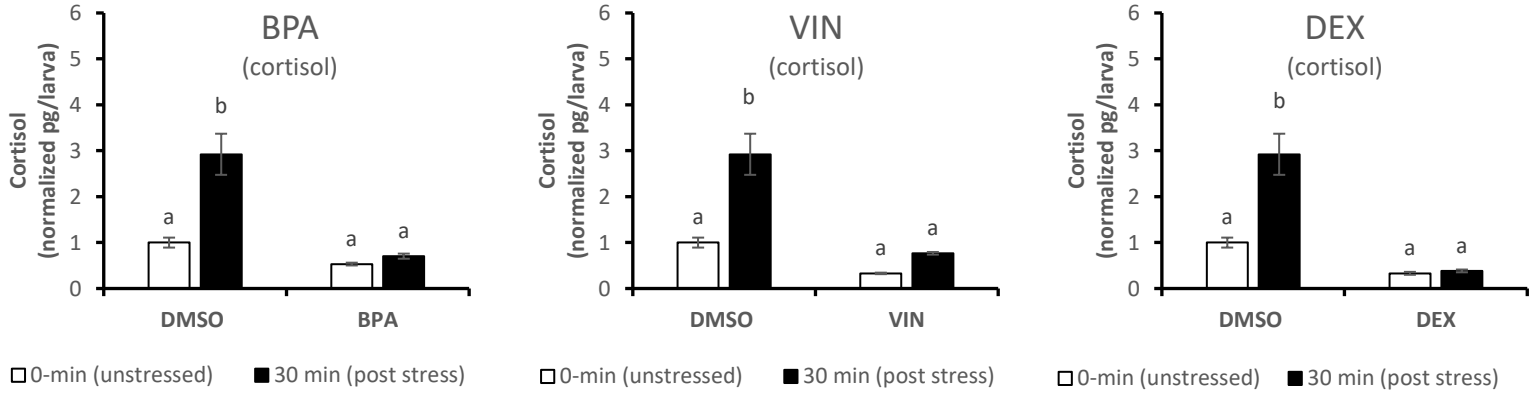

Figure 4.1 Whole-body cortisol levels in 7dpf transgenic zebrafish larvae exposed to different chemicals before and after handling stress. The cortisol levels are measured in pg/larva and normalized to the control unstressed condition. Panel **A** shows the whole-body cortisol measurement in fluoxetine treated groups with their corresponding control groups. The white bars represent cortisol levels in the unstressed condition (sacrificing subjects at 0 minutes

before the handling stress) and the black bars represent cortisol levels 30 minutes after the final round of handling stress. FLX-O/N: overnight exposure to fluoxetine; FLX-6D: daily exposure to fluoxetine from 0 to 6 days post fertilization(dpf); Ethanol-O/N: overnight exposure to ethanol, Ethanol-6D: daily exposure to ethanol from 0dpf to 6dpf; 0 min: unstressed; 30 min: 30 minutes post handling stress. Ethanol final concentrations in all experiments were 0.005%. Panel **B** shows the whole-body cortisol measurement in 7dpf SR4G larva exposed to BPA, VIN, DEX, and DMSO. BPA: overnight exposure to bisphenol A; VIN: overnight exposure to vinclozolin; DEX: overnight exposure to dexamethasone, DMSO: overnight exposure to DMSO; 0 min: unstressed; 60 min: 60 minutes post handling stress. DMSO was used as the vehicle for BPA, VIN, and DEX experiments in a final concentration of 0.001%. The DMSO data in each graph is the same data portrayed for comparison purposes. Two-way ANOVA was performed between each treatment group and its related control group in both unstressed and stressed state. No statistical comparison was performed between different treatment groups. Tukey's post-hoc test followed the significant ANOVA results for pairwise comparisons. Means (± SEM) with different letters (a, b) are significantly different; $p \leq 0.05$; N=6. Each sample contained a pool of 22-28 7dpf SR4G transgenic zebrafish larvae.

4.3.2. The whole-body eGFP mRNA response to handling stress is blunted following exposure to FLX, BPA, VIN, and DEX

Our findings showed that the mean of whole-body eGFP mRNA levels 60 minutes after the handling stress increased by 4.4-fold in the Ethanol-6D group compared to the unstressed condition ($p \leq 0.01$). This increase was not observed upon developmental exposure to FLX (FLX-6D) (Figure 4.2). There was an apparent 6-fold decrease in the whole-body eGFP mRNA levels in FLX exposed group in unstressed condition (FLX-6D-0 min); however, this decrease was not significant based on Tukey's test ($p > 0.05$) (Figure 4.2). Our findings show that the developmental exposure to FLX blunted the elevation of the whole-body eGFP mRNA in response to the handling stress in a similar matter to that of whole-body cortisol. Moreover, the two-way ANOVA performed to study the effect of stress, and overnight exposure to FLX (FLX-O/N) did not support any significant difference regarding this variable; therefore, no pairwise comparison performed (Figure 4.2).

The two-way ANOVA showed that treatment (BPA vs DMSO, $p \leq 0.01$; VIN vs DMSO, $p \leq 0.01$; and DEX vs DMSO, $p \leq 0.01$), stress state (stressed vs unstressed; $p \leq 0.001$) and their interaction (the treatment*the stress status; $p \leq 0.001$) had significant effects on the whole-body eGFP mRNA levels. A post-hoc Tukey's test was followed. Our findings showed that the mean of whole-body eGFP mRNA levels 60 minutes after the handling stress increased by 3-fold in the DMSO group compared to the unstressed condition ($p \leq 0.01$). This increase was not observed in all other treatment groups when compared to the control unstressed state (0.4-fold in BPA, $p > 0.05$; 0.6-fold in VIN, $p > 0.05$; 1.3-fold in DEX, $p > 0.05$). There was no significant difference between stressed and unstressed state within each treatment groups (BPA, VIN and DEX; $p > 0.05$), and both values (stressed and unstressed) were similar to the whole-body eGFP mRNA levels in the unstressed state in the control (DMSO) group ($p > 0.05$; Figure 4.2). Our findings showed that overnight exposure to BPA, VIN, and DEX disrupt the whole-body eGFP mRNA's elevation in response to handling stress.

In our study, the cortisol (CORT) group exposed to 10µM of cortisol overnight was used as the positive control and had a distinct pattern compared to the other groups (Supplementary

Figure 5). The larvae in the pre-handling stress group (equivalent to the unstressed compared to the other treatment groups studies) showed a higher elevation of whole-body eGFP mRNA; 12-fold. The two-way ANOVA showed that the treatment (CORT vs DMSO; $p \leq 0.05$) and the stress state (stressed vs unstressed; $p \leq 0.05$) had significant effects on the whole-body cortisol levels CORT and its associated control group. However, their interaction (the treatment*the stress status) was not significant; Therefore, pairwise comparison was not performed between the treatment groups ($p > 0.05$).

Overall, our whole-body eGFP mRNA levels measurements showed that BPA, VIN, and FLX in the concentrations and exposure times used in this study could decrease whole-body eGFP mRNA levels transgenic SR4G zebrafish larvae ($p \leq 0.05$, Figure 4.2). A similar finding was observed for DEX as the elected positive control for blunted stress response in our study (Figure 4.2). Further details regarding whole-body eGFP mRNA levels upon exposure to different chemicals and associated statistical parameters are shown in Appendix 1.

A)

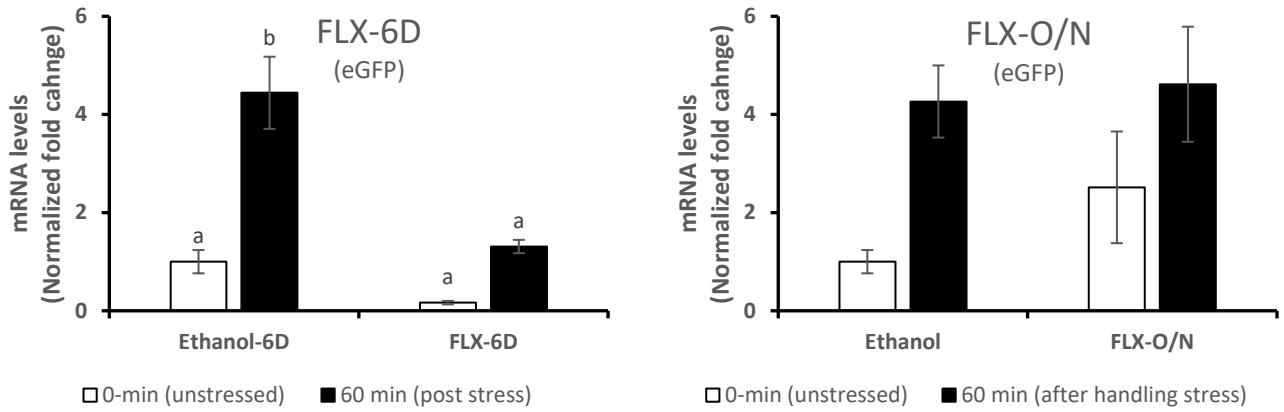

B)

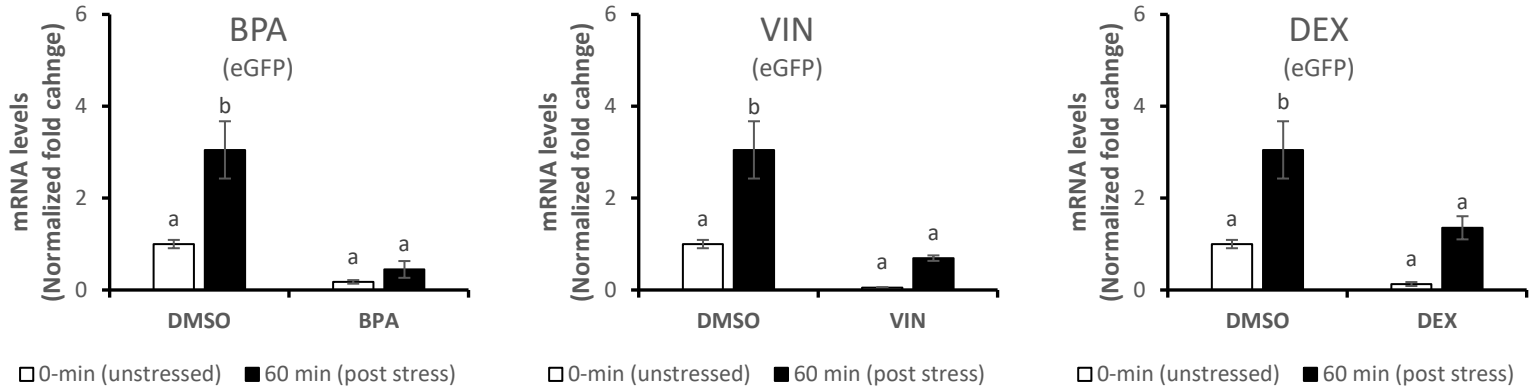

Figure 4.2 Whole-body eGFP mRNA levels in 7dpf transgenic zebrafish larvae exposed to different chemicals before and after the handling stress. The whole-body eGFP mRNA levels are measured in pg/larva and normalized to the control unstressed condition. Panel **A** shows the eGFP mRNA levels

in fluoxetine treated groups with their corresponding control groups. The white bars represent cortisol levels in the unstressed condition (sacrificing subjects at 0 minutes before the handling stress) and the black bars represent eGFP mRNA levels 60 minutes after the final round of handling stress. FLX-O/N: overnight exposure to fluoxetine; FLX-6D: daily exposure to fluoxetine from 0 to 6 days post fertilization(dpf); Ethanol-O/N: overnight exposure to ethanol, Ethanol-6D: daily exposure to ethanol from 0dpf to 6dpf; 0 min: unstressed; 60 min: 60 minutes post handling stress. Ethanol final concentrations in all experiments were 0.005%. Panel **B** shows the whole-body cortisol measurement in 7dpf SR4G larva exposed to BPA, VIN, DEX, and DMSO. BPA: overnight exposure to bisphenol A; VIN: overnight exposure to vinclozolin; DEX: overnight exposure to dexamethasone, DMSO: overnight exposure to DMSO; 0 min: unstressed; 60 min: 60 minutes post handling stress. DMSO was used as the vehicle for BPA, VIN, and DEX experiments in a final concentration of 0.001%. The DMSO data in each graph is the same data portrayed for comparison purposes. Two-way ANOVA was performed between each treatment group and its related control group in both unstressed and stressed state. No statistical comparison was performed between different treatment groups. Tukey's post-hoc test followed the significant ANOVA results for pairwise comparisons. Means (± SEM) with different letters (a, b) are significantly different; $p \leq 0.05$; N=6. Each sample contained a pool of 22-28 7dpf SR4G transgenic zebrafish larvae.

4.3.3. Whole-body eGFP mRNA are correlated to the whole-body cortisol levels in SR4G transgenic zebrafish larvae.

The two-way ANOVA performed for whole-body cortisol levels and whole-body eGFP mRNA levels. The whole-body cortisol experiment indicated that the stress condition (unstressed vs stressed; $p \leq 0.0001$) was the only significant factor. Our analysis showed that the whole-body cortisol levels increased by 4.2-fold and 3-fold 30 minutes after the handling stress in Ethanol and DMSO groups compared to the related unstressed condition, respectively (Figure 4.3). In the whole-body eGFP mRNA experiment, the stress condition (unstressed vs stressed; $p \leq 0.0001$) was the only significant factor. Our analysis showed that the whole-body eGFP mRNA levels increased by 4.4-fold and 3-fold 30 minutes after the handling stress in Ethanol and DMSO groups compared to the related unstressed condition, respectively (Figure 4.3).

The Pearson correlation coefficient was calculated for whole-body cortisol and whole-body eGFP mRNA regarding response to stress (unstressed vs stressed). A significant positive correlation was observed ($r=0.94$). The very close approximation to 1 indicates that the whole-body eGFP mRNA levels measurement may significantly represent the whole-body cortisol levels in SR4G transgenic zebrafish larvae (Figure 4.3).

A)

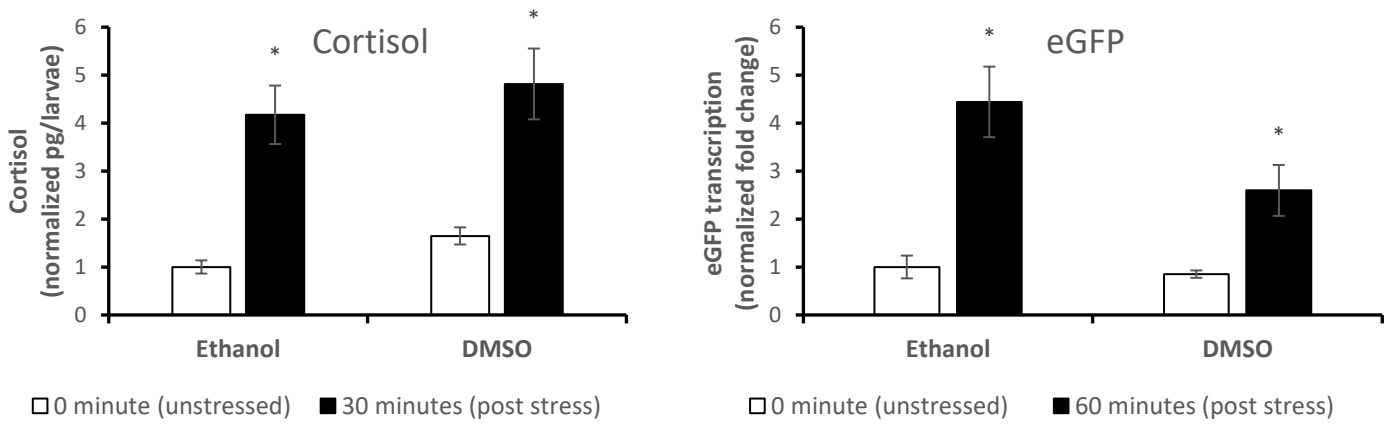

B)

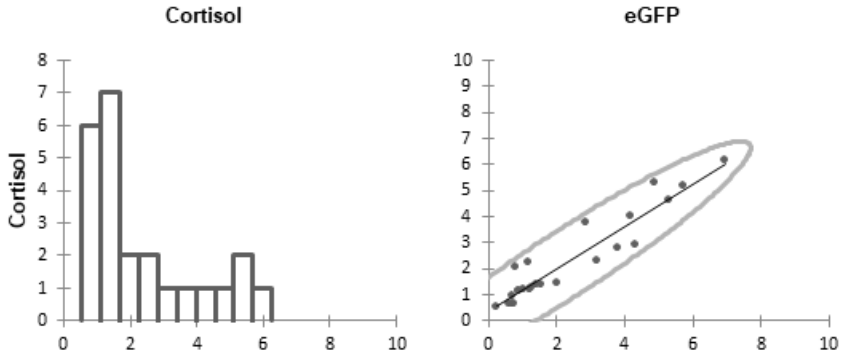

Correlation matrix (Pearson):

Variables	Cortisol	eGFP
Cortisol	**1**	**0.947**

Figure 4.3. The correlation between whole-body cortisol and total eGFP mRNA levels in SR4G transgenic zebrafish larvae. The graphs in panel **A** show normalized whole-body cortisol levels (left) and normalized whole-body eGFP mRNA levels (right) in the two control groups, Ethanol and DMSO, under the two unstressed and stressed conditions. Two-way ANOVA was performed to evaluate the effect of treatments and stress conditions on whole-body cortisol levels and whole-body eGFP mRNA levels. Means (± SEM) marked by an asterisk (*) are significantly different within each category (whole-body cortisol or whole-body

eGFP mRNA study); $p \leq 0.0001$; N=6. Ethanol: overnight exposure to 0.005% ethanol; DMSO: overnight exposure to 0.001% DMSO. The time points,30 min or 60 min, show the time-lapsed following the handling stress before euthanizing the subjects for sample collection. Each sample contained a pool of 22-28 7dpf SR4G transgenic zebrafish larvae. Panel **B** shows the correlation coefficient between whole-body cortisol and whole-body eGFP mRNA illustrated by graphs and determined by the Pearson test.

4.3.4. Whole-body eGFP mRNA levels are predictive of blunted stress response following exposure to stress disruptive chemicals in SR4G transgenic zebrafish larvae.

The potential of whole-body eGFP mRNA level to predict the stress response upon exposure to different chemicals were evaluated. The stressed condition was used as the qualitative dependent variable based on the significant variation to the unstressed control (Ethanol). Based on the whole-body cortisol levels measured upon exposure to different chemicals (FLX-6D, FLX-O/N, BPA, VIN, and DEX), the significant stressed condition (significant higher cortisol levels compared to the unstressed state, $p \leq 0.05$) was assigned a binary value 1 (one), and the statistically non- significant measures were assigned a binary value 0 (zero). The whole-body eGFP mRNA levels in the Ethanol group in both stressed and unstressed conditions were used as the training data set for predictive modelling, regression forest (RDF) and logistic regression (LOG). The out-of-bag (OOB) error estimate for RDF was 0.4, and the validation misclassification rate was 0.00. The R^2 for LOG was 0.774. The positive predictive value (PPV) and the negative predictive value (NPV) was calculated for both models for each treatment group (Table 4.1). Table 4.1 summarize the prediction of the stress response in all the treatment and control groups studied based on the whole-body eGFP mRNA levels. The stress column shows the actual binary stress code retrieved from the normalized whole-body cortisol measurement (pg/larva). The predicted classification of the individual FC is shown based on RDF and LOG models. The bolded values show the correct prediction of the individual FC's stress status based on the actual binary stress code retrieved from normalized whole-body cortisol measurement (pg/larva). Our findings show that the models based on the whole-body mRNA levels of eGFP could determine the altered stress response upon exposure to different chemicals.

Table 4.1. Prediction of stress response based on the whole-body eGFP mRNA levels using regression random forest (RDF) and logistic regression (LOG) model trained by Ethanol (control) group.

Ethanol (control)			Predicted stress status																	
			FLX_O/N			FLX-6D			DMSO			BPA			VIN			DEX		
Samples	FC	**Stress**	FC	**LOG**	**RDF**	FC	**LOG**	**RDF**	FC	**LOG**	**RDF**	FC	**LOG**	**RDF**	FC	**LOG**	**RDF**	FC	**LOG**	**RDF**
Unstressed S-1	2.05	0	9.33	1	1	0.23	**0**	**0**	1.33	**0**	**0**	0.16	**0**	**0**	0.10	**0**	**0**	0.06	**0**	**0**
Unstressed S-2	0.90	0	5.69	1	1	0.16	**0**	**0**	0.72	**0**	**0**	0.24	**0**	**0**	0.08	**0**	**0**	0.36	**0**	**0**
Unstressed S-3	0.64	0	1.27	**0**	**0**	0.39	**0**	**0**	0.93	**0**	**0**	0.37	**0**	**0**	0.04	**0**	**0**	0.10	**0**	**0**
Unstressed S-4	0.27	0	0.74	**0**	**0**	0.10	**0**	**0**	1.09	**0**	**0**	0.07	**0**	**0**	0.06	**0**	**0**	0.04	**0**	**0**
Unstressed S-5	0.72	0	1.12	**0**	**0**	0.24	**0**	**0**	0.80	**0**	**0**	0.16	**0**	**0**	0.00	**0**	**0**	0.07	**0**	**0**
Unstressed S-6	1.41	0	0.04	**0**	**0**	0.07	**0**	**0**	1.28	**0**	**0**	0.09	**0**	**0**	0.01	**0**	**0**	0.17	**0**	**0**
Stressed S-1	6.95	1	12.81	**1**	**1**	0.99	**0**	**0**	3.93	**1**	**1**	0.00	**0**	**0**	0.55	**0**	**0**	0.06	**0**	**0**
Stressed S-2	4.18	1	5.80	**1**	**1**	1.32	**0**	**0**	0.84	0	0	0.00	**0**	**0**	0.58	**0**	**0**	0.36	**0**	**0**
Stressed S-3	1.57	1	2.77	**1**	0	1.64	**0**	**0**	1.24	0	0	1.01	**0**	**0**	0.86	**0**	**0**	0.10	**0**	**0**
Stressed S-4	2.89	1	2.80	**1**	0	1.55	**0**	**0**	5.00	**1**	**1**	0.79	**0**	**0**	0.78	**0**	**0**	0.04	**0**	**0**
Stressed S-5	5.32	1	3.60	**1**	**1**	2.32	1	**0**	4.45	**1**	**1**	0.01	**0**	**0**	0.57	**0**	**0**	0.07	**0**	**0**
Stressed S-6	5.74	1	5.60	**1**	**1**	1.65	**0**	**0**	3.30	**1**	**1**	0.94	**0**	**0**	0.92	**0**	**0**	0.17	**0**	**0**
PPV				**75%**	**67%**		**N/A**	**N/A**		**100%**	**100%**		**N/A**	**N/A**		**N/A**	**N/A**		**N/A**	**N/A**
NPV				**100%**	**67%**		**100%**	**100%**		**75%**	**75%**		**100%**	**100%**		**100%**	**100%**		**100%**	**100%**

FC: fold change, FLX-6D: daily exposure to from 0 to 6 days post fertilization(dpf); FLX-O/N, BPA, VIN, DEX, CORT representing overnight exposure to fluoxetine, bis-phenol A, vinclozolin, dexamethasone, and cortisol, respectively. LOG: logistic regression, RFD: random forest. PPV: positive predictive value, NPV: negative predictive value. (LOG; R^2: 0.774) (RDF; OOB: 0.4)

4.3.5. The global pattern of whole-body mRNA levels of 11 genes related to stress, depression, and neurogenesis was suggestive of blunted stress response following exposure to stress disruptive chemicals in SR4G transgenic zebrafish larvae

The qPCR experiment targeting 11 genes that their Homo sapiens' orthologues are associated with neurogenesis, development of depression, and stress response showed significant downregulation of several members upon exposure to FLX, BPA VIN (Figure 4.6, 4.7, 4.8, and 4.9).

The two-way ANOVA analysis performed showed that developmental six days exposure to FLX (FLX-6D) resulted in significant downregulation of several target genes in stressed condition to levels significantly similar to unstressed condition; including *npas4a* (7-fold, $p \leq 0.001$), *nr4a1* (6-fold, $p \leq 0.001$), *per2* (6-fold, $p \leq 0.001$), *rorcb* (11-fold, $p \leq 0.001$), and *fosab* (12-fold, $p \leq 0.001$) (Figure 4.6 and 4.7). Moreover, our analysis showed that developmental exposure to FLX resulted in significant downregulation of *htr1b*, regardless of the stress state ($p \leq 0.05$; Figure 4.6. An interesting pattern was observed for *fkbp5*, with significant 5-fold downregulation in the unstressed condition and a significant 2-fold in the stressed condition ($p \leq 0.05$; Figure 4.6). For *crhb* and *bdnf,* no significant effect was observed upon developmental exposure to FLX in 7-dpf zebrafish larvae ($p > 0.05$). Moreover, we showed that overnight exposure to FLX (FLX-O/N) did not have any significant effect on the whole-body mRNA levels of any of the 11 genes studied in both unstressed and stressed conditions ($p > 0.05$ for individual genes; Figure 4.6 and 4.7).

Furthermore, the two-way ANOVA performed showed that overnight exposure to VIN resulted in a significant downregulation of several target genes studied in the stressed condition; including *egr2a* (5.4-fold, $p \leq 0.001$), *npas4a* (19-fold, $p \leq 0.001$), *nr4a1* (3-fold, $p \leq 0.001$), *per2* (9-fold, $p \leq 0.001$), *rorcb* (5-fold, $p \leq 0.001$), and *fosab* (26-fold, $p \leq 0.001$) (Figure 4.8 and 4.9). For *crhb, htr1b,* and *bdnf* the two-way ANOVA test performed did not show any significant difference ($p > 0.05$; Figure 4.8 and 4.9).

Moreover, our analysis showed an interesting similar transcription pattern between BPA and the DEX group. The two-way ANOVA showed that fosab was the only affected gene upon overnight exposure to BPA and DEX that showed significant downregulation in stressed

conditions (3-fold, p≤0.01for BPA and 7-fold, p≤0.01 for DEX, Figure 4.9). For *crhb, htr1b,* and *bdnf,* the two-way ANOVA test performed did not show any significant difference (p>0.05; Figure 4.8 and 4.9).

A series of separate one-way ANOVA test was performed to study the effect of chemical exposure on the unstressed state of 7-dpf zebrafish larvae. As expected, overnight exposure to FLX (FLX-O/N) did not have any significant effect on the 11 genes (p>0.05; Figure 4.10). In the other hand, developmental exposure to FLX (FLX-6D) resulted in significant downregulation of several genes, including: *egr2a* (2.4-fold; p≤0.05), *fkbp5* (5.4-fold; p≤0.01), *htr1b* (2-fold; p≤0.01), *npas4a* (4-fold; p≤0.05), *nr4a1* (3-fold; p≤0.05), and *per2* (6-fold; p≤0.05) (Figure 4.10). Moreover, significant downregulation of several of these genes was observed in the unstressed larvae upon overnight exposure to BPA; including *egr2a* (3.2-fold; p≤0.01), *fkbp5* (4.4-fold; p≤0.001), *fosl1* (6.4-fold; p≤0.001), *npas4a* (4.6-fold; p≤0.001), *per2* (13-fold; p≤0.01), *rorcb* (6-fold; p≤0.001), and *fosab* (3.4-fold; p≤0.05) (Figure 4.11 and 4.12). Similar downregulation effect was also observed upon overnight exposure to VIN, our findings showed significant downregulation of *egr2a* (2.2-fold; p≤0.05), *fkbp5* (14-fold; p≤0.001), *fosl1* (7-fold; p≤0.001), *npas4a* (7.5-fold; p≤0.001), *nr4a1* (2.2-fold; p≤0.01), *per2* (12-fold; p≤0.01), and *fosab* (15-fold; p≤0.01) (Figure 4.11 and 4.12). Interestingly, a significant upregulation of *bdnf* was observed upon overnight exposure to VIN in the unstressed 7-dpf larvae (3.4-fold; p≤0.01). Also, our findings showed significant downregulation of *fkbp5* (3-fold; p≤0.01), *fosl1* (6-fold; p≤0.001), *per2* (9.5-fold; p≤0.01), and *fosab* (2.6-fold; p≤0.05) upon overnight exposure to DEX in 7-dpf larvae (Figure 4.11 and 4.12).

Overall, our findings showed several genes with reported association with neurogenesis, development of depression and stress response in human and mammalian models are affected by exposure to stress altering compounds studied here in a zebrafish model. The downregulation of these genes was the prominent effect of such exposure. Further details regarding individual gene's transcript upon exposure to different chemicals and associated statistical parameters are shown in Appendix 1.

4.3.5. Whole-body mRNA levels of 11 genes related to stress, depression, and neurogenesis are predictive of altered stress response following chemical exposures in SR4G transgenic zebrafish larvae.

The orthologue of 11 genes associated with the development of depression, stress response and neurogenesis in mammalian models were studied in this thesis. Table 4.2 shows these genes and their orthologous pathways. The potential of whole-body mRNA levels of this minimal library to predict the stress response following chemical exposures was evaluated. The stressed condition was used as the qualitative dependent variable based on the significant variation to the unstressed control (ethanol). The significant stressed condition was assigned binary value 1 (one), and the nonsignificant measure was assigned a binary value 0 (zero). The whole-body mRNA levels of the 11 target genes in the control (Ethanol) group in both stressed and unstressed conditions were used to train the predictive model (Figure 4.5). A model based on regression random forest (RDF) was initially trained and used to predict the stress response based on the whole-body mRNA levels of the 11 target genes. The out-of-bag (OOB) error estimate for RDF was 0.4, and the validation misclassification rate was 0.00. A logistic regression (LOG) model was created based on 11 target genes' whole-body mRNA levels using the Ethanol group as the training data set. The R^2 for LOG was 0.741. These two models were used to predict the stress response in the treatment groups (Table 4.3). The positive predictive value (PPV) and the negative predictive value (NPV) was calculated for both models for each treatment group (Table 4.3). Our findings show that the models based on the whole-body mRNA levels of selected 11 genes could determine the altered stress response upon exposure to different chemicals.

Table 4.2. The 11 genes implicated in stress response, neural plasticity, and development of depression.

Gene Symbol		Gene name	Homo sapiens orthologue pathway
Danio rerio	***Homo sapiens***		
d4EGFP	NA	transgene-Green Fluorescent Protein	NA
bdnf	BDNF	Brain-derived neurotrophic factor	Development of depression, Stress, Neural plasticity
crhb	CRH	corticotropin releasing hormone b	Stress response
egr2a	EGR+	early growth response 2a	Neural plasticity
fkbp5	FKBP5	FKBP Prolyl Isomerase 5	Development of depression, Stress response
fosab	FOS	v-fos FBJ murine osteosarcoma viral oncogene homolog Ab	Development of depression, Neural plasticity
fosl1a	FOSL1	FOS Like 1, AP-1 Transcription Factor Subunit	Development of depression
htr1b	HTR1D	5-hydroxytryptamine (serotonin) receptor 1B	Development of depression
npas4a	NPAS4	neuronal PAS domain protein 4a	Neural plasticity
nr4a1	NR4A1	nuclear receptor subfamily 4, group A	Stress response
per2	PER2	period circadian clock 2	Stress response, Neural plasticity
rorcb	RORC+	RAR-related orphan receptor C b	Stress response

NA: not applicable; * Indicates a gene that did not pass FDR≤ 0.05; (+): potential orthologue (the exact ortholog was unknown at the time of writing this chapter).

A)

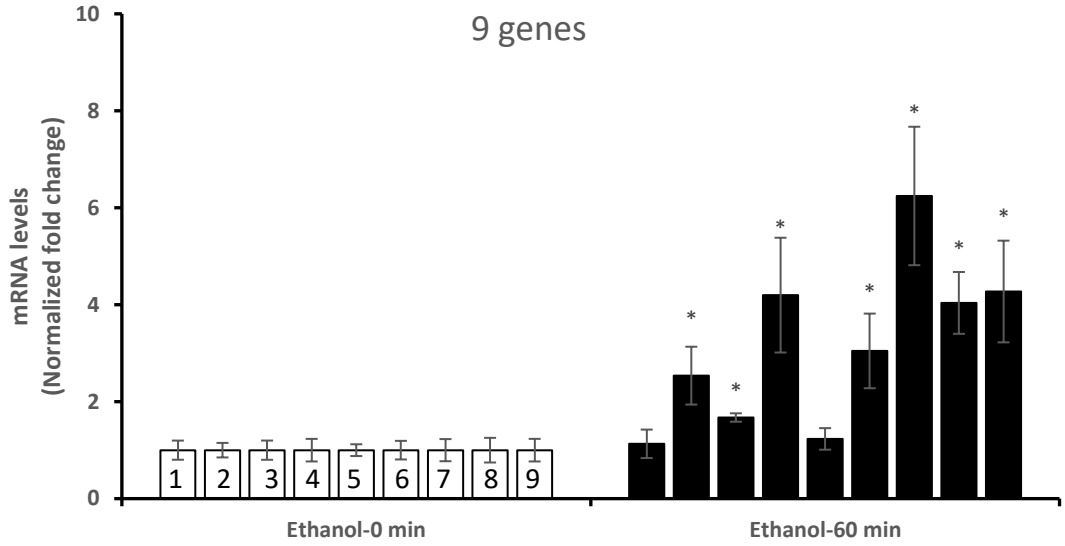

B)

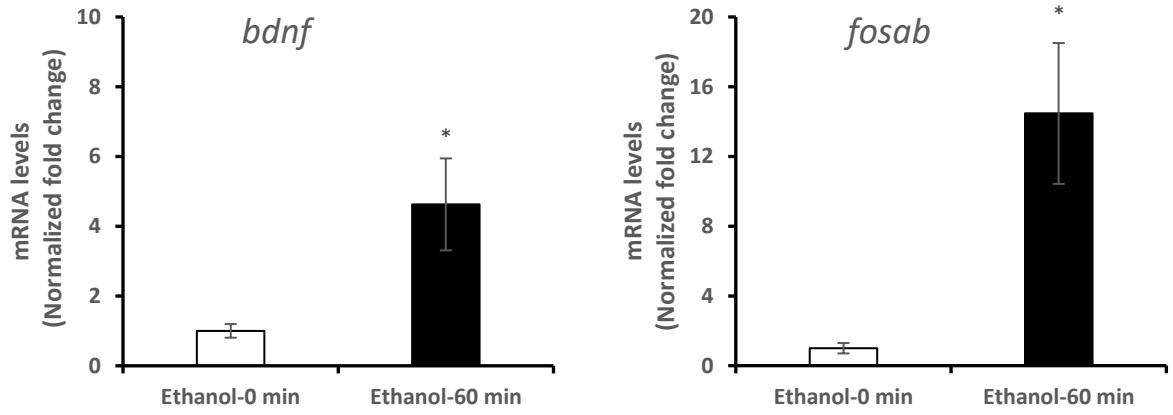

Figure 4.5. The whole-body mRNA levels of the 11 genes in 7dpf SR4G transgenic zebrafish larvae in the control group (normal stress response). The values are shown in normalized fold changes using the unstressed Ethanol as the control. The white and black bars show unstressed and stressed conditions, respectively. In each treatment and control groups the 9 genes are arranged alphabetically; from left to right: 1:*crhb, 2:egr2a, 3:fkbp5, 4:fosl1a, 5:htr1b, 6:npas4a, 7:nr4a1, 8:per2, and 9:rorcb.* Panel **A** shows the mRNA levels of the 9 genes in the Ethanol (overnight exposure to ethanol) group. Panel **B** shows the mRNA levels of *bdnf* and *fosab* in the Ethanol (overnight exposure to ethanol) group. 0 min: unstressed; 60 min: 60 minutes post-handling stress. Ethanol final concentrations in all experiments were 0.005%. One-way ANOVA was performed. The means (± SEM) with an

asterisk (*) are significantly different; p≤0.05; N=6. Each sample was a pool of 22-28 7dpf SR4G transgenic zebrafish larvae.

A)

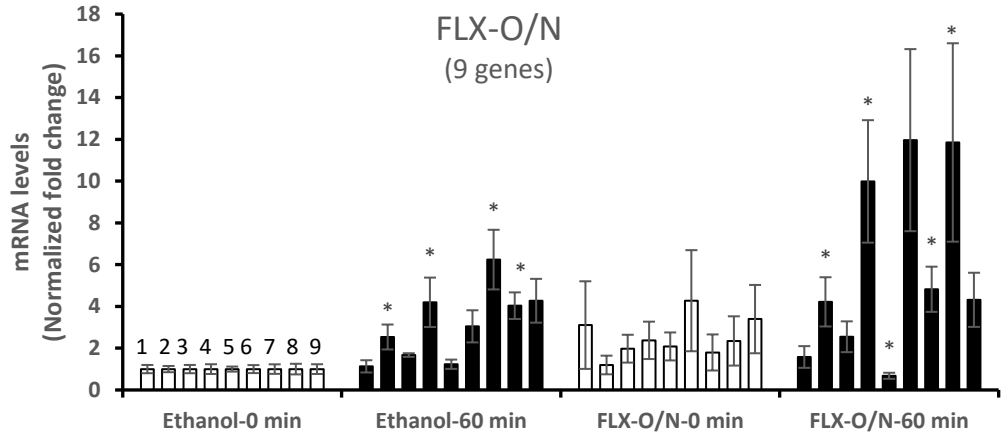

B)

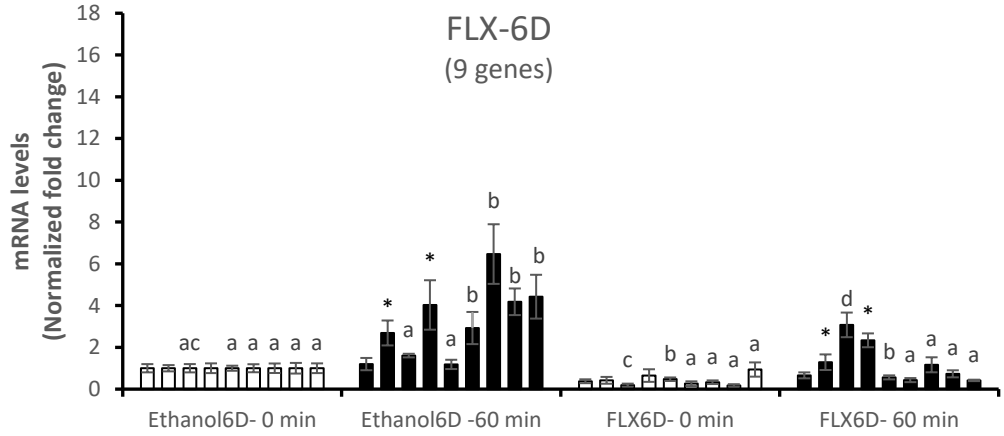

Figure 4.6. The whole-body mRNA levels of the 9 genes in FLX exposed 7dpf SR4G transgenic zebrafish larvae. The values are shown in normalized fold changes using the unstressed Ethanol as the control. The 9 genes with similar fold change ranges are separated from *bdnf* and *fosab* for visual illustration purposes. The white and black bars show unstressed and stressed conditions, respectively. In each treatment and control groups the 9 genes are arranged alphabetically; from left to right: 1:*crhb, 2:egr2a, 3:fkbp5, 4:fosl1a, 5:htr1b, 6:npas4a, 7:nr4a1, 8:per2, and 9:rorcb..* Panel A shows the mRNA levels of the 9 genes in the FLX-O/N group and its related control group. Panel B shows the mRNA levels of the 9 genes in the FLX-6D group and its related control group. FLX-O/N: overnight exposure to fluoxetine; FLX-6D: daily exposure to fluoxetine from 0 to 6 days post fertilization(dpf); Ethanol: overnight exposure to ethanol, Ethanol6D: daily exposure to ethanol from 0dpf to 6dpf; 0 min: unstressed; 60 min: 60 minutes post handling stress. Ethanol final concentrations in all experiments were 0.005%. Two-way ANOVA was performed for each gene in each treatment group and its related control group in both unstressed and stressed state. No statistical comparison was performed between different genes or different treatment

groups. If the ANOVA for treatment, stress state and interaction between them (treatment vs stress state) was significant (intercept $p \leq 0.05$), Tukey's post-hoc test was performed for all conditions. The means (± SEM) with different letters (a, b) are significantly different; $p \leq 0.05$; N=6. If the ANOVA for treatment and stress state was significant ($p \leq 0.05$) and ANOVA for interaction between them (treatment vs stress state) was not significant (intercept $p > 0.05$), Tukey's post-hoc test was only performed for stress state within each treatment group. The means (± SEM) with a significant difference is marked with an asterisk (*) in this case; $p \leq 0.05$; N=6. Each sample was a pool of 22-28 7dpf SR4G transgenic zebrafish larvae.

A)

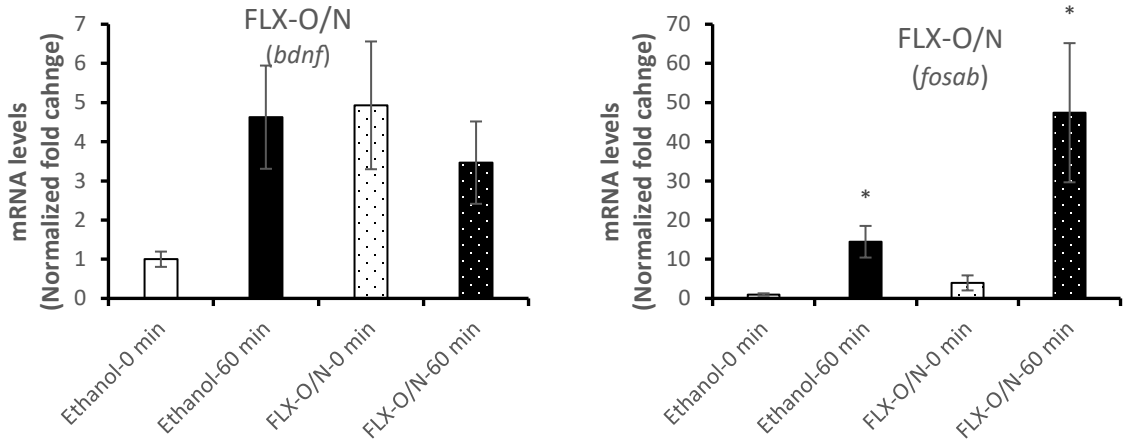

B)

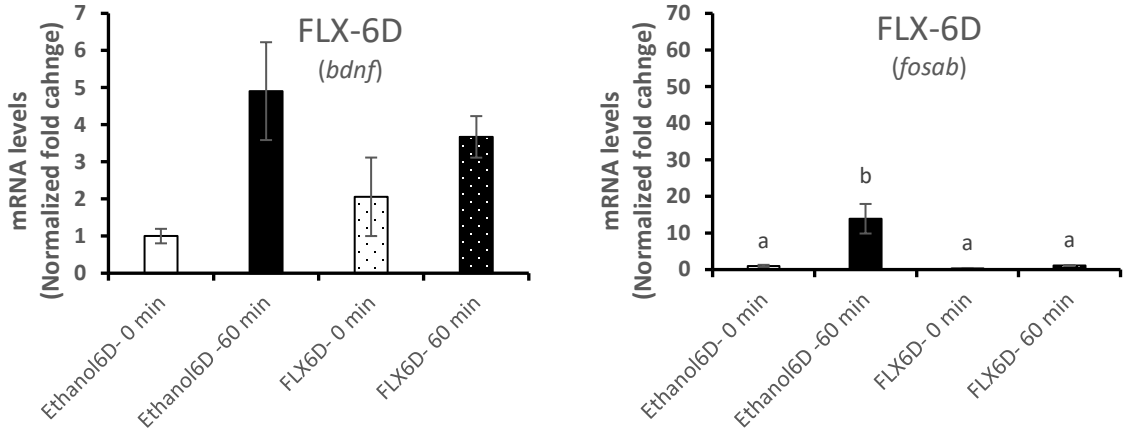

Figure 4.7 The whole-body mRNA levels of bdnf and fosab in FLX-exposed 7dpf SR4G transgenic zebrafish larvae. The values are shown in normalized fold changes using the unstressed Ethanol as the control. The 9 genes with similar fold change ranges are separated from *bdnf* and *fosab* for visual illustration purposes. The white and black bars show unstressed and stressed conditions, respectively. Panel **A** shows the mRNA levels of *bdnf* and *fosab* in the FLX-O/N group and its related control group. Panel **B** shows the mRNA levels of *bdnf* and *fosab* in the FLX-6D group and its related control group. FLX-O/N: overnight exposure to fluoxetine; FLX-6D: daily exposure to fluoxetine from 0 to 6 days post fertilization(dpf); Ethanol: overnight exposure to ethanol, Ethanol6D: daily exposure to ethanol from 0dpf to 6dpf; 0 min: unstressed; 60 min: 60 minutes post handling stress. Ethanol final concentrations in all experiments were 0.005%. Two-way ANOVA was performed for each gene in each treatment group and its related control group in both unstressed and stressed state. No statistical comparison was performed between different genes or different treatment groups. If the ANOVA for treatment, stress state and interaction between them (treatment vs stress state) was significant (intercept $p \leq 0.05$), Tukey's post-hoc test was performed for all conditions. The means (± SEM) with different letters (a, b) are significantly

different; p≤0.05; N=6. If the ANOVA for treatment and stress state was significant (p≤0.05) and ANOVA for interaction between them (treatment vs stress state) was not significant (intercept p >0.05), Tukey's post-hoc test was only performed for stress state within each treatment group. The means (± SEM) with a significant difference is marked with an asterisk (*) in this case; p≤0.05; N=6. Each sample was a pool of 22-28 7dpf SR4G transgenic zebrafish larvae.

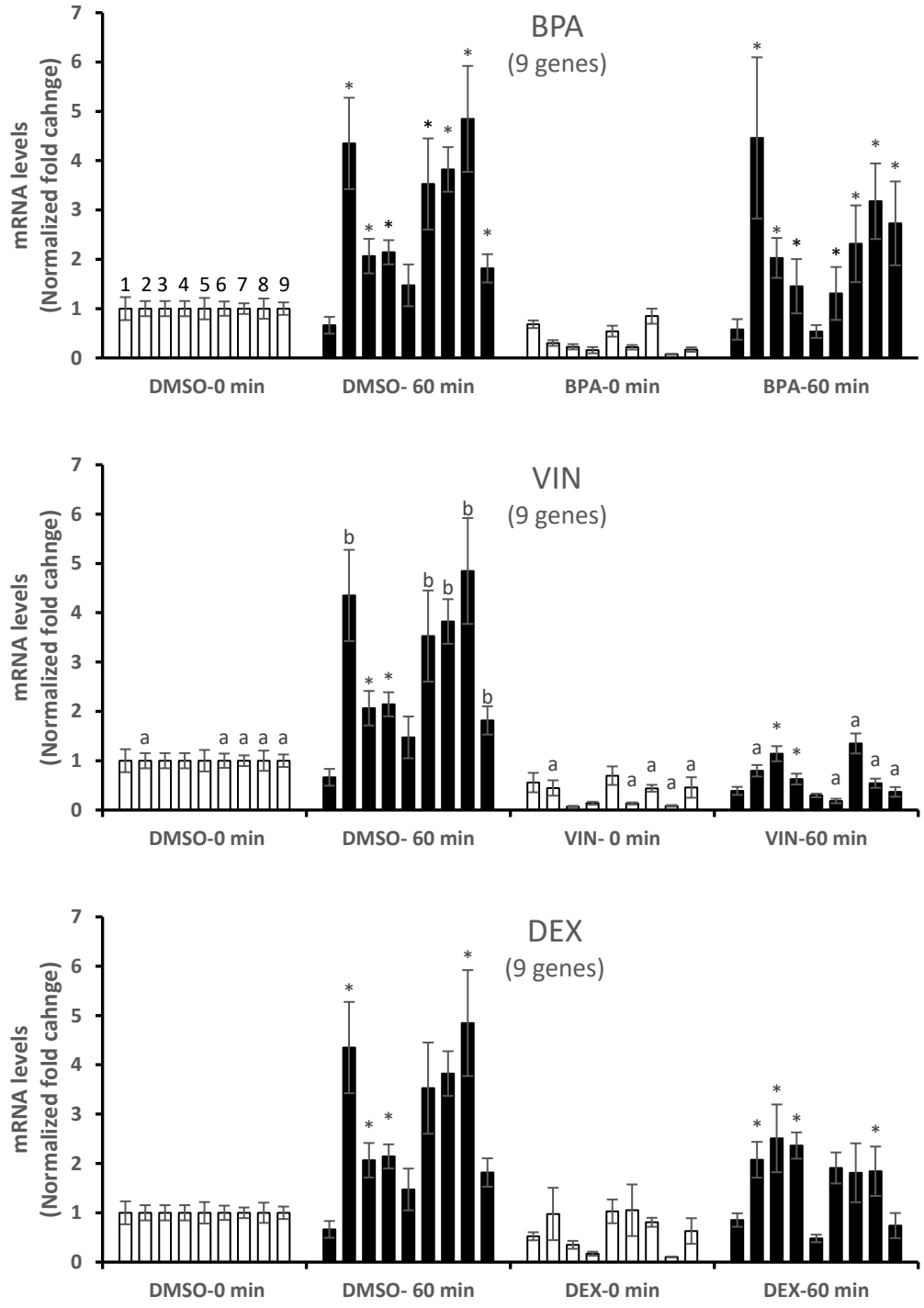

Figure 4.8. The whole-body mRNA levels of the nine genes in BPA, VIN and DEX, exposed 7dpf SR4G transgenic zebrafish larvae. The values are shown in normalized fold changes using the unstressed DMSO as the control. The 9 genes with similar fold change range are separated from *bdnf* and *fosab* for visual

illustration purposes. The white and black bars show unstressed and stressed conditions, respectively. In each treatment and control groups the 9 genes are arranged alphabetically; from left to right: 1:*crhb, 2:egr2a, 3:fkbp5, 4:fosl1a, 5:htr1b, 6:npas4a, 7:nr4a1, 8:per2, and 9:rorcb.* BPA: overnight exposure to bisphenol A; VIN: overnight exposure to vinclozolin; DEX: overnight exposure to dexamethasone; DMSO: overnight exposure to DMSO; 0 min: unstressed; 60 min: 60 minutes post handling stress. DMSO was used as the vehicle for BPA, VIN, and DEX experiments in a final concentration of 0.001%. Two-way ANOVA was performed between each gene in each treatment group and its related control group in both unstressed and stressed states. No statistical comparison was performed between different genes or different treatment groups. If the ANOVA for treatment, stress state and interaction between them (treatment vs stress state) was significant (intercept $p \leq 0.05$), Tukey's post-hoc test was performed for all conditions. The Means (± SEM) with different letters (a, b) are significantly different; $p \leq 0.05$; N=6. . If the ANOVA for treatment and stress state was significant ($p \leq 0.05$) and ANOVA for interaction between them (treatment vs stress state) was not significant (intercept $p > 0.05$), Tukey's post-hoc test was only performed for stress vs unstressed state within each treatment group. The Means (± SEM) with a significant difference are marked with an asterisk in this case (*); $p \leq 0.05$; N=6. Each sample contained 22-28, 7dpf SR4G transgenic zebrafish larvae.

A)

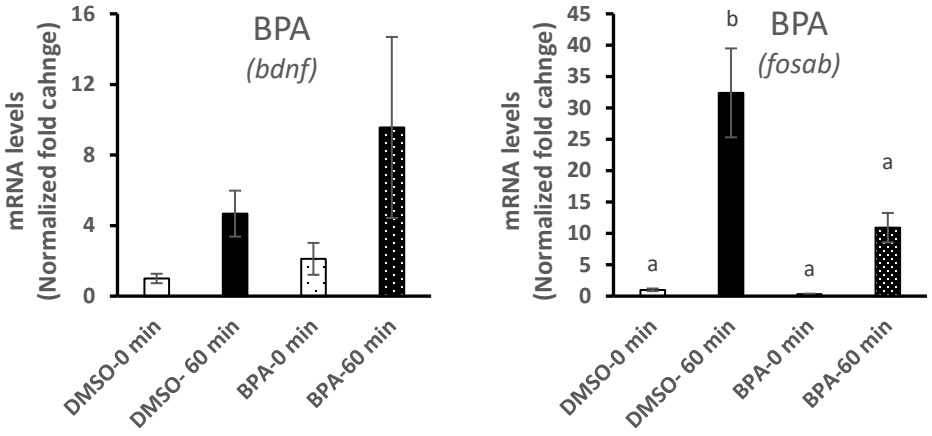

B)

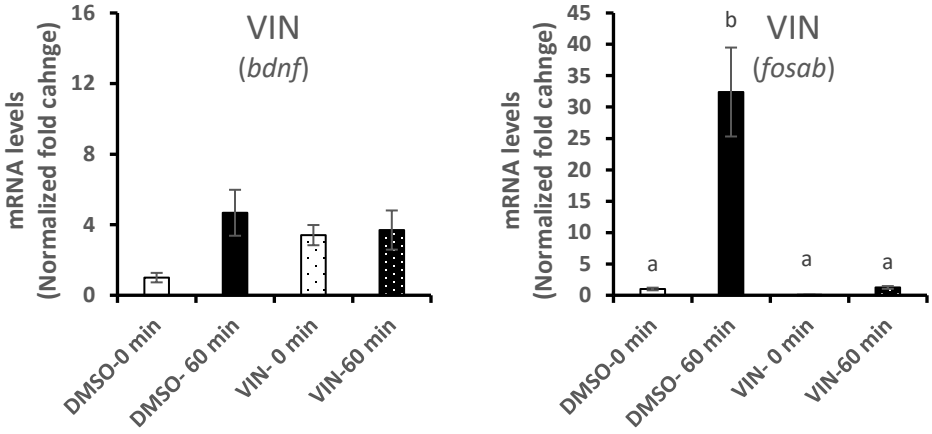

C)

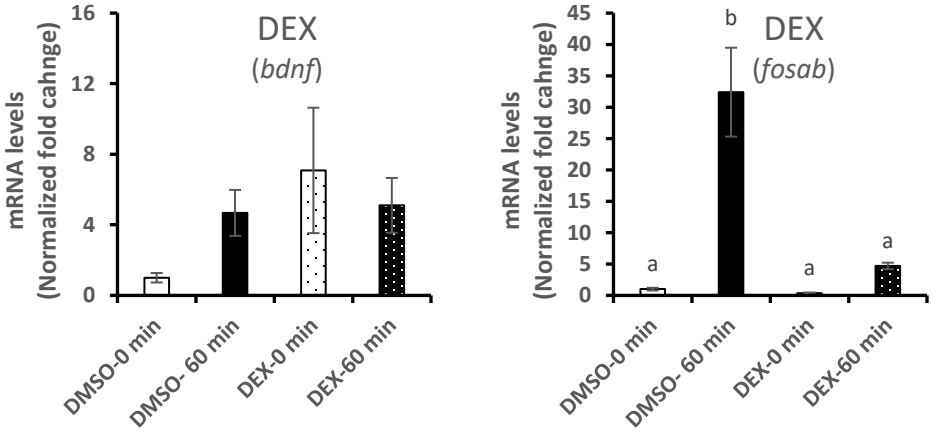

Figure 4.9. The whole-body mRNA levels of bdnf and fosab in BPA-, VIN- and DEX-exposed 7dpf SR4G

transgenic zebrafish larvae. The values are shown in normalized fold changes using the unstressed DMSO as the control. The mRNA levels for *bdnf* and *fosab* are separated from the other 9 genes for visual illustration purposes. The white and black bars show unstressed and stressed conditions, respectively. Panel **A** shows the mRNA levels for *bdnf* and *fosab* in BPA treated group and its associated control. Panel **B** shows the mRNA levels for *bdnf* and *fosab* in VIN treated group and its associated control. Panel **C** shows the mRNA levels for *bdnf* and *fosab* in DEX treated group and its associated control. BPA: overnight exposure to bisphenol A; VIN: overnight exposure to vinclozolin; DEX: overnight exposure to dexamethasone; DMSO: overnight exposure to DMSO; 0 min: unstressed; 60 min: 60 minutes post handling stress. DMSO was used as the vehicle for BPA, VIN, and DEX experiments in a final concentration of 0.001%. Two-way ANOVA was performed between each gene in each treatment group and its related control group in both unstressed and stressed states. No statistical comparison was performed between different genes or different treatment groups. If the ANOVA for treatment, stress state and interaction between them (treatment vs stress state) was significant (intercept $p \leq 0.05$), Tukey's post-hoc test was performed for all conditions. The Means (± SEM) with different letters (a, b) are significantly different; $p \leq 0.05$; N=6. If the ANOVA for treatment and stress state was significant ($p \leq 0.05$) and ANOVA for interaction between them (treatment vs stress state) was not significant (intercept $p > 0.05$), Tukey's post-hoc test was only performed for stress state within each treatment group. The Means (± SEM) with a significant difference is marked with an asterisk in this case (*); $p \leq 0.05$; N=6. Each sample contained 22-28, 7dpf SR4G transgenic zebrafish larvae.

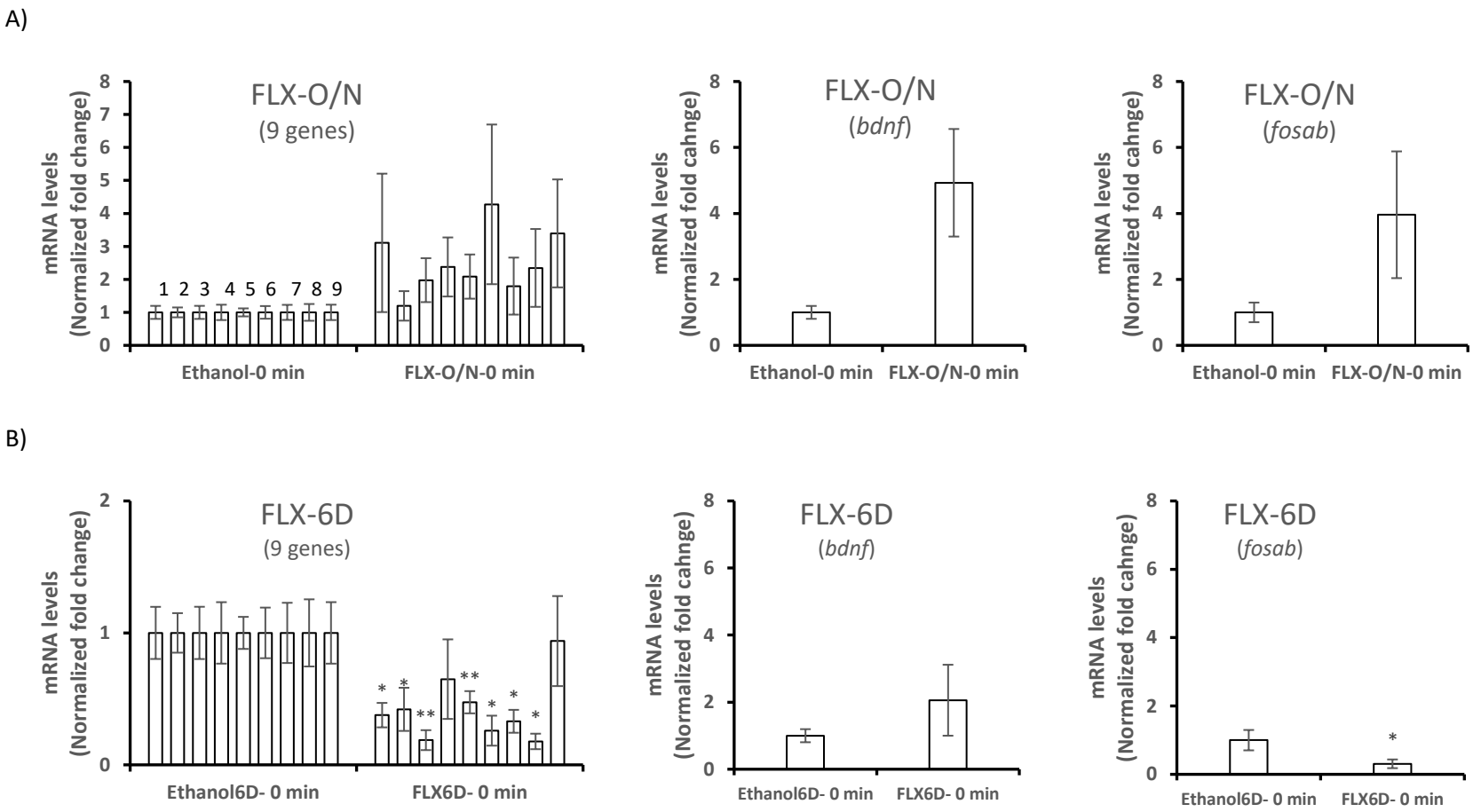

Figure 4.10. Comparing the whole-body mRNA levels of the 11 genes in FLX exposed 7dpf SR4G transgenic zebrafish larvae in the unstressed condition. The values are shown in normalized fold changes using the unstressed control group. The mRNA levels for *bdnf* and *fosab* are separated from the other 9 genes for visual illustration purposes. In each treatment and control groups the 9 genes are arranged alphabetically; from left to right: 1:*crhb, 2:egr2a, 3:fkbp5, 4:fosl1a, 5:htr1b, 6:npas4a, 7:nr4a1, 8:per2, and 9:rorcb.* Panel **A** shows the whole-body mRNA levels of the 11 gens in the FLX-O/N group compared to the Ethanol group in the unstressed condition. Panel **B** shows the whole-body mRNA levels of the 11 gens

in the FLX-6D group compared to the Ethanol-6D group in the unstressed condition. FLX-O/N: overnight exposure to fluoxetine; FLX-6D: daily exposure to fluoxetine from 0 to 6 days post fertilization(dpf); Ethanol: overnight exposure to ethanol, Ethanol6D: daily exposure to ethanol from 0dpf to 6dpf; 0 min: unstressed; 60 min: 60 minutes post handling stress. Ethanol final concentrations in all experiments were 0.005%. One-way ANOVA was performed for each gene in each treatment group and its related control group. No statistical comparison was performed between different genes or different treatment groups. The Means (± SEM) with a significant difference is marked with an asterisk in this case (*****); $p \leq 0.05$; N=6. Each sample contained 22-28, 7dpf SR4G transgenic zebrafish larvae.

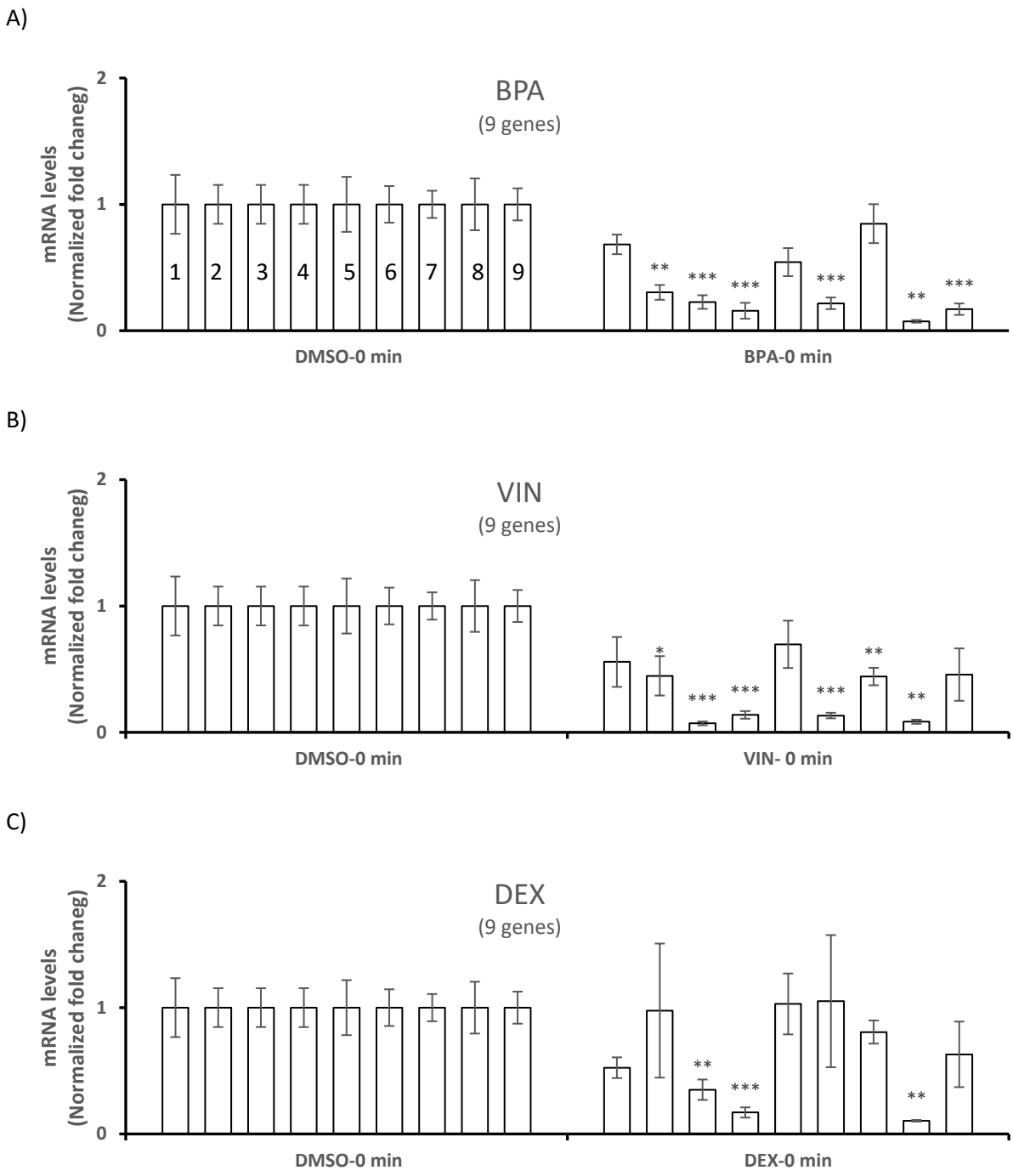

Figure 4.11. Comparing the whole-body mRNA levels of the nine genes in BPA, VIN, and DEX exposed 7dpf SR4G transgenic zebrafish larvae in the unstressed condition. The values are shown in normalized fold changes using the unstressed control group. The mRNA levels for *bdnf* and *fosab* are separated from the other 9 genes for visual illustration purposes. In each treatment and control groups the 9 genes are arranged alphabetically; from left to right: 1:*crhb, 2:egr2a, 3:fkbp5, 4:fosl1a, 5:htr1b, 6:npas4a, 7:nr4a1, 8:per2, and 9:rorcb.* Panel **A** shows the whole-body mRNA levels of the 9 genes in the BPA group compared to the DMSO group in the unstressed condition. Panel **B** shows the whole-body mRNA levels of the 9 genes in the VIN group compared to the DMSO group in the unstressed condition. Panel **C** shows the whole-

body mRNA levels of the 9 genes in the DEX group compared to the DMSO group in the unstressed condition. BPA: overnight exposure to bisphenol A; VIN: overnight exposure to vinclozolin; DEX: overnight exposure to dexamethasone; DMSO: overnight exposure to DMSO; 0 min: unstressed; 60 min: 60 minutes post handling stress. DMSO was used as the vehicle for BPA, VIN, and DEX experiments in a final concentration of 0.001%. One-way ANOVA was performed for each gene in each treatment group and its related control group. No statistical comparison was performed between different genes or different treatment groups. The Means (± SEM) with a significant difference is marked with an asterisk in this case (*); $p \leq 0.05$; N=6. Each sample contained 22-28, 7dpf SR4G transgenic zebrafish larvae.

A)

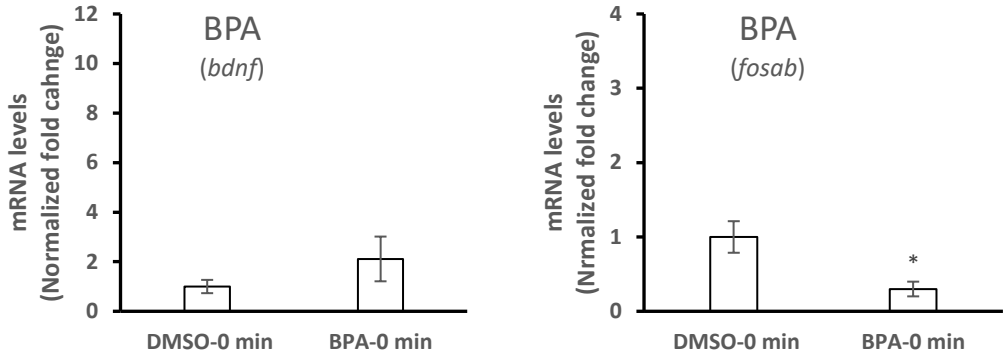

B)

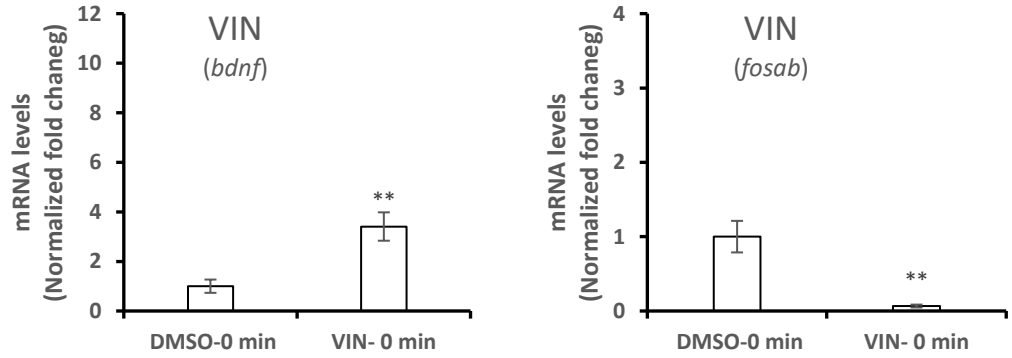

C)

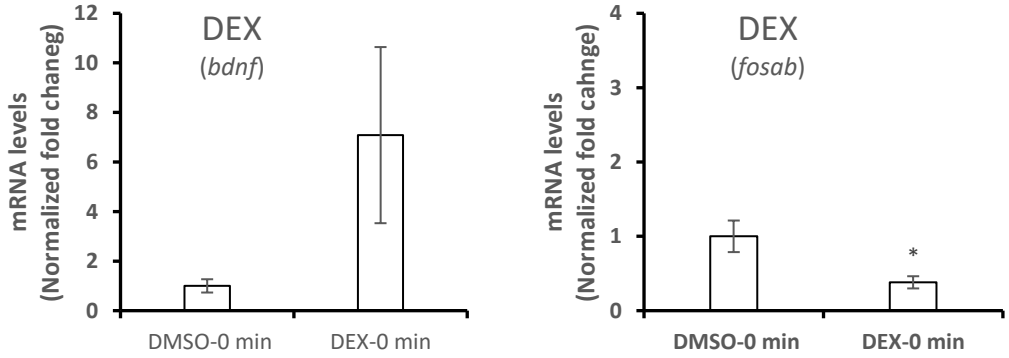

Figure 4.12. Comparing the whole-body mRNA levels of bdnf and fosab in BPA, VIN, and DEX exposed 7dpf SR4G transgenic zebrafish larvae in the unstressed condition. The values are shown in normalized fold changes using the unstressed control group. The mRNA levels for *bdnf* and *fosab* are separated from the other 9 genes for visual illustration purposes. Panel **A** shows the whole-body mRNA levels of the *bdnf* and *fosab* in the BPA group compared to the DMSO group in the unstressed condition. Panel **B** shows the whole-body mRNA levels of *bdnf* and *fosab* in the VIN group compared to the DMSO group in the

unstressed condition. Panel **C** shows the whole-body mRNA levels of *bdnf* and *fosab* in the DEX group compared to the DMSO group in the unstressed condition. BPA: overnight exposure to bisphenol A; VIN: overnight exposure to vinclozolin; DEX: overnight exposure to dexamethasone; DMSO: overnight exposure to DMSO; 0 min: unstressed; 60 min: 60 minutes post handling stress. DMSO was used as the vehicle for BPA, VIN, and DEX experiments in a final concentration of 0.001%. One-way ANOVA was performed for each gene in each treatment group and its related control group. No statistical comparison was performed between different genes or different treatment groups. The Means (± SEM) with a significant difference is marked with an asterisk in this case (*); $p \leq 0.05$; N=6. Each sample contained 22-28, 7dpf SR4G transgenic zebrafish larvae.

Table 4.3. Prediction of stress response based on the whole-body mRNA levels of the 11 genes using regression random forest (RDF) and logistic regression (LOG) model.

Control (ethanol)	Predicted stress status											
	FLX_O/N		FLX-6D		DMSO		BPA		VIN		DEX	
Samples	**LOG**	**RDF**	**LOG**	**RDF**	**LOG**	**RDF**	**LOG**	**RDF**	**LOG**	**RDF**	**LOG**	**RDF**
Unstressed S-1	**0**	1	**0**	**0**	**0**	**0**	**0**	**0**	**0**	**0**	**0**	**0**
Unstressed S-2	1	1	**0**	**0**	**0**	**0**	**0**	**0**	**0**	**0**	**0**	**0**
Unstressed S-3	**0**	**0**	**0**	**0**	**0**	**0**	**0**	**0**	**0**	**0**	**0**	**0**
Unstressed S-4	**0**	**0**	**0**	**0**	**0**	**0**	**0**	**0**	**0**	**0**	**0**	**0**
Unstressed S-5	1	**0**	**0**	**0**	**0**	**0**	**0**	**0**	**0**	**0**	**0**	**0**
Unstressed S-6	1	1	**0**	**0**	**0**	**0**	**0**	**0**	**0**	**0**	**0**	1
Stressed S-1	**1**	**1**	**0**	1	**1**	**1**	1	1	**0**	**0**	**0**	1
Stressed S-2	**1**	**1**	1	1	**1**	**1**	1	1	**0**	**0**	**0**	1
Stressed S-3	**1**	**1**	1	**0**	**1**	**1**	**0**	1	1	**0**	**0**	1
Stressed S-4	0	0	**0**	**0**	**1**	**1**	1	1	**0**	**0**	**0**	1
Stressed S-5	**1**	**1**	**0**	1	**1**	**1**	1	1	**0**	**0**	**0**	1
Stressed S-6	**1**	**1**	1	1	**1**	**1**	1	1	1	**0**	**0**	1
PPV	**62%**	**62%**	N/A	N/A	**100%**	**100%**	N/A	N/A	N/A	N/A	N/A	N/A
NPV	**75%**	**75%**	**100%**	**100%**	**100%**	**100%**	**100%**	**100%**	**100%**	**100%**	**100%**	**100%**

FC: fold change, FLX-6D: daily exposure to from 0 to 6 days post fertilization(dpf); FLX-O/N, BPA, VIN, DEX, CORT represents overnight exposure to fluoxetine, bis-phenol A, vinclozolin, dexamethasone, and cortisol, respectively. LOG: logistic regression, RFD: random forest. PPV: positive predictive value, NPV: negative predictive value. (LOG; R^2: 0.774) (RDF; OOB: 0.4)

4.3.6. Whole-body fluorescence measurements are not sensitive enough to detect disruption of the stress response following chemical. exposure

To determine the potential of fluorescence intensity to predict an altered stress response, transgenic larvae were exposed to a similar set of chemicals as described earlier. The fluorescence intensity was measured on the crude protein extract of a pool of 7dpf SR4G transgenic larvae at two different time points 0 minutes (unstressed) and 120 minutes (2 hours post the handling stress. The two-way ANOVA showed no significant difference regarding the treatment (FLX-6D vs Ethanol-6D; $p>0.05$) and the stress state (stressed vs unstressed; $p>0.05$) on the whole-body fluorescence intensity levels in FLX-6D and its associated control group. Similar findings were observed for the FLX-O/N group (Figure 4.6). Furthermore, two-way ANOVA performed showed no significant difference regarding the treatment (BPA vs DMSO, $p>0.05$; VIN vs DMSO, $p>0.05$; DEX vs DMSO, $p>0.05$) and the stress state (stressed vs unstressed; $p>0.05$) on the whole-body fluorescence intensity levels in all other treatment chemicals and their associated control group (Figure 4.6). Therefore, our findings indicate that fluorescence intensity measured in the described way is not sensitive and does not discriminate between stressed and unstressed state and treatment and control groups.

A)

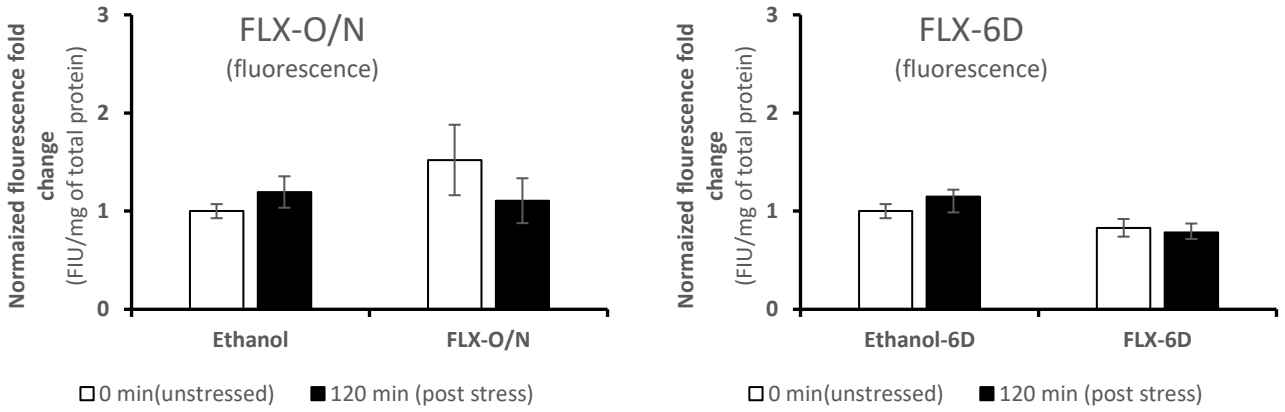

B)

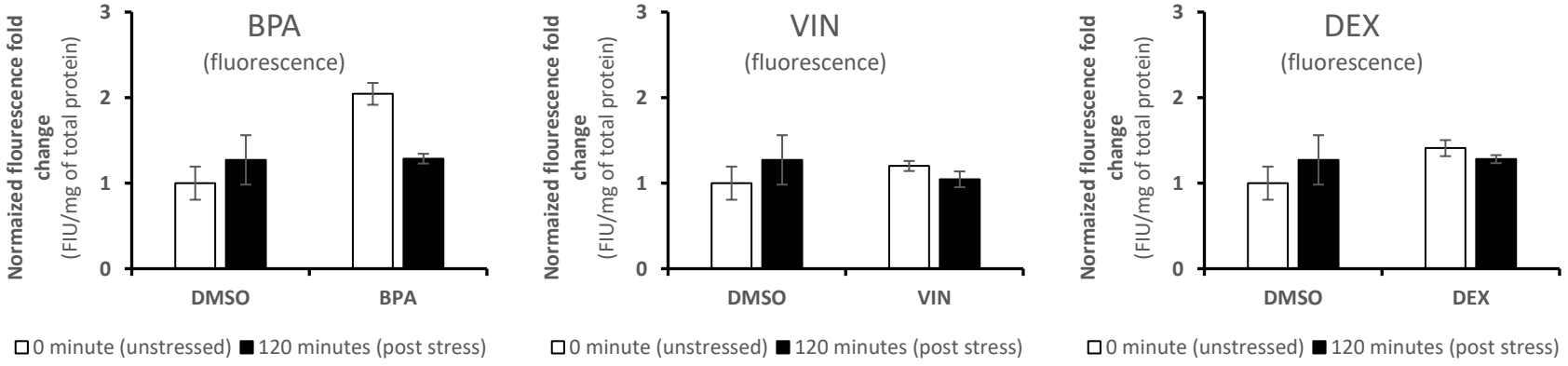

Figure 4.10. The whole-body fluorescence intensity in the crude homogenized extract of 7dpf transgenic zebrafish larvae exposed to different chemicals before and after handling stress. The fluorescence values are measured in fluorescence intensity unit (FIU)/mg of total protein and normalized to the control unstressed condition. Panel **A** shows the whole-body fluorescence intensity measurement in FLX treated groups with their corresponding control groups. The white bars represent fluorescence intensity levels in the unstressed condition (sacrificing subjects at 0

minutes before the handling stress) and the black bars represent fluorescence intensity levels 120 minutes after the final round of handling stress. FLX-O/N: overnight exposure to fluoxetine; FLX-6D: daily exposure to fluoxetine from 0 to 6 days post fertilization(dpf); Ethanol-O/N: overnight exposure to ethanol, Ethanol-6D: daily exposure to ethanol from 0dpf to 6dpf; 0 min: unstressed; 120 min: 120 minutes post handling stress Ethanol final concentrations in all experiments was 0.005%. Panel **B** shows the whole-body fluorescence intensity measurement in 7dpf SR4G larva exposed to BPA, VIN, DEX, and DMSO. BPA: overnight exposure to bisphenol A; VIN: overnight exposure to vinclozolin; DEX: overnight exposure to dexamethasone, DMSO: overnight exposure to DMSO; 0 min: unstressed; 120 min: 120 minutes post handling stress. DMSO was used as the vehicle for BPA, VIN, and DEX experiments in a final concentration of 0.001%. The DMSO data in each graph is the same data portrayed for comparison purposes. Two-way ANOVA was performed between each treatment group and its related control group in both unstressed and stressed state. No statistical comparison was performed between different treatment groups. The ANOVA results were not significant across all treatment and control groups; $p>0.05$; N=6. Each sample contained 22-28, 7dpf SR4G transgenic zebrafish larvae.

4.4. Discussion

We showed a significant positive linear correlation between whole-body levels of cortisol and whole-body eGFP mRNA levels in SR4G larvae. Indeed, eGFP mRNA levels could predict a blunted stress response upon exposure to various EDCs. The eGFP transgene in the SR4G line controls six consecutive glucocorticoid response elements (GRE), making it very sensitive to dynamic changes in the stress-axis line [5]. Measurement of cortisol using immunoassays is the standard approach to determine the stress-axis state and how certain chemicals might affect it [276]. However, this assessment mode requires multiple quality control and optimization steps, and is also time-consuming and expensive [277].

Commonly used immunoassays have cross-reactivity with other steroids and suffer from inter-assay and intra-laboratory variability [27, 278-280]. Other endpoints have been suggested for evaluation of the stress response such as behavioural (e.g. explosive activity, locomotor activity), physiological (e.g. heart rate, blood pressure, pain), metabolic (e.g. glucose, insulin, ketone bodies), neurochemical (e.g. catecholamines, serotonin, dopamine), and endocrine (e.g. ACTH, CRH, vasopressin) [27]. However, the challenges of measuring these endpoints may be greater than immunoassays. Alternatively, the transcriptional analysis of stress-axis genes has been suggested [27]. Several genes such as CRH and POMC (the ACTH precursor protein) have been considered but nervous system sampling is required [27]. This may limit the number size for *in vivo* studies and affect the experiments' associated cost and statistical power. The other alternative is behavioural studies, however, strict study design is necessary to achieve replicable results [281].

In the current study, we suggested measuring eGFP mRNA as an alternative route to assess stress-axis activation in the SR4G zebrafish model. The two predictive models, random forest (RDF) and logistic regression (LOG), trained using whole-body eGFP mRNA in a control group (ethanol), could correctly predict the blunted stress response upon exposure to BPA and VIN in 7-dpf zebrafish larvae.The overnight exposure to BPA and VIN blunted the increase of whole-body cortisol and eGFP mRNA after a handling stressor compared to the control groups. The

negative predictive value of 100% showed that the proposed models could effectively screen these stress-disruptive compounds.

The generated predictive models could discriminate between the two exposure-mode to FLX. A common antidepressant, FLX, elicits its therapeutic and even adverse effects after prolonged exposure [194]. The overnight (18 hours) exposure to FLX did not significantly affect whole-body cortisol levels and, consequently, whole-body eGFP mRNA levels. On the other hand, prolonged developmental exposure (0 to 6-dpf in zebrafish) to FLX resulted in a blunted stress response; evident by a significant decrease in the whole-body cortisol and the whole-body eGFP mRNA after a handling stress in zebrafish larvae.

It was found that the predictive models (RFD and LOG) based on mRNA levels of 11 different genes had similar NPV to the models based on eGFP mRNA only. The selected genes are associated with stress responses, development of depression, and neurogenesis in mammalian and teleost models [215]. Several of the selected genes are considered a member of the immediate early gene (IEG) class. A variety of external stimuli could induce the expression of IEGs, which is rapid, transient, and protein synthesis-independent [282]. The dysregulation of these genes in human and rodent models is associated with altered stress responses and impaired neural plasticity [282-287]. Our study showed that the disruption of the normal stress response upon overnight exposure to BPA and VIN resulted in a marked downregulation of *fosab* after handling stress. Downregulation of *fosab* was observed after the developmental exposure to FLX (FLX-6D group). Similar downregulation was observed in the negative control (DEX). Upregulation of Fos (orthologue of *fosab*) has been observed in specific brain regions following a seizure, tactile sensory stimulation, visual stimulation, cocaine administration, and nursing newborn offspring in rodent models [287, 288]. Alternate splicing and downregulation of Fos have been reported following chronic stress and FLX therapy in rodent models [289].

Several members of the 11 target genes were downregulated following overnight exposure to BPA, VIN, and DEX in unstressed larvae, including *per2, egra2* and *fosl1*. Similar downregulation in unstressed condition was observed following developmental exposure to FLX, and interestingly not the overnight exposure to FLX. Our findings showed a distinct

downregulation of *npas4, nr4a1, per2,* and *rorcb* following developmental exposure to FLX and overnight exposure to VIN in both stressed and unstressed larvae. These four genes are involved in neurogenesis and neural activity in rodent models [287, 290]. This pattern was not observed for BPA and DEX, demonstrating some specificity of the responses, which might be explained by differences in the mechanism of action of these compounds.

Our findings showed that *bdnf, crhb,* and *htr1b* were not affected by exposure to the studied compounds. Brain-derived neurotrophic factor (BDNF) is a critical gene in regulating neural growth, synaptic maturation, and neurogenesis [60]. Although BDNF is not precisely an IEG member, it has activity-associated behaviour and responds to a wide range of external and internal stimuli [290, 291]. The decreased levels of BDNF are associated with the development of major depressive disorder, and its increase following antidepressant therapy is measured as a response to therapy criteria in humans [292]. The neurogenesis induction following TrkB (BDNF receptor) signalling has been implicated in memory formation, addictive behaviour to cocaine, and recovery after stroke [290]. We observed a wide variation in *bdnf* mRNA levels across samples and treatments in our study. The only significant upregulation of *bdnf* was observed upon exposure to VIN when the unstressed conditions were compared. This could be due to the background noise of measuring a gene in whole-body settings [293]. In our study, *crhb* and *htr1b* were not affected by the treatments. However, downregulation of *htr1b* following developmental exposure to FLX was observed when the comparison was performed only in an unstressed condition. There is a discrepancy of findings regarding htr1b alteration following exposure to SSRIs, with some studies showing an apparent dysregulation while others do not report such changes [294, 295]. The exact reason for such discrepancies is presently unknown. The study of mRNA level of the selected 11 genes had similar predictive value as the study of eGFP mRNA only in SR4G transgenic larvae. Although the study of these genes in both unstressed and stressed conditions is likely more sensitive to show disrupted stress response, the study in only unstressed condition could also be as effective; at least for potent stress-disruptive compounds such as BPA and VIN. This will affect the time and the costs associated with the potential screening experiments.

We also measured the whole-body fluorescence signal in the crude homogenized pooled sample of SR4G transgenic larvae. Our preliminary experiments in the previous chapter (Chapter 2) using microscopic fluorescence imaging showed that measurement of fluorescence intensity in four anatomical regions (including telencephalon and diencephalon) could discriminate between the stressed and unstressed conditions in 4 dpf SR4G zebrafish larvae. However, using the homogenized sample to measure the fluorescence signal was not as accurate and as predictive as whole-body cortisol measurement and whole-body eGFP mRNA measurement to assess stress-response. Previously, two transgenic zebrafish line with the eGFP reporter gene under the control of estrogen response elements were developed and provided promising results in detecting low levels of estrogenic compounds (17α-ethynylestradiol, diethylstilbestrol, and BPA) in environmental samples [162]. The main drawbacks in the wide-spread use of these reporter lines are the need for individual imaging of zebrafish embryos/larvae, the need for sensitive fluorescence detection devices, and the long half-life of the eGFP protein, which could not reflect the dynamic nature of toxicity [150, 162, 169, 296]. Improving the extraction method, enhancing protein integrity preservation after extraction, and optimizing the number of larvae per sample, may improve the outcome and need further study.

The major obstacles in the design and development of environmental risk assessment surveillance tools are defining exposure settings (acute vs chronic), appropriate biomarkers, ideal tissue specimens, ability to detect the effect of a single or combinations of toxicants, ability to screen for potential within-generational and transgenerational effects, and finally the associated cost and volume capacity of screening an array of compounds [162]. Using transgenic zebrafish larvae, such as SR4G, could address many of these obstacles. For example, we showed that predictive models can be created to detect a physiologic response using the transgene alone, or in combination with other genes of interest. Additionally, this approach has the potential to discriminate between different exposure settings (e.g., chronic vs acute). This approach potentially can be adapted to detect different types of chemical exposures by introducing different transgenic constructs.

4.5. Statement of contribution

Amin Nozari designed the study, developed the methodology, conducted the experiments, and prepared the manuscript. Dr. Vance Trudeau, helped with the design of the study, development of methodology and manuscript editing.

Chapter 5: General discussion and future directions

5.1. Thesis summary and discussion

Our transcriptomic study and orthologue pathways analysis on larval and adult brain showed a life-long dysregulation of numerous genes involved in nervous system development, stress response, and lipid metabolism. Many endocrine pathways, mainly regulated by the hypothalamus, were affected by developmental exposure to FLX, including GnRH signalling, glucocorticoid receptor signalling, androgen, relaxin signalling, and prolactin signalling. The upstream transcription factor analysis showed that the dysregulations of *clocka* and *nr3c1, amongst others,* were the potential drivers of the observed life-long effects. Life-long dysregulation of *bdnf*, *trkb*, and *npas4,* critical genes in neurogenesis, was observed [60]. Several genes associated with epigenetic machinery, including *dnmt3a, adarb1, adaeb2, hdac4, hdac5, hdac8,* and *atf2* were affected by developmental exposure to FLX. To our knowledge, only a handful of studies investigated the global transcriptomic effects of FLX in the zebrafish brain. Our findings suggest that the observed long-lasting effects on brain transcriptome might be mediated through the effects of glucocorticoids on neurodevelopment with likely involvement of epigenetic mechanism. There is extensive evidence of the long-lasting effects of SSRIs in human, rodents, and teleost upon prenatal and developmental exposure [89, 122].

The developmental origin of health and disease (DOHaD) hypothesis states that conditioning during antenatal and prenatal development shapes an individual's risk to acquire chronic illness over the lifespan [297]. Based on observational studies in humans, there is a direct association between perinatal/early-post natal exposure to adverse conditions and mental health disorder later in life during adolescence and likely adulthood [298]. A meta-analysis review by Su *et al.* (2020) summarized this association. Several biological factors (low birth weight, gestational age, young gestational age, and parent's age), psychological factors (maternal stress, maternal anxiety, and maternal prenatal depression), and sociological factors (maternal education, socioeconomic status, maternal smoking, and paternal smoking) were found to be significantly related to increased risk of the developmental of depression in offspring [298]. Studies in human and rodent models suggest that prenatal adversities result in altered

neurodevelopment [75, 82, 233]. For example, postnatal MRI (magnetic resonance imaging) studies in children of mothers suffering from depression and anxiety have shown structural changes in the right insula, dorsolateral prefrontal cortex, right middle occipital cortex, right angular gyrus, uncinate fasciculus, posterior cingulate, and parahippocampus [299, 300]. Increased functional connectivity between these structures is observed in a patient with the major depressive disorder [301]. Numerous studies have shown a potential role for glucocorticoids as the mediator between maternal adversity and offspring development. The glucocorticoid receptors are expressed ubiquitously in the developing nervous system, and their precise regulations are necessary for the proper development of neural circuits. There is extensive evidence for the effects of glucocorticoid levels and the rate of neural apoptosis in different developing brain regions, particularly the hippocampus and amygdala [25, 302].

Our orthologue pathways analysis showed that zebrafish is a good model organism to study the life-long effects of psychopharmaceuticals. The short development period from embryonic stages to adulthood, easy exposure routine in different life stages, and highly conserved CNS structure, both in molecular and neural circuits levels, are making zebrafish an excellent model organism to study the neuropharmacology [122]. Our upstream transcription regulator analysis was suggestive of the involvement of NR3C1 related pathways in the zebrafish nervous system. The previous studies in our lab have shown that the developmental exposure to FLX in zebrafish resulted in transgenerational hypocortisolism, which could explain the observed increased anxiety-like behaviour of the exposed male adult zebrafish [1, 2]. Although we did not measure whole-body cortisol levels in adult zebrafish, the previous studies in our lab [1, 2] and the measurements performed on exposed larvae in Chapter 4 showed decreased whole-body cortisol level in male adults and 7-dpf zebrafish larvae, respectively.

Several limitations should be noted while interpreting the findings of the current study. We have used *Homo sapiens* orthologue annotations to interpret the pathways affected upon developmental exposure to FLX in zebrafish. Although there are high levels of conservation between gene functions and overall molecular pathways between human and zebrafish, the exact mechanistic networking might not exist in zebrafish. Since the effects of duplicated genes were not considered in the current study, several pathways and networks might be over- or

under-represented in our study. The advancement of pathway analysing algorithms based on existing zebrafish annotated pathways shall alleviate this problem.Although we focused our study on adult male individuals, the sexual separation was not possible for larvae study. It is well known that the long-lasting effects of developmental exposure to both stress and SSRIs are sex and time dependant. This should be considered while interpreting the life-long effects of the observed transcriptomics.

In Chapter 4, we showed a significant positive linear correlation between the whole-body cortisol levels and the whole-body transcription levels of eGFP in SR4G transgenic zebrafish larvae (R^2> 0.9). The two predictive models trained based on the eGFP mRNA levels could correctly predict the blunted stress response upon exposure to BPA, VIN, DEX, and FLX. The negative predictive value (NPV) of these models was 100%. The proposed model could discriminate between short exposure and more prolonged developmental exposure to FLX. We also found that models based on the mRNA transcription levels of 11 genes, associated with immediate-early response genes, resulted in a similar 100% NPV as eGFP mRNA based models. This finding emphasized that eGFP transcription in the SR4G zebrafish line could be used as the tier-1 test in environmental risk assessment studies to screen for stress-disruptive compounds like SSRI antidepressants. The SSRIs are considered emerging environmental contaminants. Their high levels of prescription results in high levels of the active compounds and/or their metabolites in the effluents of swage treatment facilities [142, 303-305]. Given the similarities between serotonergic systems in humans and different fish species, the risk of drug-induced interference with hormonal systems in these non-target organisms is high [254-256]. For instance, zebrafish has a similar gene sequence and genomic structure regarding the superfamily of serotonin receptors and serotonin transporters compared to the mammalian models [306]. It has been shown that 15 days of exposure to FLX (50 µg/L) in adult zebrafish could result in a blunted response to an acute stressor [127]. In another example, Theodoridi *et al.,* (2017) showed acute 2 hours exposure to FLX (5 mg/L) could decrease offensive behaviour in the dominant zebrafish and decrease freezing behaviour (an anxiety-like response) in the subordinate zebrafish [232]. These behaviour changes were accompanied by a change in the mRNA levels of several genes involved in the stress-axis and neural activity, including *nr3c1, nr3c2, bdnf, fosab, htr2b,* and

slc6a4b [232]. Altered feeding behaviour (5µg/g body weight), delayed sexual maturation (71µg/L), decreased growth (0.5 µg/L), altered anxiety-like behaviours (1 µg/L), and developmental abnormalities (0.1-5 µg/L) have been reported in zebrafish following exposure to FLX [307].

We showed that SR4G transgenic line could be used as an *in vivo* screening model to screen stress disruption. The previously described capacity for automation of zebrafish-based tests [261] could facilitate the high throughput screening of a large library of potential stress disruptive compounds using this transgenic model. Several strategies have been introduced for using zebrafish in biomonitoring studies, including mortality (e.g., LC50), morphological assessment, transgene biomarkers and behavioural monitoring [115]. The transgenic zebrafish lines with fluorescent reporter genes are particularly of interest in the study of developmental disease, reproduction, neurobehavior and toxicology [145, 151]. Recently, several transgenic zebrafish models have been created for biomonitoring of heavy metals (luciferase reporter gene under the control of mouse metal response element promoter [308]), xenoestrogens (GFP reporter gene under the control of the *vtg* promoter [309]), and aromatic hydrocarbons (luciferase reporter gene under the control of human aryl hydrocarbon response elements promoter [308]) in environmental smaples. The major obstacles in designing a novel biomonitoring approach based on the zebrafish model include the ability to detect the effect of a single toxicant or combination of toxicants, the ability to screen for potential life-long and transgenerational effects, the high throughput capacity, and the cost of screening an extensive library of chemical [162]. Zebrafish have been proposed to address majority of these obstcles and is considered as the model to bridge *in vitro* and *in vivo* studies [146, 150, 160, 169]..

5.2. Significance of these findings

The findings reported in this doctoral thesis contribute to our understanding of the potential life-long effects of FLX in an amenable vertebrate model. More than 264 million people worldwide suffer from depression, and antidepressants are widely prescribed as the first line of treatment [75]. The consumption of antidepressants during pregnancy, particularly SSRIs like FLX, increases the risks of fetal exposure to antidepressants. Adverse effects such as disruption of the

normal stress response and altered social behaviour have been reported in humans and animal models [56, 203, 206, 310] upon prenatal exposure to SSRIs. Moreover, it has been shown that FLX reaches the water bodies through sewage treatment facilities and could disrupt the normal function of the endocrine pathways and fish behaviour [303, 311, 312].

Recently, in our lab, for the first time, we showed the evidence of transgenerational effects of developmental exposure to FLX, demonstrated by altered exploratory behaviour and hypocortisolism three generations withdrew from FLX in zebrafish [1-3]. The findings presented here provide extensive information about the underlying mechanisms for a life-long transfer of such traits, including response to stress and neural development. Moreover, a proof-of-concept for a biomonitoring tool based on the SR4G zebrafish line to screen the adverse effects of environmental pollutant has been established. We showed that our proposed model could detect a blunted stress response upon exposure to BPA (a widely used plasticizer with a high level of environmental contamination) and VIN (a fungicide commonly used in agriculture which is determined as an EDC).

5.3. Future perspectives

The research presented in this doctoral thesis generated extensive "big data" outcomes that can be used as a strong foundation for future studies. Some of the direct lines of investigation are presented below:

1. Assessment of promoter regions of the genes of interest for potential epigenetic marking sites such as CpG islands and microRNA binding sites followed by targeted studies such as RRBS (reduced representation bisulfite sequencing) BisPCR^2.
2. The transgenerational whole-genome DNA methylation analysis in targeted brain regions including telencephalon and hypothalamus; life-longly and trans-generationally.
3. *In situ* hybridization and immunohistochemistry studies to localize affected neural circuits upon developmental exposure to FLX in zebrafish larva and adult brain

4. The automation of eGFP transcription analysis in the SR4G transgenic line to create dose-response plots for known EDCs followed by screening a medium to a large number of chemicals for their stress disruption potentials.
5. Improvement of whole-body fluorescence assessment analysis in the SR4G transgenic line, using an improved extraction method or more sensitive fluorescence imaging system to substitute the eGFP transcription analysis for screening stress-disrupting compounds.

Supplementary data

A) B)

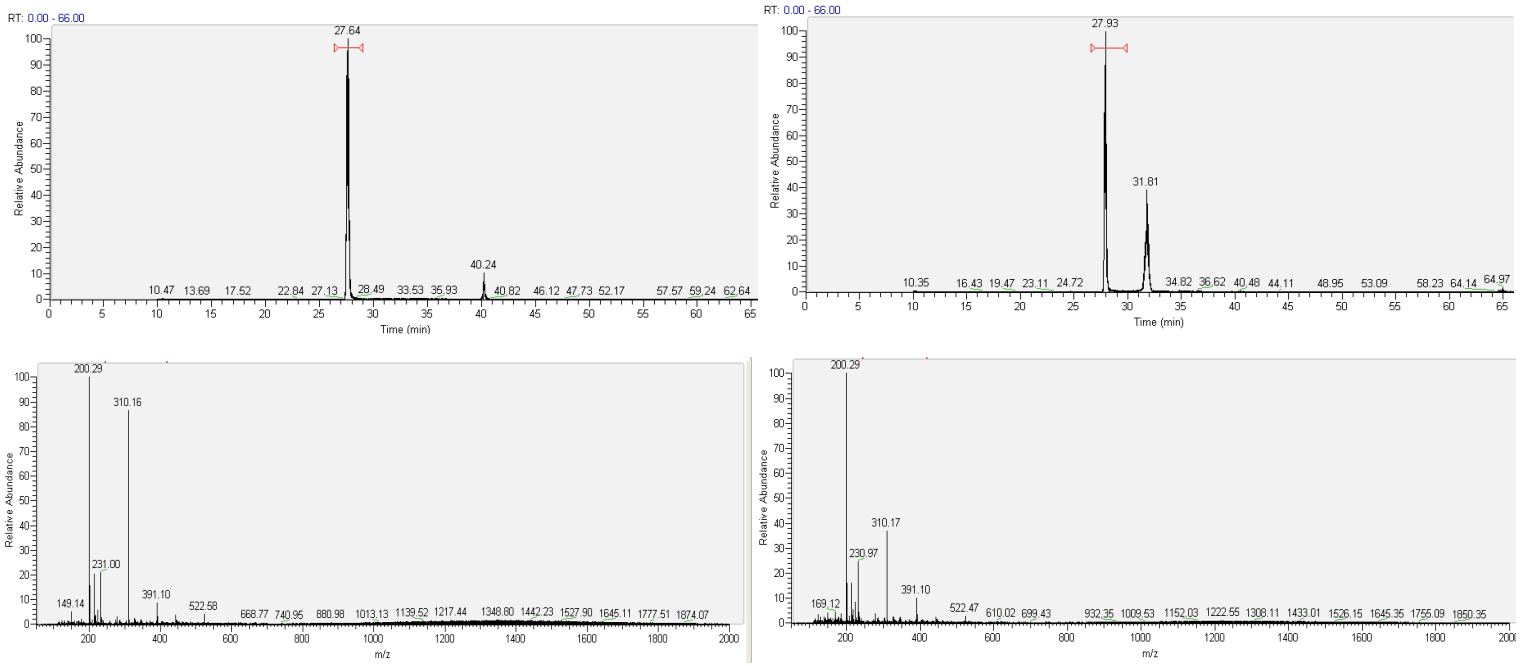

Supplementary Figure 1. The mass spectrometry analysis of the fluoxetine stock preparations. To confirm that the storage in -80 oC does not affect the concentration of FLX, in freshly prepared working dilution from stock solution, the concentration working solution (54 µg/L) was assessd by liquid chromatography-Mass spectropmetry. Two stock of fluoxetine were compared; FLX-ethanol (1mg/ml fluoxetine prepared in 95% ethanol), and FLX-water (4mg/ml fluoxetine prepared in water). Several dilutions were prepared and compared for the m/z ratio. Panel **A** shows the detected relative abundance and m/z ratio for 0.17mM concentration prepared from FLX-ethanol stock. Panel **B** shows the detected relative

abundance and m/z ratio for 0.17mM concentration prepared from FLX-water stock. Similar relative abundance and m/z ratio was detected for both stocks in working concentration of 0.17mM concentration.

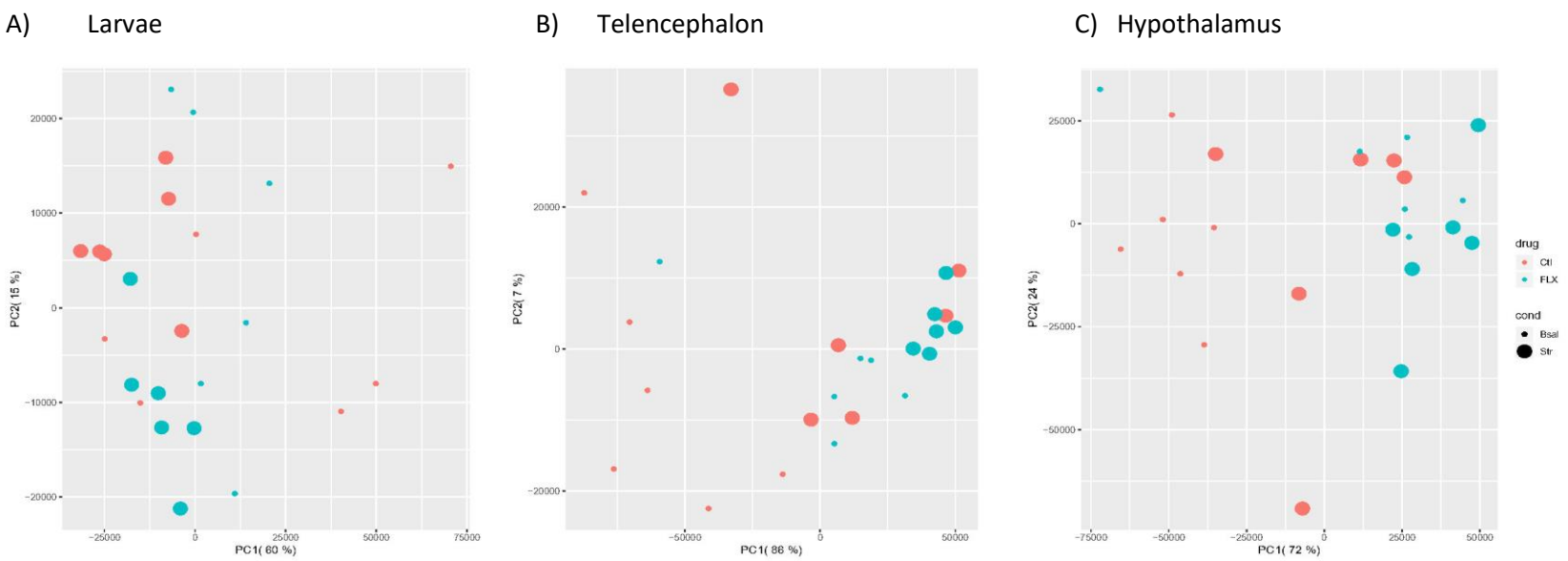

Supplementary Figure 2. Principle component analysis of the differentially expressed genes obtained from each tissue sample in 24 samples. EL-larvae (a), Each graph shows the gene clustering across all 24 samples based on the PC1(x-axis) and PC2 (y-axis). Panel (A) depicts the data set for FLX exposed larvae compared to the control larvae. Panel (B) depicts the data set for telencephalon from adults exposed to FLX in the early life developmental stage compared to control adults exposed to vehicle compound (ethanol) in the early life developmental stage. Panel (C) depicts the data set for the hypothalamus from adults exposed to FLX in the early life developmental stage compared to control adults exposed to vehicle compound (ethanol) in the early life developmental stage. Blue: FLX treated, red: control (ethanol), small circles: unstressed condition, big circles: stressed condition.

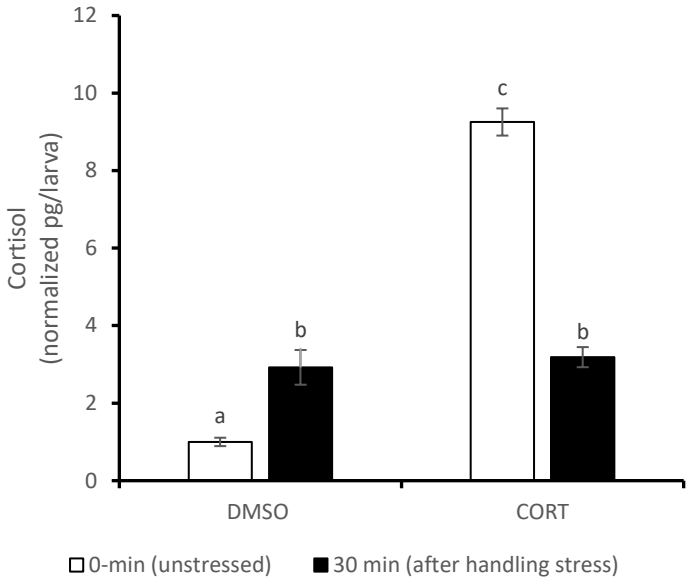

Supplementary Figure 3. Whole-body cortisol levels in 7dpf transgenic zebrafish larvae exposed to cortisol before and after handling stress. The cortisol levels are measured in pg/larva and normalized to the control unstressed condition. The graph shows the whole-body cortisol measurement in the cortisol treated group (CORT) with their corresponding control group (DMSO). The white bars represent cortisol levels in the unstressed condition (sacrificing subjects at 0 minutes before the handling stress) and the black bars represent cortisol levels 30 minutes after the final round of handling stress. CORT: overnight exposure to 10mM cortisol; DMSO: overnight exposure to DMSO; 0 min: unstressed; 60 min: 60 minutes post handling stress. DMSO was used as the vehicle in a final concentration of 0.001%. Two-way ANOVA was performed. Tukey's post-hoc test followed the significant ANOVA results for pairwise comparisons. Means (± SEM) with different letters (a, b) are significantly different; $p \leq 0.05$; N=6. Each sample contained a pool of 22-28 7dpf SR4G transgenic zebrafish larvae.

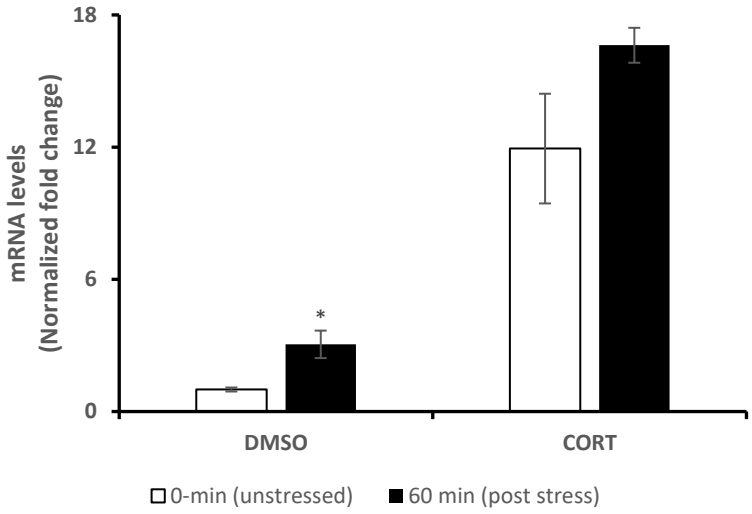

Supplementary Figure 4. Whole-body eGFP mRNA levels in 7dpf transgenic zebrafish larvae exposed to cortisol before and after the handling stress. The whole-body eGFP mRNA levels are measured in pg/larva and normalized to the control unstressed condition. The graph shows the eGFP mRNA levels in cortisol (CORT) treated groups with its corresponding control group (DMSO). The white bars represent cortisol levels in the unstressed condition (sacrificing subjects at 0 minutes before the handling stress) and the black bars represent eGFP mRNA levels 60 minutes after the final round of handling stress. CORT: overnight exposure to cortisol 10mM; DMSO: overnight exposure to DMSO; 0 min: unstressed; 60 min: 60 minutes post handling stress. DMSO was used as the vehicle in a final concentration of 0.001%. The DMSO data in each graph is the same data portrayed for comparison purposes. Two-way ANOVA was performed. Means (± SEM) with an asterisk (*) are significantly different compare to the control unstressed state ($p \leq 0.05$); N=6. Each sample contained a pool of 22-28 7dpf SR4G transgenic zebrafish larvae.

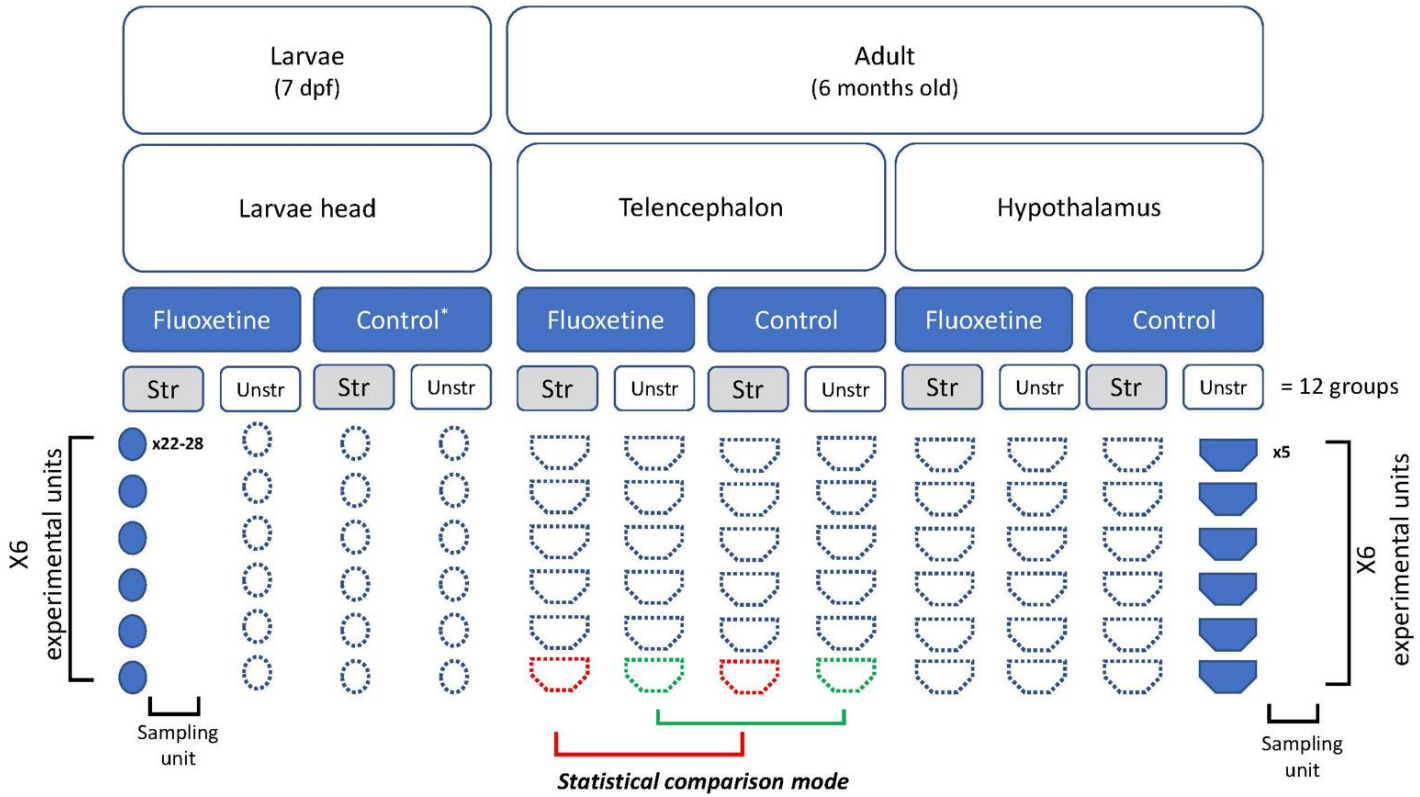

Supplementary Figure 5. The experimental design to study the life-long effects of developmental exposure to fluoxetine in zebrafish. Zebrafish larvae (each petri dish containing 22-28 larvae) were daily exposed to fluoxetine (54µg/L) or control (ethanol 0.005%) from 0 to 6 dpf. Each group was further divided into stressed (Str) and unstressed (Unstr) based on the handling stress routine described elsewhere in this manuscript. A pooled sample of larvae head (22-28 larvae, 7 dpf) was prepared. Each experiment was conducted in 6 experimental replicates. Several subgroups of developmentally exposed and not-exposed larvae were raised to adulthood (6 months of age) in separate tanks. They were further divided into stressed and unstressed based on the handling stress routine described elsewhere in this manuscript. Telencephalon and hypothalamus were harvested from 5 male individuals in each group and pooled in a single sample tube. A total of 6 experimental replicates was assessed. The statistical comparison for the RNAseq study was performed between unstressed and stressed condition considering the fluoxetine exposure background.

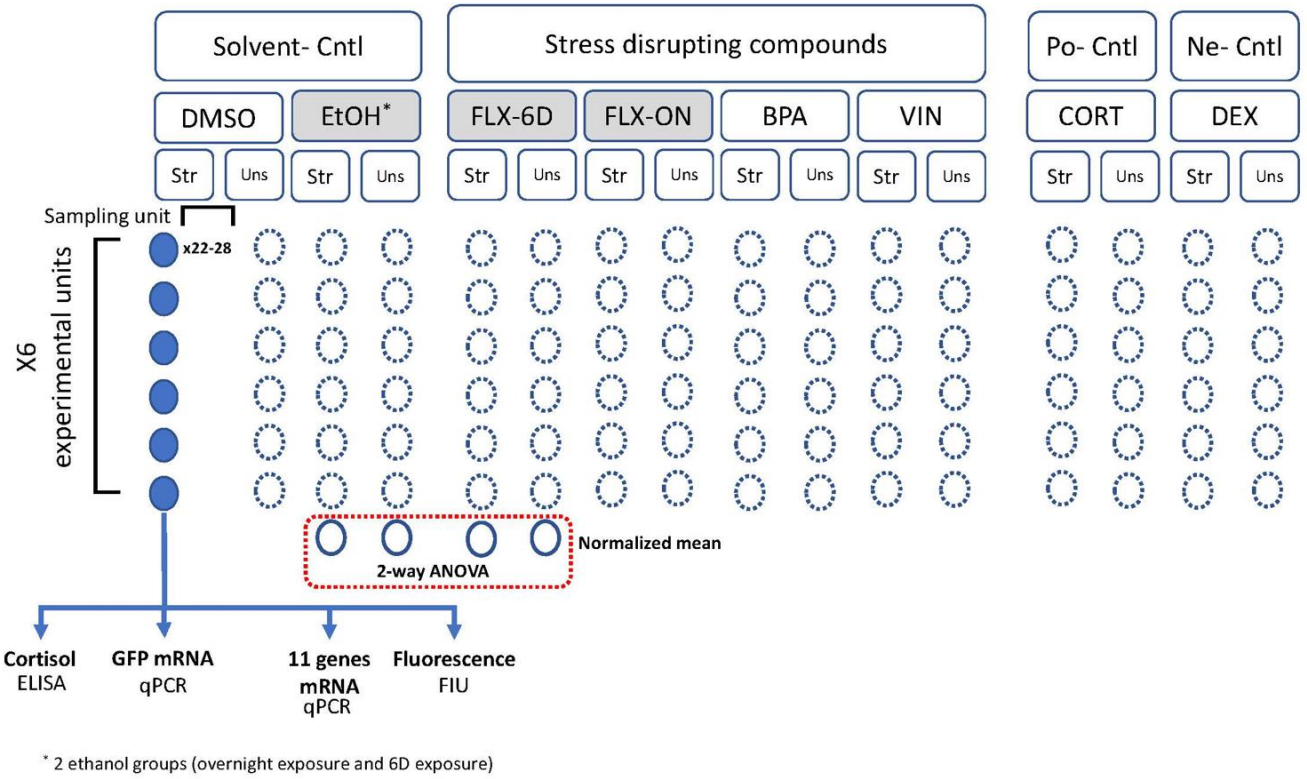

Supplementary Figure 6. The experimental design to study the life-long effects of developmental exposure to fluoxetine in zebrafish. Zebrafish larvae (6 dpf, each petri dish containing 22-28 larvae) were exposed overnight to different treatment (FLX- O/N: fluoxetine, BPA: bisphenol A, VIN: vinclozolin, DEX: dexamethasone, CORT: cortisol) and controls (DMSO and EtOH: ethanol). Also, one group of larvae (each petri dish containing 22-28 larvae) were daily exposed to fluoxetine (54µg/L) or control (ethanol 0.005%) from 0 to 6 dpf. All groups were further divided into stressed (Str) and unstressed (Uns) based on the handling stress described elsewhere in this manuscript. All experiments were conducted on 7 dpf larvae and with 6 experimental replicates. Several endpoints were studied at different time points described elsewhere, including cortisol (ELISA), eGFP mRNA (qPCR), eGFP fluorescence (FIU: fluorescence intensity unit in microscope imaging), and mRNA of 11 target genes. CORT was selected as a positive control (Po-Cntl), and DEX was selected as a negative

control (Ne-Cntl) in this study. 2-way ANOVA was used to determine the statistical significance of treatment exposure on stress response compared to control groups.

Supplementary Table 1. Pathways affected life-longly by developmental exposure to fluoxetine in the unstressed condition

Canonical pathway	unstressed		
	L	H	T
Apelin Cardiac Fibroblast Signaling Pathway			
Caveolar-mediated Endocytosis Signaling			
Choline Biosynthesis III			
D-myo-inositol (1,4,5)-Trisphosphate Biosynthesis			
Ephrin A Signaling			
Glycolysis I			
GP6 Signaling Pathway			
HIPPO signaling			
Ketogenesis			
Mevalonate Pathway I			
Nitric Oxide Signaling in the Cardiovascular System			
Phagosome Formation			
Phagosome Maturation			
RhoA Signaling			
14-3-3-mediated Signaling			
3-phosphoinositide Biosynthesis			
3-phosphoinositide Degradation			
4-1BB Signaling in T Lymphocytes			
Actin Cytoskeleton Signaling			
Actin Nucleation by ARP-WASP Complex			
Acute Myeloid Leukemia Signaling			
Adrenomedullin signaling pathway			
Aldosterone Signaling in Epithelial Cells			
Androgen Signaling			
Angiopoietin Signaling			
Antioxidant Action of Vitamin C			
Antiproliferative Role of Somatostatin Receptor 2			
Apelin Adipocyte Signaling Pathway			
Apelin Cardiomyocyte Signaling Pathway			
Apelin Muscle Signaling Pathway			
Apoptosis Signaling			
April Mediated Signaling			
Arginine Degradation I (Arginase Pathway)			

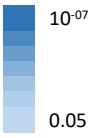

Supplementary Table 1. Pathways affected life-longly by developmental exposure to fluoxetine in the unstressed condition (cont…)

Canonical pathway	unstressed		
	L	H	T
B Cell Activating Factor Signaling			
B Cell Receptor Signaling			
BMP signaling pathway			
Breast Cancer Regulation by Stathmin1			
cAMP-mediated signaling			
Cancer Drug Resistance By Drug Efflux			
Cardiac β-adrenergic Signaling			
CCR3 Signaling in Eosinophils			
CCR5 Signaling in Macrophages			
CDK5 Signaling			
Ceramide Signaling			
Chemokine Signaling			
Chronic Myeloid Leukemia Signaling			
Circadian Rhythm Signaling			
CNTF Signaling			
Colorectal Cancer Metastasis Signaling			
Corticotropin Releasing Hormone Signaling			
D-myo-inositol (1,4,5,6)-Tetrakisphosphate Biosynthesis			
D-myo-inositol (3,4,5,6)-tetrakisphosphate Biosynthesis			
D-myo-inositol-5-phosphate Metabolism			
EGF Signaling			
EIF2 Signaling			
Endocannabinoid Cancer Inhibition Pathway			
Endocannabinoid Developing Neuron Pathway			
Endocannabinoid Neuronal Synapse Pathway			
Endometrial Cancer Signaling			
Endothelin-1 Signaling			
Ephrin B Signaling			
Ephrin Receptor Signaling			
ErbB Signaling			
ErbB2-ErbB3 Signaling			
ErbB4 Signaling			
ERK5 Signaling			

Supplementary Table 1. Pathways affected life-longly by developmental exposure to fluoxetine in the unstressed condition (cont…)

Canonical pathway	unstressed		
	L	H	T
Erythropoietin Signaling			
Estrogen Receptor Signaling			
Estrogen-Dependent Breast Cancer Signaling			
FAK Signaling			
FAT10 Cancer Signaling Pathway			
Fc Epsilon RI Signaling			
Fcγ Receptor-mediated Phagocytosis in Macrophages and Monocytes			
FcγRIIB Signaling in B Lymphocytes			
FGF Signaling			
FLT3 Signaling in Hematopoietic Progenitor Cells			
fMLP Signaling in Neutrophils			
G Beta Gamma Signaling			
GABA Receptor Signaling			
Gap Junction Signaling			
GDNF Family Ligand-Receptor Interactions			
Glioma Signaling			
Glucocorticoid Receptor Signaling			
Glutamate Receptor Signaling			
GM-CSF Signaling			
GPCR-Mediated Nutrient Sensing in Enteroendocrine Cells			
G-Protein Coupled Receptor Signaling			
Growth Hormone Signaling			
Gustation Pathway			
Gα12/13 Signaling			
Gαi Signaling			
Gαs Signaling			
HER-2 Signaling in Breast Cancer			
Hereditary Breast Cancer Signaling			
HGF Signaling			
HIF1α Signaling			
HMGB1 Signaling			
Huntington's Disease Signaling			

Supplementary Table 1. Pathways affected life-longly by developmental exposure to fluoxetine in the unstressed condition (cont…)

Canonical pathway	unstressed		
	L	H	T
IL-15 Signaling			
IL-17 Signaling			
IL-17A Signaling in Airway Cells			
IL-2 Signaling			
IL-22 Signaling			
IL-3 Signaling			
IL-6 Signaling			
IL-9 Signaling			
Inhibition of Angiogenesis by TSP1			
Insulin Receptor Signaling			
JAK/Stat Signaling			
L-carnitine Biosynthesis			
Leptin Signaling in Obesity			
LPS-stimulated MAPK Signaling			
Melanocyte Development and Pigmentation Signaling			
Melanoma Signaling			
Melatonin Signaling			
Molecular Mechanisms of Cancer			
Mouse Embryonic Stem Cell Pluripotency			
Myc Mediated Apoptosis Signaling			
Natural Killer Cell Signaling			
Neuregulin Signaling			
Neurotrophin/TRK Signaling			
NF-κB Activation by Viruses			
NGF Signaling			
nNOS Signaling in Neurons			
Non-Small Cell Lung Cancer Signaling			
NRF2-mediated Oxidative Stress Response			
Oncostatin M Signaling			
Opioid Signaling Pathway			
P2Y Purigenic Receptor Signaling Pathway			
Pancreatic Adenocarcinoma Signaling			

Supplementary Table 1. Pathways affected life-longly by developmental exposure to fluoxetine in the unstressed condition (cont…)

Canonical pathway	unstressed		
	L	H	T
PDGF Signaling			
PEDF Signaling			
PFKFB4 Signaling Pathway			
PI3K Signaling in B Lymphocytes			
PKCθ Signaling in T Lymphocytes			
PPAR Signaling			
PPARα/RXRα Activation			
Production of Nitric Oxide and Reactive Oxygen Species in Macrophages			
Prolactin Signaling			
Prostate Cancer Signaling			
RANK Signaling in Osteoclasts			
RAR Activation			
Reelin Signaling in Neurons			
Regulation of Cellular Mechanics by Calpain Protease			
Regulation of eIF4 and p70S6K Signaling			
Regulation of IL-2 Expression in Activated and Anergic T Lymphocytes			
Regulation of the Epithelial-Mesenchymal Transition Pathway			
Relaxin Signaling			
Renal Cell Carcinoma Signaling			
Renin-Angiotensin Signaling			
RhoGDI Signaling			
Role of JAK family kinases in IL-6-type Cytokine Signaling			
Role of JAK1 and JAK3 in γc Cytokine Signaling			
Role of MAPK Signaling in the Pathogenesis of Influenza			
Role of NANOG in Mammalian Embryonic Stem Cell Pluripotency			
Role of NFAT in Regulation of the Immune Response			
Role of Tissue Factor in Cancer			
SAPK/JNK Signaling			
Sertoli Cell-Sertoli Cell Junction Signaling			
Small Cell Lung Cancer Signaling			
Sphingosine-1-phosphate Signaling			
SPINK1 General Cancer Pathway			

Supplementary Table 1. Pathways affected life-longly by developmental exposure to fluoxetine in the unstressed condition (cont…)

Canonical pathway	unstressed		
	L	H	T
Sumoylation Pathway			
Superpathway of Inositol Phosphate Compounds			
Synaptic Long Term Depression			
Synaptic Long Term Potentiation			
Systemic Lupus Erythematosus In T Cell Signaling Pathway			
T Cell Exhaustion Signaling Pathway			
T Cell Receptor Signaling			
Tec Kinase Signaling			
Telomerase Signaling			
TGF-β Signaling			
Thrombin Signaling			
Thrombopoietin Signaling			
Thyroid Cancer Signaling			
tRNA Splicing			
Type II Diabetes Mellitus Signaling			
UVA-Induced MAPK Signaling			
UVB-Induced MAPK Signaling			
UVC-Induced MAPK Signaling			
VEGF Family Ligand-Receptor Interactions			
VEGF Signaling			
White Adipose Tissue Browning Pathway			
Wnt/Ca+ pathway			
Xenobiotic Metabolism Signaling			
α-Adrenergic Signaling			

Different shades of blue representing the negative logarithmic scale of the associated p-value (-log p-value); the dense colours present lower p values, and lighter colours present a higher p-value. Only significant data ($p \leq 0.05$) are shown in the blue gradient. Gray represent non-significant data. L: larvae (unstr-FLX-L); H: hypothalamus (unstr-FLX-Hyp); T: telencephalon (unstr-FLX-Tel).

Supplementary Table 2. Pathways affected life-longly by developmental exposure to fluoxetine in stressed condition

Canonical pathways	stressed		
	L	H	T
Adenine and Adenosine Salvage VI			
Cancer Drug Resistance By Drug Efflux			
Chemokine Signaling			
Cholecystokinin/Gastrin-mediated Signaling			
Coagulation System			
CXCR4 Signaling			
D-myo-inositol (1,4,5,6)-Tetrakisphosphate Biosynthesis			
D-myo-inositol (3,4,5,6)-tetrakisphosphate Biosynthesis			
Endothelin-1 Signaling			
eNOS Signaling			
Ephrin B Signaling			
Ephrin Receptor Signaling			
ERK5 Signaling			
Folate Polyglutamylation			
Glucocorticoid Receptor Signaling			
Glycogen Degradation II			
Glycogen Degradation III			
GNRH Signaling			
HER-2 Signaling in Breast Cancer			
JAK/Stat Signaling			
NAD Salvage Pathway II			
Prolactin Signaling			
RAR Activation			
Relaxin Signaling			
Retinol Biosynthesis			
Role of Tissue Factor in Cancer			
Superoxide Radicals Degradation			
Thrombopoietin Signaling			
UVA-Induced MAPK Signaling			
VEGF Family Ligand-Receptor Interactions			
Vitamin-C Transport			
γ-glutamyl Cycle			

Supplementary Table 2. Pathways affected life-longly by developmental exposure to fluoxetine in stressed condition (cont…).

Canonical pathways	stressed		
	L	H	T
Antioxidant Action of Vitamin C			
Apelin Cardiomyocyte Signaling Pathway			
Biotin-carboxyl Carrier Protein Assembly			
Calcium Signaling			
Cardiac β-adrenergic Signaling			
Cellular Effects of Sildenafil (Viagra)			
Cysteine Biosynthesis III (mammalia)			
Dopamine Degradation			
Dopamine-DARPP32 Feedback in cAMP Signaling			
Fatty Acid α-oxidation			
Glycolysis I			
GP6 Signaling Pathway			
Intrinsic Prothrombin Activation Pathway			
Leucine Degradation I			
Melatonin Signaling			
Methionine Degradation I (to Homocysteine)			
Mitochondrial Dysfunction			
Neuropathic Pain Signaling In Dorsal Horn Neurons			
Nitric Oxide Signaling in the Cardiovascular System			
Noradrenaline and Adrenaline Degradation			
Proline Degradation			
Protein Ubiquitination Pathway			
Putrescine Degradation III			
S-adenosyl-L-methionine Biosynthesis			
Salvage Pathways of Pyrimidine Ribonucleotides			
Sucrose Degradation V (Mammalian)			

Different shades of blue representing the negative logarithmic scale of the associated p-value (-log p-value); the dense colours present lower p values, and lighter colours present a higher p-value. Only significant data ($p \leq 0.05$) are shown in the blue gradientGray represent non-significant data. L: larvae (str-FLX-L); H: hypothalamus (str-FLX-Hyp); T: telencephalon (str-FLX-Tel).

Supplementary Table 3. Life-long dysregulation of genes associated with depressive disorders upon developmental exposure to fluoxetine.

Gene symbol		Unstressed			Stressed		
Homo sapiens	***Danio rerio***	**L**	**H**	**T**	**L**	**H**	**T**
ABCB10	abcb10						
ABCC1	abcc1						
ABCC10	abcc6a						
ABCC10	abcc6b.2						
ABCC10	abcc6b.1						
ABI3BP	abi3bpa						
ABI3BP	abi3bpb						
ACER2	acer2						
ACER3	acer3						
ADAR	adar						
ADARB1	adarb1b						
ADARB1	adarb1a						
ADARB2	adarb2						
ADCY3	adcy3a						
ADCY5	adcy5						
ADCYAP1R1	adcyap1r1b						
ADRA1A	adra1aa						
ADRA2B	adra2b						
ADRB1	adrb1						
AKAP8L	akap8l						
AMACR	amacr						
ANK3	ank3b						
ANPEP	si:ch211-106j24.1						
APAF1	apaf1						
APOE	apoea						
APP	appb						
APPBP2	appbp2						
APPL1	appl1						
APPL2	appl2						
ARRB1	arrb1						

Supplementary Table 3. Life-long dysregulation of genes associated with depressive disorders upon developmental exposure to fluoxetine (cont…)

Gene symbol		Unstressed			Stressed		
Homo sapiens	***Danio rerio***	**L**	**H**	**T**	**L**	**H**	**T**
ARSA	arsa						
ATP7B	atp7b						
AVPI1	si:ch211-197k17.3						
AVPR1A	avpr1aa						
BCL2	bcl2a						
BCL2L1	bcl2l1						
BDNF	bdnf						
BICC1	bicc1b						
CACNA1C	cacna1c						
CAMK2A	camk2a						
CC2D1A	FO704915.1						
CD34	si:dkey-261h17.1						
CD9	cd9b						
CD93	cd248b						
CD93	cd248a						
CDK5	cdk5						
CDK5R1	cdk5r1a						
CDK5R1	cdk5r1b						
CDK5R2	cdk5r2a						
CDK5RAP2	zgc:55582						
CDKN2AIPNL	cdkn2aipnl						
CFP	si:ch73-237c6.1						
CHP1	chp1						
CHRFAM7A	chrna7						
CHRM2	chrm2a						
CHRNA4	chrna4b						
CIT	citb						
CIT	cita						
CITED1	cited1						
CITED2	cited2						

Supplementary Table 3. Life-long dysregulation of genes associated with depressive disorders upon developmental exposure to fluoxetine (cont…)

Gene symbol		Unstressed			Stressed		
Homo sapiens	***Danio rerio***	**L**	**H**	**T**	**L**	**H**	**T**
CITED4	cited4a						
CLOCK	clockb						
CLOCK	clocka						
CMYA5	cmya5						
CMYA5	si:ch1073-398f15.1						
CNR1	cnr1						
CNTNAP2	cntnap2b						
COMT	comtb						
CREB1	creb1b						
CREM	crema						
CRH	crhb						
CRHBP	crhbp						
CRHR2	CABZ01033000.1						
CRPPA	ispd						
CRTC1	crtc1a						
CRTC1	crtc1b						
CRY1	cry1ab						
CRY1	cry1aa						
CTNND2	ctnnd2b						
CTNND2	ctnnd2a						
CYP1A2	cyp1a						
DDC	ddc						
DISC1	disc1						
DLG2	dlg2						
DLG4	dlg4a						
DRD1	drd1b						
DST	CABZ01044277.1						
DST	si:ch211-165e15.1						
DST	CABZ01044281.1						
DUSP1	dusp1						

Supplementary Table 3. Life-long dysregulation of genes associated with depressive disorders upon developmental exposure to fluoxetine (cont…)

Gene symbol		Unstressed			Stressed		
Homo sapiens	***Danio rerio***	**L**	**H**	**T**	**L**	**H**	**T**
DUSP11	dusp11						
DUSP12	dusp12						
DUSP13	AL929334.1						
DUSP16	dusp16						
DUSP19	dusp19b						
DVL3	dvl3b						
ECT2L	BX323819.1						
EGFLAM	CT737133.1						
EHD3	ehd3						
ELOVL5	elovl5						
EPHB1	ephb1						
EPHB1	FQ377603.1						
EPHB2	ephb2a						
ERBB3	erbb3b						
EXOSC6	exosc6						
F2R	si:dkey-163m14.2						
F2RL1	f2rl1.1						
F2RL1	f2rl1.2						
F2RL2	CABZ01071020.1						
FAAH2	faah2b						
FABP2	fabp2						
FADS2	fads2						
FGFR1	fgfr1b						
FGFR1OP2	fgfr1op2						
FGFR2	fgfr2						
FKBP4	fkbp4						
FMR1	fmr1						
FOSB	fosb						

Supplementary Table 3. Life-long dysregulation of genes associated with depressive disorders upon developmental exposure to fluoxetine (cont…)

Gene symbol		Unstressed			Stressed		
Homo sapiens	***Danio rerio***	**L**	**H**	**T**	**L**	**H**	**T**
FOSL1	fosl1a						
FREM3	frem3						
GABBR1	gabbr1b						
GABBR1	gabbr1a						
GABBR2	gabbr2						
GABRA3	gabra3						
GAD1	gad1a						
GAL	galn						
GAL3ST2	gal3st2						
GALC	galca						
GALK2	galk2						
GALNS	galns						
GALNT12	galnt12						
GALNT17	galnt17						
GALNT18	galnt18b						
GALNT2	galnt2						
GALR1	galr1a						
GALR2	galr2a						
GCHFR	gchfr						
GDE1	gde1						
GJA1	cx40.8						
GMIP	gmip						
GNB3	gnb3b						
GNB3	gnb3a						
GPR50	mtnr1c						
GRIA1	gria1b						
GRIA2	gria2a						
GRIA4	gria4a						

Supplementary Table 3. Life-long dysregulation of genes associated with depressive disorders upon developmental exposure to fluoxetine (cont…)

Gene symbol		Unstressed			Stressed		
Homo sapiens	***Danio rerio***	**L**	**H**	**T**	**L**	**H**	**T**
GRIK3	GRIK3						
GRIN2A	grin2aa						
GRIN2B	LO018552.1						
GRM2	grm2a						
GRM2	grm2b						
GRM3	grm3						
GRM5	grm5b						
GRM7	GRM7						
GRM7	CR974456.1						
GSK3B	gsk3b						
GSK3B	GSK3B (1 of many)						
HDAC5	hdac5						
HIF1AN	hif1an						
HLF	hlfb						
HOMER1	homer1b						
HPCA	hpca						
HPCAL4	hpcal4						
HPD	hpdb						
HPS3	hps3						
HSP90AA1	hsp90aa1.1						
HSP90AA1	hsp90aa1.2						
HSPA12A	hspa12a						
HSPA4	hspa4a						
HTR4	htr4						
IGFBP2	igfbp2b						
IL22RA1	ifngr1						
IL2RB	il2rb						
IL6R	lifra						

Supplementary Table 3. Life-long dysregulation of genes associated with depressive disorders upon developmental exposure to fluoxetine (cont…)

Gene symbol		Unstressed			Stressed		
Homo sapiens	***Danio rerio***	**L**	**H**	**T**	**L**	**H**	**T**
ISG20	isg20						
JUNB	junba						
JUNB	junbb						
KALRN	kalrna						
KCNK2	kcnk2b						
KCNK2	kcnk2a						
KDR	kdr						
KLC1	klc1a						
KLC4	klc3						
KLC4	klc4						
KLF11	klf11b						
KLF11	klf11a						
KLF12	klf12b						
KLF15	klf15						
KLF16	klf13						
KLF18	sp5l						
KLF4	klf4						
KLF5	klf5b						
KLF7	klf7a						
KLF8	klf8						
KLF9	klf9						
KLHL11	klhl11						
KLHL12	KLHL12 (1 of many)						
KLHL17	klhl17						
KLHL18	klhl18						
KLHL23	klhl23						
KLHL25	enc2						
KLHL29	zmp:0000000619						

Supplementary Table 3. Life-long dysregulation of genes associated with depressive disorders upon developmental exposure to fluoxetine (cont…)

Gene symbol		Unstressed			Stressed		
Homo sapiens	***Danio rerio***	**L**	**H**	**T**	**L**	**H**	**T**
KLHL36	klhl36						
KLHL4	klhl4						
KLHL40	klhl40a						
KLHL41	klhl41a						
KLHL5	klhl5						
KLHL6	klhl24a						
KLHL8	klhl8						
KLHL9	klhl13						
KLHL9	klhl13						
KYAT3	si:ch73-97h19.2						
KYAT3	kyat3						
KYAT3	FO818711.1						
KYNU	kynu						
LDHA	ldha						
LEPR	lepr						
LEPROTL1	LEPROTL1						
LHPP	lhpp						
LINC02210-CRHR1	crhr1						
LRFN5	lrfn5a						
LRP1	lrp1ab						
LRP8	lrp8						
LSAMP	CABZ01099795.1						
MAFG	mafga						
MAFG	mafgb						
MAFK	mafk						
MAG	mag						
MAGI1	magi1b						
MAGI1	magi1a						

Supplementary Table 3. Life-long dysregulation of genes associated with depressive disorders upon developmental exposure to fluoxetine (cont…)

Gene symbol		Unstressed			Stressed		
Homo sapiens	***Danio rerio***	**L**	**H**	**T**	**L**	**H**	**T**
MAGI2	magi2b						
MAGI3	magi3b						
MAGIX	magixa						
MAGIX	magixb						
MAGT1	magt1						
MAOB	mao						
MAOB	zgc:66484						
MAP2K4	map2k4a						
MAP2K6	map2k6						
MAP2K7	map2k7						
MAPK1	mapk1						
MAPK10	mapk10						
MAPK13	mapk13						
MAPK14	mapk14b						
MAPK15	mapk15						
MAPK3	mapk3						
MARS2	mars2						
MDGA1	mdga1						
MDM4	mdm4						
MECP2	mecp2						
MED12	med12						
MET	met						
METTL1	mettl1						
METTL11B	mettl11b						
METTL21C	zgc:172067						
METTL24	mettl24						
METTL25	mettl25						
METTL7A	si:ch211-173n18.3						

Supplementary Table 3. Life-long dysregulation of genes associated with depressive disorders upon developmental exposure to fluoxetine (cont…)

Gene symbol		Unstressed			Stressed		
Homo sapiens	***Danio rerio***	**L**	**H**	**T**	**L**	**H**	**T**
MYT1L	myt1la						
NCAM1	ncam1b						
NCAM1	ncam1a						
NCAN	ncanb						
NCAN	CU861477.1						
NDUFV1	ndufv1						
NOS1	nos1						
NOTCH1	notch1b						
NPY	npy						
NPY2R	npy2rl						
NQO1	nqo1						
NR3C2	nr3c2						
NRGN	nrgna						
NTM	opcml						
NTMT1	ntmt1						
NTRK2	ntrk2a						
NTRK2	ntrk2b						
NTRK3	ntrk3b						
NTSR1	ntsr1						
NVL	nvl						
OLIG1	olig1						
OPRM1	oprm1						
P2RX7	p2rx7						
PARP15	si:ch211-244b2.4						
PARP15	parp12b						
PARP15	si:ch211-244b2.3						
PARP15	CABZ01079480.1						
PAWR	pawr						

Supplementary Table 3. Life-long dysregulation of genes associated with depressive disorders upon developmental exposure to fluoxetine (cont…)

Gene symbol		Unstressed			Stressed		
Homo sapiens	***Danio rerio***	**L**	**H**	**T**	**L**	**H**	**T**
PCLO	pclob						
PDE11A	pde11al						
PDE11A	si:dkey-219c10.4						
PDE9A	pde9a						
PEA15	pea15						
PER1	per1b						
PER1	per1a						
PER2	per2						
PER3	per3						
PFKFB3	pfkfb3						
PHF21B	PHF21B						
PINK1	pink1						
PLCB1	PLCB1						
PLCB4	PLCB4						
PLXNA3	plxna3						
POMC	pomca						
POU3F1	pou3f1						
POU3F1	pou3f3a						
POU3F1	pou3f2a						
POU3F1	pou3f3b						
PPP1R9B	ppp1r9bb						
PRKCB	prkcba						
PROM1	prom1b						
PSMD13	psmd13						
PTGS2	ptgs2b						
PTPRR	ptprr						
PVALB	pvalb6						
PVALB	pvalb7						

Supplementary Table 3. Life-long dysregulation of genes associated with depressive disorders upon developmental exposure to fluoxetine (cont…)

Gene symbol		Unstressed			Stressed		
Homo sapiens	***Danio rerio***	**L**	**H**	**T**	**L**	**H**	**T**
QKI	qkib						
RAC1	rac1b						
RAC1	RAC1						
RAF1	raf1b						
RAPGEF5	rapgef5a						
RAPH1	raph1a						
RAPH1	raph1b						
RBFOX3	rbfox3a						
RBFOX3	rbfox3b						
REEP5	reep5						
RGS4	rgs4						
SAT1	sat1b						
SAT1	sat1a.1						
SAT1	sat1a.2						
SCD	scd						
SERPINE1	serpine1						
SIGMAR1	sigmar1						
SLC17A6	slc17a6a						
SLC17A7	slc17a7b						
SLC18A2	slc18a2						
SLC1A1	slc1a1						
SLC1A2	slc1a2a						
SLC1A2	slc1a2b						
SLC1A3	slc1a3b						
SLC1A6	slc1a6						
SLC22A16	slc22a16						
SLC25A42	slc25a42						
SLC25A43	slc25a43						

Supplementary Table 3. Life-long dysregulation of genes associated with depressive disorders upon developmental exposure to fluoxetine (cont…)

Gene symbol		Unstressed			Stressed		
Homo sapiens	***Danio rerio***	**L**	**H**	**T**	**L**	**H**	**T**
SLC25A46	slc25a46						
SLC25A47	slc25a47a						
SLC25A48	slc25a48						
SLC25A6	slc25a6						
SLC2A1	slc2a1a						
SLC2A1	slc2a1b						
SLC2A12	slc2a12						
SLC2A13	CABZ01043955.1						
SLC6A13	SLC6A13						
SLC6A15	slc6a15						
SLC6A3	slc6a3						
SLIT3	slit3						
SNAP25	snap25a						
SNAP25	snap25b						
SOD1	sod1						
SOD2	sod2						
SOX9	sox9a						
SOX9	sox9b						
SRRT	srrt						
SSTR2	sstr2a						
SSTR5	sstr3						
STARD13	stard13b						
STARD4	stard4						
STARD5	stard5						
TAL1	tal1						
TBC1D9	tbc1d9						
TBC1D9B	tbc1d9						
TDO2	tdo2a						

Supplementary Table 3. Life-long dysregulation of genes associated with depressive disorders upon developmental exposure to fluoxetine (cont…)

Gene symbol		Unstressed			Stressed		
Homo sapiens	***Danio rerio***	**L**	**H**	**T**	**L**	**H**	**T**
TEF	tefa						
TEF	tefb						
TESC	tescb						
THAP11	thap11						
THAP4	thap4						
THAP6	si:dkey-50i6.5						
THAP7	thap7						
THBS2	thbs2b						
THBS3	thbs3b						
THBS4	thbs4b						
THEM6	THEM6						
THRA	thraa						
THRA	thrab						
THRAP3	thrap3a						
THRB	thrb						
THSD7A	thsd7aa						
THSD7A	thsd7ab						
THSD7B	thsd7ba						
THTPA	thtpa						
THUMPD1	thumpd1						
THYN1	thyn1						
TMED2	tmed2						
TNFAIP2	tnfaip2a						
TNFAIP3	tnfaip3						
TNFAIP8L2	tnfaip8l2a						
TNFAIP8L3	tnfaip8l3						
TNFRSF4	tnfrsfa						
TNFRSF4	tnfrsf1b						

Supplementary Table 3. Life-long dysregulation of genes associated with depressive disorders upon developmental exposure to fluoxetine (cont…)

Gene symbol		Unstressed			Stressed		
Homo sapiens	***Danio rerio***	**L**	**H**	**T**	**L**	**H**	**T**
TOMM40	tomm40						
TPH1	tph1a						
TPH1	tph1b						
TPH2	tph2						
TPPP	TPPP						
TPPP2	tppp2						
TPPP3	tppp3						
TRH	trh						
TRHDE	trhde.1						
TRHDE	trhde.2						
TRHR	trhra						
TSNAX-DISC1	tsnax						
TSPO2	tspo						
USP46	usp46						
VDR	vdrb						
VEGFA	vegfab						
VEGFA	vegfaa						
VIP	vip						
VIPAS39	vipas39						
VIPR1	vipr1b						
WDR26	wdr26a						
XBP1	xbp1						
ZBTB20	zbtb20						
ZNF804A	znf804a						

Gene symbol is shown for *Danio rerio* (zebrafish) and its associated *Homo sapiens* (human) orthologue. red: upregulation, green: downregulation, gray: non-significant fold change. L: larvae, T: telencephalon, H: hypothalamus.

Supplementary Table 4. Gene list associate to neural plasticity, synaptogenesis, and neurogenesis in Homo sapiens

Gene symbol *(Homo Sapiens)*	Full name
LRRTM1	Leucine-rich repeat transmembrane neuronal protein 1
LRRTM2	Leucine-rich repeat transmembrane neuronal protein 2
NSG1	Neuronal vesicle trafficking-associated protein 1
NPAS4	Neuronal PAS domain-containing protein 4
CHRNA7	Neuronal acetylcholine receptor subunit alpha-7
NSMF	NMDA receptor synaptonuclear signaling and neuronal migration factor
PPFIA3	Liprin-alpha-3
NCDN	Neurochondrin
SHISA8	Protein shisa-8
SYNGR1	Synaptogyrin-1
SYP	Synaptophysin
SYNPO	Synaptopodin
SLC4A10	Sodium-driven chloride bicarbonate exchanger
SHISA9	Protein shisa-9
MCTP1	Multiple C2 and transmembrane domain-containing protein 1
RIN1	Ras and Rab interactor 1
GRIK2	Glutamate receptor ionotropic, kainate 2
UNC13A	Protein unc-13 homolog A
NETO1	Neuropilin and tolloid-like protein 1
CAMK2B	Calcium/calmodulin-dependent protein kinase type II subunit beta
RAB8A	Ras-related protein Rab-8A
SLC8A2	Sodium/calcium exchanger 2
RAB5A	Ras-related protein Rab-5A
SHISA6	Protein shisa-6
KCNJ10	ATP-sensitive inward rectifier potassium channel 10
SYNGAP1	Ras/Rap GTPase-activating protein SynGAP
SHISA7	Protein shisa-7
JPH3	Junctophilin-3
SYT4	Synaptotagmin-4
SORCS2	VPS10 domain-containing receptor SorCS2
NPTN	Neuroplastin
UNC13B	Protein unc-13 homolog B
UNC13C	Protein unc-13 homolog C
SHANK3	SH3 and multiple ankyrin repeat domains protein 3

Supplementary Table 4. Gene list associate to neural plasticity, synaptogenesis, and neurogenesis in Homo sapiens (cont…)

Gene symbol *(Homo Sapiens)*	Full name
RAB3A	Ras-related protein Rab-3A
RAB3GAP1	Rab3 GTPase-activating protein catalytic subunit
GRM5	Metabotropic glutamate receptor 5
NRGN	Neurogranin
NEURL1	E3 ubiquitin-protein ligase NEURL1
DBN1	Drebrin
CPLX2	Complexin-2
S100B	Protein S100-B
STAU1	Double-stranded RNA-binding protein Staufen homolog 1
MAP1B	Microtubule-associated protein 1B
RASGRF1	Ras-specific guanine nucleotide-releasing factor 1
ACP4	Testicular acid phosphatase
CNTN2	Contactin-2
KRAS	GTPase KRas
RAB11A	Ras-related protein Rab-11A
DLG4	Disks large homolog 4
CLN3	Battenin
EPHB2	Ephrin type-B receptor 2
ARC	Activity-regulated cytoskeleton-associated protein
SLC24A2	Sodium/potassium/calcium exchanger 2
SLC24A1	Sodium/potassium/calcium exchanger 1
SNAP47	Synaptosomal-associated protein 47
KIT	Mast/stem cell growth factor receptor Kit
CAMK2A	Calcium/calmodulin-dependent protein kinase type II subunit alpha
EGR2	E3 SUMO-protein ligase EGR2
STAR	Steroidogenic acute regulatory protein, mitochondrial
SHANK2	SH3 and multiple ankyrin repeat domains protein 2
HRAS	GTPase HRas
NF1	Neurofibromin
GRIN1	Glutamate receptor ionotropic, NMDA 1
CALB1	Calbindin
GIP	Gastric inhibitory polypeptide
KCNB1	Potassium voltage-gated channel subfamily B member 1
P2RX3	P2X purinoceptor 3

Supplementary Table 4. Gene list associate to neural plasticity, synaptogenesis, and neurogenesis in Homo sapiens (cont…)

Gene symbol *(Homo Sapiens)*	Full name
PPP1R9A	Neurabin-1
GRIA1	Glutamate receptor 1
SYT7	Synaptotagmin-7
DGKI	Diacylglycerol kinase iota
MME	Neprilysin
CRTC1	CREB-regulated transcription coactivator 1
ITPR3	Inositol 1,4,5-trisphosphate receptor type 3
MAP1A	Microtubule-associated protein 1A
DRD2	D(2) dopamine receptor
ADCY8	Adenylate cyclase type 8
APP	Amyloid-beta precursor protein
PICK1	PRKCA-binding protein
AGT	Angiotensinogen
abeta-42-oligomer_human	Amyloid-beta protein 42 oligomeric complex
SLC8A3	Sodium/calcium exchanger 3
SNAP25	Synaptosomal-associated protein 25
CX3CR1	CX3C chemokine receptor 1
FMR1	Synaptic functional regulator FMR1
BAIAP2	Brain-specific angiogenesis inhibitor 1-associated protein 2
STXBP1	Syntaxin-binding protein 1
APOE	Apolipoprotein E
RAPGEF2	Rap guanine nucleotide exchange factor 2
NLGN1	Neuroligin-1
NTRK2	BDNF/NT-3 growth factors receptor
MAPT	Microtubule-associated protein tau
ADORA2A	Adenosine receptor A2a
EPHA4	Ephrin type-A receptor 4
CRH	Corticoliberin
DRD1	D(1A) dopamine receptor
CDC42	Cell division control protein 42 homolog
ADORA1	Adenosine receptor A1
CDK5	Cyclin-dependent-like kinase 5
PRKCZ	Protein kinase C zeta type
MAPK1	Mitogen-activated protein kinase 1

Supplementary Table 4. Gene list associate to neural plasticity, synaptogenesis, and neurogenesis in Homo sapiens (cont…)

Gene symbol *(Homo Sapiens)*	Full name
CX3CL1	Fractalkine
ABL1	Tyrosine-protein kinase ABL1
PSEN1	Presenilin-1
PTK2B	Protein-tyrosine kinase 2-beta

Supplementary Table 5. The primer list for qPCR experiments.

Gene symbol	**Primer sequence**	
Danio rerio	Forward primer 5' to 3'	Forward primer 5' to 3'
eef1a1l1	CCG TCT GCC ACT TCA GGA TGT GT	TTG AGG ACA CCA GTC TCC ACA CGA
d4EGFP	CGA GCA ACT GAG GAT CCC ATT CTC T	CAC CCC GGT GAA CAG CTC CT
bdnf	AGC ATC TGT TGG AGT GTG TGG	TAA CCT GTT GGA ACA TTT TCC CCT
crhb	CAC AGA TTC TCC TCG CCA CT	TGG AAA GGC AAC GAG CAG AG
egr2a	CAA CAC AAG CCC TCA GAG CAA	GTC GCT GTC ATT TTG ATC CTC G
fkbp5	CGC CGG TGA GAC TAA ACA GA	ACA TGC CCT TGT TCC CAA AA
fosab	TAC CCG CTC AAC CAG ACT CA	CGT GAC AGT TGG CAC GAA AG
fosl1a	CCC TGA CTC CAT TTA CCG CC	GAC GGA TGA GAC GTG ACG AG
htr1b	TTC CCC TCT GTT CGT CTT GC	TGA GTT GAC GTA GCC AAG CC
npas4a	GGT CCA CTA AAG GAG CCT CG	TCG GAG ATG GGC AAC AAG TC
nr4a1	TCG CTT ACG GTT TCT CTG CT	AGG TCT TCA AAC ACA GGC GT
per2	GAG AGG GGT CCA CGC TTT TA	GGG ACT GCT TCA GAC GTG AC
rorcb	ACC TGT CAA CAT GAG AGC CC	CCT TGC ACC CTT CAC ACG TA

Supplementary Table 6. Gene list associate to epigenetics in *Homo sapiens*

Gene symbol (*Homo sapiens*)	Full name
POLR2F	DNA-directed RNA polymerases I, II, and III subunit RPABC2
PHF19	PHD finger protein 19
HDAC4	Histone deacetylase 4
POLR1G	DNA-directed RNA polymerase I subunit RPA34
H2AX	Histone H2AX
DNMT1	DNA (cytosine-5)-methyltransferase 1
MORF4L2	Mortality factor 4-like protein 2
H2AC21	Histone H2A type 2-B
ERCC6	DNA excision repair protein ERCC-6
METTL3	N6-adenosine-methyltransferase catalytic subunit
PPM1D	Protein phosphatase 1D
PRDM14	PR domain zinc finger protein 14
POLR1E	DNA-directed RNA polymerase I subunit RPA49
EXOSC10	Exosome component 10
TNP1	Spermatid nuclear transition protein 1
POLR1C	DNA-directed RNA polymerases I and III subunit RPAC1
RLIM	E3 ubiquitin-protein ligase RLIM
LRIF1	Ligand-dependent nuclear receptor-interacting factor 1
H3C1	Histone H3.1
MYO1C	Unconventional myosin-Ic
CTBP1	C-terminal-binding protein 1
MTA1	Metastasis-associated protein MTA1
TRIM27	Zinc finger protein RFP
SIN3A	Paired amphipathic helix protein Sin3a
HAT1	Histone acetyltransferase type B catalytic subunit
PRMT7	Protein arginine N-methyltransferase 7
RIF1	Telomere-associated protein RIF1
ACTB	Actin, cytoplasmic 1
POLR1B	DNA-directed RNA polymerase I subunit RPA2
ATAD2	ATPase family AAA domain-containing protein 2
CDCA4	Cell division cycle-associated protein 4
PCGF5	Polycomb group RING finger protein 5
H2AB2	Histone H2A-Bbd type 2/3
H2AB1	Histone H2A-Bbd type 1
RBBP7	Histone-binding protein RBBP7

Supplementary Table 6. Gene list associate to epigenetics in *Homo sapiens* (cont…)

Gene symbol (*Homo sapiens*)	Full name
H1-0	Histone H1.0
AEBP2	Zinc finger protein AEBP2
H2AC6	Histone H2A type 1-C
CTCF	Transcriptional repressor CTCF
H2AC20	Histone H2A type 2-C
H1-6	Histone H1t
WBP2	WW domain-binding protein 2
H3C13	Histone H3.2
PADI2	Protein-arginine deiminase type-2
MYBBP1A	Myb-binding protein 1A
POLR2E	DNA-directed RNA polymerases I, II, and III subunit RPABC1
DDX21	Nucleolar RNA helicase 2
TAF1D	TATA box-binding protein-associated factor RNA polymerase I subunit D
PABPC1L	Polyadenylate-binding protein 1-like
GSK3A	Glycogen synthase kinase-3 alpha
ARID4A	AT-rich interactive domain-containing protein 4A
DPY30	Protein dpy-30 homolog
SMARCA5	SWI/SNF-related matrix-associated actin-dependent regulator of chromatin 5
SPI1	Transcription factor PU.1
ZNF335	Zinc finger protein 335
CDC45	Cell division control protein 45 homolog
SMARCD1	SWI/SNF-related matrix-associated actin-dependent regulator of chromatin 1
ATAD2B	ATPase family AAA domain-containing protein 2B
DYDC2	DPY30 domain-containing protein 2
IFI16	Gamma-interferon-inducible protein 16
MTHFR	Methylenetetrahydrofolate reductase
GPX1	Glutathione peroxidase 1
BAZ1B	Tyrosine-protein kinase BAZ1B
SF3B1	Splicing factor 3B subunit 1
EED	Polycomb protein EED
KLF2	Krueppel-like factor 2
POLR2L	DNA-directed RNA polymerases I, II, and III subunit RPABC5
H4-16	Histone H4
POLR2H	DNA-directed RNA polymerases I, II, and III subunit RPABC3
MTF2	Metal-response element-binding transcription factor 2

Supplementary Table 6. Gene list associate to epigenetics in *Homo sapiens* (cont…)

Gene symbol (*Homo sapiens*)	Full name
ASIP	Agouti-signaling protein
RBM15B	Putative RNA-binding protein 15B
PHF1	PHD finger protein 1
H3-3A	Histone H3.3
SERTAD1	SERTA domain-containing protein 1
CTCFL	Transcriptional repressor CTCFL
H1-4	Histone H1.4
SIRT1	NAD-dependent protein deacetylase sirtuin-1
H2AZ1	Histone H2A.Z
H2AC7	Histone H2A type 1-D
ARID1B	AT-rich interactive domain-containing protein 1B
TASOR	Protein TASOR
ASF1A	Histone chaperone ASF1A
DNMT3L	DNA (cytosine-5)-methyltransferase 3-like
MORF4L1	Mortality factor 4-like protein 1
YTHDC1	YTH domain-containing protein 1
SERTAD2	SERTA domain-containing protein 2
EPC1	Enhancer of polycomb homolog 1
DNMT3B	DNA (cytosine-5)-methyltransferase 3B
DNMT3A	DNA (cytosine-5)-methyltransferase 3A
MACROH2A1	Core histone macro-H2A.1
DIRAS3	GTP-binding protein Di-Ras3
PPHLN1	Periphilin-1
HMGA1	High mobility group protein HMG-I/HMG-Y
ZMIZ2	Zinc finger MIZ domain-containing protein 2
POLR1A	DNA-directed RNA polymerase I subunit RPA1
POLR1F	DNA-directed RNA polymerase I subunit RPA43
H2AC12	Histone H2A type 1-H
MACROH2A2	Core histone macro-H2A.2
KAT2B	Histone acetyltransferase KAT2B
JARID2	Protein Jumonji
POLR2K	DNA-directed RNA polymerases I, II, and III subunit RPABC4
H2AC11	Histone H2A type 1
H1-10	Histone H1.10
KCNQ1	Potassium voltage-gated channel subfamily KQT member 1

Supplementary Table 6. Gene list associate to epigenetics in *Homo sapiens* (cont…)

Gene symbol (*Homo sapiens*)	Full name
MSL3	Male-specific lethal 3 homolog
IGF2	Insulin-like growth factor II
H2AW	Histone H2A type 3
H2AP	Huntingtin-interacting protein M
MSL3P1	Putative male-specific lethal-3 protein-like 2
HDAC6	Histone deacetylase 6
BRCA1	Breast cancer type 1 susceptibility protein
PCGF3	Polycomb group RING finger protein 3
MIER1	Mesoderm induction early response protein 1
TFAP2C	Transcription factor AP-2 gamma
HDAC2	Histone deacetylase 2
EZH2	Histone-lysine N-methyltransferase EZH2
H1-9P	Putative spermatid-specific linker histone H1-like protein
ELOF1	Transcription elongation factor 1 homolog
HMGB1	High mobility group protein B1
HDAC5	Histone deacetylase 5
H1-1	Histone H1.1
TAF1B	TATA box-binding protein-associated factor RNA polymerase I subunit B
SMCHD1	Structural maintenance of chromosomes flexible hinge domain-containing protein 1
ARID1A	AT-rich interactive domain-containing protein 1A
SUZ12	Polycomb protein SUZ12
H2AL1RP	Histone H2A
SPHK2	Sphingosine kinase 2
ZFP57	Zinc finger protein 57 homolog
CHEK1	Serine/threonine-protein kinase Chk1
RBM15	RNA-binding protein 15
POLR1H	DNA-directed RNA polymerase I subunit RPA12
HNRNPU	Heterogeneous nuclear ribonucleoprotein U
SIRT6	NAD-dependent protein deacetylase sirtuin-6
EP300	Histone acetyltransferase p300
DEK	Protein DEK
CREBZF	CREB/ATF bZIP transcription factor
PCGF1	Polycomb group RING finger protein 1
KMT2D	Histone-lysine N-methyltransferase 2D
RBBP4	Histone-binding protein RBBP4

Gene symbol (*Homo sapiens*)	Full name
PCGF2	Polycomb group RING finger protein 2
BMI1	Polycomb complex protein BMI-1
H2AC1	Histone H2A type 1-A
H2AJ	Histone H2A.J
H2AC14	Histone H2A type 1-J
TAF1A	TATA box-binding protein-associated factor RNA polymerase I subunit A
TAF1C	TATA box-binding protein-associated factor RNA polymerase I subunit C
KAT2A	Histone acetyltransferase KAT2A
UBE2B	Ubiquitin-conjugating enzyme E2 B
H2AC4	Histone H2A type 1-B/E
MPHOSPH8	M-phase phosphoprotein 8
EZH1	Histone-lysine N-methyltransferase EZH1
DOT1L	Histone-lysine N-methyltransferase, H3 lysine-79 specific
H2AC18	Histone H2A type 2-A
GLMN	Glomulin
H1-2	Histone H1.2
H1-3	Histone H1.3
H1-5	Histone H1.5
UPF1	Regulator of nonsense transcripts 1
MORC2	ATPase MORC2
H1-8	Histone H1.8
SIRT2	NAD-dependent protein deacetylase sirtuin-2
MECP2	Methyl-CpG-binding protein 2
UBR2	E3 ubiquitin-protein ligase UBR2
H2AZ2	Histone H2A.V
DYDC1	DPY30 domain-containing protein 1
TDG	G/T mismatch-specific thymine DNA glycosylase
MORC1	MORC family CW-type zinc finger protein 1
CDYL	Chromodomain Y-like protein
TBP	TATA-box-binding protein
KDM1B	Lysine-specific histone demethylase 1B
ZMIZ1	Zinc finger MIZ domain-containing protein 1

Supplementary Table 6. Gene list associate to epigenetics in *Homo sapiens* (cont…)

Appendix 1- The statistical details for eGFP mRNA and 11-target genes alteration

The two-way ANOVA showed that treatment (FLX-6D vs Ethanol-6D; $F(1,20)=21.24$, $p=0.0001$), stress state (stressed vs unstressed; $F(1,20)=28.39$, $p=3.2^{E0-5}$) and their interaction (the treatment*the stress status; $F(1,20)=7.1$, $p=0.01$) had significant effects on the whole-body eGFP mRNA levels in FLX-6D and its associated control groups. A post-hoc Tukey's test was performed for pairwise comparisons. Our findings showed that the mean of whole-body eGFP mRNA levels 60 minutes after the handling stress increased by 4.4-fold in the Ethanol-6D group compared to the unstressed condition ($p\leq0.01$). This increase was not observed in the FLX-6D group. There was an apparent 6-fold decrease in the whole-body eGFP mRNA levels in FLX exposed group in unstressed condition (FLX-6D-0 min), however this decrease was not significant based on Tukey's test ($p>0.05$). Therefore, there was no significant difference between the stressed and the unstressed state in FLX-6D group ($p>0.05$), and both of these values were similar to the whole-body eGFP mRNA levels in the unstressed state in control (Ethanol-6D-0 min) group ($p>0.05$). Our findings show that the developmental exposure to FLX blunted the elevation of the whole-body eGFP mRNA in response to the handling stress in a similar matter to that of whole-body cortisol.

A post-hoc Tukey's test was performed for pairwise comparison within each treatment or control group to evaluate the difference between unstressed vs stressed condition on the whole-body eGFP mRNA levels.

The two-way ANOVA indicated that stress state (stressed vs unstressed; $F(1,20)= 7.8$, $p=0.01$) had significant effects on the whole-body eGFP mRNA levels in FLX-O/N and its associated control group; however treatment (FLX-O/N vs Ethanol-O/N; $F(1,20)=0.7$, $p=0.40$) and their interaction (the treatment*the stress status; $F(1,20)=0.45$, $p=0.5$) did not have any significant effects. A post-hoc Tukey's test was performed for pairwise comparisons between the unstressed and stressed within each treatment. Our findings showed that the mean of whole-body eGFP mRNA levels 60 minutes after the handling stress increased by 4.3-fold in the Ethanol group compared to the unstressed condition ($p\leq0.05$). An increase of 4.6-fold was also observed in the FLX-O/N-60 min group. The mean of whole-body eGFP mRNA levels 60 minutes after the handling stress increased by 4.6-fold in the FLX-O/N group compared to the unstressed condition ($p\leq0.05$). Our findings show that overnight exposure to FLX does not affect the elevation of whole-body eGFP mRNA in response to the handling stress.

Similar statistical analysis was performed for other treatment groups. All these treatment groups were compared to a single control group; DMSO. The two-way ANOVA performed showed that treatment (BPA vs DMSO, $F(1,20)=22.63$, $p=0.0001$; VIN vs DMSO, $F(1:20)= 16.41$, $p=0.0001$), stress state (stressed vs unstressed; BPA: $F(1,20)=10.39$, $p=0.004$; VIN: $F(1,20)=15.08$, $p=0.0009$) and their interaction (the treatment*the stress status; BPA: $F(1,20)=6.1$, $p=0.02$; VIN: $F(1,20)=4.1$, $p=0.05$) had significant effects on the whole-body eGFP mRNA levels in the treatment (BPA and VIN) groups and their associated control group (DMSO) . Our findings showed that the mean of whole-body eGFP mRNA levels 60 minutes after the handling stress increased by 3-fold in the DMSO group compared to the unstressed condition ($p\leq0.01$). This increase was not observed in all other treatment groups when compared to the control unstressed state (0.4-fold in BPA, $p>0.05$; 0.6-fold in VIN, $p>0.05$). There was no significant difference between stressed and unstressed state within each treatment groups (BPA and VIN) and both values (stressed and unstressed) were similar to the whole-body eGFP mRNA levels in the unstressed state in the control (DMSO) group ($p>0.05$). Our findings show that overnight exposure to BPA and VIN disrupt the elevation of the whole-body eGFP mRNA in response to the handling stress.

In our study, the cortisol (CORT) group, the larvae in the pre-handling stress group (equivalent to the unstressed compared to the other treatment groups studies) showed a higher elevation of whole-body eGFP mRNA; 12-fold ($F(1,20)=69.28$, $p=6.28^{E0-8}$). The two-way ANOVA performed showed that the treatment (CORT vs DMSO; $F(1,20)=69.28$, $p=6.28^{E0-8}$), and the stress state (stressed vs unstressed; $F(1,20)=5.23$, $p=0.03$) had significant effects on the whole-body cortisol levels in CORT and its associated control group. However, their interaction (the treatment*the stress status; $F(1,20)=0.8$, $p=0.38$) was not significant; Therefore, pairwise comparison was not performed between the treatment groups. A post-hoc Tukey's test was performed for pairwise comparison within the treatment and control groups. Our findings showed that the mean of whole-body eGFP mRNA after overnight exposure to cortisol was elevated regardless of the sampling time; 12-fold and 17-fold in 0-min and 60-min sampling time, respectively ($p<0.05$). However, no statistical comparison to the control group was valid, given the interaction (the treatment*the stress status) was not significant ($p>0.05$).

Also, in our study, DEX group was used as the negative control. The two-way ANOVA performed showed that treatment (DEX vs DMSO, $F(1:20)= 11.86$, $p=0.002$), stress state (stressed vs unstressed: $F(1,20)=19.31$, $p=0.0002$) and their interaction (the treatment*the stress status; $F(1,20)=4.2$, $p=0.05$) had significant effects on the whole-body cortisol levels in the treatment (DEX) groups and its associated control group (DMSO). A post-hoc Tukey's test was performed for pairwise comparison. Our findings showed that the mean of whole-body cortisol levels 30 minutes after the handling stress increased by 3-fold in the DMSO group compared to the unstressed condition ($p\leq0.01$). This increase was not observed in the DEX group (1.3-fold, $p>0.05$) and both values (stressed and unstressed) were similar to the whole-body cortisol levels in the unstressed state in control (DMSO) group when compared to each treatment groups (DEX $p>0.05$).

Our whole-body eGFP mRNA levels measurements showed that BPA, VIN, DEX, and FLX in the concentrations and exposure times used in this study could blunt the stress response in the transgenic SR4G zebrafish larvae ($p\leq0.05$).

Nine genes belonging to IEG class of genes were analyzed; including: *bdnf, egr2a, fkbp5, fosab, fosl1a, npas4a, nr4a1, per2,* and *rorcb*. Two more genes, *crhb* and *htr1b,* were also added to the list of genes given their important role in HPI axis and depression development. The whole-body mRNA levels of these 11 target genes were measured in unstressed and stressed conditions by quantitative SYBR®green PCR (qPCR) after exposure to different chemicals (FLX-O/N, FLX-6D, BPA, VIN, and DEX) and the two related control groups (Ethanol and DMSO).

For all 11 genes in each treatment group, two-way ANOVA was performed to compare each treatment group to its related control group. For FLX-6D group, the two-way ANOVA performed showed that the treatment (FLX-6D vs Ethanol-6D), the stress state (stressed vs unstressed) and their interaction (the treatment*the stress status) had significant effects on the whole-body mRNA levels of the following genes: *htr1b, fkbp5, npas4a, nr4a1, per2, rorcb, and fosab*. A post hoc test, Tukey's test, was performed for pairwise comparison for these genes. Our findings showed that although *npas4a, nr4a1, per2, rorcb, and fosab* showed apparent downregulation, there was no significant difference in the whole-body mRNA levels between the FLX-6D group and the Ethanol-6D groups in the unstressed (0-min) condition for each gene ($p>0.05$ for individual genes; Figure 4.6 and 4.7). However, our findings showed significant downregulation of these genes in the stressed (60-min) condition when FLX-6D groups and Ethanol-6D groups compared: *npas4a* (7-fold, $p\leq0.001$), *nr4a1* (6-fold, $p\leq0.001$), *per2* (6-fold, $p\leq0.001$), *rorcb* (11-

fold, p≤0.001), and *fosab* (12-fold, p≤0.001). The whole-body mRNA levels for these genes in the stressed condition (FLX-6D-60 min) was similar to the control unstressed condition (Ethanol-6D-0 min) (p>0.05 for individual genes). Our findings for *fkbp5* gene showed significant 5-fold downregulation of the whole-body mRNA levels in the unstressed condition (0-min) when FLX-6D compared to Ethanol-6D (p≤0.05). Also, our findings for *fkbp5* gene showed significant 2-fold upregulation of the whole-body mRNA levels in the stressed condition (60-min) when FLX-6D compared to Ethanol-6D (p≤0.05). The pairwise comparison showed there was no significant difference between the unstressed (0-min) and stressed (60-min) state for the whole-body mRNA levels of *htr1b* within FLX-6D and Ethanol-6D groups. However, the levels of whole-body mRNA of *htr1b* were significantly downregulated in FLX-6D by 2-fold in both unstressed (0-min) and stressed (60-min) conditions (p≤0.05). The two-way ANOVA performed showed that the treatment (FLX-6D vs Ethanol-6D) and the stress state (stressed vs unstressed) had significant effects on the whole-body mRNA levels of the following genes: *fosl1a, egr2a*. A post hoc test, Tukey's test was performed for pairwise comparison for these genes on the main factor of the stress status. The whole-body mRNA levels were upregulated when the stressed condition (60-min) was compared to the unstressed condition (0-min). For *fosl1a,* 4-fold (p≤0.05) in Ethanol-6D and 3.5-fold (p≤0.05) in FLX-6D; for *egr2a,* 2.7-fold (p≤0.05) in Ethanol-6D and 3-fold (p≤0.05) in FLX-6D. Given the interaction of the treatment and the stress state (the treatment*the stress state) was not significant on ANOVA (p>0.05) pairwise comparison between these groups was not valid for these two genes. For *crhb* and *bdnf,* the ANOVA test performed did not show any significant difference with regards to the three variables studied (treatment, stress status, and treatment*stress status interaction; p>0.05). Therefore, pairwise comparison was not valid for these genes.

For FLX-O/N group, the two-way ANOVA performed showed that interaction between the treatment and the stress status (the treatment*the stress status) did not have significant effects on the whole-body mRNA levels of any of the 11 genes studied (intercept p>0.05 for individual genes). Therefore, pairwise comparison was not valid for such interactions. The two-way ANOVA performed showed that the treatment (FLX-O/N vs Ethanol) and the stress state (unstressed vs stressed) had significant effects on the whole-body mRNA levels of the following genes within each treatment: *egr2a, fosl1a, nr4a1, per2,* and *fosab*. A post hoc test, Tukey's test was performed for pairwise comparison for these genes on the main factor of the stress status. Our findings showed that in all five genes, the whole-body mRNA levels were upregulated after the handling stress (60-min vs 0-min) within each treatment group. For *egr2a,* 2.5-fold (p≤0.05) in Ethanol and 3.5-fold (p≤0.05) in FLX-O/N, for *fosl1a,* 4-fold (p≤0.05) in Ethanol and 4-fold (p≤0.05) in FLX-O/N; for *nr4a1,* 6-fold (p≤0.05) in Ethanol and 2.6-fold (p≤0.05) in FLX-O/N; for *per2,* 4-fold (p≤0.05) in Ethanol and 5-fold (p≤0.05) in FLX-O/N; and for *fosab,* 14-fold (p≤0.05) in Ethanol and 12-fold (p≤0.05) in FLX-O/N. For *crhb, fkbp5, htr1b, rorcb,* and *bdnf,* the ANOVA test performed did not show any significant difference with regards to the three variables studied (the treatment, the stress status, and the treatment*stress status interaction; p>0.05). Therefore, pairwise comparison was not valid for these genes.

For BPA group, the two-way ANOVA performed showed that the treatment (BPA vs DMSO), the stress state (stressed vs unstressed) and their interaction (the treatment*the stress status) had significant effects on the whole-body mRNA levels only for *fosab*. A post hoc test, Tukey's test was performed for pairwise comparison. Our findings showed that although an apparent downregulation was appreciated, there was no significant difference between the BPA group and the DMSO group in the unstressed (0-min) condition (p>0.05). Our findings showed significant downregulation of *fosab* whole-body mRNA levels (3-

fold, p≤0.01) in the stressed (60-min) condition when the BPA group and the DMSO group were compared . Furthermore, the whole-body mRNA levels for *fosab* in BPA-60 min (stressed condition) was similar to the DMSO-0 min (control unstressed condition), statistically (p>0.05). For BPA group, the two-way ANOVA performed showed that the treatment (BPA vs DMSO) and the stress state (stressed vs unstressed) had significant effects on the whole-body mRNA levels of the following genes *egr2a, fkbp5, fosl1a, npas4a, nr4a1, per2,* and *rorcb.* A post hoc test, Tukey's test was performed for pairwise comparison for these genes on the main factors of the stress status. Our findings showed that in these genes, the whole-body mRNA levels were upregulated after the handling stress when the stressed condition (60-min) was compared to the unstressed condition. For *egr2a,* 4-fold (p≤0.05) in DMSO and 14-fold (p≤0.05) in BPA; for *fkbp5* 2-fold (p≤0.05) in DMSO and 9-fold (p≤0.05) in BPA; for *fosl1a,* 2-fold (p≤0.05) in DMSO and 9-fold (p≤0.05) in BPA; for *npas4a* 3.5-fold (p≤0.05) in DMSO and 6-fold (p≤0.05) in BPA; for *nr4a1,* 4-fold (p≤0.05) in DMSO and 3-fold (p≤0.05) in BPA; for *per2* 4-fold (p≤0.05) in DMSO and 42-fold (p≤0.05) in BPA; for *rorcb* 2-fold (p≤0.05) in DMSO and 16-fold (p≤0.05) in BPA. For *crhb, htr1b,* and *bdnf* the ANOVA test performed did not show any significant difference with regards to the three variables studied (the treatment, the stress status, and the treatment*stress status interaction, p>0.05). Therefore, pairwise comparison was not valid for these genes.

For VIN group, the two-way ANOVA performed showed that the treatment (VIN vs DMSO), the stress state (stressed vs unstressed) and their interaction (the treatment*the stress status) had significant effects on the whole-body mRNA levels only for *egr2a, npas4a, nr4a1, per2, rorcb* and *fosab.* A post hoc test, Tukey's test was performed for pairwise comparison. Our findings showed that although an apparent downregulation was appreciated, there was no significant difference between the VIN group and the DMSO group in the unstressed (0-min) condition (p>0.05). However, our findings showed significant downregulation of these genes in the stressed (60-min) condition when the VIN groups and the DMSO groups compared: *egr2a* (5.4-fold, p≤0.001), *npas4a* (19-fold, p≤0.001), *nr4a1* (3-fold, p≤0.001), *per2* (9-fold, p≤0.001), *rorcb* (5-fold, p≤0.001), and *fosab* (26-fold, p≤0.001). For VIN group, the two-way ANOVA performed showed that the treatment (VIN vs DMSO) and the stress state (stressed vs unstressed) had significant effects on the whole-body mRNA levels of the following genes *fkbp5,* and *fosl1a.* A post hoc test, Tukey's test was performed for pairwise comparison for these genes on the main factors of the stress status. Our findings showed that in these genes the whole-body mRNA levels were upregulated after the handling stress when the stressed condition (60-min) was compared to the unstressed condition (0-min) in the treatment (VIN) and control (DMSO) groups separately; for *fkbp5* 2-fold (p≤0.05) in DMSO and 16-fold (p≤0.01) in VIN; and for *fosl1a,* 2-fold (p≤0.05) in DMSO and 5-fold (p≤0.01) in VIN. For *htr1b* there was an apparent treatment effect when VIN and DMSO groups were compared; however, the two-way ANOVA performed did not show any significant difference with regards to the stress status, and the treatment*stress status interaction (p>0.05). For *crhb* and *bdnf* the ANOVA test performed did not show any significant difference with regards to the three variables studied (the treatment, the stress status, and the treatment*stress status interaction, p>0.05). Therefore, pairwise comparison was not valid for these genes.

For DEX group, the two-way ANOVA performed showed that the treatment (DEX vs DMSO), the stress state (stressed vs unstressed) and their interaction (the treatment*the stress status) had significant effects on the whole-body mRNA levels only for *fosab*. A post hoc test, Tukey's test was performed for pairwise comparison. Our findings showed that although an apparent downregulation was appreciated, there was no significant difference between the DEX group and the DMSO group in the unstressed (0-min)

condition (p>0.05; Figure 11, panel **C**). Our findings showed significant downregulation of *fosab* whole-body mRNA levels (7-fold, p≤0.01) in the stressed (60-min) condition when the DEX group and the DMSO group were compared (Figure 11, panel **C**). Furthermore, the whole-body mRNA levels for *fosab* in DEX-60 min (stressed condition) was similar to the DMSO-0 min (control unstressed condition), statistically (p>0.05; Figure 11, panel **C**). For DEX group, the two-way ANOVA performed showed that the treatment (DEX vs DMSO) and the stress state (stressed vs unstressed) had significant effects on the whole-body mRNA levels of the following genes *egr2a, fkbp5, fosl1a,* and *per2.* A post hoc test, Tukey's test was performed for pairwise comparison for these genes on the main factors of the stress status. Our findings showed that in these genes the whole-body mRNA levels were upregulated after the handling stress when the stressed condition (60-min) was compared to the unstressed condition (0-min) in the treatment (BPA) and control (DMSO) groups separately. For *egr2a,* 4-fold (p≤0.05) in DMSO and 2-fold (p≤0.01) in DEX; for *fkbp5* 2-fold (p≤0.05) in DMSO and 7-fold (p≤0.05) in DEX; for *fosl1a,* 2-fold (p≤0.05) in DMSO and 13-fold (p≤0.001) in DEX; for *per2* 4-fold (p≤0.05) in DMSO and 18-fold (p≤0.001) in DEX (Figure 10, panel **C**). For *crhb, htr1b, npas4a, nr4a1,* and *rorcb* the ANOVA test performed did not show any significant difference with regards to the three variables studied (the treatment, the stress status, and the treatment*stress status interaction, p>0.05). Therefore, pairwise comparison was not valid for these genes.

To focus on the effects of the treatment chemicals in the unstressed condition, separate one-way ANOVA was performed. For FLX-O/N group, there was no significant difference between the treatment and the control (Ethanol) group for all 11 genes studied (p>0.05). For FLX-6D group, our findings showed significant downregulation of *egr2a* (2.4-fold; p≤0.05), *fkbp5* (5.4-fold; p≤0.01), *htr1b* (2-fold; p≤0.01), *npas4a* (4-fold; p≤0.05), *nr4a1* (3-fold; p≤0.05), and *per2* (6-fold; p≤0.05) (Figure). For *crhb*, *fosl1a, rorcb, bdnf,* and *fosab* the ANOVA test performed did not show any significant difference between the treatment (FLX-6D-0 min) and the control (Ethanol-6D- 0min) groups. For BPA, our findings showed significant downregulation of *egr2a* (3.2-fold; p≤0.01), *fkbp5* (4.4-fold; p≤0.001), *fosl1* (6.4-fold; p≤0.001), *npas4a* (4.6-fold; p≤0.001), *per2* (13-fold; p≤0.01), *rorcb* (6-fold; p≤0.001), and *fosab* (3.4-fold; p≤0.05). For *crhb, htr1b, bdnf,* and *nr4a1,* the ANOVA test performed did not show any significant difference between the treatment (BPA-0 min) and the control (DMSO- 0 min) groups. For VIN, our findings showed significant downregulation of *egr2a* (2.2-fold; p≤0.05), *fkbp5* (14-fold; p≤0.001), *fosl1* (7-fold; p≤0.001), *npas4a* (7.5-fold; p≤0.001), *nr4a1* (2.2-fold; p≤0.01), *per2* (12-fold; p≤0.01), and *fosab* (15-fold; p≤0.01). For VIN, our findings showed significant upregulation of *bdnf* (3.4-fold; p≤0.01) in the treatment (VIN- 0 min) group compared to the control (DMSO- 0 min). For *crhb, htr1b, and rorcb,* the ANOVA test performed did not show any significant difference between the treatment (VIN-0 min) and the control (DMSO- 0 min) groups. For DEX, our findings showed significant downregulation of *fkbp5* (3-fold; p≤0.01), *fosl1* (6-fold; p≤0.001), *per2* (9.5-fold; p≤0.01), and *fosab* (2.6-fold; p≤0.05). For *crhb, egr2a, htr1b, npas4a, nr4a1, rorcb* and *bdnf* the ANOVA test performed did not show any significant difference between the treatment (DEX-0 min) and the control (DMSO- 0 min) groups.

Our findings showed several genes associated with stress response, neurogenesis and development of depression in mammalian models (the minimal library) are affected by exposure to different chemicals in SR4G transgenic larvae. The downregulation of these genes was the prominent effect of such exposure.

References

1. Vera-Chang, M.N., T.W. Moon, and V.L. Trudeau, *Cortisol disruption and transgenerational alteration in the expression of stress-related genes in zebrafish larvae following fluoxetine exposure.* Toxicology and Applied Pharmacology, 2019. **382**: p. 114742.
2. Vera-Chang, M.N., et al., *Transgenerational hypocortisolism and behavioral disruption are induced by the antidepressant fluoxetine in male zebrafish Danio rerio.* Proceedings of the National Academy of Sciences of the United States of America, 2018. **115**(52): p. E12435-E12442.
3. Vera-Chang, M.N., T.W. Moon, and V.L. Trudeau, *Ancestral Fluoxetine Exposure Sensitizes Zebrafish to Venlafaxine-Induced Reductions in Cortisol and Spawning.* Endocrinology, 2019. **160**(9): p. 2137-2142.
4. Martinez, R., et al., *Developmental fluoxetine exposure in zebrafish reduces offspring basal cortisol concentration via life stage-dependent maternal transmission.* PLOS ONE, 2019. **14**(2): p. e0212577.
5. Krug, R.G., et al., *A transgenic zebrafish model for monitoring glucocorticoid receptor activity.* Genes, Brain and Behavior, 2014. **13**(5): p. 478-487.
6. Ulrich-Lai, Y.M. and J.P. Herman, *Neural regulation of endocrine and autonomic stress responses.* Nature Reviews Neuroscience, 2009. **10**(6): p. 397-409.
7. Dayas, C.V., et al., *Stressor categorization: acute physical and psychological stressors elicit distinctive recruitment patterns in the amygdala and in medullary noradrenergic cell groups.* European Journal of Neuroscience, 2001. **14**(7): p. 1143-1152.
8. Skoluda, N., et al., *Intra-individual psychological and physiological responses to acute laboratory stressors of different intensity.* Psychoneuroendocrinology, 2015. **51**: p. 227-236.
9. Russo, S.J. and E.J. Nestler, *The brain reward circuitry in mood disorders.* Nature Reviews Neuroscience, 2013. **14**(9): p. 609-625.
10. de Kloet, E.R., M. Joëls, and F. Holsboer, *Stress and the brain: from adaptation to disease.* Nature Reviews Neuroscience, 2005. **6**(6): p. 463-475.
11. Joëls, M. and T.Z. Baram, *The neuro-symphony of stress.* Nature Reviews Neuroscience, 2009. **10**(6): p. 459-466.
12. Herman, J.P., et al., *Central mechanisms of stress integration: hierarchical circuitry controlling hypothalamo–pituitary–adrenocortical responsiveness.* Frontiers in Neuroendocrinology, 2003. **24**(3): p. 151-180.
13. Senst, L. and J. Bains, *Neuromodulators, stress and plasticity: a role for endocannabinoid signalling.* The Journal of Experimental Biology, 2014. **217**(1): p. 102-108.
14. Bains, J.S., J.I.W. Cusulin, and W. Inoue, *Stress-related synaptic plasticity in the hypothalamus.* Nature Reviews Neuroscience, 2015. **16**(7): p. 377-388.
15. JJ, R., *Toward a limbic cortical inhibitory network: implications for hypothalamic-pituitary-adrenal responses following chronic stress.* Front. Behav. Neurosci., 2012. **6**(7).
16. Carlos, C.C., et al., *Mechanisms in the Bed Nucleus of the Stria Terminalis Involved in Control of Autonomic and Neuroendocrine Functions: A Review.* Current Neuropharmacology, 2013. **11**(2): p. 141-159.
17. Godoy, L.D., et al., *A Comprehensive Overview on Stress Neurobiology: Basic Concepts and Clinical Implications.* Frontiers in Behavioral Neuroscience, 2018. **12**.
18. Anacker, C., et al., *The glucocorticoid receptor: pivot of depression and of antidepressant treatment?* Psychoneuroendocrinology, 2011. **36**(3): p. 415-25.

19. Kerr, D., et al., *Hippocampal glucocorticoid receptor activation enhances voltage-dependent Ca2+ conductances: relevance to brain aging.* PNAS, 1992. **89**: p. 8527-8531.
20. Shirazi, S.N., et al., *Glucocorticoids and the Brain: Neural Mechanisms Regulating the Stress Response*. 2015, Springer New York. p. 235-252.
21. Joëls, M., *Corticosteroids and the brain.* Journal of Endocrinology, 2018. **238**(3): p. R121-R130.
22. Almeida, O.F.X., et al., *Subtle shifts in the ratio between pro- and antiapoptotic molecules after activation of corticosteroid receptors decide neuronal fate.* The FASEB Journal, 2000. **14**(5): p. 779-790.
23. Heine, V.M., et al., *Suppressed proliferation and apoptotic changes in the rat dentate gyrus after acute and chronic stress are reversible.* European Journal of Neuroscience, 2004. **19**(1): p. 131-144.
24. Mayer, J.L., et al., *Brief Treatment With the Glucocorticoid Receptor Antagonist Mifepristone Normalises the Corticosterone-Induced Reduction of Adult Hippocampal Neurogenesis.* Journal of Neuroendocrinology, 2006. **18**(8): p. 629-631.
25. Mifsud, K.R. and J.M.H.M. Reul, *Mineralocorticoid and glucocorticoid receptor-mediated control of genomic responses to stress in the brain.* Stress, 2018. **21**(5): p. 389-402.
26. Odermatt, A. and C. Gumy, *Glucocorticoid and mineralocorticoid action: Why should we consider influences by environmental chemicals?* Biochemical Pharmacology, 2008. **76**(10): p. 1184-1193.
27. Patchev, V.K. and A.V. Patchev, *Experimental models of stress.* Dialogues in clinical neuroscience, 2006. **8**(4): p. 417-432.
28. Ridder, S., et al., *Mice with Genetically Altered Glucocorticoid Receptor Expression Show Altered Sensitivity for Stress-Induced Depressive Reactions.* The Journal of Neuroscience, 2005. **25**(26): p. 6243-6250.
29. Tronche, F., et al., *Disruption of the glucocorticoid receptor gene in the nervous system results in reduced anxiety.* Nature Genetics, 1999. **23**(1): p. 99-103.
30. Boyle, M.P., et al., *Forebrain Glucocorticoid Receptors Modulate Anxiety-Associated Locomotor Activation and Adrenal Responsiveness.* The Journal of Neuroscience, 2006. **26**(7): p. 1971-1978.
31. Schmidt, M.V., et al., *Postnatal Glucocorticoid Excess Due to Pituitary Glucocorticoid Receptor Deficiency: Differential Short- and Long-Term Consequences.* Endocrinology, 2009. **150**(6): p. 2709-2716.
32. Wagner, K.V., et al., *Pituitary glucocorticoid receptor deletion reduces vulnerability to chronic stress.* Psychoneuroendocrinology, 2011. **36**(4): p. 579-587.
33. Wei, Q., et al., *Glucocorticoid receptor overexpression in forebrain: A mouse model of increased emotional lability.* Proceedings of the National Academy of Sciences of the United States of America, 2004. **101**(32): p. 11851-11856.
34. Rozeboom, A.M., H. Akil, and A.F. Seasholtz, *Mineralocorticoid receptor overexpression in forebrain decreases anxiety-like behavior and alters the stress response in mice.* Proceedings of the National Academy of Sciences, 2007. **104**(11): p. 4688-4693.
35. Alderman, S.L. and N.J. Bernier, *Ontogeny of the corticotropin-releasing factor system in zebrafish.* General and Comparative Endocrinology, 2009. **164**(1): p. 61-69.
36. Rajakumar, A. and B. Senthilkumaran, *Steroidogenesis and its regulation in teleost-a review.* Fish Physiology and Biochemistry, 2020. **46**(3): p. 803-818.
37. Alsop, D. and M. Vijayan, *The zebrafish stress axis: Molecular fallout from the teleost-specific genome duplication event.* General and Comparative Endocrinology, 2009. **161**(1): p. 62-66.
38. Balasch, J.C. and L. Tort, *Netting the Stress Responses in Fish.* Frontiers in Endocrinology, 2019. **10**.
39. Harper, C. and J.C. Wolf, *Morphologic Effects of the Stress Response in Fish.* ILAR Journal, 2009. **50**(4): p. 387-396.

40. Sørensen, C., I.B. Johansen, and Ø. Øverli, *Neural plasticity and stress coping in teleost fishes.* General and Comparative Endocrinology, 2013. **181**: p. 25-34.
41. Xavier, M.J., et al., *Transgenerational inheritance: how impacts to the epigenetic and genetic information of parents affect offspring health.* Human Reproduction Update, 2019. **25**(5): p. 519-541.
42. Crews, D., et al., *Epigenetic transgenerational inheritance of altered stress responses.* Proc Natl Acad Sci U S A, 2012. **109**(23): p. 9143-8.
43. Argentieri, M.A., et al., *Epigenetic Pathways in Human Disease: The Impact of DNA Methylation on Stress-Related Pathogenesis and Current Challenges in Biomarker Development.* EBioMedicine, 2017. **18**: p. 327-350.
44. Gillette, R., et al., *Distinct actions of ancestral vinclozolin and juvenile stress on neural gene expression in the male rat.* Front Genet, 2015. **6**: p. 56.
45. Stouder, C. and A. Paoloni-Giacobino, *Transgenerational effects of the endocrine disruptor vinclozolin on the methylation pattern of imprinted genes in the mouse sperm.* Reproduction, 2010. **139**(2): p. 373-9.
46. Franklin, T.B., et al., *Epigenetic transmission of the impact of early stress across generations.* Biol Psychiatry, 2010. **68**(5): p. 408-15.
47. Anway, M.D., et al., *Epigenetic transgenerational actions of endocrine disruptors and male fertility.* Science, 2005. **308**(5727): p. 1466-9.
48. Skinner, M.K., et al., *Transgenerational epigenetic programming of the brain transcriptome and anxiety behavior.* PLoS One, 2008. **3**(11): p. e3745.
49. Harada, B.T. and C. He, *Epigenetics: Making your mark on DNA.* Nat Chem, 2017. **9**(11): p. 1040-1042.
50. Lyko, F., *The DNA methyltransferase family: a versatile toolkit for epigenetic regulation.* Nat Rev Genet, 2017.
51. Pang, Y.Y., R.J.H. Lu, and P.Y. Chen, *Behavioral Epigenetics: Perspectives Based on Experience-Dependent Epigenetic Inheritance.* Epigenomes, 2019. **3**(3).
52. Park, C., et al., *Stress, epigenetics and depression: A systematic review.* Neuroscience and Biobehavioral Reviews, 2019. **102**: p. 139-152.
53. Dietz, D.M., et al., *Paternal Transmission of Stress-Induced Pathologies.* Biological Psychiatry, 2011. **70**(5): p. 408-414.
54. Saavedra-Rodríguez, L. and L.A. Feig, *Chronic Social Instability Induces Anxiety and Defective Social Interactions Across Generations.* 2013. **73**(1): p. 44-53.
55. Franklin, T.B., et al., *Influence of Early Stress on Social Abilities and Serotonergic Functions across Generations in Mice.* PLoS ONE, 2011. **6**(7): p. e21842.
56. Pei, S.R., et al., *Risk of prenatal depression and stress treatment: alteration on serotonin system of offspring through exposure to Fluoxetine.* Scientific Reports, 2016. **6**.
57. Jiang, S., et al., *Epigenetic Modifications in Stress Response Genes Associated With Childhood Trauma.* Frontiers in Psychiatry, 2019. **10**.
58. Fogelman, N. and T. Canli, *Early Life Stress, Physiology, and Genetics: A Review.* Frontiers in Psychology, 2019. **10**.
59. Chen, D., et al., *A review of DNA methylation in depression.* Journal of Clinical Neuroscience, 2017. **43**: p. 39-46.
60. Castrén, E. and T. Rantamäki, *The role of BDNF and its receptors in depression and antidepressant drug action: Reactivation of developmental plasticity.* Developmental Neurobiology, 2010. **70**(5): p. 289-297.
61. Sarkar, A., et al., *Hippocampal HDAC4 Contributes to Postnatal Fluoxetine-Evoked Depression-Like Behavior.* Neuropsychopharmacology, 2014. **39**(9): p. 2221-2232.

62. Torres-Berrio, A., et al., *Unraveling the epigenetic landscape of depression: focus on early life stress.* Dialogues Clin Neurosci, 2019. **21**(4): p. 341-357.
63. Elliott, E., et al., *Resilience to social stress coincides with functional DNA methylation of the Crf gene in adult mice.* 2010. **13**(11): p. 1351-1353.
64. Duman, E.A. and T. Canli, *Influence of life stress, 5-HTTLPR genotype, and SLC6A4 methylation on gene expression and stress response in healthy Caucasian males.* Biology of Mood & Anxiety Disorders, 2015. **5**(1).
65. Alexander, N., et al., *DNA methylation profiles within the serotonin transporter gene moderate the association of 5-HTTLPR and cortisol stress reactivity.* 2014. **4**(9): p. e443.
66. Uchida, S., et al., *Epigenetic Status of Gdnf in the Ventral Striatum Determines Susceptibility and Adaptation to Daily Stressful Events.* Neuron, 2011. **69**(2): p. 359-372.
67. Zheng, Y., et al., *Gestational stress induces depressive-like and anxiety-like phenotypes through epigenetic regulation of BDNF expression in offspring hippocampus.* Epigenetics, 2016. **11**(2): p. 150-162.
68. Turecki, G. and M.J. Meaney, *Effects of the Social Environment and Stress on Glucocorticoid Receptor Gene Methylation: A Systematic Review.* Biological Psychiatry, 2016. **79**(2): p. 87-96.
69. Braun, K., et al., *Experience-induced transgenerational (re-)programming of neuronal structure and functions: Impact of stress prior and during pregnancy.* Neuroscience & Biobehavioral Reviews, 2020. **117**: p. 281-296.
70. Prasanth, G.K., L.M. Divya, and C. Sadasivan, *Bisphenol-A can bind to human glucocorticoid receptor as an agonist: an in silico study.* Journal of Applied Toxicology, 2010. **30**(8): p. 769-774.
71. Chen, F., et al., *Sex differences in the adult HPA axis and affective behaviors are altered by perinatal exposure to a low dose of bisphenol A.* 2014. **1571**: p. 12-24.
72. Giesbrecht, G.F., et al., *Prenatal bisphenol a exposure and dysregulation of infant hypothalamic-pituitary-adrenal axis function: findings from the APrON cohort study.* Environmental Health, 2017. **16**(1).
73. Giesbrecht, G.F., et al., *Urinary bisphenol A is associated with dysregulation of HPA-axis function in pregnant women: Findings from the APrON cohort study.* 2016. **151**: p. 689-697.
74. Aitken, M., et al., *Medicines Use and Spending in the US: A Review of 2015 and Outlook to 2020.* 2016, IMS Institute for Healthcare Informatics: Parsippany, NJ.
75. Boas, G.R.V., et al., *Molecular aspects of depression: A review from neurobiology to treatment.* European Journal of Pharmacology, 2019. **851**: p. 99-121.
76. Micheli, L., et al., *Depression and adult neurogenesis: Positive effects of the antidepressant fluoxetine and of physical exercise.* Brain Research Bulletin, 2018. **143**: p. 181-193.
77. Uguz, F., *Selective serotonin reuptake inhibitors and the risk of congenital anomalies: a systematic review of current meta-analyses.* Expert Opinion on Drug Safety, 2020: p. 1-10.
78. Albert, P.R. and C. Benkelfat, *The neurobiology of depression—revisiting the serotonin hypothesis. II. Genetic, epigenetic and clinical studies.* Philosophical Transactions of the Royal Society B: Biological Sciences, 2013. **368**(1615): p. 20120535.
79. Tang, S.W., D. Helmeste, and B. Leonard, *Is neurogenesis relevant in depression and in the mechanism of antidepressant drug action? A critical review.* The World Journal of Biological Psychiatry, 2012. **13**(6): p. 402-412.
80. Ma, K., et al., *Molecular Mechanism for Stress-Induced Depression Assessed by Sequencing miRNA and mRNA in Medial Prefrontal Cortex.* Plos One, 2016. **11**(7).
81. Mitjans, M. and B. Arias, *The genetics of depression: What information can new methodologic approaches provide?* Actas Espanolas De Psiquiatria, 2012. **40**(2): p. 70-83.
82. Chaudhury, D., H. Liu, and M.H. Han, *Neuronal correlates of depression.* Cellular and Molecular Life Sciences, 2015. **72**(24): p. 4825-4848.

83. Bleakley, S., *Review of the choice and use of antidepressant drugs.* Progress in Neurology and Psychiatry, 2013. **17**(6): p. 18-26.
84. Schatzberg A, Blier P, and Delgada P, *Antidepressant Discontinuation syndrome: Consensus panel recommendations for clinical management and additional research.* J Clin Psychiatry, 2006. **67**(4): p. 27-30.
85. Glover, M.E. and S.M. Clinton, *Of rodents and humans: A comparative review of the neurobehavioral effects of early life SSRI exposure in preclinical and clinical research.* International Journal of Developmental Neuroscience, 2016. **51**(C): p. 50-72.
86. Kroeze, Y., H. Zhou, and J.R. Homberg, *The genetics of selective serotonin reuptake inhibitors.* Pharmacology & Therapeutics, 2012. **136**(3): p. 375-400.
87. Ramos, É., et al., *Prevalence and predictors of antidepressant use in a cohort of pregnant women.* BJOG: An International Journal of Obstetrics & Gynaecology, 2007. **114**(9): p. 1055-1064.
88. Alwan, S., et al., *Patterns of Antidepressant Medication Use Among Pregnant Women in a United States Population.* The Journal of Clinical Pharmacology, 2011. **51**(2): p. 264-270.
89. Susan E. Maloney, et al., *Examining the Reversibility of Long-Term Behavioral Disruptions in Progeny of Maternal SSRI Exposure.* Disorders of the Nervous System, 2008.
90. Lebrand, C., et al., *Transient developmental expression of monoamine transporters in the rodent forebrain.* J Comp Neurol, 1998. **401**(4): p. 506-24.
91. Zou, D., et al., *DREADD in parvalbumin interneurons of the dentate gyrus modulates anxiety, social interaction and memory extinction.* Curr Mol Med, 2016. **16**(1): p. 91-102.
92. Whitaker-Azmitia, P.M., *Serotonin and brain development: role in human developmental diseases.* Brain Research Bulletin, 2001. **56**(5): p. 479-485.
93. Riccio, O., et al., *Excess of serotonin affects neocortical pyramidal neuron migration.* Translational Psychiatry, 2011. **1**(10): p. e47-e47.
94. Riccio, O., et al., *Excess of serotonin affects embryonic interneuron migration through activation of the serotonin receptor 6.* Molecular Psychiatry, 2009. **14**(3): p. 280-290.
95. Cases, O., et al., *Lack of Barrels in the Somatosensory Cortex of Monoamine Oxidase A–Deficient Mice: Role of a Serotonin Excess during the Critical Period.* Neuron, 1996. **16**(2): p. 297-307.
96. Xu, Y., Y. Sari, and F.C. Zhou, *Selective serotonin reuptake inhibitor disrupts organization of thalamocortical somatosensory barrels during development.* Developmental Brain Research, 2004. **150**(2): p. 151-161.
97. Lee, L.-J., *Neonatal Fluoxetine Exposure Affects the Neuronal Structure in the Somatosensory Cortex and Somatosensory-Related Behaviors in Adolescent Rats.* Neurotoxicity Research, 2009. **15**(3): p. 212-223.
98. Arumugasaamy, N., et al., *Assessing SSRIs' effects on fetal cardiomyocytes utilizing placenta-fetus model.* Acta Biomaterialia, 2019. **99**: p. 258-268.
99. Arumugasaamy, N., et al., *Model Placental Barrier Phenotypic Response to Fluoxetine and Sertraline: A Comparative Study.* Advanced Healthcare Materials, 2019. **8**(18).
100. Goeden, N., et al., *Maternal Inflammation Disrupts Fetal Neurodevelopment via Increased Placental Output of Serotonin to the Fetal Brain.* The Journal of Neuroscience, 2016. **36**(22): p. 6041-6049.
101. Gemmel, M., et al., *Perinatal fluoxetine effects on social play, the HPA system, and hippocampal plasticity in pre-adolescent male and female rats: Interactions with pre-gestational maternal stress.* Psychoneuroendocrinology, 2017. **84**: p. 159-171.
102. Grieb, Z.A. and C.M. Ragan, *The effects of perinatal SSRI exposure on anxious behavior and neurobiology in rodent and human offspring.* European Neuropsychopharmacology, 2019. **29**(11): p. 1169-1184.

103. Klinger, G. and P. Merlob, *Selective serotonin reuptake inhibitor induced neonatal abstinence syndrome.* Isr J Psychiatry Relat Sci, 2008. **45**(2): p. 107-13.
104. Klinger, G., et al., *Long-term outcome following selective serotonin reuptake inhibitor induced neonatal abstinence syndrome.* Journal of Perinatology, 2011. **31**(9): p. 615-620.
105. Pawluski, J.L., et al., *Prenatal SSRI exposure alters neonatal corticosteroid binding globulin, infant cortisol levels, and emerging HPA function.* Psychoneuroendocrinology, 2012. **37**(7): p. 1019-1028.
106. Oberlander, T.F., et al., *Hypothalamic–pituitary–adrenal (HPA) axis function in 3-month old infants with prenatal selective serotonin reuptake inhibitor (SSRI) antidepressant exposure.* Early Human Development, 2008. **84**(10): p. 689-697.
107. Oberlander, T.F., et al., *Pain Reactivity in 2-Month-Old Infants After Prenatal and Postnatal Selective Serotonin Reuptake Inhibitor Medication Exposure.* Pediatrics, 2005. **115**(2): p. 411-425.
108. Oberlander, T.F., et al., *Prolonged Prenatal Psychotropic Medication Exposure Alters Neonatal Acute Pain Response.* Pediatric Research, 2002. **51**(4): p. 443-453.
109. Malm, H., et al., *Gestational Exposure to Selective Serotonin Reuptake Inhibitors and Offspring Psychiatric Disorders: A National Register-Based Study.* Journal of the American Academy of Child & Adolescent Psychiatry, 2016. **55**(5): p. 359-366.
110. Schultz, M.M., et al., *Antidepressant Pharmaceuticals in Two U.S. Effluent-Impacted Streams: Occurrence and Fate in Water and Sediment, and Selective Uptake in Fish Neural Tissue.* Environmental Science & Technology, 2010. **44**(6): p. 1918-1925.
111. Metcalfe, C.D., et al., *Antidepressants and their metabolites in municipal wastewater, and downstream exposure in an urban watershed.* Environmental Toxicology and Chemistry, 2010. **29**(1): p. 79-89.
112. Metcalfe, C.D., et al., *Distribution of acidic and neutral drugs in surface waters near sewage treatment plants in the lower Great Lakes, Canada.* Environmental Toxicology and Chemistry, 2003. **22**(12): p. 2881-2889.
113. Kolpin, D.W., et al., *Pharmaceuticals, Hormones, and Other Organic Wastewater Contaminants in U.S. Streams, 1999–2000: A National Reconnaissance.* Environmental Science & Technology, 2002. **36**(6): p. 1202-1211.
114. Mennigen, J.A., et al., *Pharmaceuticals as Neuroendocrine Disruptors: Lessons Learned from Fish on Prozac.* 2011. **14**(5-7): p. 387-412.
115. Li, C., et al., *An integrated approach with the zebrafish model for biomonitoring of municipal wastewater effluent and receiving waters.* Water Research, 2018. **131**: p. 33-44.
116. McDonald, M.D., *An AOP analysis of selective serotonin reuptake inhibitors (SSRIs) for fish.* Comparative Biochemistry and Physiology C-Toxicology & Pharmacology, 2017. **197**: p. 19-31.
117. Valenti, T.W., et al., *Human Therapeutic Plasma Levels of the Selective Serotonin Reuptake Inhibitor (SSRI) Sertraline Decrease Serotonin Reuptake Transporter Binding and Shelter-Seeking Behavior in Adult Male Fathead Minnows.* Environmental Science & Technology, 2012. **46**(4): p. 2427-2435.
118. Margiotta-Casaluci, L., et al., *Quantitative Cross-Species Extrapolation between Humans and Fish: The Case of the Anti-Depressant Fluoxetine.* PLoS ONE, 2014. **9**(10): p. e110467.
119. Cunha, D.L., M.P. Mendes, and M. Marques, *Environmental risk assessment of psychoactive drugs in the aquatic environment.* Environmental Science and Pollution Research, 2019. **26**(1): p. 78-90.
120. Gould, G.G., B.W. Brooks, and A. Frazer, *[3H] Citalopram Binding to Serotonin Transporter Sites in Minnow Brains.* Basic & Clinical Pharmacology & Toxicology, 2007. **101**(3): p. 203-210.

121. Mennigen, J.A., et al., *Waterborne fluoxetine disrupts feeding and energy metabolism in the goldfish Carassius auratus.* Aquatic Toxicology, 2010. **100**(1): p. 128-137.
122. Kreke, N. and D.R. Dietrich, *Physiological Endpoints for Potential SSRI Interactions in Fish.* Critical Reviews in Toxicology, 2008. **38**(3): p. 215-247.
123. Winberg, S., et al., *Serotonin as a regulator of hypothalamic-pituitary-interrenal activity in teleost fish.* Neurosci Lett, 1997. **230**(2): p. 113-6.
124. McDonald, M.D., A. Gonzalez, and K.A. Sloman, *Higher levels of aggression are observed in socially dominant toadfish treated with the selective serotonin reuptake inhibitor, fluoxetine.* Comparative Biochemistry and Physiology Part C: Toxicology & Pharmacology, 2011. **153**(1): p. 107-112.
125. Morando, M.B., L.R. Medeiros, and M.D. McDonald, *Fluoxetine treatment affects nitrogen waste excretion and osmoregulation in a marine teleost fish.* Aquatic Toxicology, 2009. **95**(2): p. 164-171.
126. Sebire, M., et al., *Prozac affects stickleback nest quality without altering androgen, spiggin or aggression levels during a 21-day breeding test.* Aquatic Toxicology, 2015. **168**: p. 78-89.
127. Giacomini, A., et al., *Environmental and Pharmacological Manipulations Blunt the Stress Response of Zebrafish in a Similar Manner.* Scientific Reports, 2016. **6**.
128. Kalueff, A.V., et al., *Zebrafish neurobehavioral phenomics for aquatic neuropharmacology and toxicology research.* Aquatic Toxicology, 2016. **170**: p. 297-309.
129. Whitaker, K.W., et al., *Serotonergic modulation of startle-escape plasticity in an African cichlid fish: a single-cell molecular and physiological analysis of a vital neural circuit.* Journal of Neurophysiology, 2011. **106**(1): p. 127-137.
130. Nowicki, M., et al., *Serotonin antagonists induce anxiolytic and anxiogenic-like behavior in zebrafish in a receptor-subtype dependent manner.* Pharmacology Biochemistry and Behavior, 2014. **126**: p. 170-180.
131. Nathan, F.M., S. Ogawa, and I.S. Parhar, *Kisspeptin1 modulates odorant-evoked fear response via two serotonin receptor subtypes (5-HT1A and 5-HT2) in zebrafish.* Journal of Neurochemistry, 2015. **133**(6): p. 870-878.
132. Maximino, C., et al., *Interaction between 5-HT1B receptors and nitric oxide in zebrafish responses to novelty.* Neuroscience Letters, 2015. **588**: p. 54-56.
133. Egan, R.J., et al., *Understanding behavioral and physiological phenotypes of stress and anxiety in zebrafish.* Behavioural Brain Research, 2009. **205**(1): p. 38-44.
134. Kellner, M., et al., *Environmentally relevant concentrations of citalopram partially inhibit feeding in the three-spine stickleback (Gasterosteus aculeatus).* Aquatic Toxicology, 2015. **158**: p. 165-170.
135. Carlini, V.P., et al., *Selective serotonin reuptake inhibitor (fluoxetine) decreases the effects of ghrelin on memory retention and food intake.* Regulatory Peptides, 2007. **140**(1): p. 65-73.
136. Rubio, V.C., F.J. Sánchez-Vázquez, and J.A. Madrid, *Oral serotonin administration affects the quantity and the quality of macronutrients selection in European sea bass Dicentrarchus labrax L.* Physiology & Behavior, 2006. **87**(1): p. 7-15.
137. Pérez Maceira, J.J., M.J. Mancebo, and M. Aldegunde, *The involvement of 5-HT-like receptors in the regulation of food intake in rainbow trout (Oncorhynchus mykiss).* Comparative Biochemistry and Physiology Part C: Toxicology & Pharmacology, 2014. **161**: p. 1-6.
138. Ortega, V., D. Lovejoy, and N. Bernier, *Appetite-suppressing effects and interactions of centrally administered corticotropin-releasing factor, urotensin I and serotonin in rainbow trout (Oncorhynchus mykiss).* Frontiers in Neuroscience, 2013. **7**(196).

139. Mager, E.M., et al., *The toadfish serotonin 2A (5-HT2A) receptor: molecular characterization and its potential role in urea excretion.* Comparative Biochemistry and Physiology Part A: Molecular & Integrative Physiology, 2012. **163**(3): p. 319-326.
140. Prasad, P., S. Ogawa, and I.S. Parhar, *Serotonin reuptake inhibitor citalopram inhibits GnRH synthesis and spermatogenesis in the male zebrafish.* Biol Reprod, 2015. **93**(4): p. 102.
141. Mennigen, J.A., et al., *Effects of fluoxetine on the reproductive axis of female goldfish (Carassius auratus).* Physiological Genomics, 2008. **35**(3): p. 273-282.
142. Mennigen, J.A., et al., *Endocrine disrupting effects of waterborne fluoxetine exposure on the reproductive axis of female goldfish, Carassius auratus.* Comparative Biochemistry and Physiology Part C: Toxicology & Pharmacology, 2017. **202**: p. 70-78.
143. Lister, A., et al., *Inhibition of egg production in zebrafish by fluoxetine and municipal effluents: A mechanistic evaluation.* Aquatic Toxicology, 2009. **95**(4): p. 320-329.
144. Schreck, C.B., *Stress and fish reproduction: The roles of allostasis and hormesis.* General and Comparative Endocrinology, 2010. **165**(3): p. 549-556.
145. Shen, C. and Z. Zuo, *Zebrafish (Danio rerio) as an excellent vertebrate model for the development, reproductive, cardiovascular, and neural and ocular development toxicity study of hazardous chemicals.* Environmental Science and Pollution Research, 2020.
146. Chakravarthy, S., et al., *Zebrafish as an In Vivo High-Throughput Model for Genotoxicity.* 2014. **11**(2): p. 154-166.
147. Cassar, S., et al., *Use of Zebrafish in Drug Discovery Toxicology.* Chemical Research in Toxicology, 2020. **33**(1): p. 95-118.
148. Clark, K.J., N.J. Boczek, and S.C. Ekker, *Stressing zebrafish for behavioral genetics.* Reviews in the neurosciences, 2011. **22**(1): p. 49-62.
149. Gunnarsson, L., et al., *Evolutionary conservation of human drug targets in organisms used for environmental risk assessments.* Environ Sci Technol, 2008. **42**(15): p. 5807-13.
150. Horzmann, K.A. and J.L. Freeman, *Making Waves: New Developments in Toxicology With the Zebrafish.* Toxicological Sciences, 2018. **163**(1): p. 5-12.
151. Lee, O., J.M. Green, and C.R. Tyler, *Transgenic fish systems and their application in ecotoxicology.* Critical Reviews in Toxicology, 2015. **45**(2): p. 124-141.
152. Fox, H.E., et al., *Stress and dominance in a social fish.* J Neurosci, 1997. **17**(16): p. 6463-9.
153. Larson, E.T., D.M. O'Malley, and R.H. Melloni, Jr., *Aggression and vasotocin are associated with dominant-subordinate relationships in zebrafish.* Behav Brain Res, 2006. **167**(1): p. 94-102.
154. Howe, K., et al., *The zebrafish reference genome sequence and its relationship to the human genome.* Nature, 2013. **496**(7446): p. 498-503.
155. Howe, K., et al., *Erratum: Corrigendum: The zebrafish reference genome sequence and its relationship to the human genome.* Nature, 2014. **505**(7482): p. 248-248.
156. Gonzalez-Nunez, V., R. Gonzalez-Sarmiento, and R.E. Rodríguez, *Identification of two proopiomelanocortin genes in zebrafish (Danio rerio).* Brain Res Mol Brain Res, 2003. **120**(1): p. 1-8.
157. Schaaf, M.J., et al., *Discovery of a functional glucocorticoid receptor beta-isoform in zebrafish.* Endocrinology, 2008. **149**(4): p. 1591-9.
158. Roest Crollius, H. and J. Weissenbach, *Fish genomics and biology.* Genome Res, 2005. **15**(12): p. 1675-82.
159. Busquet, F., et al., *OECD validation study to assess intra- and inter-laboratory reproducibility of the zebrafish embryo toxicity test for acute aquatic toxicity testing.* Regulatory Toxicology and Pharmacology, 2014. **69**(3): p. 496-511.
160. Dai, Y.-J., et al., *Zebrafish as a model system to study toxicology.* Environmental Toxicology and Chemistry, 2014. **33**(1): p. 11-17.

161. Garcia, G.R., P.D. Noyes, and R.L. Tanguay, *Advancements in zebrafish applications for 21st century toxicology.* Pharmacology & Therapeutics, 2016. **161**: p. 11-21.
162. Bambino, K. and J. Chu, *Zebrafish in Toxicology and Environmental Health*. 2017, Elsevier. p. 331-367.
163. Nishimura, Y., et al., *Using zebrafish in systems toxicology for developmental toxicity testing.* Congenital Anomalies, 2016. **56**(1): p. 18-27.
164. Zhang, K. and Y. Zhao, *Reduced Zebrafish Transcriptome Atlas toward Understanding Environmental Neurotoxicants.* Environmental Science & Technology, 2018. **52**(12): p. 7120-7130.
165. Brady, C., et al., *Intestinal Transit Time and Cortisol-Mediated Stress in Zebrafish.* Zebrafish, 2017. **14**(5): p. 404-410.
166. Chen, Q., et al., *Common deregulated gene expression profiles and morphological changes in developing zebrafish larvae exposed to environmental-relevant high to low concentrations of glucocorticoids.* Chemosphere, 2017. **172**: p. 429-439.
167. Van Den Bos, R., et al., *Early Life Glucocorticoid Exposure Modulates Immune Function in Zebrafish (Danio rerio) Larvae.* Frontiers in Immunology, 2020. **11**.
168. Ge, W., *Zebrafish*, in *Encyclopedia of Reproduction (Second Edition)*, M.K. Skinner, Editor. 2018, Academic Press: Oxford. p. 704-710.
169. D'Amora, M. and S. Giordani, *The Utility of Zebrafish as a Model for Screening Developmental Neurotoxicity.* Frontiers in Neuroscience, 2018. **12**.
170. Sonavane, M., et al., *Zebrafish-based reporter gene assays reveal different estrogenic activities in river waters compared to a conventional human-derived assay.* 2016. **550**: p. 934-939.
171. Gorelick, D.A., et al., *Transgenic Zebrafish Reveal Tissue-Specific Differences in Estrogen Signaling in Response to Environmental Water Samples.* 2014.
172. Ramsay, J.M., et al., *Whole-body cortisol response of zebrafish to acute net handling stress.* Aquaculture, 2009. **297**(1-4): p. 157-162.
173. Alsop, D. and M.M. Vijayan, *Development of the corticosteroid stress axis and receptor expression in zebrafish.* Am J Physiol Regul Integr Comp Physiol, 2008. **294**(3): p. R711-9.
174. Kates, M., *Chapter 3 Lipid extraction procedures*, in *Laboratory Techniques in Biochemistry and Molecular Biology*, T.S. Work and E. Work, Editors. 1972, Elsevier. p. 347-353.
175. Westerfield, M., *The zebrafish book. A guide for the laboratory use of zebrafish (Danio rerio).* 4th ed, ed. M. Westerfield. 2000, Eugene: Univ. of Oregon Press.
176. Machluf, Y., A. Gutnick, and G. Levkowitz, *Development of the zebrafish hypothalamus*, in *Trends in Neuroendocrinology*, H. Vaudry and M.C. Tonon, Editors. 2011, Blackwell Science Publ: Oxford. p. 93-105.
177. Fuzzen, M.L.M., G. Van Der Kraak, and N.J. Bernier, *Stirring Up New Ideas About the Regulation of the Hypothalamic-Pituitary-Interrenal Axis in Zebrafish (Danio rerio).* Zebrafish, 2010. **7**(4): p. 349-358.
178. Steenbergen, P.J., M.K. Richardson, and D.L. Champagne, *The use of the zebrafish model in stress research.* Progress in Neuro-Psychopharmacology and Biological Psychiatry, 2011. **35**(6): p. 1432-1451.
179. White, R.M., et al., *Transparent Adult Zebrafish as a Tool for In Vivo Transplantation Analysis.* Cell Stem Cell, 2008. **2**(2): p. 183-189.
180. Antinucci, P. and R. Hindges, *A crystal-clear zebrafish for in vivo imaging.* Scientific Reports, 2016. **6**(1): p. 29490.
181. Chan, K.M., et al., *Metallothionein gene expression in zebrafish embryo-larvae and ZFL cell-line exposed to heavy metal ions.* Mar Environ Res, 2006. **62 Suppl**: p. S83-7.

182. Chen, X., et al., *BDE-47 disrupts axonal growth and motor behavior in developing zebrafish.* Aquat Toxicol, 2012. **120-121**: p. 35-44.
183. Wang, R.-L., et al., *A transcriptomics-based biological framework for studying mechanisms of endocrine disruption in small fish species.* Aquatic Toxicology, 2010. **98**(3): p. 230-244.
184. Yu, L., et al., *Exposure to DE-71 alters thyroid hormone levels and gene transcription in the hypothalamic-pituitary-thyroid axis of zebrafish larvae.* Aquat Toxicol, 2010. **97**(3): p. 226-33.
185. Massoni-Badosa, R., et al., *Sampling time-dependent artifacts in single-cell genomics studies.* Genome Biology, 2020. **21**(1).
186. Reichholf, B., et al., *Time-Resolved Small RNA Sequencing Unravels the Molecular Principles of MicroRNA Homeostasis.* Molecular Cell, 2019. **75**(4): p. 756-768.e7.
187. Mesches, G.A., K.L. Wisner, and H.K. Betcher, *A common clinical conundrum: Antidepressant treatment of depression in pregnant women.* Seminars in Perinatology, 2020. **44**(3).
188. Biffi, A., et al., *Use of antidepressants during pregnancy and neonatal outcomes: An umbrella review of meta-analyses of observational studies.* Journal of Psychiatric Research, 2020. **124**: p. 99-108.
189. Lucki, I., *The spectrum of behaviors influenced by serotonin.* Biol Psychiatry, 1998. **44**(3): p. 151-62.
190. Whitaker-Azmitia, P.M., et al., *Serotonin as a developmental signal.* Behav Brain Res, 1996. **73**(1-2): p. 19-29.
191. Whitaker-Azmitia, P.M., *Behavioral and cellular consequences of increasing serotonergic activity during brain development: a role in autism?* Int J Dev Neurosci, 2005. **23**(1): p. 75-83.
192. Sodhi, M.S. and E. Sanders-Bush, *Serotonin and brain development.* Int Rev Neurobiol, 2004. **59**: p. 111-74.
193. Xing, L., et al., *Serotonin Receptor 2A Activation Promotes Evolutionarily Relevant Basal Progenitor Proliferation in the Developing Neocortex.* Neuron, 2020.
194. Gemmel, M., et al., *Perinatal fluoxetine has enduring sexually differentiated effects on neurobehavioral outcomes related to social behaviors.* Neuropharmacology, 2019. **144**: p. 70-81.
195. Abreu, M.S., et al., *Divergent effect of fluoxetine on the response to physical or chemical stressors in zebrafish.* Peerj, 2017. **5**.
196. Ansai, S., et al., *Deficiency of Serotonin in Raphe Neurons and Altered Behavioral Responses in Tryptophan Hydroxylase 2-Knockout Medaka (Oryzias latipes).* Zebrafish, 2017. **14**(6): p. 495-507.
197. Avitsur, R., *Prenatal fluoxetine modifies the behavioral and hormonal responses to stress in male mice.* Behavioural Pharmacology, 2017: p. 1.
198. Torres, G., et al., *Fluoxetine induces the transcription of genes encoding c-fos, corticotropin-releasing factor and its type 1 receptor in rat brain.* 1998. **87**(2): p. 463-477.
199. Vera-Chang, M.N., et al., *Fluoxetine Exposure During Sexual Development Disrupts the Stress Axis and Results in Sex- and Time-Dependent Effects on the Exploratory Behavior in Adult Zebrafish Danio rerio.* Frontiers in Neuroscience, 2019. **13**.
200. Iniguez, S.D., et al., *Fluoxetine Exposure during Adolescence Alters Responses to Aversive Stimuli in Adulthood.* 2014. **34**(3): p. 1007-1021.
201. Giacomini, A.C.V.V., et al., *Fluoxetine and diazepam acutely modulate stress induced-behavior.* Behavioural Brain Research, 2016. **296**: p. 301-310.
202. Bailey, J., A. Oliveri, and E.D. Levin, *Zebrafish model systems for developmental neurobehavioral toxicology.* Birth Defects Research Part C: Embryo Today: Reviews, 2013. **99**(1): p. 14-23.
203. Grzeskowiak, L.E., A.L. Gilbert, and J.L. Morrison, *Long term impact of prenatal exposure to SSRIs on growth and body weight in childhood: evidence from animal and human studies.* Reprod Toxicol, 2012. **34**(1): p. 101-9.

204. Oberlander, T.F., et al., *Hypothalamic-pituitary-adrenal (HPA) axis function in 3-month old infants with prenatal selective serotonin reuptake inhibitor (SSRI) antidepressant exposure.* Early Hum Dev, 2008. **84**(10): p. 689-97.
205. Davidson, S., et al., *Effect of exposure to selective serotonin reuptake inhibitors in utero on fetal growth: potential role for the IGF-I and HPA axes.* Pediatr Res, 2009. **65**(2): p. 236-41.
206. Pawluski, J.L., et al., *Prenatal SSRI exposure alters neonatal corticosteroid binding globulin, infant cortisol levels, and emerging HPA function.* Psychoneuroendocrinology, 2012. **37**(7): p. 1019-28.
207. Pawluski, J.L., et al., *Developmental fluoxetine exposure differentially alters central and peripheral measures of the HPA system in adolescent male and female offspring.* Neuroscience, 2012. **220**: p. 131-41.
208. Zhou, Q.G., et al., *Hippocampal Neuronal Nitric Oxide Synthase Mediates the Stress-Related Depressive Behaviors of Glucocorticoids by Downregulating Glucocorticoid Receptor.* 2011. **31**(21): p. 7579-7590.
209. Meloni, E.G., et al., *Activation of raphe efferents to the medial prefrontal cortex by corticotropin-releasing factor: correlation with anxiety-like behavior.* Biol Psychiatry, 2008. **63**(9): p. 832-9.
210. Loveland, J.L., et al., *Social status differences regulate the serotonergic system of a cichlid fish, <em>Astatotilapia burtoni</em&gt.* The Journal of Experimental Biology, 2014. **217**(15): p. 2680.
211. Abreu, M.S., et al., *Divergent effect of fluoxetine on the response to physical or chemical stressors in zebrafish.* PeerJ, 2017. **5**: p. e3330.
212. Schroeder, A., et al., BMC Molecular Biology, 2006. **7**(1): p. 3.
213. Love, M.I., W. Huber, and S. Anders, *Moderated estimation of fold change and dispersion for RNA-seq data with DESeq2.* Genome Biology, 2014. **15**(12).
214. Francisco, D.M.F., et al., *Advancing brain barriers RNA sequencing: guidelines from experimental design to publication.* Fluids and Barriers of the CNS, 2020. **17**(1).
215. Piñero, J., et al., *The DisGeNET knowledge platform for disease genomics: 2019 update.* Nucleic Acids Research, 2019.
216. Wu, M.H., et al., *Global transcriptomic analysis of zebrafish in response to embryonic exposure to three antidepressants, amitriptyline, fluoxetine and mianserin.* Aquatic Toxicology, 2017. **192**: p. 274-283.
217. Park, J.W., et al., *Global gene expression in larval zebrafish (Danio rerio) exposed to selective serotonin reuptake inhibitors (fluoxetine and sertraline) reveals unique expression profiles and potential biomarkers of exposure.* Environmental Pollution, 2012. **167**: p. 163-170.
218. Wong, R.Y., S.E. Oxendine, and J. Godwin, *Behavioral and neurogenomic transcriptome changes in wild-derived zebrafish with fluoxetine treatment.* BMC Genomics, 2013. **14**(1): p. 348.
219. Huang, W., et al., *A transcriptomics-based analysis of toxicity mechanisms of zebrafish embryos and larvae following parental Bisphenol A exposure.* Ecotoxicology and Environmental Safety, 2020. **205**: p. 111165.
220. Takahashi, J.S., *Transcriptional architecture of the mammalian circadian clock.* Nature Reviews Genetics, 2017. **18**(3): p. 164-179.
221. Maiese, K., *Moving to the Rhythm with Clock (Circadian) Genes, Autophagy, mTOR, and SIRT1 in Degenerative Disease and Cancer.* Curr Neurovasc Res, 2017. **14**(3): p. 299-304.
222. Kiryanova, V., et al., *Circadian behavior of adult mice exposed to stress and fluoxetine during development.* 2016.
223. Knaepen, L., et al., *Developmental Fluoxetine Exposure Normalizes the Long-Term Effects of Maternal Stress on Post-Operative Pain in Sprague-Dawley Rat Offspring.* 2013. **8**(2): p. e57608.
224. Pawluski, J.L., et al., *Prenatal SSRI exposure alters neonatal corticosteroid binding globulin, infant cortisol levels, and emerging HPA function.* 2012. **37**(7): p. 1019-1028.

225. Brennan, P.A., et al., *Maternal depression and infant cortisol: influences of timing, comorbidity and treatment.* Journal of Child Psychology and Psychiatry, 2008. **49**(10): p. 1099-1107.
226. Pawluski, J.L., et al., *Developmental fluoxetine exposure differentially alters central and peripheral measures of the HPA system in adolescent male and female offspring.* Neuroscience, 2012. **220**: p. 131-141.
227. Abreu, M.S., et al., *Effects of waterborne fluoxetine on stress response and osmoregulation in zebrafish.* Environmental Toxicology and Pharmacology, 2015. **40**(3): p. 704-707.
228. Faught, E. and M.M. Vijayan, *The mineralocorticoid receptor is essential for stress axis regulation in zebrafish larvae.* Scientific Reports, 2018. **8**(1).
229. Diotel, N., et al., *Common and Distinct Features of Adult Neurogenesis and Regeneration in the Telencephalon of Zebrafish and Mammals.* Frontiers in Neuroscience, 2020. **14**.
230. Labusch, M., et al., *Conserved and Divergent Features of Adult Neurogenesis in Zebrafish.* Frontiers in Cell and Developmental Biology, 2020. **8**.
231. Pavlidis, M., A. Theodoridi, and A. Tsalafouta, *Neuroendocrine regulation of the stress response in adult zebrafish, Danio rerio.* Progress in Neuro-Psychopharmacology and Biological Psychiatry, 2015. **60**: p. 121-131.
232. Theodoridi, A., A. Tsalafouta, and M. Pavlidis, *Acute Exposure to Fluoxetine Alters Aggressive Behavior of Zebrafish and Expression of Genes Involved in Serotonergic System Regulation.* Frontiers in Neuroscience, 2017. **11**.
233. Doan, L., T. Manders, and J. Wang, *Neuroplasticity Underlying the Comorbidity of Pain and Depression.* Neural Plasticity, 2015.
234. David, D.J., et al., *Neurogenesis-Dependent and -Independent Effects of Fluoxetine in an Animal Model of Anxiety/Depression.* Neuron, 2009. **62**(4): p. 479-493.
235. Mateus-Pinheiro, A., et al., *Sustained remission from depressive-like behavior depends on hippocampal neurogenesis.* Translational Psychiatry, 2013. **3**(1): p. e210-e210.
236. Santarelli, L., *Requirement of Hippocampal Neurogenesis for the Behavioral Effects of Antidepressants.* Science, 2003. **301**(5634): p. 805-809.
237. Hill, A.S., A. Sahay, and R. Hen, *Increasing Adult Hippocampal Neurogenesis is Sufficient to Reduce Anxiety and Depression-Like Behaviors.* Neuropsychopharmacology, 2015. **40**(10): p. 2368-2378.
238. Guidotti, G., et al., *Developmental Influence of the Serotonin Transporter on the Expression of Npas4 and GABAergic Markers: Modulation by Antidepressant Treatment.* 2012. **37**(3): p. 746-758.
239. Rodriguez-Porcel, F., et al., *Neonatal Exposure of Rats to Antidepressants Affects Behavioral Reactions to Novelty and Social Interactions in a Manner Analogous to Autistic Spectrum Disorders.* 2011. **294**(10): p. 1726-1735.
240. Simpson, K.L., et al., *Perinatal antidepressant exposure alters cortical network function in rodents.* 2011. **108**(45): p. 18465-18470.
241. Pawluski, J.L. and M. Gemmel, *Perinatal SSRI medications and offspring hippocampal plasticity: interaction with maternal stress and sex.* Hormones, 2018. **17**(1): p. 15-24.
242. Albert, P.R., B. Le Francois, and F. Vahid-Ansari, *Genetic, epigenetic and posttranscriptional mechanisms for treatment of major depression: the 5-HT1A receptor gene as a paradigm.* Journal of Psychiatry & Neuroscience, 2019. **44**(3): p. 164-176.
243. Athira, K.V., et al., *An Overview of the Heterogeneity of Major Depressive Disorder: Current Knowledge and Future Prospective.* Current Neuropharmacology, 2020. **18**(3): p. 168-187.
244. Ciobanu, L.G., et al., *Differential gene expression in brain and peripheral tissues in depression across the life span: A review of replicated findings.* Neuroscience and Biobehavioral Reviews, 2016. **71**: p. 281-293.

245. Hack, L.M., et al., *Moving pharmacoepigenetics tools for depression toward clinical use.* Journal of Affective Disorders, 2019. **249**: p. 336-346.
246. Haenisch, B. and H. Bönisch, *Depression and antidepressants: Insights from knockout of dopamine, serotonin or noradrenaline re-uptake transporters.* Pharmacology & Therapeutics, 2011. **129**(3): p. 352-368.
247. Vetencourt, J.F.M., et al., *Serotonin triggers a transient epigenetic mechanism that reinstates adult visual cortex plasticity in rats.* European Journal of Neuroscience, 2011. **33**(1): p. 49-57.
248. Wang, Y., et al., *Fluoxetine Increases Hippocampal Neurogenesis and Induces Epigenetic Factors But Does Not Improve Functional Recovery after Traumatic Brain Injury.* Journal of Neurotrauma, 2011. **28**(2): p. 259-268.
249. Robison, A.J., et al., *Fluoxetine Epigenetically Alters the CaMKIIα Promoter in Nucleus Accumbens to Regulate ΔFosB Binding and Antidepressant Effects.* Neuropsychopharmacology, 2014. **39**(5): p. 1178-1186.
250. Zaidan, H., et al., *Pre-reproductive stress and fluoxetine treatment in rats affect offspring A-to-I RNA editing, gene expression and social behavior.* Environmental Epigenetics, 2018. **4**(2).
251. Wang, W. and G.-Z. Wang, *Understanding Molecular Mechanisms of the Brain Through Transcriptomics.* Frontiers in Physiology, 2019. **10**(214).
252. Moosa, A., et al., *Are endocrine disrupting compounds environmental risk factors for autism spectrum disorder?* Hormones and Behavior, 2018. **101**: p. 13-21.
253. Tijani, J.O., et al., *Pharmaceuticals, endocrine disruptors, personal care products, nanomaterials and perfluorinated pollutants: a review.* Environmental Chemistry Letters, 2016. **14**(1): p. 27-49.
254. Nelson, W., et al., *Review of the Effects of Perinatal Exposure to Endocrine-Disrupting Chemicals in Animals and Humans*. 2019, Springer International Publishing. p. 131-184.
255. Nesan, D. and D.M. Kurrasch, *Gestational Exposure to Common Endocrine Disrupting Chemicals and Their Impact on Neurodevelopment and Behavior.* Annual Review of Physiology, 2020. **82**(1): p. 177-202.
256. Walley, S.N. and T.A. Roepke, *Perinatal exposure to endocrine disrupting compounds and the control of feeding behavior—An overview.* Hormones and Behavior, 2018. **101**: p. 22-28.
257. Silva, A.S., et al., *Maternal Exposure to Fluoxetine during Gestation and Lactation Induces Long Lasting Changes in the DNA Methylation Profile of Offspring's Brain and Affects the Social Interaction of Rat.* Brain Research Bulletin, 2018.
258. Wiersielis, K.R., B.A. Samuels, and T.A. Roepke, *Perinatal exposure to bisphenol A at the intersection of stress, anxiety, and depression.* Neurotoxicology and Teratology, 2020. **79**: p. 106884.
259. William A. Thompson, V.I. Arnold, and M.M. Vijayan, *Venlafaxine in Embryos Stimulates Neurogenesis and Disrupts Larval Behavior in Zebrafis.* Environ. Sci. Technol., 2017. **51**: p. 12889-12897.
260. Sukardi, H., et al., *Zebrafish for drug toxicity screening: bridging thein vitrocell-based models andin vivomammalian models.* Expert Opinion on Drug Metabolism & Toxicology, 2011. **7**(5): p. 579-589.
261. Teixidó, E., et al., *Automated Morphological Feature Assessment for Zebrafish Embryo Developmental Toxicity Screens.* Toxicological Sciences, 2019. **167**(2): p. 438-449.
262. Peterson, R.T. and C.A. Macrae, *Systematic Approaches to Toxicology in the Zebrafish.* Annual Review of Pharmacology and Toxicology, 2012. **52**(1): p. 433-453.
263. Kinch, C.D., et al., *Low-dose exposure to bisphenol A and replacement bisphenol S induces precocious hypothalamic neurogenesis in embryonic zebrafish.* Proceedings of the National Academy of Sciences, 2015. **112**(5): p. 1475.

264. Ma, Y., et al., *The adverse health effects of bisphenol A and related toxicity mechanisms.* Environmental Research, 2019. **176**: p. 108575.
265. Aquilino, M., P. Sánchez-Argüello, and J.-L. Martínez-Guitarte, *Vinclozolin alters the expression of hormonal and stress genes in the midge Chironomus riparius.* 2016. **174**: p. 179-187.
266. Crews, D., et al., *Epigenetic transgenerational inheritance of altered stress responses.* 2012. **109**(23): p. 9143-9148.
267. Song, M., et al., *Assessing developmental toxicity and estrogenic activity of halogenated bisphenol A on zebrafish (Danio rerio).* Chemosphere, 2014. **112**: p. 275-81.
268. Marty, M.S., et al., *Population-relevant endpoints in the evaluation of endocrine-active substances (EAS) for ecotoxicological hazard and risk assessment.* Integrated Environmental Assessment and Management, 2017. **13**(2): p. 317-330.
269. Sánchez-Argüello, P., N. Aparicio, and C. Fernández, *Linking embryo toxicity with genotoxic responses in the freshwater snail Physa acuta: Single exposure to benzo(a)pyrene, fluoxetine, bisphenol A, vinclozolin and exposure to binary mixtures with benzo(a)pyrene.* 2012. **80**: p. 152-160.
270. Martinović-Weigelt, D., et al., *Gene expression profiling of the androgen receptor antagonists flutamide and vinclozolin in zebrafish (Danio rerio) gonads.* 2011. **101**(2): p. 447-458.
271. Ali, S., H.G.J.V. Mil, and M.K. Richardson, *Large-Scale Assessment of the Zebrafish Embryo as a Possible Predictive Model in Toxicity Testing.* PLoS ONE, 2011. **6**(6): p. e21076.
272. Horie, Y., et al., *Assessment of the lethal and sublethal effects of 20 environmental chemicals in zebrafish embryos and larvae by using OECD TG 212.* Journal of Applied Toxicology, 2017.
273. Hendrick, V., et al., *Placental passage of antidepressant medications.* American Journal of Psychiatry, 2003. **160**(5): p. 993-996.
274. Rampono, J., et al., *A pilot study of newer antidepressant concentrations in cord and maternal serum and possible effects in the neonate.* International Journal of Neuropsychopharmacology, 2004. **7**(3): p. 329-334.
275. Kim, J., et al., *Stereoselective disposition of fluoxetine and norfluoxetine during pregnancy and breast-feeding.* British Journal of Clinical Pharmacology, 2006. **61**(2): p. 155-163.
276. Canavello, P.R., et al., *Measuring Endocrine (Cortisol) Responses of Zebrafish to Stress*. 2011, Humana Press. p. 135-142.
277. Yeh, C.-M., M. Glöck, and S. Ryu, *An Optimized Whole-Body Cortisol Quantification Method for Assessing Stress Levels in Larval Zebrafish.* PLoS ONE, 2013. **8**(11): p. e79406.
278. Roberts, R.F. and W.L. Roberts, *Performance characteristics of five automated serum cortisol immunoassays.* 2004. **37**(6): p. 489-493.
279. Jensen, M.A., et al., *An interlaboratory comparison between similar methods for determination of melatonin, cortisol and testosterone in saliva.* Scandinavian Journal of Clinical and Laboratory Investigation, 2014. **74**(5): p. 454-461.
280. El-Farhan, N., D.A. Rees, and C. Evans, *Measuring cortisol in serum, urine and saliva – are our assays good enough?* Annals of Clinical Biochemistry, 2017. **54**(3): p. 308-322.
281. Basnet, R., et al., *Zebrafish Larvae as a Behavioral Model in Neuropharmacology.* Biomedicines, 2019. **7**(1): p. 23.
282. Gallo, F.T., et al., *Immediate Early Genes, Memory and Psychiatric Disorders: Focus on c-Fos, Egr1 and Arc.* Frontiers in Behavioral Neuroscience, 2018. **12**.
283. Barbosa, F.F. and R.H. Silva, *Immediate-Early Gene Expression in Neural Circuits Related to Object Recognition Memory*. 2018, Elsevier. p. 261-271.
284. Minatohara, K., M. Akiyoshi, and H. Okuno, *Role of Immediate-Early Genes in Synaptic Plasticity and Neuronal Ensembles Underlying the Memory Trace.* Frontiers in Molecular Neuroscience, 2016. **8**.

285. Bahrami, S. and F. Drabløs, *Gene regulation in the immediate-early response process.* Advances in Biological Regulation, 2016. **62**: p. 37-49.
286. Lindecke, A., et al., *Long-term depression activates transcription of immediate early transcription factor genes: involvement of serum response factor/Elk-1.* European Journal of Neuroscience, 2006. **24**(2): p. 555-563.
287. Chottekalapanda, R.U., et al., *AP-1 controls the p11-dependent antidepressant response.* Molecular Psychiatry, 2020. **25**(7): p. 1364-1381.
288. Heroux, N.A., et al., *Differential expression of the immediate early genes c-Fos, Arc, Egr-1, and Npas4 during long-term memory formation in the context preexposure facilitation effect (CPFE).* Neurobiol Learn Mem, 2018. **147**: p. 128-138.
289. Vialou, V., et al., *Differential induction of FosB isoforms throughout the brain by fluoxetine and chronic stress.* 2015. **99**: p. 28-37.
290. Hogan, M.K., G.F. Hamilton, and P.J. Horner, *Neural Stimulation and Molecular Mechanisms of Plasticity and Regeneration: A Review.* Frontiers in Cellular Neuroscience, 2020. **14**.
291. Flavell, S.W. and M.E. Greenberg, *Signaling mechanisms linking neuronal activity to gene expression and plasticity of the nervous system.* Annu Rev Neurosci, 2008. **31**: p. 563-90.
292. Mikics, É., et al., *Social Learning Requires Plasticity Enhanced by Fluoxetine Through Prefrontal Bdnf-TrkB Signaling to Limit Aggression Induced by Post-Weaning Social Isolation.* Neuropsychopharmacology, 2018. **43**(2): p. 235-245.
293. Feder, M.E. and J.C. Walser, *The biological limitations of transcriptomics in elucidating stress and stress responses.* Journal of Evolutionary Biology, 2005. **18**(4): p. 901-910.
294. Wang, P., et al., *HTR1A/1B DNA methylation may predict escitalopram treatment response in depressed Chinese Han patients.* Journal of Affective Disorders, 2018. **228**: p. 222-228.
295. Gassó, P., et al., *Epigenetic and genetic variants in the HTR1B gene and clinical improvement in children and adolescents treated with fluoxetine.* Progress in Neuro-Psychopharmacology and Biological Psychiatry, 2017. **75**: p. 28-34.
296. Alexander-Dann, B., et al., *Developments in toxicogenomics: understanding and predicting compound-induced toxicity from gene expression data.* Molecular Omics, 2018. **14**(4): p. 218-236.
297. Gluckman, P.D., T. Buklijas, and M.A. Hanson, *The Developmental Origins of Health and Disease (DOHaD) Concept*. 2016, Elsevier. p. 1-15.
298. Su, Y., C. D'Arcy, and X. Meng, *Research Review: Developmental origins of depression – a systematic review and meta-analysis.* Journal of Child Psychology and Psychiatry, 2020.
299. Goodman, S.H., et al., *Maternal depression and child psychopathology: a meta-analytic review.* Clin Child Fam Psychol Rev, 2011. **14**(1): p. 1-27.
300. Qiu, A., et al., *COMT Haplotypes Modulate Associations of Antenatal Maternal Anxiety and Neonatal Cortical Morphology.* American Journal of Psychiatry, 2015. **172**(2): p. 163-172.
301. Qiu, A., et al., *Prenatal maternal depression alters amygdala functional connectivity in 6-month-old infants.* Translational Psychiatry, 2015. **5**(2): p. e508-e508.
302. Hamada, H. and S.G. Matthews, *Prenatal programming of stress responsiveness and behaviours: Progress and perspectives.* Journal of Neuroendocrinology, 2019. **31**(3): p. e12674.
303. Comber, S., et al., *Active pharmaceutical ingredients entering the aquatic environment from wastewater treatment works: A cause for concern?* Science of The Total Environment, 2018. **613-614**: p. 538-547.
304. Kalichak, F., et al., *Waterborne psychoactive drugs impair the initial development of Zebrafish.* Environmental Toxicology and Pharmacology, 2016. **41**: p. 89-94.
305. Abreu, M.S., et al., *Acute exposure to waterborne psychoactive drugs attract zebrafish.* Comparative Biochemistry and Physiology C-Toxicology & Pharmacology, 2016. **179**: p. 37-43.

306. Klee, E.W., et al., *Zebrafish: a model for the study of addiction genetics.* Hum Genet, 2012. **131**(6): p. 977-1008.
307. Mishra, P., Z. Gong, and B.C. Kelly, *Assessing biological effects of fluoxetine in developing zebrafish embryos using gas chromatography-mass spectrometry based metabolomics.* Chemosphere, 2017. **188**: p. 157-167.
308. Nebert, D.W., et al., *Use of reporter genes and vertebrate DNA motifs in transgenic zebrafish as sentinels for assessing aquatic pollution.* Environ Health Perspect, 2002. **110**(1): p. A15.
309. Chen, H., et al., *Generation of a fluorescent transgenic zebrafish for detection of environmental estrogens.* Aquat Toxicol, 2010. **96**(1): p. 53-61.
310. Avitsur, R., et al., *Prenatal SSRI alters the hormonal and behavioral responses to stress in female mice: Possible role for glucocorticoid resistance.* Hormones and Behavior, 2016. **84**: p. 41-49.
311. Arnnok, P., et al., *Selective Uptake and Bioaccumulation of Antidepressants in Fish from Effluent-Impacted Niagara River.* Environmental Science & Technology, 2017. **51**(18): p. 10652-10662.
312. Arpin-Pont, L., et al., *Occurrence of PPCPs in the marine environment: a review.* Environmental Science and Pollution Research, 2016. **23**(6): p. 4978-4991.